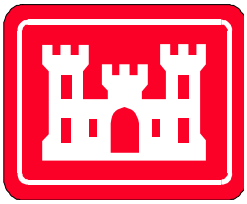

US Army Corps of Engineers
Engineering and Support Center,
Huntsville

Innovative Navigation Systems to Support Digital Geophysical Mapping ESTCP #200129

Phase III APG Demonstrations & Phase IV Development

Final Report

17 February 2006

ARMY Environmental Quality Technology Program

EQT

Report Documentation Page

Form Approved
OMB No. 0704-0188

1. REPORT DATE	2. REPORT TYPE	3. DATES COVERED
17 FEB 2006		**00-00-2006 to 00-00-2006**

4. TITLE AND SUBTITLE	5a. CONTRACT NUMBER
Innovative Navigation Systems to Support Digital Geophysical Mapping	5b. GRANT NUMBER
	5c. PROGRAM ELEMENT NUMBER
6. AUTHOR(S)	5d. PROJECT NUMBER
	5e. TASK NUMBER
	5f. WORK UNIT NUMBER
7. PERFORMING ORGANIZATION NAME(S) AND ADDRESS(ES) **U.S. Army Corps of Engineers, Engineering & Support Center?Huntsville (CEHNC),P.O. Box 1600 ,Huntsville,AL,35807**	8. PERFORMING ORGANIZATION REPORT NUMBER
9. SPONSORING/MONITORING AGENCY NAME(S) AND ADDRESS(ES)	10. SPONSOR/MONITOR'S ACRONYM(S)
	11. SPONSOR/MONITOR'S REPORT NUMBER(S)

12. DISTRIBUTION/AVAILABILITY STATEMENT
Approved for public release; distribution unlimited

13. SUPPLEMENTARY NOTES

14. ABSTRACT

15. SUBJECT TERMS

16. SECURITY CLASSIFICATION OF:			17. LIMITATION OF ABSTRACT	18. NUMBER OF PAGES	19a. NAME OF RESPONSIBLE PERSON
a. REPORT	b. ABSTRACT	c. THIS PAGE			
unclassified	**unclassified**	**unclassified**	**Same as Report (SAR)**	**229**	

Innovative Navigation Systems to Support Digital Geophysical Mapping
Final Report

Table of Contents

Acronyms and Abbreviations

3-D	three-dimensional
AEC	Army Environmental Center
APG	Aberdeen Proving Grounds
BRAC	Base Realignment and Closure
CEHNC	U. S. Army Corps of Engineers, Engineering and support Center—Huntsville
cm	centimeter
DGM	digital geophysical mapping
DGPS	differential global positioning system
DOD	Department of Defense
DSSS	direct sequence spread spectrum
EM	electromagnetic
EDM	electronic distance measurement (laser)
EQT	Environmental Quality Technology
ERDC	Engineering Research and Development Center
ESTCP	Environmental Security Technology Certification Program
FCC	Federal Communications Commission
FUDS	formerly used defense sites
GFE	government furnished equipment
GIS	geographic information system
GPR	ground-penetrating radar
GPS	global positioning system
Hz	hertz
IMU	inertial measurement unit
INS	inertial navigation system
ISM	industrial, scientific, and medical
m	meter
mm	millimeter
NEMA	National Electrical Manufacturers Association
OE	ordnance and explosive
OE-IT	ordnance and explosive-innovative technology
QA	quality assurance
QAPP	Quality Assurance Project Plan
RFP	request for proposals
RTK DGPS	real-time kinematic differential global positioning system
RTS	Robotic Total Station
SAINT	Small Area Inertial Navigation Tracking
SAM	sub-audio magnetics
SERDP	Strategic Environmental Research and Development Program
SQUID	Superconducting Quantum Interference Device
USRADS	Ultrasonic Ranging and Data System
UTM	Universal Transverse Mercator
UXO	unexploded ordnance

Figures

Tables

Innovative Navigation Systems to Support Digital Geophysical Mapping
Final Report

Acknowledgements:

The U.S. Army Corps of Engineers, Engineering & Support Center–Huntsville (CEHNC) managed and evaluated this demonstration effort. Efforts were funded by the Environmental Security Technology Certification Program (ESTCP) through Projects 200029 and 200129, Environmental Quality Technology (EQT), the Engineering Research and Development Center (ERDC) and by the Center's formerly used defense sites (FUDS) ordnance and explosive-innovative technology (OE-IT). The Center acknowledges the continued contributions and support of these programs.

Abstract:

Phase I demonstrated the basic navigation technologies without geophysical equipment and Phase II integrated the Geonics EM-61 MK1 and demonstrated at the McKinley Range, Redstone Arsenal, Huntsville, Alabama.

This report covers the Phase III demonstrations of innovative navigation systems to support geophysical mapping and related Phase IV development efforts. Phase III continued to focus on positioning equipment integrated with a Geometrics G-858 magnetometer geophysical sensors applied in the search for potential ordnance and explosive (OE) items. Demonstrations were performed at the Aberdeen Proving Ground unexploded ordnance (UXO) Demonstration Site, Aberdeen, Maryland. Phase IV focuses on collecting and integrating complete position information: x, y, z, multi-axis twist, tilt and rotation of a sensor head as applied to typical and advanced sensors under EQT and Strategic Environmental Research and Development Program (SERDP) development.

For Phase III, four demonstrators were evaluated for their position performance in the open at the calibration lanes, for obstructions in the woods, and for the effect of slope and elevation at the mogul test scenarios. Eleven individual tests using 78 surface fixed points, 35 interrogation areas, and the subsurface anomalies were performed and evaluated to measure accuracy of the navigation equipment and the system when integrated with a geophysical sensor. The focus was to measure the effect of obstructions and terrain, and the ability to collect accurate dense anomaly interrogation data for small areas. The following systems were demonstrated:

Shaw *UXO Mapper*- The Leica TSP 1100 dual laser robotic total station (RTS) system uses a single laser measurement unit to track a rover. It provides highly accurate line-of-sight positioning that interpolates for obstructed points. It provides local high three-dimensional (3-D) accuracy for anomaly interrogation. A position accuracy of 0.07 - 0.27 meters (m) was demonstrated.

GIS *GeoVisor*- Navigation/visualization system with differential global positioning system (DGPS) as primary positioning, Hexamite ultrasonic positioning as secondary positioning with an electronic compass, and real-time visualization software. The navigation/visualization system provides high 3-D accuracy to a relative position for anomaly interrogation by using the ultrasonics. A position accuracy of 0.25 - 1.01 m was demonstrated for the principal DGPS navigation with 0.1 - 0.15 m for the ultrasonic relative positioning system.

ArcSecond UXO *Constellation*- Multiple laser transmitter stations are used to track the rover system. The system provides highly accurate line-of-sight positioning that interpolates for obstructed points and local high 3-D accuracy for anomaly interrogation. A position accuracy of 0.01 - 0.18 m was demonstrated (average 0.01 m interrogations, 0.04 m area navigation, and 0.11 m, as picked from the geophysics)

ENSCO *Ranger*- A radio navigation system is augmented with inertial navigation system (INS). The INSs use the *Ranger* position as a starting point and acquire a high accuracy relative position for 3-D instrument tracking. A position accuracy of 0.17 - 0.57 m was demonstrated for *Ranger*. The INS enhancement for the interrogation areas demonstrated a relative position accuracy of 0.03 - 0.05 m.

Phase IV continues work on interrogation data analysis as acquired in Phase III demonstrations, in interrogation system positioning development, and with commercial application demonstrations. Based on Phase III results, the ArcSecond system was developed as a flexible integrated system that provides a full multi-axis position-tracking hardware and software solution. Position outputs use an extended National Electrical Manufacturers Association (NEMA) data format standard. The system was integrated with the EQT-funded Handheld Dual Magnetic/EM Sensor by AETC Inc, the SQUID by Battele, and the EM-61 MK II and G-858 by CEHNC. Controlled independent testing validated position accuracy of 0.003 - 0.004 m when used for local area interrogation.

The results summary (Table ES-1) compares the four positioning system demonstration results for the 11 individual tests including an average for locations from items picked from the magnetometer readings, an average for the principal navigation methodology, and an average for the secondary position augmentation system when used for anomaly interrogations by local area navigation positioning.

Description	Shaw	GIS	ArcSecond	ENSCO
Average (Geophysics)	0.22	0.48	0.10	0.31
Average Principal Nav	0.10	0.57	0.04	0.39
Average Local Area Nav	0.07	0.10	0.01	0.04

Table ES-1. Results Summary (all values are shown in meters).

1. Introduction

1.1 Background

General- Unexploded ordnance (UXO) poses a threat to both human life and the environment. Millions of UXO may be located in the United States on active test and training ranges and formerly used defense sites (FUDS). There are more than 10 million acres suspected to be contaminated in approximately 1,400 sites. Essentially all the project investigations involve the use of digital geophysical mapping (DGM). One of the major problems with DGM is the need for accurate navigation for sensor position. This is especially problematic with vegetation and under tree canopies. Accurate, inexpensive, and easy-to-use navigation systems with consistent quality are needed for surveys in all terrain and vegetation cover. Navigation accuracy is critical to acquiring the DGM data required for anomaly discrimination.

The technology will support geophysical mapping of FUDS, active Department of Defense (DoD) installations, defense sites identified under the Base Realignment and Closure (BRAC) Act, property adjoining DoD installations, and other federally controlled or owned sites that have been impacted by ordnance and explosive (OE) operations.

1.2 Objectives of the Demonstration

The primary objective of this project is to demonstrate and compare multiple navigation systems to support DGM. Phase I navigation demonstration efforts were fully funded by the Environmental Security Technology Certification Program (ESTCP) under Project 200129 with participants selected by a full request for proposal (RFP) competitive process. In Phase I, eight vendors demonstrated technologies during Fall 2001. The focus was specifically on demonstrating navigation equipment without geophysical equipment integration. Results were presented at the 2002 UXO and Countermine Forum and 2002 Strategic Environmental Research and Development Program (SERDP)/ESTCP Partners in Environmental Technology Conference.[1]

In Phase II, eight vendors demonstrated technologies from Fall 2002-Summer 2003. All demonstrators had their positioning systems fully integrated with the typical geophysical sensors commonly used for UXO investigations, the EM-61, and the G-858 magnetometer. Demonstration efforts were focused to determine position accuracy for open and wooded areas for known and unknown surface and subsurface items as selected from the captured geophysical data. Phase II efforts were sponsored by the combination of the ESTCP Projects 200029, 200129, 200207, the Army Environmental Quality Technology (EQT) program and U.S. Army Corps of Engineers, Engineering and Support Center—Huntsville (CEHNC) funding, and in-house support as outlined in the workplan[2] and under the final report.[3]

[1] Innovative Navigation Systems to Support Digital Geophysical Mapping, UXO/Countermine Forum September 3-6, 2002, Scott Millhouse

[2] Innovative Navigation Systems to Support Digital Geophysical Mapping Phase II Demonstrations Final Workplan 15 October 2002, Scott Millhouse, CEHNC)

[3] Innovative Navigation Systems to Support Digital Geophysical Mapping ESTCP #200129 Phase II Demonstrations Revised Draft Report 25 June 2004, Scott Millhouse, CEHNC

Phase III demonstrations were performed December 2003-July 2004 as outlined in the workplan.[4] Navigation equipment from four vendors was fully integrated with a government-furnished Geometrics 858 cesium vapor magnetometer. Demonstrations were performed in a consistent manner to minimize the effects of the geophysical sensor. Demonstrations were held at the Aberdeen Proving Grounds (APG) UXO Demonstration Site. The emphasis was to determine the applicability of the demonstrated technologies to support in-the-wood navigation, terrain-obstructed geophysical mapping activities, and precision anomaly interrogation. These are applications where differential global positioning system (DGPS) generally drops position or has greatly reduced accuracy.

This report focuses on Phase III results but is supplemented with related follow-on developments identified as Phase IV. Phase IV results follow the Phase III results, as shown in Section 4.6. Individual papers and reports are included in Appendices J-N.

For Phase III, the vendors demonstrated the integrated systems first at the Calibration Lanes and then in the challenging environment of the wooded and mogul scenarios. The initial focus was on acquiring high accuracy, fixed point navigation, and mass mapping data using integrated navigation and geophysical sensor equipment. In the Calibration Lane, 19 representative items larger than 57 mm were interrogated by a fixed position array for static measurements, as well as in a dynamic mode to compare position accuracy.

Systems were evaluated on the accuracy of positions recorded for known and unknown surface control points, as well as on dig list locations for unknown subsurface anomalies. Systems were separately evaluated based on the accuracy of surface point positions determined from G-858 sensor profiles and gridded geophysical data. The surface points at all areas and subsurface anomalies' locations at the Calibration Lanes were evaluated independently by CEHNC. The Wooded Scenario subsurface items were evaluated by APG with emphasis on the position error rather than the typical detection metrics. The vendors did not attempt to discriminate anomalies during selection. A threshold value was set based on the Calibration Lane results for typical instrument readings for the 57 mm M86 and larger items.

The Phase III field demonstration campaign included four demonstrations. The Shaw/IT *UXO Mapper* and the GIS *GeoVizor* (funded by EQT), the ArcSecond UXO *Constellation* (funded jointly by EQT and ESTCP Project 200129), and the ENSCO *Ranger* with inertial navigation system (INS) augmentation (jointly funded by EQT and ESTCP Projects 200029 and 200129).

Phase IV continues work on interrogation data analysis as acquired in Phase III demonstrations, interrogation system positioning development, and commercial application demonstrations. Funding for this effort has been split equally by FUDS ordnance and explosive-initiative technology (OE-IT), ERDC EQT, AEC EQT and by ESTCP Project 200129. Based on Phase III results, the ArcSecond system was developed as a flexible integrated system that provides a full multi-axis position tracking hardware and software solution.

[4] Innovative Navigation Systems to Support Digital Geophysical Mapping Phase III Demonstrations Final Workplan 4 November 2003, Scott Millhouse, CEHNC

There are three levels of accuracy needed to support the OE program as outlined in the original RFP:

1. Screening level to determine areas of interest as implemented by airborne sensors or characterization efforts by ground-based sensors by corridors, transects or meandering pathways.
2. Area mapping as performed by man portable and towed arrays.
   - Phase III focuses initially for area mapping in the Calibration Lanes and the challenging wooded environment. Navigation accuracy was compared to 78 unknown fixed points that have been surveyed in by APG. Subsurface anomaly locations from the integrated sensor readings were separately evaluated by APG for position accuracy.
3. Interrogation where highly accurate dense data is acquired to interrogate and then, by post-processing the accurate layered data, discriminate a previously located target anomaly.
   - For Phase III, selected anomalies with sensor reading above the threshold established for the 57 mm at the Calibration Lanes were interrogated

Position tolerance of 0.5 m, 0.05 m, and 0.02 m is desired for these scenarios, as outlined in the original RFP. For this demonstration, tolerance is defined as the leeway for variation from a standard, with the standard being the civil surveyed position of the known and unknown points. Accuracy (or average error) is the demonstrated deviation from the location of the surveyed points.

Phase I demonstrations at the McKinley Range Test Site, Huntsville, Alabama, with only navigation equipment have shown that these goals are still somewhat ambitious but they can be approached. For the three mission scenarios, the best system average error was 1 m, 0.04 mm, and 0.006 m demonstrated in the open areas with the known points and 3 m, 0.6 m, and 0.09 m demonstrated in the wooded area for unknown points. The demonstrations' results supported additional development of navigation equipment with emphasis on obstructed and wooded areas.

For Phase II at McKinley Range, demonstrators were challenged to integrate with the EM-61 and G-858 geophysical sensors and survey to locate 10 known and 15 unknown surface points and 20 known and 130 unknown subsurface anomalies. The characterization mapping system demonstrated an average error of 1.5 m for the known surface points and 3.3 m for unknown surface points in the open with 5.4 m in the woods by navigation alone to 3.6 m for the known open and 4.5 m for the unknown open locations, as picked from the integrated geophysical sensor readings. The area mapping systems demonstrated an average error of 0.04 m-0.3 m for the known surface points and 0.09 m-0.79 m for unknown surface points in the open with 0.1 m-1 m in the woods by navigation alone to 0.37 m-1.39 m for locations as picked from the integrated geophysical sensor readings. Average error for subsurface anomalies varied from 0.18 m-0.42 m for known open and 0.32 m-0.95 m for unknown open to 0.31 m-1.36 m for unknown wooded locations. Based on these results, four demonstrators were selected to continue development for Phase III demonstrations.

The following goals are desired for highly performing equipment, as quoted from the Navigation RFP:

- 10-minute setup
- 1,000'+ range per setup
- Ability to map a 5-acre area
- Ability to have multiple crews working in the same area without interference
- Less that $20,000 per system cost
- Voice communication capability without interference
- Go-to-point capability (reacquisition)
- Real-time data transmission to a central location (could allow real-time geophysical analysis)
- Ability to capture the z or elevation data along with position
- Ability to determine relative position of individual sensor heads when coupled with geophysical instrumentation (skew, lifting, tilting, etc.)
- Flexible use with geophysical instruments (mag, electromagnetic (EM), ground-penetrating radar (GPR), etc.)
- Selectable accuracy mode to allow higher accuracy for interrogation of anomalies (most likely at slower rate of sensor travel speed)
- Real-time track map display for surveyor
- Ability to support real-time grid generation and display of geophysical data when coupled with geophysical sensors
- Capability of the system to inform users when accuracy levels are being achieved (to avoid collecting bad data)
- Capability to survey in wooded conditions with varying degrees of topography.

1.3 Regulatory Drivers

This project is primarily motivated by the desire for more efficient and accurate OE field operations to achieve both better technical remediation performance and to reduce cost. Precise navigation and positioning technology is an important part of the infrastructure of OE remediation efforts as an enabling tool to allow faster, better and cheaper detection, characterization, and excavation. Regulatory issues do not affect the need for this technology.

1.4 Stakeholder/End-User Issues

Results of this demonstration will provide end users with an understanding of the technical, logistical, and financial impact of these technologies and will allow informed decision making by end users for appropriate applications.

2. Technology Description

2.1 Technology Development and Application

This demonstration includes the navigation systems that have demonstrated in Phase I and II to have the best opportunity to provide accurate positioning in the challenging wooded and mogul Scenarios at APG. They also provide highly accurate interrogation positioning by Universal Transverse Mercator (UTM) coordinates or by relative positioning. The demonstrated systems cover most known technologies for positioning. There are six basic navigation technologies being demonstrated: DGPS, laser, ultrasonic, inertial, electronic compass, and radio. The demonstrators are applying the technologies in various fashions, as follows:

- Two systems are line-of-sight laser-based with Shaw/IT using a Robotic Total Station (RTS) as a variation on traditional single unit surveying technology and ArcSecond using multiple laser transmitters to create a form of laser global positioning system (GPS).
- The geographic information system (GIS) system is a hybrid that uses DGPS for primary positioning with ultrasonic for secondary relative positioning and an electronic compass for a direction vector.
- The ENSCO system uses radio frequency for primary positioning with an INS augmentation for accurate small area local positioning relative to the radio position location.

Navigation Demonstration Systems Overview:

Shaw *UXO Mapper*-

Demonstration December 1-5, 2003— The RTS system uses a single laser measurement unit to track a rover. The system provides highly accurate line-of-sight positioning that interpolates for obstructed points and local high 3-D accuracy for anomaly interrogation. RTS requires local reference points for principle coordinates. The system was validated by Gtek with the sub-audio magnetics (SAM) (TM-6) in June 2004 as shown in Appendix J: Gtek Application of Robotic Total Station Navigation to Sub-Audio Magnetic Surveys.

GIS *GeoVisor*-

Demonstration January 12-22 2004—The GIS system is a navigation/visualization system that uses DGPS for primary positioning, hexamite ultrasonic positioning, electronic compass, and real-time visualization software. The navigation/visualization system provides high 3-D accuracy to a relative position for anomaly interrogation using the ultrasonics.

ArcSecond UXO *Constellation*-

Demonstration April 12-15 2004—The ArcSecond system uses multiple laser transmitter stations with rover system. The system provides highly accurate line-of-sight positioning that interpolates for obstructed points and provides local high 3-D accuracy

for anomaly interrogation. The system requires local reference points for principal coordinates.

ENSCO *Ranger*-

Demonstration July 12-16, 2004—The ENSCO radio navigation system is augmented with INS. The INS systems use the *Ranger* position as a starting point and the INS to acquire a high accuracy relative position for 3-D instrument tracking. The system requires local reference points for principal coordinates.

2.1.1 Shaw *UXO Mapper*—The Robotic Total Station laser-based system was demonstrated in Phase I and Phase II as a man-portable, cart-based system by ESTCP Project 200129. Phase III efforts are fully funded by EQT. This demonstration continues development with the focus on applying the RTS methodology to handheld sensors. The sensor will be tracked in 3-D with the addition of sensor orientation data. The RTS concept is a pure line-of-sight application but, even with obstructions caused by tree trunks and branches, it provided one of the highest accuracies in the wooded areas with a reasonable range. This was attributed mostly to software enhancements that allowed the base unit to maintain track of the rover by predicting its location when emerging from obstructions.

RTS operates under a different concept from either GPS or the ultrasonic systems. It essentially is a survey station that derives its position from traditional survey methodology and then tracks the relative position of the sensor. The robotic portion maintains track on the moving prism. The unique quality of this demonstration is to have procedural and software modifications to allow the RTS to maintain lock in heavy vegetation by predicting the location of the sensor and then reacquiring it. Figure 2-1 shows the basic concept.

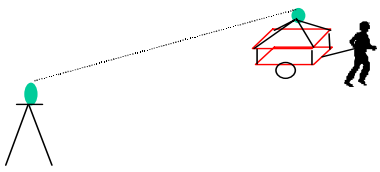

Figure 2-1 Robotic Total Station Concept

Shaw *UXO Mapper* Description:

Shaw's geophysical mapping technology is an engineered combination of off-the-shelf geophysical sensors, innovative navigation technologies, a flexible and configurable deployment system, and customized data acquisition software. The Shaw *UXO Mapper* has hardware and software components:

- Leica TPS1100 RTS for in-the-tree and open-area navigation

- Off-the-shelf magnetic (G858) sensor
- Software for data acquisition system for sensor, navigation, and gyro data collection
- Software to achieve robust navigation and sensor time-base synchronization
- Software to implement real-time telemetry and data merging.

Hardware: The Leica TPS1100 RTS is a motorized robotic total station that uses automatic target recognition to track the location of the prism and has a highly accurate distance/azimuth measurement system to produce +/-5 mm+2 ppm accuracy, which translates to 0.25 inches (3-D) at distances of up to 1,400 feet.

Software: The Shaw *UXO Mapper* has three software components. First, customized RTS firmware is used to track the roving prism. Developed specifically for Shaw's UXO mapping applications, this firmware allows for rapid collection of data to 4 hertz (Hz) and outputs solutions to the base station and rover units. The firmware enables the user to optimize prism-tracking parameters for rapid recovery of lock if obstructed by trees during a survey. Second, Shaw's data control software determines precise time synchronization between the RTS and sensor time bases, ensuring accurate collection of all data. Third, Shaw's software for data merging accommodates various sensor navigation geometries used during data collection and provides a robust framework to spatially configure sensors relative to each other and with respect to the prism location. Additionally, this software allows RTS and sensor data to be merged in either a straightforward interpolation mode (for open areas) or in hybrid switching mode that alternates to "dead reckoning" for the brief periods when the RTS is obstructed in the woods.

Figure 2-2. Shaw *UXO Mapper*

2.1.2 Gifford Integrated Sciences *GeoVisor*—This system is a low-cost DGPS/acoustic hybrid system integrated with an electronic compass. Its development and demonstration has been fully funded by EQT. The primary system (DGPS) locates the operator within the global coordinate system. The secondary system locates the instrument head relative to the DGPS antenna or a fixed stationary point. The primary positioning system is CEHNC's government furnished equipment (GFE) 2 cm capable Novatel DGPS system. Secondary relative positioning is provided by the ultrasonics. The ultrasonic positioning system is designed to provide highly accurate position information (<2 cm) in both terrestrial and underwater environments. In the hybrid system, this component is used to track the XY and Z position of the instrument head. It is also used to accurately determine the pitch and roll of the head or antenna surface. The real-time display allows the operator to "see" the survey as it is taking place through a head-mounted computer display. The operator has various views of the data that he can select for different survey objectives. The extremely rapid refresh rate of the ultrasonic system allows the operator to move the geophysical instrument in real time while keeping track of its position. The combination of the ultrasonic position information with the geophysical signal results in a volumetric representation of geophysical response around a target.

Primary Positioning System, real-time kinematic differential global positioning system (RTK DGP) Description—The GPS system is a spread-spectrum distance measuring system, where the distance from a user to several satellites is measured. Knowing the positions of the satellites, the position of the user is computed. GPS measures the distance from the satellites to the user, using one-way communications (from the satellite to the user), generating the so-called pseudo-range, and the unknown clock time of the user is solved in the solution. The RTK portion of the GPS is accomplished by a base station GPS unit occupying an existing known bench mark and recording and relaying its measured position and creating a differential correction from the known position. It then sends that correction to the rover unit, which applies the correction to its calculated position to derive a more precise DGPS position.

Secondary Positioning Ultrasonic System—Hardware Specification

- Hexamite - HE860 series positioning device (three required, one for each axis)
- Hexamite - HE240SRX receiver (three required, one for each HE860)
- Hexamite - HE240STX transmitter, for use in tethered mode (variable number required, depending on specific setup)
- Hexamite - Miniature Ultrasonic Transponder Positioning Tag, for use in untethered mode (variable number required, depending on specific setup)
- MapStar compass module (+/-0.3° accuracy)

The complete *GeoVizor* system is a backpack mounted geophysical mapping and visualization system with the following components:

- Laptop computer
- Heads-up display
- Ultrasonic positioning systems (2)
- Electronic compass
- DGPS system (Novatel)
- Integration and visualization software
- Geophysical instrument (Geometrics 858)

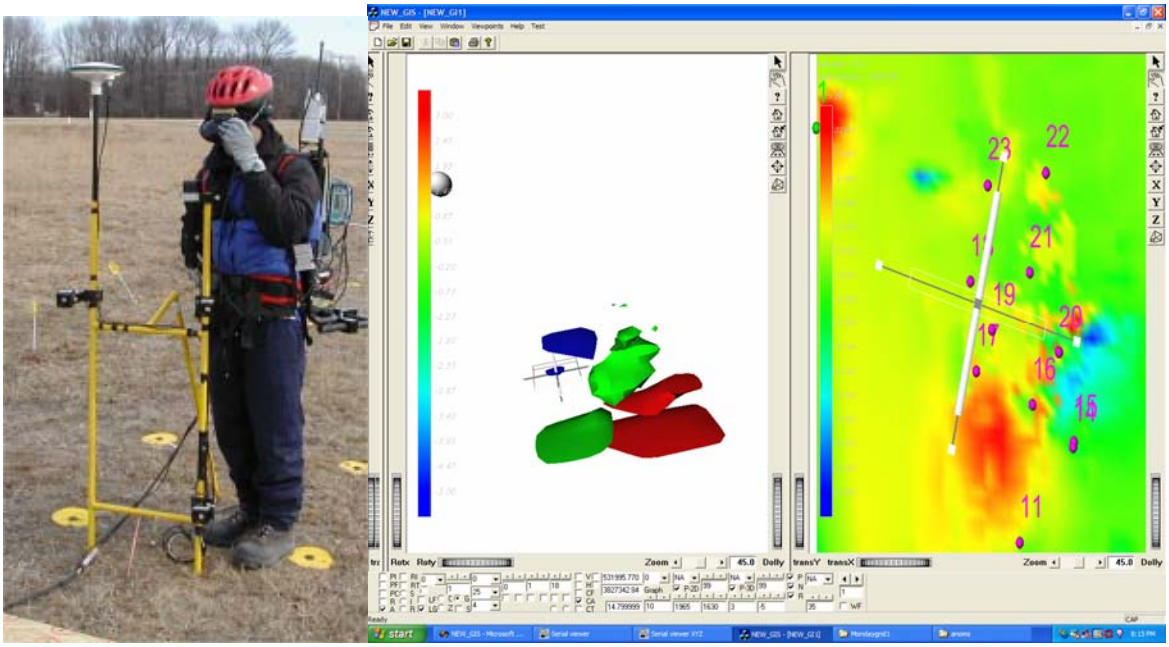

Figure 2-3. *GeoVizor* System

For Phase III demonstrations, the demonstrated system separated the work flow process into two mission areas. For acquiring area mapping geophysical data, the heads-up-display provided a visual representation of the planned survey path and the as-surveyed track to ensure complete coverage. For reacquisition, the heads-up-display directed the operator to the selected anomaly for interrogation. Once located, the display shows a real-time 3-D volume representation of the sensor position and the instrument readings.

The following enhancements were performed:

1. Separate systems for DGM surveys and reacquisition/interrogation.
2. Weight and system comfort
3. System setup complexity
4. Waterproofing the system
5. Software issues

2.1.3 ArcSecond *Constellation* System—The original Vulcan Laser Station was demonstrated in Phase I with dual transmitters and then with enhanced range and four transmitter stations as the *Constellation* System for Phase II. Phase I was funded by ESTCP project 200129, with Phase II 100% funded by CEHNC FUDS Innovative Technology. Current Phase III efforts are jointly funded by ESTCP Project 200129 and EQT. Phase IV improvements were equally funded by ESTCP Project 200129, the Engineering Research and Development Center (ERDC) and Army Environmental Center (AEC) EQT programs.

This highly accurate system is being developed for demonstration to cover large areas with additional transmitter capability and higher power output. Accuracy is high enough that it currently meets the goals for gathering data for geophysical anomaly discrimination for small open areas. Phase III adds a leap-frogging concept to facilitate corridor and large surveys and adds interrogation-capable 3-D point positioning.

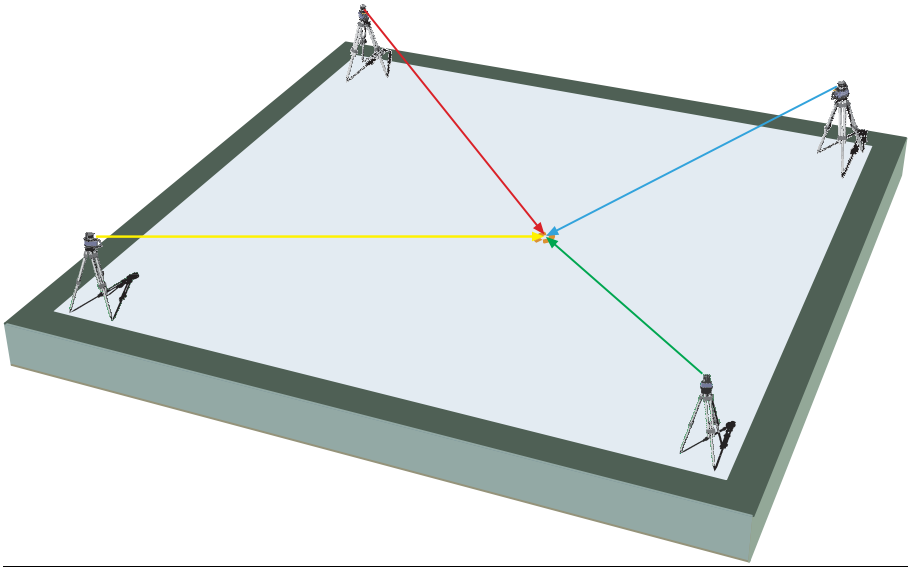

Figure 2-4. Dual Transmitter *Constellation*

Constellation works very much like a portable, highly accurate RTK-GPS alternative. The portable nature of the system allows the user to map areas where traditional methods (optical, acoustical, and GPS-based) dramatically degrade or fail—primarily under and near tree canopy, but also in relatively open areas with poor satellite visibility. In addition, the system's ability to support any number of 3-D sensors simultaneously opens two intriguing benefits for UXO: (1) the ability for multiple users to map simultaneously, and (2) the ability to track the full position and orientation of a geophysical sensor (e.g., to allow 3-D discrimination of UXO). The latter was developed as part of Phase IV.

The system consists of stationary laser transmitters/beacons (like GPS satellites) and portable sensors that can be carried or mounted on objects. The system can support any number of sensors working off the same transmitters, so multiple users could be conducting geophysical mapping surveys in the same work area. In order for a sensor to calculate its 3-D position, it must see at least two laser transmitters. Consequently, for open areas, two transmitters work well; under tree canopy or in areas where line-of-sight is restricted (e.g., close to buildings), three or four transmitters provide fuller coverage. Position location is by triangulation from the fixed transmitters.

Figure 2-5. Phase III ArcSecond System Demonstration

<u>Phase IV</u>:

For Phase IV, the ArcSecond system was developed as a flexible integrated system that provides a full multi-axis position tracking hardware and software solution. Position outputs are by an extended National Electrical Manufacturers Association (NEMA) data format standard. The system transmits a one-second timing pulse and provides a position from the primary optical sensor. Data from all four sensors is stored at 40 Hz in the system for post-processing for attitude and synchronization with the geophysical data. The system was integrated with the EQT-funded Handheld Dual Magnetic/EMI Sensor by AETC Incorporated (see Figure 2-5), the Superconducting Quantum Interference Device (SQUID) by Battelle, and the EM-61 MK II and G-858 by CEHNC. Controlled independent testing validated position accuracy of 0.003-0.004 m when used for local area interrogation as performed by Bruce Barrows of AETC Inc[5].

[5] Evaluations of Laser Based Positioning for Characterization of EMI Signals from UXO, Bruce Barrow, Nagi Khadr, Thomas Bell, AETC, Incorporated

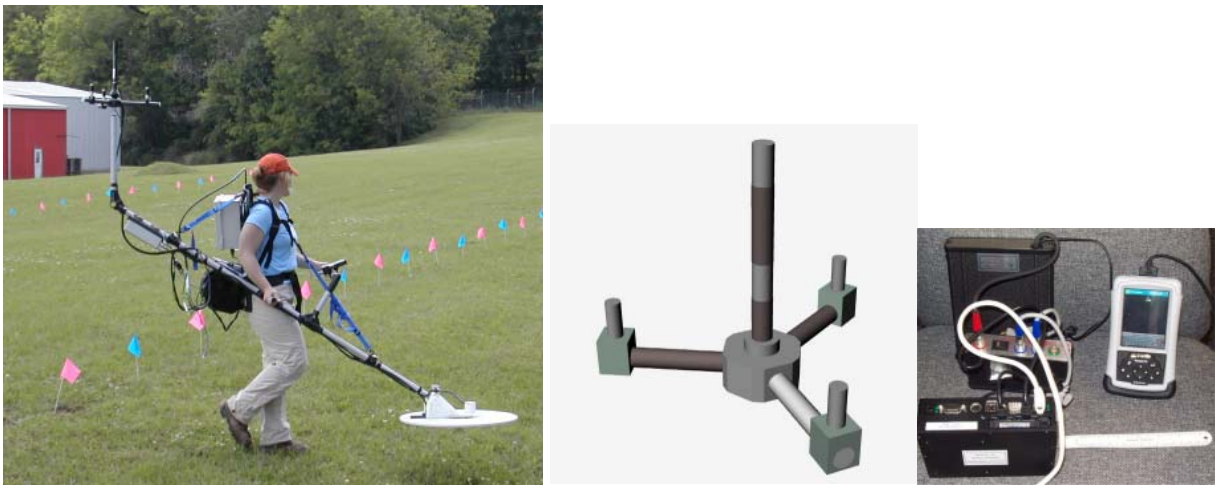

Figure 2-6. Phase IV ArcSecond Triad System

2.1.4 ENSCO *Ranger*—Under ESCTP Project 200029, CEHNC and ENSCO demonstrated a new position, location, tracking, and communication system known as *Ranger* that is designed to support DGM for UXO operations. The initial demonstration report was submitted December 2001. A follow-on effort was initiated and completed, designed to improved the technical performance of *Ranger* in several ways, with the demonstration report submitted April 2003. Efforts were combined with this project for demonstrations and comparison reporting. Phase II demonstration at the McKinley Range showed *Ranger* to be a viable navigation technology to support DGM in wooded terrain. Phase III leverages prior effort under ESTCP Project 200029 with funding from EQT and ESTCP Project 200129 to augment *Ranger* with an inertial navigation system (INS). The INS systems use the *Ranger* position as a starting point and the INS to acquire a high accuracy relative position for 3-D instrument tracking.

Ranger exploits a unique direct sequence spread spectrum measuring system to provide precision geolocation and simultaneous data communications. Multiple base-station radios (referred to as fixed radios) are used to measure their distance to one or more mobile radios. These multiple distance measurements can then be used to compute the coordinates of the mobile radios. Repeated, sequential distance measurements and coordinate computation enables tracking the mobile radio's path. This navigation system is directly integrated with a data logger and geophysical instrumentation for Phase III demonstration. Figure 2-7 shows a system block diagram.

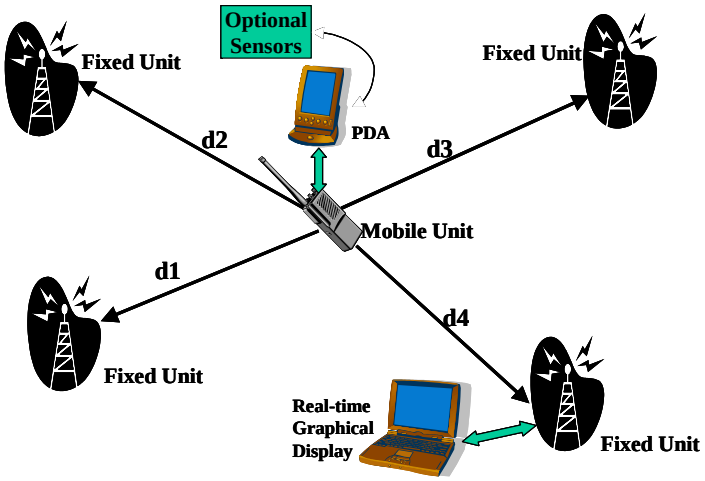

Figure 2-7. Block Diagram of *Ranger* System

The *Ranger* communications architecture is based on direct sequence spread spectrum (DSSS) in the 2.4 GHz industrial, scientific, and medical (ISM) band. This allows *Ranger* to operate as unlicensed transmitters under Federal Communications Commission (FCC) rules with a 1-watt transmit power. Core circuitry takes advantage of widely available and inexpensive components commonly used in 802.1 lb wireless network products.

The key element of *Ranger* is the ability to accurately measure distance. Methods for using a DSSS radio for semiprecise time-of-flight measurement are well understood for coarse measurement. *Ranger* differs in that a fine measurement is made to estimate more precisely the time of arrival (and hence the distance traveled) of a signal. It is this fine measurement that provides the submeter accuracy of *Ranger*.

The Phase II demonstration showed significant improvement over the Phase I effort, specifically:

- Navigation accuracy in the open site was better than the 20 cm objective and exceeded the dynamic performance of GPS systems when integrated with geophysical sensors.
- Navigation in the wooded site was successful uniformly across the entire wooded site with no gaps in coverage.
- Range of operation in the wooded site routinely exceeded 125 m, and the maximum range through the woods was not reached.

As a result of this demonstration and analysis, *Ranger* appears ready for wider use within the UXO and DGM community as a navigation tool to support geophysical data acquisition, particularly for those locations where GPS is unavailable due to obstructed visibility to the sky.

Phase III supports commercialization of *Ranger*, making it available to and usable by the UXO community, and implementing a high-precision, small area inertial navigation capability for data collection to support characterization of relocated anomalies. Commercialization effort is primarily focused on making the system easier for a non-expert user to operate. Commercial applications were demonstrated at Sibert, Anniston, Alabama, by CEHNC in November 2004 and by ARM Geophysics at Fort Devens, Massachusetts, in June 2005. See Appendix K: ARM Group Inc. Commercial Test of Ranger Positioning System for details.
Specific issues addressed:

1. Radio calibration. Temperature calibration of the signal delays in the radios were more accurately quantified to be removed from the overall error budget.
2. The Kalman filter was moved as a post-process on a PC to the Pocket PC handheld. Having a real-time Kalman filter running on the Pocket PC provides the operator with a real-time position estimate, a benefit during target relocation.
3. Simplify the user controls to both the Kalman filter and sofTRAC, our data collection, processing, and display package.
4. Develop and provide user manuals for the hardware and software.
5. Deliver a preproduction prototype to CEHNC for further evaluations and direct field application.

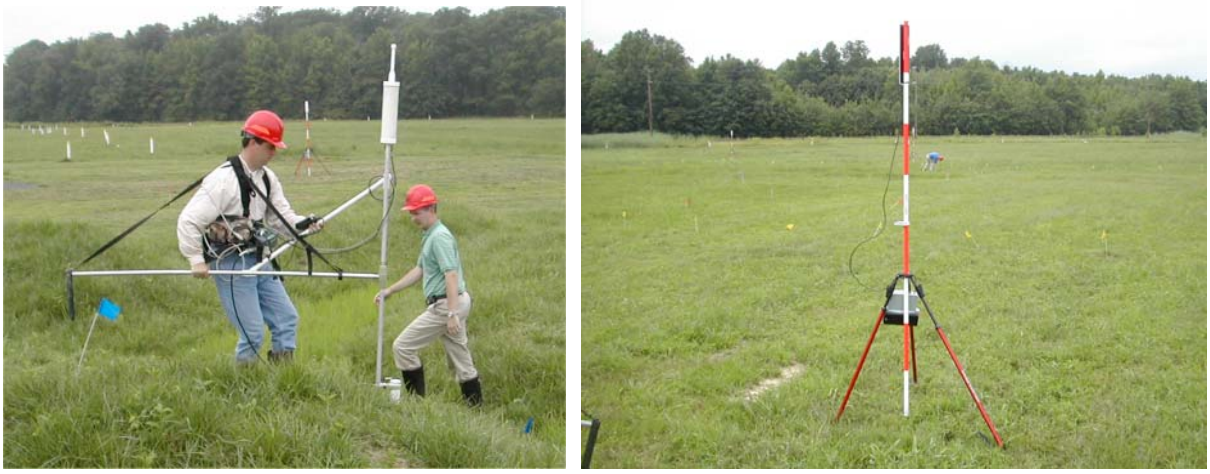

Figure 2-8. *Ranger* System

Small area inertial: The second component addresses geolocation technology to support target characterization. Studies in recent years have identified that target characterization, usually achieved through modeling and simulation, requires high-precision geolocation of sensor data. Sensor data location accuracies on the order of 2 cm are needed for high-performance analysis.

The device is based on tactical-grade inertial navigation technology, providing precise position data for target relocation. Operationally, a survey would first be conducted in a wide area search using *Ranger* to locate targets with submeter accuracy. These targets would then be relocated and marked (possibly flagged) for characterization. Data collection with this inertial device and a sensor would then be conducted over a small area with very high precision. The objective is to achieve accuracy of ±2 cm horizontally and ±4 cm vertically for the coordinates of all sensor data.

The INS system consists of the following components:

1. Tactical-grade inertial measurement unit (IMU), the Honeywell HG1700
2. A data logger Compaq iPaq
3. Integration with a Geometrics 858 magnetometer
4. Pin flag or other means to record the orientation of the local survey grid
5. Post-processing software.

Figure 2-9. *Ranger* INS Augmentation

Analysis of the optimum data acquisition and computational methods to achieve highly accurate inertial-based geolocation requires further analysis, but the key to any inertial technology is to constrain sensor drift. The developed methodology has the following features:

1. Data collection over the entire target location will require no more than several minutes.
2. An arbitrary location will be reoccupied several times during the data collection to provide further constraint.

2.2 Previous Testing of the Technology

A low-cost demonstration of eight vendors' navigation technology was demonstrated at the McKinley Range during October and November 2001 as Phase I**.** The focus was for navigation equipment without a geophysical sensor integrated for fixed surface points. Accuracy ranged from 0.04 m to 11.7 m for the open areas and 0.08 m to 25.9 m for the obstructed wooded areas.

Phase II demonstrations were also held at McKinley Range from October 2002 to June 2003. The most successful vendors from Phase I, CEHNC, and other ESTCP project demonstrators were included. Demonstrators were challenged to integrate with the EM-61 and G-858 geophysical sensors and survey to locate 10 known and 15 unknown surface points and 20 known and 130 unknown subsurface anomalies in both wooded and open areas.

Systems demonstrated and evaluated included the following:

1. CEHNC independent baseline, commercially available Novetel 20 cm accuracy RTK GPS and USRADS acoustic navigation
2. Shaw/IT Corp. ESTCP Project 200129: RTS laser, based system
3. Blackhawk ESTCP Project 200129: DGPS integrated with an improved low-cost INS
4. Where Co. ESTCP Project 200207: Improved UlTra, ultrasonic navigation with auto-correlation signal recovery
5. ENSCO ESTCP Project 200029: Local area radio frequency positioning system
6. ArcSecond (CEHNC-funded): *Constellation* with enhanced range and four transmitter stations
7. PaperPilot (EQT-funded): low-cost GPS/INS integrated with electronic compass (for characterization use)

8. Gifford Integrated Sciences (EQT-funded): GeoVizor low-cost GPS/acoustic integrated with electronic compass (for characterization use with GPS) more flexible precise use with DGPS for area mapping.

Subsurface anomaly location evaluations were only possible for the more accurate area mapping systems since the error radius was too large for the characterization systems to allocate to the individual anomalies. The six area mapping systems demonstrated an accuracy of 0.04 m-0.3 m for the known surface points and 0.09 m-0.8 m for unknown surface points in the open with 0.1 m-1 m in the woods by navigation alone to 0.37 m-1.39 m for locations as picked from the integrated geophysical sensor readings. Accuracy for subsurface anomalies varied from 0.18 m-0.42 m for known open and 0.32 m-0.95 m for unknown open to 0.31 m-1.36 m for unknown wooded locations. The top four of the six demonstrated area mapping systems are participating in this Phase III demonstration.

2.3 Factors Affecting Cost and Performance

For the Phase III demonstrations, limited application costs and productivity were recorded. This includes items such as: 1) daily/weekly/monthly technology costs for rental, purchase, and maintenance; 2) technology availability and downtime considerations; 3) survey productivity factors that include setup, survey area limitations, operating personnel labor requirements, and cost; and 4) data processing considerations for position and geophysical instrument integration. Details are shown in the applicable contractor reports.

2.4 Advantages and Limitations of the Technology

Determination of the advantages and limitations of the demonstration technologies is the key goal of this project. The technologies' objectives are: 1) to obtain a higher accuracy than traditional technologies in the more challenging environment of wooded areas and areas with varying terrain and 2) to get ultra high accuracy 3-D positioning for small areas for anomaly interrogation. These technologies were compared to the ground truth for the surface and subsurface points. In addition the demonstrators were directly compared to the typical RTK DGPS and the Ultrasonic Ranging and Data System (USRADS) results as demonstrated in Phase II by the government.

	RTK DGPS	*Ultrasonic*
Range of operation	Limited to radio link 2-7 miles typical	30-40 m
Precision	2-20 cm	10-20 cm
Number of transponders in addition to mobile	1 (base station)	12
Effect of vegetation/ canopy	Blocked	Some loss of range.
Purchase cost	$35,000	$70,000

Table 2-1. Comparison of DGPS and Ultrasonic

3. Demonstration Design

3.1 Performance Objectives

Technical performance of the planned equipment is the primary issue to quantify in this demonstration. Table 3.1 outlines the objectives.

Type of performance objective	*Performance criteria*	*Expected performance*
Quantitative	Unobstructed range of operation	100-1000 m
	Unobstructed average error	0.5-200 cm
	Obstructed range of operation	50-500 m
	Obstructed average error	1-200 cm
	2D position error	1-200 cm
	Setup time	10-30 min
	Multiple crew capability	Yes or no
	Voice communication	Yes or no
	Ability to capture elevation data (3-D)	Yes or no
	Selectable accuracy	Yes or no
	Flexible use of geophysical equipment	Yes or no
	Real-time display of geophysical grid data	Yes or no
	Ability to display position data in near-real-time on mobile data logger	Yes or no
	Ability to display position data in near-real-time on remote computer	Yes or no
	Ability to survey grids in wooded areas	Yes or no
	Integrated with G858	Yes or no
	Integrated with EM61	Yes or no
Semi-quantitative	System easy to setup and calibrate by two-person team	Yes or no
	System easy to operate by two-person crew	Yes or no
Qualitative	Reoccupation of position easily accomplished	Yes or no

Table 3-1. Performance Objectives

The project objectives are outlined in paragraph 1.2 as presented in the Navigation RFP. For the Calibration Lanes test, the technology's demonstrated position locations were compared to the known locations of all surface features and subsurface anomalies.

The Wooded Scenario position accuracy was compared to 46 new unknown points that were accurately located by precise civil surveying techniques. The subsurface anomalies were evaluated by APG with an emphasis on location accuracy. Evaluations were focused as relative system comparisons based on the average performance since obstructions to line-of-sight are random with each setup, view angle, equipment methodology, and mobilization.

For the Mogul Scenario 20, unknown surface points were surveyed for evaluations. They were placed to emphasize the varied slopes and elevations to gauge 3-D navigation capability and identify offsets by the navigation systems and as integrated with the G-858 magnetometer.

Deviations from the true locations were identified and categorized separately for surface features in the Calibration, Mogul, and Wooded areas for the initial dig list locations of the subsurface anomalies in the areas from the area mapping and for the reacquired and interrogated locations of the anomalies. The average and standard deviation were reported for each location category and each demonstrator for each test.

3.2 Selecting Test Site(s)

Criteria for selecting a test site are the following:

- Accessible to all project participants
- Sufficient space to accommodate the distances required for the planned tests
- Combination of open areas and areas with a variety of densities of vegetation
- Buried metallic targets that can be used to compare sensor data both with and without the presence of navigation equipment
- Moderate terrain so that elevation effects will not dominate the demonstration
- A controlled site with locations of items unknown to the demonstrators so that it may be revisited to gauge improvement and compare to other technologies.

Our approved test site is the APG UXO demonstration site. It meets all these selection criteria.

3.3 Test Site History/Characteristics

The Standardized UXO Test Sites Program utilizes standardized test methodologies, procedures, and facilities to help ensure that critical UXO technology performance parameters such as detection capability, false alarms, discrimination, reacquisition, and system efficiency are accurate and repeatable. The APG site is a 17-acre complex composed of five independently scored scenarios. The scenarios include calibration lanes, blind grid, wooded, moguls, and open field. Within the open field there are a variety of challenges, including electrical lines, gravel roads, fence line, wet areas, and clutter fields.

This test will utilize the Calibration, Mogul and Wooded Areas as shown in the following figures. Ground truth for the Calibration Lanes is included in Appendix F.

Figure 3-1. APG UXO Demonstration Site Layout

Figure 3-2. Calibration Lanes

Figure 3-3. Moguls

Figure 3-4. Wooded Area

3.4 Present Operations

The APG UXO Demonstration Site is maintained to provide quantitative, benchmarked evaluation of sensors and DGM systems and components. Prior demonstrations have been conducted at this facility under the supervision of AEC.

3.5 Pre-Demonstration Testing and Analysis

The performance of the systems will stand alone and is not closely tied to site conditions. The vegetation that existed on site at the time of the demonstration provided the basis for evaluating through-vegetation properties. Because there is no standard or objective description of vegetation that will potentially interfere with signal propagation, these conditions were documented in field note descriptions and with photographs. This allows qualitative conclusions to be drawn and will allow potential users to make a reasoned projection of the impact of vegetation at their project site from the conditions at this test site.

3.6 Testing and Evaluation Plan

3.6.1 Demonstration Setup and Start-Up

Demonstration setup requires installation of the fixed position sensors as appropriate and calibration of the systems. All equipment is battery powered and requires no external power.

3.6.2 Period of Operation

The demonstration was performed by four separate campaigns: 1-5 December 2003 for Shaw, 12-22 January 2004 for GIS, 12-15 April 2004 for ArcSecond, and 12-16 July 2004 for ENSCO. The tests described in Section 3.6.6 were conducted.

3.6.3 Amount /Treatment Rate of Material to be Treated

No intrusive activities were undertaken nor any material handled.

3.6.4. Residuals Handling

This section is not applicable.

3.6.5 Operating Parameters for the Technology

This is variable among the demonstrated systems. The systems are designed for reasonable all-weather use. At low temperatures we had problems with reduced battery life. Below 15-20°F, the G-858 magnetometer in-sensor heater was insufficient to maintain temperature and ceased functioning.

3.6.6. Experimental Design

Testing was performed to validate performance as outlined in Table 3.1. All surface points for navigation performance evaluations were previously surveyed by traditional civil surveying techniques by APG using a Total Station electronic distance measurement (EDM). Each area had four known surface control points established along the perimeter of the area for establishing the local coordinates reference grid.

The following outlines basic tests:

Test 1: Calibration Lane—Area Mapping

- Area map the 29 m by 37 m site (0.25 acre) using the GFE G-858 sensor (with magnetometer base station) integrated with the navigation equipment at 1 m spacing in an approximately E-W direction.
- Post-process the data set (prior to the wooded area mapping) to create a dig list for the anomalies that are above a threshold established by the typical 57 mm M86 items in the Calibration Lanes. The dig list selected based on this threshold was compared to the ground truth for position accuracy. This threshold value was used for anomaly selection for the wooded area mapping dig list.

Test 2: Calibration Lane—Reacquisition

- Reacquire the coordinates of the 19 items that included three each of 57 mm, 60 mm, 81 mm, 2.75", 105 mm, and 155 mm seeded items at different orientations and depths as well as one 8# shotput. The items are lane 6 A, C, & D; 7 A, C, E, H, J, & L; 8 A, C, &E; 13 B, F, & J; 14 B, F, & J; and Shotput lane 10 G (shown in Appendix F). Use the integrated system to reacquire and flag the position real time. The reacquired coordinates were compared to the seeded location coordinates.

Test 3: Calibration Lane Area—Fixed Grid Anomaly Interrogations Evaluations

- These 19 locations were interrogated in both a fixed grid and dynamic mode. The fixed grid data set was gathered based on a fixed grid marked on a 1.0 m square board at 0.2 m intervals with a sensor height at 0.15 m (36 points). Twelve points were captured in an "x" pattern for the 0.30 and 0.45 m heights for a total of 60 points. Standoffs were established by plastic head spacers or movement of the head position up a position pole. The individual point data captured were compared to relative positioning among the points captured to the fixed grid. Based on the 3-D data captured, a revised dig list location was selected. The refined dig list coordinates were compared to the seeded location coordinates from Appendix F.

Test 4: Calibration Lane Area—Dynamic Anomaly Interrogations Evaluations

- The 19 anomalies had a dynamic 3-D data set acquired by walking an approximately 2 m square area with the sensor head at multiple heights or by swinging and lifting the handheld sensor over the anomaly area as required by the individual systems. The objective was to capture a similar data set as in Test 3 but in a rapid more random unguided field methodology that relies on the navigation system's dynamic position accuracy with a continuous sensor and navigation data stream. Based on the 3-D data captured, a revised dig list location was selected. The refined dig list coordinates were compared to the seeded location coordinates from Appendix F.

Test 5: Wooded Area—Accuracy with Positioning System for Surface Points

- The wooded area has six unknown permanent rebar points within the interior. These positions are placed in areas without nearby adjacent geophysical anomalies. An additional widely scattered 40 points are established by PVC pipe with removable steel pins (added when required to trigger the magnetometer). Each was occupied by the

integrated navigation/geophysical sensor system to determine coordinate locations. These were compared to the ground truth for position accuracy.

Test 6: Wooded Area—Accuracy from Geophysical Data Analysis for Surface Points

- The 46 points from Test 5 were traversed dynamically by the integrated system. The points were picked from the instrument peaks and reported. These were directly compared to the ground truth for position accuracy.

Test 7: Wooded Area—Area Mapping

- The approximately 1-acre area was mapped with the data analysis using the GFE G-858 sensor integrated with the navigation equipment at approximately 1 m spacing in an approximately E-W direction. The steel pins were removed from the 40 points described in Test 5 so as not to affect the subsurface anomaly results.
- The selection threshold for anomaly selection for the wooded area was based on the instrument reading for all items larger than the 57 mm M86 as shown by the Calibration Lanes area mapping from Test 1. The dig list selected was evaluated by APG, with emphasis based on position accuracy.

Test 8: Wooded Area—Dynamic Anomaly Interrogations

- Ten well-defined anomalies were selected from the Test 7 results for interrogation. The ten anomalies then had a dynamic 3-D data set acquired as in Test 4 by walking an approximately 2 m square area with the sensor head at multiple heights or by swinging and lifting the handheld sensor over the anomaly area, as required by the individual systems.

Test 9: Wooded Area—Dynamic Anomaly Positioning

- An anomaly array board 1.2 m square was created. It had an irregular array of nails inserted for point source anomalies. This board was randomly placed in an area clear of subsurface anomalies adjacent to each of the six rebar points. These areas were mapped in a similar manner to Test 8. The individual nail positions were selected as a dig list from the instrument peaks. The government compared the relative position of the dig list points to the array positions and reported the deviation from the location.

Test 10: Mogul Area—Accuracy with Positioning System for Surface Points

- The mogul area has 20 unknown points established in a varied array traversing a portion of the large and medium moguls with widely varying slope and elevation. The points are PVC pipe with removable steel pins (to trigger the magnetometer when required). Each was occupied by the integrated navigation/geophysical sensor system to determine coordinate locations. These were directly compared to the ground truth for position accuracy.

Test 11: Mogul Area—Accuracy from Geophysical Data Analysis for Surface Points

- The 20 points from Test 10 were traversed dynamically by the integrated system. These points were picked from the instrument peaks shown in the data set and reported. These were directly compared to the ground truth for position accuracy and to the locations from Test 10.

3.6.7 Demobilization

Demobilization requires repacking equipment in shipping cases and departing the site. There should be no lasting impact to the site from this demonstration.

3.7 Selection of Analytical/Testing Methods

This section is not applicable.

3.8 Selection of Analytical/Testing Laboratory (may not be applicable to UXO)

This section is not applicable.

4. Performance Assessment

4.1 Performance Criteria

The performance objectives in Table 3-1 define the criteria by which performance will be evaluated.

4.2 Performance Confirmation Methods

Performance was evaluated by comparison of the observed measurement parameters for each test in Section 3.6.6 with the reference measurements and the actual positions of surface and subsurface items.

4.3 Data Analysis, Interpretation, and Evaluation

This performance assessment has been independently compiled by CEHNC from field observations, the demonstrator's reports, and independent analysis of the data provided, with comparison to the known and unknown survey points and subsurface seeded item locations. Deviations from the true locations were identified and categorized separately for surface features in the Calibration, Mogul and Wooded areas, for the initial dig list locations of the subsurface anomalies in the areas from the area mapping, and for the reacquired and interrogated locations of the anomalies. The average and standard deviation were reported for each location category and each demonstrator.

- All demonstrators could provide basic setups in 10-20 minutes. The INS systems required additional time for calibration as did the ArcSecond system to maintain high accuracies over larger areas. No times were considered excessive for any demonstrators.
- None of the demonstrators showed multiple crew capability but all had a procedure to make it possible by using different codes or radio channels.
- The ability to capture actual elevation data was demonstrated by all except ENSCO, but data was not specifically evaluated. As part of Test 10 for the Moguls, elevations reported were compared to surveyed elevations for the three contractors reporting values. The 3-D position accuracy for the laser-based were very similar to the x-y position accuracy, but DGPS elevation errors were more than four times larger
- All systems demonstrated at their most accurate capabilities with a form of selectable accuracy imposed by less care in setup and calibration, a greater travel speed, or more time between position updates. Reduced accuracy is only applicable to enhance productivity with reduced performance requirements.
- Ability to display position data in near-real-time was demonstrated by all contractors.
- All systems were relatively easy to set up and operate by a two-person crew.
- All demonstrators could reacquire points.

Test 1: Calibration Lane—Area Mapping

- The site was area mapped using the GFE G-858 sensor integrated with each contractor's navigation equipment at 1 m spacing in an approximately E-W direction. The data was post-processed, and a dig sheet was created for the 19 items larger than the 57 mm M86 items. The 19 items were then compared to the ground truth for position accuracy. Results varied from 0.2-0.4 m from the actual locations. A position tolerance of 0.05m was desired for this scenario as outlined in the original RFP. For this demonstration, tolerance is defined as the leeway for variation from a standard with the standard being the civil surveyed position of the known and unknown points. Distance is indicated in Table 4-1 as the radial offset from the known locations. This is the hypotenuse of the triangle formed by the changes in Easting and Northing coordinates. Accuracy, or average error, is the demonstrated deviation from the location of the surveyed points. Laser-based systems were more accurate but the differences could also be explained by procedure used in selecting anomalies from the gridded data sets.

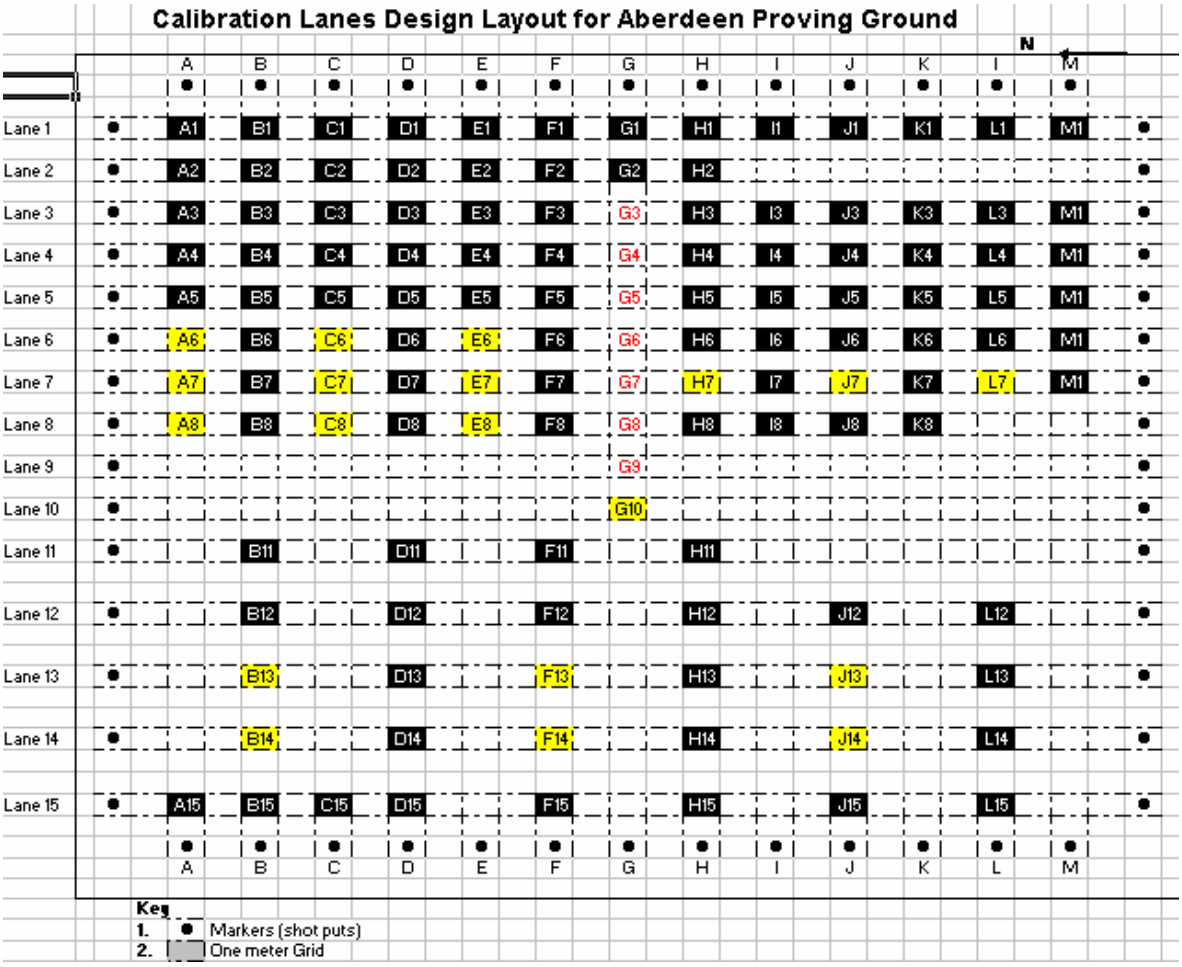

Figure 4-1. APG Calibration Lane Layout

Test 1- Calibration Lanes (Area Mapping)

19 Anomalies (Dig Sheet)

	Tolerance	Tolerance		
Contractor	Easting	Northing	Distance	
Shaw/IT	-0.0504	-0.0169	0.2186	Average Error
	0.1336	0.2492	0.1691	Standard Deviation
GIS	0.1687	0.0205	0.4083	Average Error
	0.3185	0.2953	0.2005	Standard Deviation
ArcSecond	-0.0284	0.0928	0.1812	Average Error
	0.1531	0.1500	0.1456	Standard Deviation
Ensco	0.0767	0.1759	0.3248	Average Error
	0.1717	0.4146	0.3564	Standard Deviation

Table 4-1. Test 1 Results (all values are shown in meters).

Figure 4-2. Test 1 Demonstrations (Top left, Shaw/IT; top right, GIS; bottom left, ArcSecond; bottom right, ENSCO)

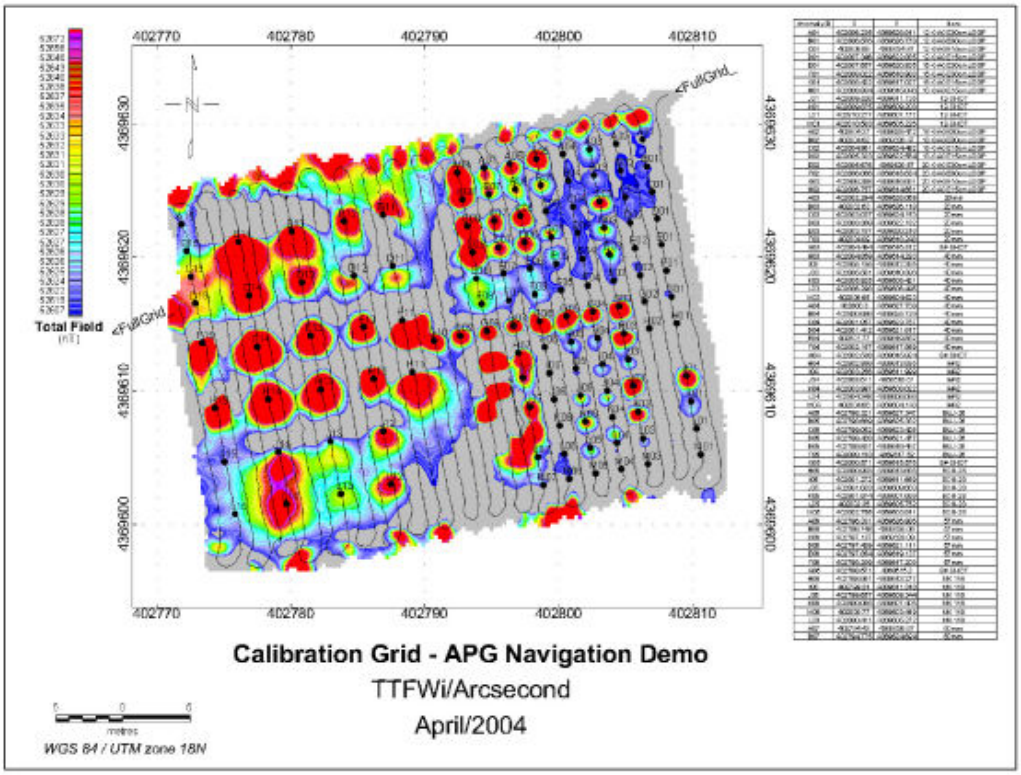

Figure 4-3. APG Calibration Lane Geophysical Representations

Test 2: Calibration Lane—Reacquisition

- The contractors then reacquired the 19 items by going to the coordinate location as designated in Test 1 and searching for the target item in real time. They recorded the apparent anomaly location directly from the instrument readings. These locations were then compared to the ground truth for position accuracy. Position accuracy improved for ENSCO but was worse for Shaw with neither GIS nor ArcSecond permanently recording positions for comparison. The difference could be based on operator skill at reacquisition rather than positioning system accuracy.

Test 2- Calibration Lanes (Reacquired)					
	19 Anomalies (Dig Sheet)				
	Tolerance	Tolerance			
Contractor	Easting	Northing	Distance		
Shaw/IT	-0.0059	0.0326	0.2547	Average Error	
	0.1941	0.2684	0.2048	Standard Deviation	
GIS	not acquired- 3D visualization				
ArcSecond	not recorded				
Ensco	-0.0016	0.0274	0.1952	Average Error	
	0.1319	0.1855	0.1112	Standard Deviation	

Table 4-2. Test 2 Results (all values are shown in meters).

Test 3: Calibration Lane Area—Fixed Grid Anomaly Interrogations Evaluations

- Nineteen cells were targeted for interrogation in both a fixed grid and then in Test 4 in a dynamic mode. The fixed grid data set was based on position reference to a fixed grid on a marked board centered for a 1.0 m square area at 0.2 m intervals with a sensor height at 0.15 m (36 points); 12 points were captured in an "x" pattern for the 0.30 and 0.45 m heights for a total of 60 points. The following four tables show cell by cell the tabulation of the comparison of the contractor designated locations and the matrix of template locations. Both Shaw and GIS had some flier points caused by obstruction to line-of-sight and/or noise and operator error. If they exceeded 0.2808 meters they could not be assigned to individual template points and were dropped. The number of these points per cell is shown under the dropped column for these two contractors. Results improved slightly when only the cells without a large number of fliers were included.

Figure 4-4. Test 3 Demonstrations (Top left, Shaw/IT; top right, GIS; bottom left, ArcSecond; bottom right, ENSCO)

- Shaw had an average error of 0.07 m with GIS at 0.1 m, ArcSecond at 0.01 m, and ENSCO with the INS local positioning augmentation at 0.03 m. Clearly, only the ArcSecond and INS met our performance objectives.

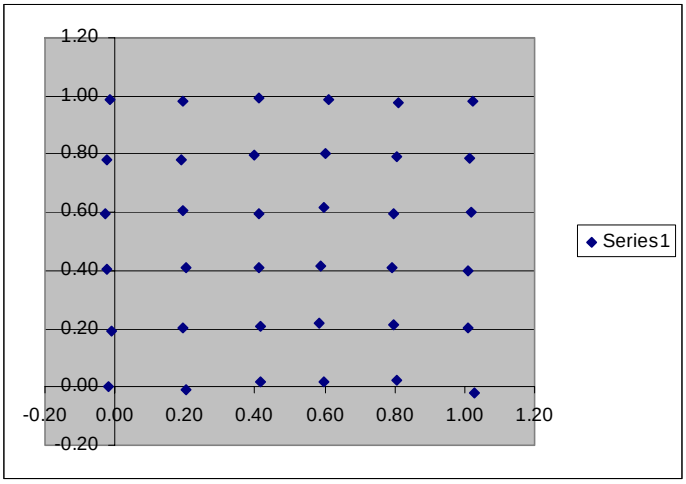

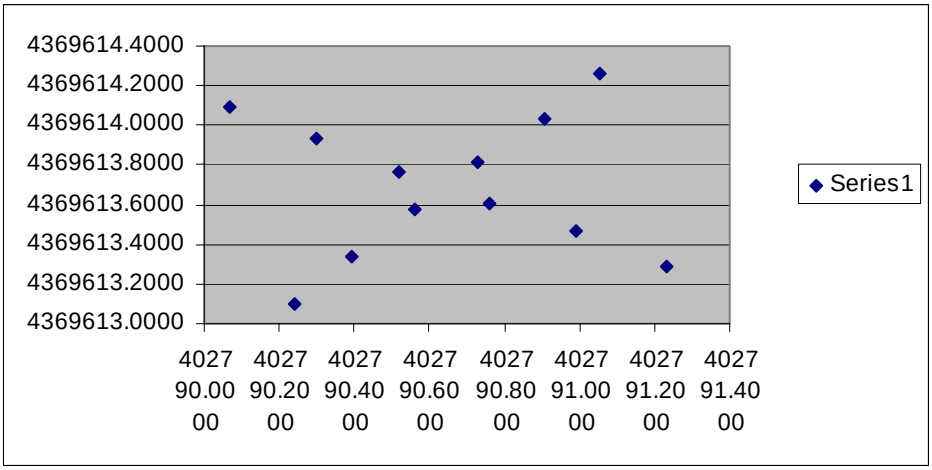

Figure 4-5. Test 3 Demonstration Grid

Shaw-RTS						
Adjusted Data: Eliminated all deviations greater than 0.2828						**Dropped**
Cell	**Average**	**St. Dev**	**Var**	**Max**	**Min**	**#**
cell 6a	0.018	0.014	0.000	0.057	0.002	0
cell 14j	0.022	0.019	0.000	0.059	0.000	0
cell 7h	0.025	0.021	0.000	0.110	0.000	0
cell 10g	0.041	0.043	0.002	0.245	0.003	0
cell 7j	0.040	0.052	0.003	0.244	0.000	0
cell 13f	0.070	0.054	0.003	0.241	0.021	0
cell 13j	0.036	0.054	0.003	0.262	0.004	1
cell 14f	0.062	0.068	0.005	0.262	0.001	1
cell 8c	0.098	0.079	0.006	0.272	0.005	1
cell 8e	0.098	0.079	0.006	0.272	0.005	1
cell 7e	0.040	0.041	0.002	0.182	0.002	2
cell 7l	0.086	0.072	0.005	0.269	0.001	2
cell 6e	0.126	0.089	0.008	0.278	0.004	2
cell 7c	0.094	0.075	0.006	0.257	0.002	3
cell 6c	0.096	0.066	0.004	0.261	0.000	3
cell 7a	0.107	0.097	0.010	0.276	0.001	4
cell 13b	0.112	0.077	0.006	0.281	0.005	8
cell 14b	0.057	0.051	0.003	0.221	0.003	9
cell 8a	0.132	0.091	0.008	0.272	0.008	11
Average	0.072	0.060	0.004	0.227	0.004	
Good only	0.063	0.055	0.004	0.218	0.003	

Table 4-3. Test 3 Fixed Grid Anomaly Interrogation Results by Test Cell—Shaw (all values are shown in meters)

GIS						
Adjusted Data: Eliminated all deviations greater than 0.2828						**Dropped**
Cell	**Average**	**St. Dev**	**Var**	**Max**	**Min**	**#**
cell 6c	0.086	0.061	0.004	0.226	0.007	0
cell 6e	0.087	0.067	0.004	0.266	0.016	1
cell 6a	0.063	0.075	0.006	0.276	0.001	2
cell 7j	0.099	0.072	0.005	0.223	0.001	3
cell 7c	0.132	0.086	0.007	0.279	0.002	3
cell 10g	0.059	0.067	0.005	0.277	0.005	4
cell 8e	0.055	0.063	0.004	0.267	0.003	4
cell 13b	0.106	0.086	0.007	0.280	0.001	5
cell 8a	0.067	0.067	0.005	0.270	0.001	6
cell 7e	0.153	0.072	0.005	0.274	0.021	7
cell 8c	0.056	0.064	0.004	0.245	0.001	7
cell 7l	0.138	0.137	0.019	0.692	0.004	8
cell 7a	0.155	0.083	0.007	0.261	0.000	14
cell 7h	0.088	0.065	0.004	0.197	0.003	16
Average	0.096	0.076	0.006	0.288	0.005	
Good only	0.088	0.071	0.005	0.262	0.005	

Table 4-4. Test 3 Fixed Grid Anomaly Interrogation Results by Test Cell—GIS (all values are shown in meters)

ArcSecond					
Cell	**Average**	**St. Dev**	**Var**	**Max**	**Min**
cell 7a	0.0051	0.0035	0.0000	0.0166	0.0008
cell 8e	0.0072	0.0043	0.0000	0.0208	0.0010
cell 7c	0.0074	0.0065	0.0000	0.0242	0.0003
cell 10g	0.0095	0.0057	0.0000	0.0205	0.0002
cell 8a	0.0108	0.0065	0.0000	0.0267	0.0009
cell 8c	0.0122	0.0048	0.0000	0.0224	0.0016
cell 7e	0.0124	0.0080	0.0001	0.0279	0.0006
cell 6a	0.0176	0.0118	0.0001	0.0456	0.0004
cell 6c	0.0231	0.0130	0.0002	0.0541	0.0031
Average	0.0117	0.0071	0.0001	0.0288	0.0010

Table 4-5. Test 3 Fixed Grid Anomaly Interrogation Results by Test Cell—ArcSecond (all values are shown in meters)

ENSCO- INS				
Cell	**Average**	**St. Dev**	**Max**	**Min**
cell 6e	0.0169	0.0082	0.0360	0.0027
cell 6c	0.0179	0.0130	0.0588	0.0038
cell 7j	0.0182	0.0126	0.0493	0.0021
cell 8c	0.0213	0.0107	0.0427	0.0044
cell 7c	0.0217	0.0120	0.0592	0.0031
cell 7a	0.0236	0.0139	0.0600	0.0025
cell 6a	0.0244	0.0148	0.0590	0.0048
cell 10g	0.0253	0.0139	0.0585	0.0043
cell 13f	0.0272	0.0120	0.0505	0.0034
cell 7e	0.0298	0.0171	0.0681	0.0061
cell 14b	0.0300	0.0171	0.0750	0.0060
cell 13b	0.0302	0.0242	0.1190	0.0053
cell 7h	0.0316	0.0120	0.0610	0.0081
cell 14f	0.0321	0.0140	0.0683	0.0086
cell 13j	0.0324	0.0181	0.0757	0.0046
cell 8e	0.0347	0.0200	0.0879	0.0077
cell 8a	0.0373	0.0164	0.0689	0.0088
cell 14j	0.0395	0.0207	0.0936	0.0079
cell 7l	0.0517	0.0318	0.1369	0.0161
AVERAGE	0.0287	0.0159	0.0699	0.0058

Table 4-6. Test 3 Fixed Grid Anomaly Interrogation Results by Test Cell—Ensco (all values are shown in meters)

As part of Test 3, the contractors also provided a dig list for the anomaly locations based on their captured geophysical instrument readings in association with the positions in the previous tables. These were submitted based on the 0.15 m, 0.3 m and 0.45 m sensor height data. The contractors' designated locations were approximately the same for all heights with average errors from 0.09-0.19 m. ENSCO was the only exception with the 0.45 m height data deviating to 0.28 m. These results appeared to show that there is little improvement in pick list location between date sets captured with a G-858 with deviation of 0.01 or 0.1 m position accuracy. This is likely a result of the spatial extent and dipole nature of the signal.

Test 3- Calibration Lanes (From Fixed Grid Interrogations)

19 Anomalies (Dig Sheet)

	Tolerance	Tolerance		
Contractor	Easting	Northing	Distance	
Shaw/IT (.15 m)	0.0292	-0.0261	0.1753	Average Error
.15 m	0.1308	0.1523	0.0973	Standard Deviation
.3 m	0.0274	-0.0813	0.1553	Average Error
.3 m	0.1467	0.1031	0.1204	Standard Deviation
.45 m	0.0385	-0.0904	0.1698	Average Error
.45 m	0.1290	0.1311	0.1164	Standard Deviation
GIS (.15 m)	0.0438	0.0039	0.1554	Average Error
.15 m	0.1422	0.0911	0.0677	Standard Deviation
.3 m	0.1082	-0.0122	0.1860	Average Error
.3 m	0.1372	0.1152	0.0864	Standard Deviation
.45 m	0.0893	-0.0426	0.1424	Average Error
.45 m	0.0820	0.1067	0.0826	Standard Deviation
ArcSecond (.15 m)	-0.0194	-0.0269	0.0927	Average Error
.15 m	0.0562	0.0794	0.0336	Standard Deviation
.3 m	-0.0048	-0.0656	0.0793	Average Error
.3 m	0.0494	0.0167	0.0233	Standard Deviation
.45 m	-0.0049	-0.0453	0.0778	Average Error
.45 m	0.0475	0.0532	0.0258	Standard Deviation
Ensco (.15 m)	0.0797	0.1125	0.1718	Average Error
.15 m	0.0879	0.1274	0.1121	Standard Deviation
.3 m	0.0678	0.0677	0.1585	Average Error
.3 m	0.1729	0.0800	0.1380	Standard Deviation
.45 m	0.1187	0.0840	0.2833	Average Error
.45 m	0.2523	0.1658	0.1646	Standard Deviation

Table 4-7. Test 3 Dig Sheet Results (all values are shown in meters)

Test 4: Calibration Lane Area—Dynamic Anomaly Interrogations Evaluations

The 19 anomalies then had a dynamic 3-D data set acquired by walking the cell with the sensor head at multiple heights to capture a data cloud. As in the previous test, the contractors designated anomaly locations that were compared to the ground truth. Selected location errors were approximately the same as for the fixed grid at 0.05-0.22 m for the contractors' chosen sensor height. Shaw and ENSCO reported locations for multiple sensor heights since they captured data dynamically but by using fixed standoffs dragging the sensor across the board. Results were degraded as expected when using just the data captured with the greater separation.

Test 4- Calibration Lanes (Dynamic Interrogations)

19 Anomalies (Dig Sheet)

	Tolerance	Tolerance		
Contractor	Easting	Northing	Distance	
Shaw/IT (.15 m)	-0.0116	0.1183	0.2246	Average Error
.15 m	0.1259	0.2020	0.1345	Standard Deviation
.3 m	0.0682	0.2422	0.2806	Average Error
.3 m	0.1480	0.2200	0.2324	Standard Deviation
.45 m	0.0208	0.0990	0.3398	Average Error
.45 m	0.2541	0.3830	0.3165	Standard Deviation
GIS	-0.0285	0.0651	0.1522	Average Error
	0.1160	0.1189	0.0898	Standard Deviation
ArcSecond (30 cm)	-0.0088	-0.0069	0.0499	Average Error
	0.0416	0.0364	0.0190	Standard Deviation
Ensco (.15 m)	0.0200	0.1707	0.2222	Average Error
.15 m	0.1186	0.1306	0.1064	Standard Deviation
.45 m	0.0173	0.2472	0.2889	Average Error
.45 m	0.1460	0.1271	0.1242	Standard Deviation

Table 4-8. Test 4 Dig Sheet Results (all values are shown in meters)

Test 5: Wooded Area—Accuracy with Positioning System for Surface Points

- The wooded area has 6 unknown permanent rebar points with an additional widely scattered 40 points established by PVC pipe with removable steel pins within the wooded interior. These positions are placed in areas without nearby adjacent geophysical anomalies. These locations were occupied by the integrated navigation/geophysical sensor system to determine coordinate locations only. Test 6 picks from geophysical sensor response. Locations were compared to the ground truth for position accuracy. Results varied from 0.05 m to 0.93 m average error for the six rebars and 0.06 m to 0.53 m for the 40 PVC points. This large variance is explained by the obstruction to GPS signal caused by the tree canopy for the GIS system, multipath caused by the tree trunks and branches for ENSCO, and line-of-sight and leveling for Shaw. Shaw used several setups to mitigate line-of-sight obstructions. The ArcSecond test was performed in one

setup and was surprisingly accurate. This was attributed to maintaining position lock by always having two of the four transmitters visible and by the nature of the system design that projects to a point in space and in the process compensates for tilt.

Figure 4-6. Test 5 Demonstrators (Top left, Shaw/IT; top right, GIS; bottom left, ArcSecond; bottom right, ENSCO)

Test 5- Wooded Surface Points (Navigation)

	6-Rebars				40-PVC Points			
	Tolerance	Tolerance			Tolerance	Tolerance		
Contractor	Easting	Northing	Distance		Easting	Northing	Distance	
Shaw/IT	0.0727	-0.0689	0.1125		0.0809	-0.0811	0.1339	Average Error
	0.0460	0.0462	0.0403		0.0608	0.0645	0.0538	Standard Deviation
GIS	-0.3843	-0.0321	0.9254		-0.1241	0.0826	0.5310	Average Error
	0.9183	0.5268	0.6428		0.3514	0.6130	0.4788	Standard Deviation
ArcSecond	0.0332	0.0282	0.0503		0.0175	0.0500	0.0649	Average Error
	0.0225	0.0225	0.0196		0.0271	0.0404	0.0303	Standard Deviation
Ensco	-0.3022	0.0300	0.4044		0.1117	-0.0631	0.5659	Average Error
	0.4155	0.1300	0.1570		0.3707	0.5213	0.3068	Standard Deviation

Table 4-9. Test 5 Picked Point Results (all values are shown in meters)

Test 6: Wooded Area—Accuracy from Geophysical Data Analysis for Surface Points

- The 46 points from Test 5 were traversed dynamically by the integrated system. The points were picked from the instrument peaks shown in the data set and reported to compare to the ground truth for position accuracy. For additional validation on the RTS, we had Gtek report out positions from a subsequent survey as a commercial application using the SAM sensor with both their standard string odometer and the RTS for positioning. Their report is included in Appendix J. For the rebars, accuracy was slightly worse and varied from 0.15 m to 1.01 m, with ArcSecond's positions lost and not recorded. Gtek improved on Shaw's RTS accuracy, but the string odometer was nearly as accurate. For the PVC points, accuracy was slightly worse at 0.14 m to 0.9 m. Although differences could be attributed to the anomaly selections process, results do clearly show the laser-based systems as being consistently more accurate.

Test 6- Wooded Points (Geophysics)

	6-Rebars			40-PVC Points				
	Tolerance	Tolerance		Tolerance	Tolerance			
Contractor	Easting	Northing	Distance	Easting	Northing	Distance		
Shaw/IT	0.1928	-0.1743	0.2651	0.1314	-0.1052	0.2493	Average Error	
	0.1302	0.0866	0.1473	0.1588	0.1371	0.0953	Standard Deviation	
GIS	0.8672	-0.5186	1.0105	-0.2748	0.0769	0.9007	Average Error	
				0.5865	0.9501	0.6753	Standard Deviation	
ArcSecond				-0.0112	0.1137	0.1397	Average Error	
				0.0569	0.0922	0.0660	Standard Deviation	
Ensco	0.2968	-0.3200	0.4369	0.1991	-0.2591	0.4666	Average Error	
	0.1360	0.1801	0.2154	0.2947	0.3841	0.3429	Standard Deviation	
Gtek (RTS)	0.0046	0.0283	0.1543	0.0410	-0.1158	0.2598	Average Error	
	0.1744	0.0493	0.0994	0.0626	0.3124	0.1898	Standard Deviation	
Gtek (String)	-0.0066	0.3300	0.3308	Average Error				
	0.0196	0.1766	0.1764	Standard Deviation				

Table 4-10. Test 6 Picked Point Results (all values are shown in meters)

Test 7: Wooded Area—Area Mapping

- The entire wooded area was area-mapped. Anomaly selection was based on the threshold instrument readings established by the Calibration Lane mapping for the target items larger than the 57 mm M86 from Test 1. There was no effort made to distinguish between clutter and UXO targets. This test failed for all data sets when only UXO targets were considered. Analysis by APG could match only three targets from the data sets for the search with a 1-m radius. APG validated that the survey control was correctly established. Analysis of the data sets did not show any systematic coordinates translation errors, and there were common anomaly correlations between the data sets.

- APG performed an analysis that included the clutter items in the woods rather than just the UXO targets. They recorded 14 hits from Shaw at an average 0.33 m offset, 10 for ArcSecond at a 0.25 m offset and 46 from ENSCO at a 0.32 m offset. Since the clutter anomaly results are valid representations, then it shows a dilution of accuracy to the Shaw and ArcSecond systems as expected when picking an irregular anomaly over a

point source as performed in Test 6 and an unexplained increase in accuracy for the ENSCO system. The data from GIS was considered unusable based on loss of DGPS positioning for the majority of the survey. The reason for the poor performance of the UXO targets is that the seeded clutter items had similar and higher amplitude responses than the threshold we established based on the items above the 57 mm size from the Calibration Lanes in Test 1.

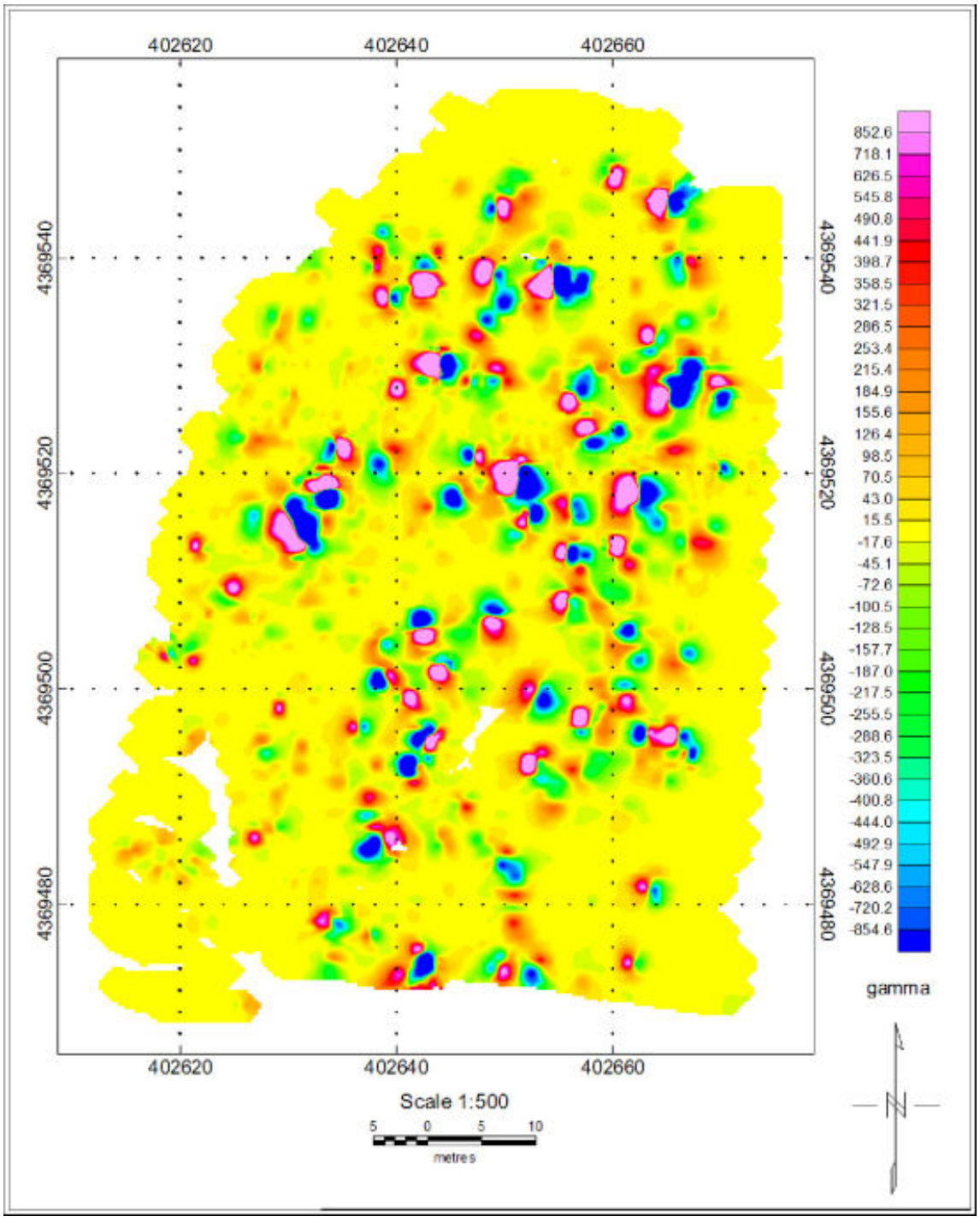

Figure 4-7. Test 7 Wooded Area Typical Geophysical Representation

Test 8: Wooded Area—Dynamic Anomaly Interrogations

- This test was intended to take the best ten well-defined anomalies selected from the Test 7 mapping results for interrogation. The locations would then be compared to the ground truth locations by APG. We would then see what improvements in anomaly location would come from interrogations with the systems using various position accuracy. This test failed since we could not associate the anomaly locations identified in Test 7 with seeded UXO. Shaw provided 10 data sets and ENSCO eight. Neither GIS nor ArcSecond completed this portion due to weather delays and equipment failures.

Test 9: Wooded Area—Dynamic Anomaly Positioning

- An anomaly array board 1.2 m square was created with an irregular array of nails inserted for point source anomalies. This board was randomly placed in an area clear of subsurface anomalies adjacent to each of the six rebar points. This was mapped in a similar manner to Test 4 and Test 8, with the individual nail location positions selected as a dig list from the instrument peaks. Shaw completed all six rebar locations with 4-15 of the 20 nail locations picked. Points could not be associated to actual locations due to lost points, unknown orientation and inaccurate positioning. GIS completed two locations with 19 and 16 nails picked, and points could not be uniquely associated with actual locations. ArcSecond did not complete due to several weather delays. ENSCO completed three locations with all 20 nails represented and reasonable positioning. This data set was the only one accurate enough to evaluate. Position accuracy averaging 0.05 m error was achieved as is shown in Table 4-11.

Figure 4-8. Test 9 Nail Array Test Board

Figure 4-9. Test 9 Demonstrators (Left, Shaw/IT; right, GIS)

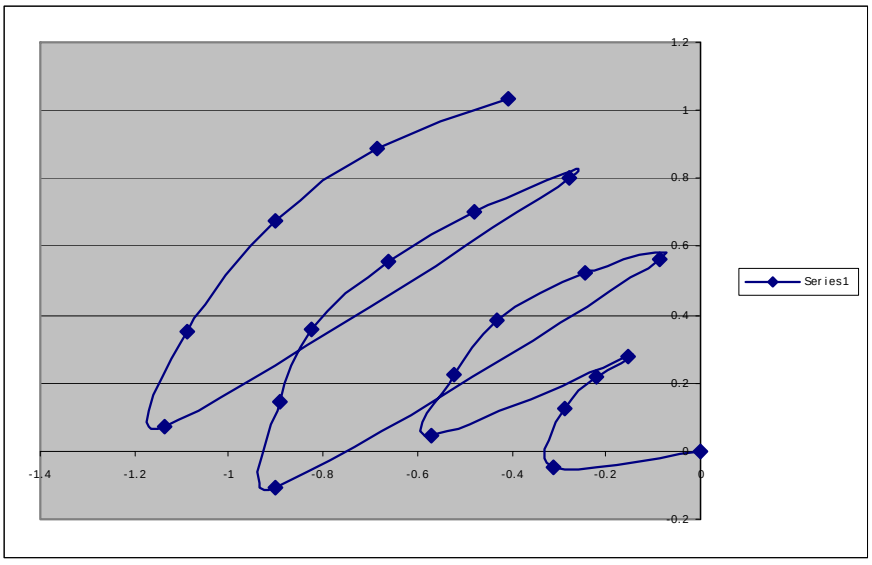

Figure 4-10. Test 9 Results Representation—ENSCO

ENSCO results

Test 9-Nail array interrogations (Woods)					
Rebar	Average	St. Dev	Var	Max	Min
1	0.046	0.031	0.001	0.099	0.012
2	0.065	0.030	0.001	0.128	0.015
3	0.043	0.030	0.001	0.097	0.001
Average	0.051	0.030	0.001	0.108	0.009

Table 4-11. Test 9 Picked Point Results (all values are shown in meters)

Test 10: Mogul Area—Accuracy with Positioning System for Surface Points

- The mogul area has 20 unknown points established in a varied array, traversing a portion of the large and medium moguls, with widely varying slope and elevation. The points are PVC pipe with removable steel pins (to trigger the magnetometer when required). Each was occupied by the integrated navigation/geophysical sensor system to determine

coordinate locations. The results showed average error of 0.01 m to 0.25 m, with the laser-based systems being the most accurate, followed by DGPS and the Tracker Radio system. ArcSecond's better accuracy is accounted for by its automatic adjustment of the effect of tilt and inclination. The moguls' reported elevations were compared to the surveyed elevations for the three contractors reporting values. The 3-D position accuracy for the laser-based systems was very similar to the x-y position accuracy, but DGPS elevation errors were more than four times larger. This is as expected since DGPS always has reduced accuracy in elevation.

Figure 4-11. Test 10 Demonstrators (Top left, Shaw/IT; top right, ArcSecond; bottom, ENSCO)

Test 10- Mogul Points (Navigation)						
	20-PVC Points					
	Tolerance	Tolerance				
Contractor	Easting	Northing	Distance		Elevation	
Shaw/IT	-0.0562	-0.0392	0.0900		-0.1486	Average Error
	0.0449	0.0551	0.0383		0.0261	Standard Deviation
GIS	-0.0538	-0.0782	0.2545		1.0938	Average Error
	0.1914	0.1883	0.1157		0.0896	Standard Deviation
ArcSecond	-0.0001	0.0115	0.0150		0.0100	Average Error
	0.0065	0.0097	0.0061		0.0105	Standard Deviation
Ensco	0.0900	-0.0098	0.2111		N/A	
	0.1400	0.1691	0.0991			

Table 4-12. Test 10 Picked Point Results (all values are shown in meters)

Test 11: Mogul Area—Accuracy from Geophysical Data Analysis for surface points

- The 20 points from Test 10 were traversed dynamically by the integrated system. These points were picked from the instrument peaks shown in the data set and reported. Comparison to the ground truth shows average errors from 0.06 m to 0.34 m. As expected, the accuracy when picking the items from the geophysical data is slightly worse. The laser-based systems are still clearly more accurate.

Test 11- Mogul Points (Geophysics)					
	20-PVC Points				
	Tolerance	Tolerance			
Contractor	Easting	Northing	Distance		
Shaw/IT	0.0010	0.0455	0.1786	Average Error	
	0.1464	0.1475	0.1041	Standard Deviation	
GIS	0.0062	-0.0536	0.2318	Average Error	
	0.1591	0.1919	0.0931	Standard Deviation	
ArcSecond	-0.0023	0.0263	0.0649	Average Error	
	0.0583	0.0441	0.0405	Standard Deviation	
Ensco	-0.1195	0.0562	0.3354	Average Error	
	0.2558	0.2178	0.1089	Standard Deviation	

Table 4-13. Test 11 Picked Point Results (all values are shown in meters)

4.4 Technology Comparison

The technologies were compared to the DGPS and USRADS baseline as shown in Section 2.4, Table 2-1, and the performance objectives shown in Table 3-1.

Shaw RTS: The Shaw Leica TSP 1100 dual laser RTS provided very high accuracy and long range that met the performance objectives. The accuracy from 0.07 m for absolute location in the open to 0.27 m for anomaly selection is better than either the baseline DGPS or USRADS solutions for all applications. Setup time is similar for open areas when considering the time for setup of a DGPS base station and similar to the USRADS in the woods where multiple RTS setups are required. Cost is approximately the same as DGPS and about 50% of USRADS cost. The contractors' report of the demonstration is included as Appendix G: Shaw Environmental Phase III Report.

GIS GeoVisor: The GIS system varied from 0.10 m for absolute location in the open to complete loss of positioning in the woods. Since the system uses DGPS for the principal positioning system, it matched the baseline DGPS in performance but fell short of the USRADS for wooded applications due to loss of GPS lock. This portion failed the obstructed range and accuracy criteria from the performance objectives. The ultrasonic local area positioning system augmentation for interrogation outperformed both baseline systems at 0.10 m. Setup time is similar to DGPS, but cost is approximately 50% more for the system augmentations. The contractor's report of the demonstration is included as Appendix H: GIS Phase III Report.

ArcSecond Constellation: The ArcSecond Constellation system showed accuracy of 0.01 m absolute for interrogations, 0.04 m for area navigation, and 0.11m for anomalies picked from geophysics. This exceeded both baseline system capabilities for all mission areas and met the performance objectives. Setup time was about twice that of DGPS but similar to that of USRADS. Cost was similar to USRADS and about twice the cost of DGPS. Range is approximately the same as a complete USRADS system for the wooded areas, but it provides several times the accuracy. The system is superior to all methodologies for wooded areas and for interrogations. Where it falls short is for open areas where its range is limited to a maximum of 100 m diagonal between transmitters. In this case, if the high accuracy or high data refresh is not needed, DGPS is a more flexible solution for one-half of the cost and setup time. The contractor's report of the demonstration is included as Appendix I: ArcSecond Phase III Report.

ENSCO Ranger: The ENSCO local area radio frequency positioning system provided an accuracy of 0.17 m for absolute location in the open to 0.57 m for anomalies selected from geophysics and it met performance objectives. Performance was poorer than can be achieved with DGPS in unobstructed areas, and it outperformed DGPS by maintaining track in obstructed areas. In comparison to the USRADS, it exceeded the range and accuracy in the open but was less accurate in obstructed areas. This was caused by multipath interference. Accuracy can be improved with additional radio transmitters, software, and system calibration improvements. The Ranger prototype system cost was approximately twice that of DGPS or equal to that of USRADS, but in limited production it could match that of DGPS. The prototype INS enhancement for high accuracy anomaly interrogation for a relative position showed accuracy of 0.03-0.05 m. This capability met objectives and exceeds accuracy produced by the commercial

systems. The contractors' report of the demonstration has been submitted to ESTCP under Project 200029 as the Final Report[6] and Cost and Performance Report.[7]

4.5 Conclusions

Table 4-14 compares the four positioning system demonstration results for the 11 individual tests, an average for locations from items picked from the magnetometer readings, and an average for the principal navigation methodology and for the secondary position augmentation system when used for anomaly interrogations by local area navigation positioning.

The two laser-based systems, Shaw RTS and the ArcSecond Constellation, used the same technology for both area mapping and interrogations, with GIS using ultrasonics and ENSCO using INS for local area positioning.

ArcSecond has the best overall performance for all testing. Shaw came in second for all categories, except for Test 3 for local area navigation positioning. For local area, ArcSecond was first at 0.01 m, with ENSCO at 0.04 m, Shaw at 0.07 m, and GIS at 0.10 m.

In comparing GIS and ENSCO, results were similar for open areas with their implementation of DGPS and radio systems varying from 0.15-0.41 m offset. In the woods, the DGPS clearly degraded more than the radio positioning with the offsets from 0.4-0.55 m for the radio to 0.53-0.93 m for DGPS. The DGPS also had so many position dropouts that the geophysical data could not be used for the wooded area. For interrogations, the INS positioning augmentation by ENSCO at 0.03 m was clearly better that the GIS ultrasonic augmentation by GIS at 0.10 m.

Based on the results, follow-on efforts detailed under Section 4.6 Phase IV were implemented to further explore and develop system capabilities for the RTS and Constellation Laser technologies, Ranger Radio, INS augmentation, and for analysis of the interrogation data captured under the APG tests.

[6] UXO Precise Position Tracking APG Demonstration ESTCP Project 200129 Final Report 15 November 2004, David Taylor, ENSCO, Inc.
[7] UXO Precise Position Tracking Ranger- Cost and Performance ESTCP Project 200029 23 November 2005, David Taylor, ENSCO, Inc.

APG Demonstration Summary

Test	Description	Shaw	GIS	ArcSecond	ENSCO
1	From Geophysics	0.22	0.41	0.18	0.32
2	From Geophysics	0.25	N/A	N/A	0.19
3a	From Geophysics	0.17	0.15	0.09	0.17
3b	Array Board (Nav)	0.07	0.10	0.01	0.03
4	From Geophysics	0.22	0.15	0.05	0.22
5a	Rebar (Nav)	0.11	0.92	0.05	0.40
5b	PVC (Nav)	0.13	0.53	0.06	0.57
6a	Rebar (Geophysics)	0.27	1.01	N/A	0.44
6b	PVC (Geophysics)	0.25	0.90	0.14	0.47
7	APG Evaluation	TBD	TBD	TBD	TBD
8	APG Evaluation	TBD	N/A	N/A	TBD
9	Nail array (Geophysics)	N/A	N/A	N/A	0.05
10	PVC (Nav)	0.09	0.25	0.02	0.21
11	PVC (Geophysics)	0.18	0.23	0.06	0.34
	Average (Geophysics)	0.22	0.48	0.10	0.31
	Average Principal Nav	0.10	0.57	0.04	0.39
	Average Local Area Nav	0.07	0.10	0.01	0.04

Table 4-14. Test 1-11 Summary Results (all values are shown in meters)

4.6 Phase IV Developments

Phase IV continues navigation and positioning system demonstration and development with commercial application demonstrations; interrogation data analysis, as acquired in the APG Phase III demonstrations and in interrogation system positioning development of the ArcSecond laser-based system; and the INS augmentation for interrogations with ENSCO. Funding for these efforts has been split equally by FUDS OE-IT, ERDC EQT, AEC EQT and by ESTCP Project 200129.

4.6.1 Commercial Application Demonstrations: Commercial system applications were performed by Gtek Geophysics for the RTS system, as included in Appendix J: Gtek Application of Robotic Total Station Navigation to Sub-Audio Magnetic Survey and for the Ranger by ARM Geophysics, as reported in Appendix K: ARM Group Inc. Commercial Test of Ranger Positioning System.

The Gtek RTS results were included in the Phase III Test 6 results for the wooded area points, as shown in Table 4-10. They improved slightly on the results from Shaw. The locations had approximately one-half the average error as their standard string odometer methodology at 0.15 m as compared to 0.33 m. Gtek reported good positioning results for the RTS for the open areas that matched or exceeded DGPS. They felt that the methodology came up short in obstructed areas. Loss of line-of-sight caused too much interpolation of positioning and reduced accuracy, causing poorly formed and smeared geophysical anomaly representation. These problems can be minimized by using more numerous RTS setups to maintain line-of-sight or by ganging multiple RTS units and

combining the best positioning. That concept is being developed by SKY Research under SERDP Project UX-1441, UXO Navigation Technology.

The ARM Ranger results from a BRAC project test showed that the system was not yet ready for commercial use. The system needs more work on durability, in radio self-location software development, and in documentation before it can be routinely used on geophysical projects. These issues have been reported in the ESTCP 200029 C&P Report[7] and in the white paper proposed effort for commercialization development.

4.6.2 Positioning System Development and Demonstration: Based on Phase III results, the ArcSecond system was developed as a flexible, integrated system that provides a full multi-axis position tracking hardware and software solution for interrogation quality data acquisition. Development was also continued on the ENSCO INS approach for small area interrogations, as demonstrated in Phase III.

The ArcSecond Constellation system demonstrated in Phase III was an enhanced version of their commercial system, enhanced by the creation of extended range strobes and additional software to enable integration of geophysical instruments and to survey large outdoor areas. That system used four laser transmitters located on an area's perimeter and a rover that included two optical sensor arrays. This system was shown to accurately capture x,y,z positions at 10 Hz when the receiver sensors were both visible to a minimum of two transmitters. This configuration could not provide geophysical sensors the desired attitude information.

For Phase IV, the system was enhanced to support four optical sensor arrays on the rover configured to a three fork "Triad" configuration. This is discussed in Section 2.1.3 and shown in Figure 2-6. Attitude information is provided when three of the four sensors are visible from two or more transmitters. The fourth optical sensor array provides redundancy. Position outputs are by an extended NEMA data format standard. The system transmits a one-second timing pulse and provides a position from the primary optical sensor. Data from all four sensors is stored at 40 Hz in the system's rover-dedicated brick computer for post-processing for attitude and synchronization with the geophysical data. Status and user input is provided by a handheld PDA. The stored data is post-processed to combine the data streams. The system was integrated with the EQT-funded Handheld Dual Magnetic/EMI Sensor by AETC Inc, the SQUID by Battele, and the EM-61 MK II and G-858 by CEHNC. The system integrated with the Handheld Dual Magnetic/EMI Sensor is planned for a production-oriented full survey at APG for Spring 2006.

Independent position system accuracy validations were performed by Bruce Barrows of AETC, Incorporated,[5] and are included in Appendix M: AETC, Incorporated, Evaluations of Laser Based Positioning for Characterization of EMI Signals from UXO. Controlled independent testing validated position accuracy of 0.003-0.004 m when used for local area interrogation.

The ENSCO Small Area Inertial Navigation Tracking (SAINT) system expands on the approach demonstrated in Phase III using an INS for small local area anomaly interrogations. CEHNC funded efforts to integrate the newer, smaller, and more accurate

Honeywell IMU with a digital magnetic compass sensor into a hardware and software solution with standard geophysical sensors. The improved system improved accuracy to an average of 0.01 error for 30 seconds of data capture as shown in Appendix N: ENSCO, Inc. Inertial Navigation System Improvements for Target Characterization Using Small Area Inertial Navigation Tracking (SAINT) - Initial Study . Efforts are continuing under ESTCP new start project MM-200604 Inertial Navigation System Improvements for Target Characterization using Small Area Inertial Navigation Tracking (SAINT).

5. Cost Assessment

5.1 Cost Reporting

Costs are included in the individual demonstrator's reports.

5.2 Cost Analysis

Cost Comparison

The demonstrated technologies are benchmarked to the baseline RTK DGPS for open areas and USRADS for wooded areas. They have been roughly compared to the baseline systems as shown in Section 4.4. Accurate comparison of cost cannot be made since all systems except the RTS are unique, one-of-a-kind prototypes.

6. Implementation Issues

6.1 Environmental Checklist

There are no permits or regulations that impact this technology.

6.2 Other Regulatory Issues

This technology is not primarily driven by regulatory issues, but instead by desire for faster, more accurate, and more successful UXO operations. Information about this technology will be disseminated via technology conferences (such as the UXO Forum and SERDP/ESTCP Symposium), by direct contact with appropriate government representatives working in UXO issues, and by direct contact with contractors who support government activities.

6.3 End-User Issues

CEHNC is the lead on this project because of their pressing need for better technology for DGM and UXO operations. CEHNC is prepared to advocate applicable technologies into the user community if it is shown to meet the defined objectives.

7. References

1. Innovative Navigation Systems to Support Digital Geophysical Mapping, UXO/Countermine Forum September 3-6, 2002, Scott Millhouse, CEHNC. Paper was augmented with additional images and charts February 2003 and published as ESTCP Cost and Performance Report (UX-0129), Innovative Navigation Systems to Support Digital Geophysical Mapping, February 2004.

2. Innovative Navigation Systems to Support Digital Geophysical Mapping, Phase II Demonstrations, Final Workplan, 15 October 2002, Scott Millhouse, CEHNC.

3. Innovative Navigation Systems to Support Digital Geophysical Mapping, ESTCP #200129 Phase II Demonstrations, Revised Draft Report, 25 June 2004, Scott Millhouse, CEHNC.

4. Innovative Navigation Systems to Support Digital Geophysical Mapping, Phase III Demonstrations, Final Workplan, 4 November 2003, Scott Millhouse, CEHNC.

5. Evaluations of Laser-Based Positioning for Characterization of EMI Signals from UXO, Bruce Barrow, Nagi Khadr, Thomas Bell, AETC, Inc. (Included in Appendix M)

6. UXO Precise Position Tracking, APG Demonstration, ESTCP Project 200129 Final Report, 15 November 2004, David Taylor, ENSCO, Inc.

7. UXO Precise Position Tracking Ranger- Cost and Performance ESTCP Project 200029, 23 November 2005, David Taylor, ENSCO, Inc.

8. Points of Contact

Demonstrator	Point of Contact	Address	Phone/Fax/Email	Role in Project
CEHNC	Scott Millhouse, PE	U.S. Army Corps of Engineers Engineering & Support Center-Huntsville 4820 University Square Huntsville, Alabama 35816-1822	Phone: 256-895-1607 Fax: 256-895-1602 scott.d.millhouse@hnd01.usace.army.mil	Principal Investigator
Shaw/IT Corp	John E. Foley, Ph.D.	SKY 15 Douglas Road Lowell MA, 10852	Phone: 978-458-9807 Fax: 978-458-0278 jfoley@TheITGroup.com	Demonstrator
ENSCO, Inc.	David W.A. Taylor, PhD, PG	ENSCO, Inc. 5400 Port Royal Road Springfield, VA 22151	Phone: 336-632-1200 Fax: 703-321-7863 taylor@ensco.com	Demonstrator
ArcSecond, Inc.	Edmund Pendleton	ArcSecond, Inc. 44880 Falcon Place, Suite 100 Dulles, VA 20166	Phone: 703-435-5400 Fax: 703-435-5994 edmundp@arcsecond.com	Demonstrator
GIS	Matthew Gifford	Gifford Integrated Sciences 31859 Rainbow Hill Road Golden, CO 80403	Phone: 303-277-9821 Fax: 303-271-1867 matthew.gifford@att.net	Demonstrator

Signature of Project Lead

D. Scott Millhouse — Scott Millhouse, PE

17 Feburary 2006 — Date

Appendix A: Analytical Methods Supporting the Experimental Design

Not required.

Appendix B: Analytical Methods Supporting the Sampling Plan

Not required.

Appendix C: Quality Assurance Project Plan (QAPP)

The QAPP was as outlined in the approved work plan; Innovative Navigation Systems to Support Digital Geophysical Mapping, Phase III Demonstrations, Final Workplan, 4 November 2003, Scott Millhouse, CEHNC.

Appendix D: Health and Safety Plan

This demonstration was conducted in compliance with the existing Health and Safety Plan at the Aberdeem Proving Grounds, Maryland.

Appendix E: Data Storage and Archiving Procedures

Field notes will be recorded in a bound surveyor's notebook. Electronic data will initially be stored in the field on computer disks. Prior to leaving the field each day, all data will be copied onto CD-R disks for permanent storage. A copy will be provided to the quality assurance (QA) officer.

Appendix F:

APG UXO Demonstration Test Site

Calibration Lanes Ground Truth

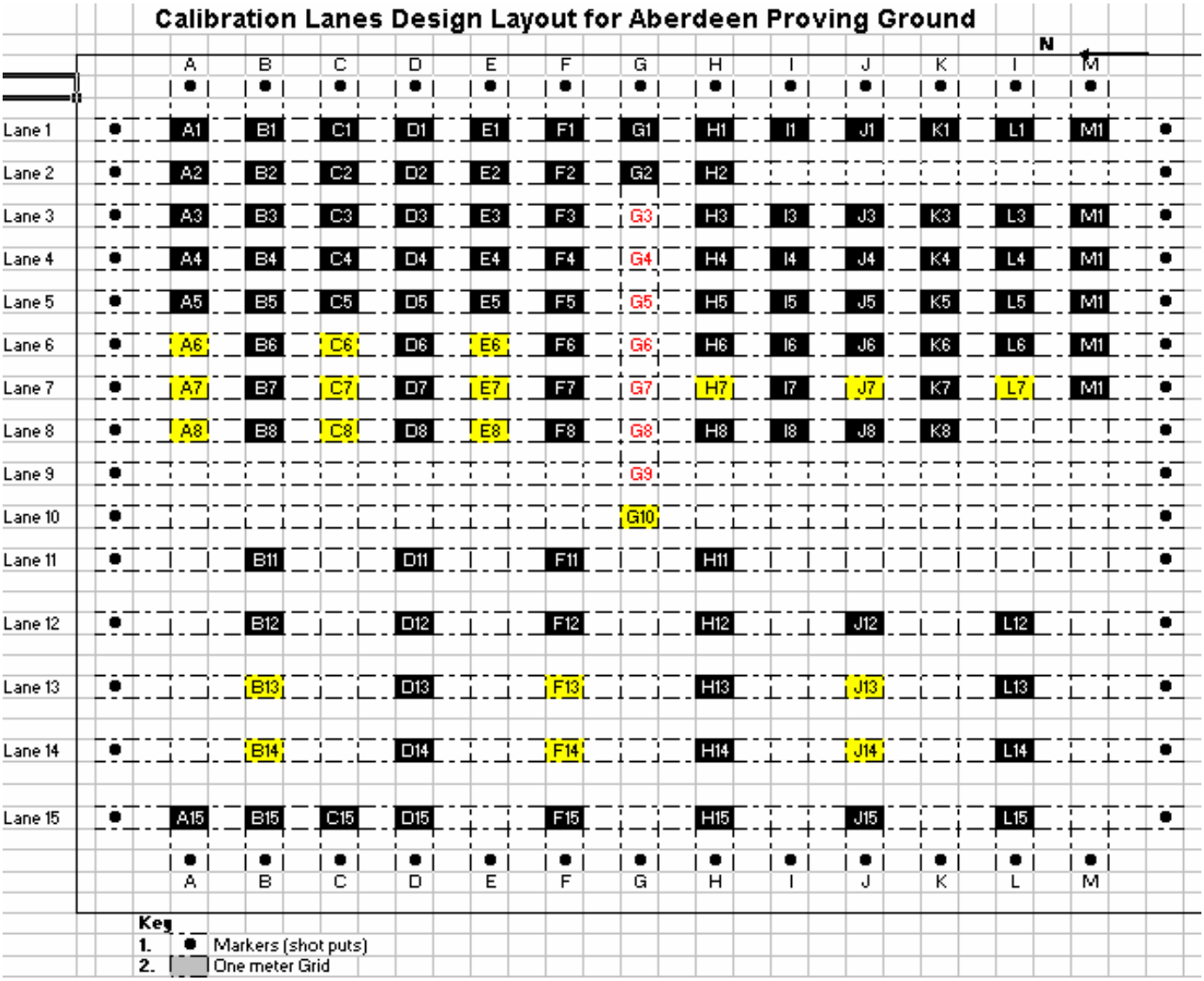
Calibration Lanes Design Layout for Aberdeen Proving Ground
N
A B C D E F G H I J K I M
Lane 1 A1 B1 C1 D1 E1 F1 G1 H1 I1 J1 K1 L1 M1
Lane 2 A2 B2 C2 D2 E2 F2 G2 H2
Lane 3 A3 B3 C3 D3 E3 F3 G3 H3 I3 J3 K3 L3 M1
Lane 4 A4 B4 C4 D4 E4 F4 G4 H4 I4 J4 K4 L4 M1
Lane 5 A5 B5 C5 D5 E5 F5 G5 H5 I5 J5 K5 L5 M1
Lane 6 A6 B6 C6 D6 E6 F6 G6 H6 I6 J6 K6 L6 M1
Lane 7 A7 B7 C7 D7 E7 F7 G7 H7 I7 J7 K7 L7 M1
Lane 8 A8 B8 C8 D8 E8 F8 G8 H8 I8 J8 K8
Lane 9 G9
Lane 10 G10
Lane 11 B11 D11 F11 H11
Lane 12 B12 D12 F12 H12 J12 L12
Lane 13 B13 D13 F13 H13 J13 L13
Lane 14 B14 D14 F14 H14 J14 L14
Lane 15 A15 B15 C15 D15 F15 H15 J15 L15
A B C D E F G H I J K L M
Key
1. Markers (shot puts)
2. One meter Grid

Grid location	Grid location	North	East	ID	Depth(M) Surface	Azimuth
Lane 6						
A6	A06	4369626.986	402796.331	57mm M86	0.40	0 az
B6	B06	4369625.060	402796.748	57mm M86	0.40	0 az
C6	C06	4369623.090	402797.137	57mm M86	0.40	0 az
D6	D06	4369621.111	402797.439	57mm M86	0.40	n/a
E6	E06	4369619.137	402797.854	57mm M86	0.91	0 az
Lane 7						
A7	A07	4369626.670	402794.430	60mm M49A3	0.50	0 az
B7	B07	4369624.694	402794.775	60mm M49A3	0.50	0 az
C7	C07	4369622.719	402795.185	60mm M49A3	0.50	0 az
D7	D07	4369620.731	402795.504	60mm M49A3	0.50	n/a
E7	E07	4369618.778	402795.871	60mm M49A3	1.00	0 az
F7	F07	4369616.767	402796.272	60mm M49A3	1.00	90 az
G7	G07	4369614.853	402796.621	8# SHOT	0.20	
H7	H07	4369612.829	402796.984	81mm M374	0.50	0 az
I7	I07	4369610.972	402797.319	81mm M374	0.50	0 az
J7	J07	4369608.786	402797.874	81mm M374	0.50	0 az
K7	K07	4369607.133	402798.046	81mm M374	0.50	n/a
L7	L07	4369605.029	402798.446	81mm M374	1.50	0 az
M7	M07	4369602.938	402798.858	81mm M374	1.50	90 az
Lane 8						
A8	A08	4369626.304	402792.426	2.75" M230	0.50	0 az
B8	B08	4369624.306	402792.801	2.75" M230	0.50	0 az
C8	C08	4369622.320	402793.186	2.75" M230	0.50	0 az
D8	D08	4369620.364	402793.557	2.75" M230	0.50	n/a
E8	E08	4369618.401	402793.836	2.75" M230	1.20	0 az
Lane 10						
G10	G10	4369613.755	402790.697	8# SHOT	0.20	
Lane 13						
B13	B13	4369621.924	402780.068	105mm M60	0.90	0 az
D13	D13	4369618.103	402780.836	105mm M60	0.90	0 az
F13	F13	4369614.115	402781.483	105mm M60	0.90	0 az
H13	H13	4369610.097	402782.234	105mm M60	0.90	n/a
J13	J13	4369606.210	402782.970	105mm M60	1.80	0 az
L13	L13	4369602.279	402783.740	105mm M60	1.80	90 az
Lane 14						
B14	B14	4369621.141	402776.104	155mm M483A1	0.90	0 az
D14	D14	4369617.121	402776.884	155mm M483A1	0.90	0 az
F14	F14	4369613.288	402777.510	155mm M483A1	0.90	0 az
H14	H14	4369609.360	402778.325	155mm M483A1	0.90	n/a
J14	J14	4369605.419	402779.063	155mm M483A1	2.00	0 az

Appendix G:

Shaw Environmental
Phase III Report

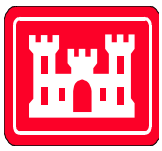

US Army Corps of Engineers
Engineering and Support Center,
Huntsville

Innovative Navigation Systems to Support Digital Geophysical Mapping

Phase III
Final Report

Prepared by
Shaw Environmental and Infrastructure
May 2004

Table of Contents

Figures

Tables

Acronyms

DoD	Department of Defense
EM	electromagnetic
ESTCP	Environmental Security Technology Certification Program
GPS	global positioning system
HIP	handheld instrument pad
LOS	line of sight
RTK	real-time kinematic
RTS	robotic total station
UXO	unexploded ordnance

1. Introduction

Shaw Environmental, Inc. (Shaw) performed Phase III of the navigation technology demonstration for geophysical mapping at Aberdeen Proving Ground on December 1 through 5, 2003. Our approach integrated the Geometrics, Inc. G858 magnetometer used for unexploded ordnance (UXO) surveys; a Leica dual-laser robotic total station (RTS) for navigation; a RIS Corp. handheld instrument pod (HIP) 12G that merges the instrument's data streams in real time; and an Xplore Technologies tablet computer for real-time data viewing and storage. It was demonstrated in Phases I and II of this Environmental Security Technology Certification Program (ESTCP) effort that the RTS technology already meets or exceeds several of the stated navigation performance goals.

Shaw's technical approach to improve navigational capabilities for UXO mapping:

- Utilized the Leica TSP1105 RTS for in-the-tree and open-area mapping
- Created standard operating procedures for successful use of RTS technology
- Integrated Geometrics, Inc. G858 magnetometer
- Implemented real-time telemetry and data merging.

The primary objective of Phase III of this demonstration was to test the viability of Shaw's RTS technology with geophysical sensors and real-time data merging and integration in a wooded area.

1.1 Background Information

This technology demonstration addressed the need for high quality digital geophysical survey data used for mapping applications related to UXO clearance. The quality of geophysical data is dependent on several factors, including the accuracy, reliability, and repeatability of the navigation information collected in conjunction with the sensor data. In the past, navigation issues have been mainly resolved in open areas through the application of real-time real-time kinematic (RTK) – global positioning system (GPS) technology, although a significant percentage of UXO sites are not suitable for this technology. GPS fails to provide

sufficient accuracy and reliability when the satellite constellation visibility is degraded due to obstructions. In tree-covered areas and adjacent to tree lines, GPS accuracy is typically greatly diminished and often ineffectual.

1.2 Objectives of the Demonstration

This Phase III demonstration integrated the Geonics, Inc. G858 magnetometer with the RTS navigation, and supporting hardware and software in order to create a real-time, seamless data collection system that acquired positional and geophysical data at high streaming rates into a single file. Although integration of geophysical sensors is critical to this demonstration, it was structured so that all participants in the demonstration utilized the same geophysical sensor and results reflected the accuracy and ease of use the navigational system rather than any discrepancies in geophysical sensor technology.

The technical objectives related to the navigational component of the demonstration are listed and described in Table 1-1.

Table 1-1. Technical Objectives

ESTCP Goal	Demonstrated Survey Capability
10-minute detup	Set-up time of 10 minutes was demonstrated.
1000-ft range per setup	RTS range over 1,400 ft (Phase I) and 1,023 feet (Phase II) demonstrated, exceeding present goals. During Phase III, proper placement of gun for use in wooded area was of higher priority than distance alone.
Multiple crews without interference	While routinely accomplished through selectable radio frequency selection, this was not demonstrated.
Less than $20,000/unit	Complete unit cost is approximately $35,000.
Voice communication	Noninterfering cell-phone operation was demonstrated.
Go-to point capability	Efficient go-to capability was demonstrated.

Real-time data transmission	Real-time data telemetry was demonstrated.
Capture Z elevation data	Full 3D positional data collected, demonstrating elevation mapping capability of system (Phase I). Z data collected during Phase III, but software requires minor modification to output this data.
Ability to measure relative position of geophysical sensors	Demonstrated Shaw software which allows multisensor configuration (not tested in Phase III).
Flexibility with multiple geophysical instruments	Present technology allows G858, EM61, and EM31 integration. EM61 demonstrated in Phase II, G858 in Phase I and III.
Selectable accuracy modes	Standard RTS accuracy of +/-5mm + 2ppm, and meets full range of accuracy goals.
Heads-up track map display for operator	Demonstrated realtime track-map display (Phase I).
Real-time grid generation/ display with geonics instruments	Not demonstrated.
Capability to determine accuracy levels	Real-time data stream can be monitored, but no accuracy detection has been implemented as of this time.
Capability to survey in wooded conditions	Successfully and efficiently able to map in all wooded conditions presented in Phase III.

Activities executed as part of the demonstration address each of the stated technology objectives:

Ten-minute setup demonstration. Shaw demonstrated the speed of system setup by establishing the Leica base station over a provided benchmark and initiated navigation activities within 10 minutes. Day 1 activities were delayed due to equipment lost during shipping as well as provided benchmark coordinate issues.

1,000-ft Range capability. Shaw demonstrated the capability of our laser-navigation technology at distances exceeding 1,000 ft in previous testing.

Multiple crews without interference. This was demonstrated in a previous test by showing that two-way data transmission and rover control of the RTS can be set to different frequencies to ensure separate communication for each survey crew.

Voice communication. Cell phones were used to demonstrate the ability of the magnetometer and Leica equipment to operate unaffected by transmission. Use of radios is also possible but was not demonstrated.

Go-to point capability. Shaw demonstrated the ability to go to points in both open and wooded conditions, capturing several previously provided or collected control points.

Real-time data transmission. The ability of the RTS to provide real-time telemetry of the solution coordinates to the roving system for integration with the onboard data logger was demonstrated.

Capture of Z-elevations. The Leica system captures real-time XYZ positional data. This was demonstrated by capturing elevation data at elevated control points and surveying the southern gully area as part of the Phase I meandering path surveys.

Ability to measure relative position of geophysical sensors. Shaw has integrated geophysical sensors with the RTS technology (EM31, EM61, and G858). We demonstrated this capability by performing both grid-based and meandering path surveys using the RTS system integrated with the Geometrics G858 magnetometers in Phase I and 3, and with the Geonics EM61 in Phase II.

Flexibility with multiple geophysical instruments. Shaw demonstrated custom software used to establish relative sensor-navigation geometry used for magnetometer or electromagnetic (EM) deployments.

Selectable accuracy mode for higher accuracy in interrogation of anomalies. Accuracy is dependent on instrument type. Typical accuracy for the model utilized in this survey (Leica TPS 1105) is +/- 5mm and meets all accuracy goals.

Real-time track map display for surveyor. Originally demonstrated in Phase I, the newest version of the software does not yet fully implement yet, but there is a software option available that has not been fully tested.

Ability to support real-time grid generation. Software does not support real-time grid generation, although real-time profiles of data can be viewed.

Capability to inform users when accuracy levels are being achieved. There are not accuracy checks built in to the software yet, but real-time streaming data can be viewed during data collection. This feature could likely be implemented in future versions of the software.

Capability to survey in wooded conditions with varying degrees of topography. The ability to quickly and easily survey with geophysical sensors and minimal positional error was demonstrated in Phase III of the navigational sensor test.

1.3 Regulatory Drivers

No regulations prohibit or limit the use of any demonstrated technology.

2. Technology Description

2.1 Technology Development and Application

The demonstrated geophysical mapping technology includes both hardware and software components. Shaw's demonstrated technical approach to improve navigational capabilities for UXO mapping included the following components.

Hardware System hardware consists of four integrated components; 1) Geometrics, Inc. G858 magnetometer, 2) Leica TPS1105 dual laser robotic total station , 3) RIS Corp. HIP box multiple data stream input and merging hardware, and 4) Xplore Technologies ruggedized, field-ready tablet PC.

The Leica TSP1105 is a motorized robotic total station that utilizes automatic target recognition to track the location of the prism and has a highly accurate distance/azimuth measurement system to produce +/-5mm +2ppm accuracy. The RIS Corp. HIP 12G will input multiple geophysical sensor data streams, as well as a data stream from a GPS or RTS, and merge these data streams in real time. It initializes itself with the tablet computer in order to synchronize with the tablet time, then time stamps all incoming data with little to no latency. This ensures that all data is collected with the most accurate ground locations possible.

Software Three software components are integrated within the demonstrated technology. First, firmware that is utilized on the RTS base station to track the roving prism provides rapid collection of data up to 4 Hz, and serial output of solutions on both the base station and rover computing units. The firmware also enables the user to optimize the prism tracking parameters for rapid recovery of lock if obstructed by trees during a survey. Second, RIS Corp. data logging software synchronizes with and controls the recording parameters in the HIP box. Third, Shaw data-merge software allows definition of the sensor geometry during collection (if prism/antenna is not directly over the geophysical sensor). This software

provides a robust framework to spatially configure sensors relative to each other and with respect to the prism location, resulting in accurate spatial representation of all collected data.

2.2 Previous Testing of the Technology

Previous testing of the Shaw RTS system includes 1) internal tests with RTS navigation equipment on a UXO demonstration site at Fort Devens, 2) demonstration/testing of the technology at the Fort Ritchie, UXO clearance site, 3) Phase I test/demonstration of the RTS as part of this ESTCP project, and 4) Phase II of the test/demonstration of the RTS as part of this ESTCP project.

Initial testing by Shaw included three controlled field experiments using the RTS at a UXO demonstration site at Fort Devens. During these Shaw-funded tests (held in March, May, and July, 2001), systematic data collection scenarios were executed in open and tree-covered areas, including both flat and hilly topography. These operations included stand-alone tests of the RTS technology, comparisons against differential GPS, and integration tests with geophysical sensors. The results were extremely positive, showing repeatable 10-25 cm target location accuracy on tree-covered hill slopes. The RTS gear has been modified to provide four-Hz real-time audio output to indicate to the operator when the RTS has lost lock with the laser prism. Additionally, Shaw's present system allows two-way communication between the roving survey equipment operator and a support technician to quickly re-establish prism lock if lost.

Survey methodologies have been modified to adjust to the differences between RTS and GPS surveying. In most cases, when an operator travels behind a tree the RTS reacquires lock on the prism after re-entering the field-of-view. However, in approximately 10% of the cases experienced at Fort Devens, the RTS lost lock and could not regain the prism location. In these cases, the RTS provides an audio alarm to the operator of "lost-lock" conditions. At this point, the operator stops and keeps the sensors stationary until the RTS regains sight of the prism. The RTS provides both an audio and visual signal indicating it is ready to continue. While the RTS navigation technology can robustly locate the prism in the woods,

the quality of the resultant geophysical survey data requires significant specific modification from typical standard operating procedures associated with GPS deployments.

2.3 Factors Affecting Cost and Performance

Table 2-1 provides performance parameters of the demonstrated system.

Table 2-1. Performance Analysis

Operational Parameter	Performance Effect
Distance from Base	Position degradation +/-5mm + 2ppm.
Line of Sight (LOS)	Unit provides solution only when LOS exists.
Prism Tracking	The RTS recovers from intermittent LOS better as distances from the base to the prism increase (up to ranges of approximately 1,000 feet). This is due to the geometrical increase in the beam search area with distance.
Prism Recovery Parameters for Recovery of Loss of Lock	Re-lock is best achieved if the search area is a defined rectangle with horizontal search range greater than vertical search range (e.g., 10° horizontal and 5° vertical). The aspect ratio of the rectangle reflects the vertical nature of the obstructions (trees). Absolute angles will depend on distance from the base.
Tree Density	Loss of LOS is easily recovered within sparse and/or isolated trees. In heavy forested areas, more care and planning is required to recover lock upon loss of LOS. Very few LOS problems were encountered during the Phase III testing.
Distance from Base to Trees	While greater distances are preferred if trees exist in the intervening area, performance is reduced.
Data Solution Rate	The present firmware produces data between 3.5 and 4 samples per second. This rate allows for capture of erratic motion of the sensors.
Tilt of the Prism Pole	Nonvertical prism pole results in inaccurate representations of the XY location of the sensors. A 10° angle of a 6-ft pole introduces 3.6 in of horizontal error.
Instrument Calibration	It is recommended that the RTS unit be calibrated yearly. A quick (< 5 min) calibration test is recommended every time the unit is shipped.

2.4 Advantages and Limitations of the Technology

The demonstrated RTS technology has advantages and disadvantages compared to conventional GPS navigation techniques, including the following, which are similar to those presented in Section 1.2.

Advantages

- Fast set-up time. Typically requires 10 minutes or less.

- Limited operational constraints. All daylight hours are available for surveying as long as weather conditions permit line-of-site operation. (Fog, rain, snow, and extreme heat may limit laser travel.) This capability eliminates constraining outside factors such as satellite availability to execute a survey.
- Modest capital costs. At approximately $35,000 for all hardware and software, this is less expensive than RTK GPS for a single unit.
- Extensive survey range. The demonstrated range of at least 1,000 ft means that under ideal conditions the effective survey area with a single setup is more than 100 acres.
- High precision. At +/-5 mm (0.2 in) + 2ppm, the RTS provides accuracy of better than 0.25 inches at distances of up to 1,400 feet from the gun. This is better than any real-time GPS accuracy.
- Elevation data. RTS accuracy is circular, providing Z elevations as accurate as XY locations. This is significantly different from GPS solutions, which are highly ellipsoidal.
- Noninterference. Cell phones and radios have no effect on the operation of the system. These are prohibited from close proximity to GPS units.
- In-the-tree capability. The RTS is operative in wooded conditions provided there is continuous or intermittent line of sight. RTK GPS fails in most wooded areas, and single-frequency GPS provides sporadic 1-2 m accuracy under favorable conditions.
- Light weight. The prism unit is less than 1 lb, easy to mount on a sensor platform, and adds no power requirements to the system.

Limitations

- Required survey control. Two control points are needed to define a baseline in absolute coordinates. If unavailable, local coordinates can be established.
- Line-of-sight required. The unit determines a location when it sees the prism. While it can survey in areas of intermittent obstructions (such as wooded areas), it cannot survey around corners of building or around walled canyons.

- Conventional survey capabilities required. In order to operate the RTS effectively, the survey personnel need to be skilled in the conventional use of a sophisticated total station.
- Multiple survey crews require multiple units. In order to operate multiple survey crews, an RTS gun and roving unit is necessary for each crew, whereas RTK GPS need only one base station with multiple rovers.

Table 2-2. RTS versus RTK GPS Comparison

Performance Factor	Demonstrated RTS Capability	GPS Capability
Set-Up Time	10 minutes for initial base station, 5 minutes for subsequent setups	Approximately 25 minutes
Operational Times	Unlimited during daylight hours	Requires sufficient satellites; no constraints on daylight.
Range per Setup	More than 1,000 ft radius distance, 100-acre radial area	Range limited to radio repeater distance, typically 1KM (3,280 ft)
Multiple Crews Without Interference	Accomplished through selectable radio frequency selection	Accomplished through selectable radio frequency selection
Cost	Gun/Rover cost, approximately $35,000	Base/Rover system cost, approximately $65,000
Voice Communication	No interfering cell-phone/radio operation	Radios and cell-phones interference with operations
Go-To Point Capability	One-person go-to capability	One-person go-to capability
Real-Time Data Transmission	Real-time data telemetry including XYZ solution to handheld unit; also allows real-time control of base unit from rover	Real-time data telemetry of XYZ solution
Z Elevation Data	Full 3D positional data; circular errors of +/5mm + 2ppm	Full 3-D positional data; highly ellipsoidal errors with XY +/- 20 mm. Z error varies, typically +/- 100 mm or greater
Relative Position of Geophysical Sensors	Shaw software allows multisensor configuration	Shaw software allows multisensor configuration
Flexibility with Multiple Geophysical Instruments	Present Shaw technology allows G858, EM61, and EM31 integration	Present Shaw technology allows G858, EM61, and EM31 integration

3. Demonstration Design

3.1 Performance Objectives

Table 3-1 provides performance objectives of the demonstrated system.

Table 3-1. Performance Objectives

Type of performance objective	*Performance criteria*	*Expected performance*
Quantitative	Unobstructed range of operation	0 - 400 m
	Range accuracy within range of operation	+/- 5 mm
	Obstructed range of operation	N/A – line of sight
	Obstructed range accuracy within range of operation	N/A – line of sight
	2-D position error	+/- 5 mm
	Set-up time	10-20 min
	Multiple crew capability	Yes (with multiple guns)
	Voice communication	No
	Ability to capture elevation data (3-D)	Yes (with high accuracy)
	Selectable accuracy	Yes or no
	Flexible use of geophysical equipment	Yes (multiple sensors of same or different make can be utilized at once)
	Real-time display of geophysical grid data	No (not yet implemented)
	Ability to display position data in near-real-time on mobile data logger	Yes (in real time text; graphical display not yet implemented)
	Ability to display position data in near-real-time on remote computer	No
	Ability to survey grids in lightly wooded areas	Yes
	Ability to survey grids in moderately wooded areas	Yes
	Integrated with G858	Yes
	Integrated with EM61	Yes
Semi-quantitative	System easy to set up and calibrate by two-person team	Yes (typical set up time is approximately 20 min)
	System easy to operate by two-person crew	Yes
Qualitative	Reoccupation of position easily accomplished	Yes (similar to popular GPS models reoccupation)

3.2 Selecting Test Site(s)

This section is not applicable.

3.3 Test Site History/Characteristics

This site consists of three primary testing areas. These consist of a flat calibration area with known sources and locations, a wooded area and a mogul area.

3.4 Present Operations

This section is not applicable

3.5 Pre-Demonstration Testing and Analysis

Prior to the Phase III demonstration, this system was tested in Phase I and Phase II of this ESTCP demonstration, as well as in house testing prior to Phase III deployment. Phase III testing involved some new hardware and software configurations previously untested. These include the RIS Corp. Handheld Instrument Pod (HIP) 12G and applicable software, the Xplore Technologies tablet PC, and a Crossbow CXM543 high-speed orientation sensor.

Given that previous deployments of this system were implemented with the Shaw cart, a new method was devised so that the system was man-portable and could easily be navigated through wooded areas. An aluminum frame backpack was used for carrying cabling, batteries, and the HIP box, while a PVC and wood assembly was constructed and attached to the backpack in which the tablet PC and RTS remote would rest in front of the user. The magnetometer sensor was mounted approximately 4 in above the ground directly on a staff consisting of the poles included with the standard G858 equipment. A PVC coupling with equal diameter of the magnetometer head was attached to the pole with the same mount that holds the magnetic sensor head. A bolt was mounted through the PVC top, which connected the RTS prism. Figure 3-1 shows that this configuration aligns the prism at the exact distance from the staff as the center of the magnetometer head.

With this configuration, the geophysicist could monitor all sensor readings in real time and assess and quickly react to any problems or data issues. Although this system could be implemented and run by one person, it was decided to use a second person for data collection. This would add distance from the sensor to the electronics as well as provide safer and easier travel in the wooded areas while carrying equipment.

Figure 3-1. Two Pictures of the RTS/Geophysical Sensor Setup Prior to Phase III Deployment. (Note: Fiberglass pole utilized in place of G858 standard poles prior to deployment.)

Initial testing of this system included the Crossbow orientation sensor in order to correct for any angular change from the sensor to the RTS prism. This was purposefully not utilized in the final design due to the distance it had to be placed from the sensor in order not to affect sensor readings. The extra weight high on the staff as well as extra cabling created a staff that was extremely top heavy and much harder to control. Because of this situation and the fact that there was no universal pivot point to provide an accurate geometric solution with which to correct with the gyro data, the gyro was not included on the staff, as it appeared that it would add more locational error than it could correct.

3.6 Testing and Evaluation Plan

Test 1: Calibration Lane—Area Mapping

- Mapped the 29 m by 37 m site (0.25 acre) using the GFE G-858 sensor (with magnetometer base station) integrated with the navigation equipment at 1 m spacing in an approximately E-W direction.
- Post processed the data set (prior to the wooded area mapping) to create a dig list for the anomalies that are above a threshold established by the typical 57 mm M86 items in the Calibration Lanes.. This threshold value was also to be used for anomaly selection for the wooded area mapping dig list.

Test 2: Calibration Lane—Reacquisition

- Reacquired the coordinates of 19 items. They included three each of 57 mm, 60 mm, 81 mm, 2.75 in, 105 mm, and 155 mm seeded items at different orientations and depths as well as one 8# shotput. The items were lane 6 A, C & D, 7 A, C, E, H, J & L, 8 A, C & E, 13 B, F & J, 14 B, F & J, and shotput lane 10 G. Used the integrated system to reacquire and flag the position real time. The reacquired coordinate was compared to the seeded location coordinates.

Test 3: Calibration Lane Area—Fixed Grid Anomaly Interrogations Evaluations

- These 19 locations were interrogated in both a fixed grid and dynamic mode. The fixed grid data set was gathered based on a fixed grid mesh or marked carpet centered on the reacquired location for a 1.2 m square area at .2 m intervals with a sensor height at .15, .30, and .45 m heights (147 points). Standoff was established by movement of the head position up a position pole. The individual point data captured was compared from relative positioning among the points captured to the fixed grid. Based on the 3-D data captured, a revised dig list location was selected. The refined dig list coordinates were compared to the seeded location coordinates, area mapping dig list coordinates from Test 1 and the flagged coordinates from Test 2.

Test 4: Calibration Lane Area—Dynamic Anomaly Interrogations Evaluations

- The 19 anomalies then had a dynamic 3-D data set acquired by walking an approximately 2 m square area with the sensor head at multiple heights or by swinging and lifting the handheld sensor over the anomaly area as required by the individual systems. The objective was to capture a similar data set as in Test 3 but in a rapid, more random unguided field methodology that relied on the navigation system's dynamic position accuracy with a continuous sensor and navigation data stream. Based on the 3-D data captured, a revised dig list location was selected. The refined dig list coordinates were compared to the seeded location coordinates, area mapping dig list coordinates from Test 1, the flagged coordinates from Test 2, and the fixed grid location from Test 3.

Test 5: Wooded Area—Accuracy with Positioning System for Surface Points

- The wooded area has six unknown permanent rebar points within the interior, which are placed in areas without nearby adjacent geophysical anomalies. An additional widely scattered 40 points are established by PVC pipe with removable steel pins (when required to trigger the magnetometer). Each was occupied by the integrated navigation and geophysical sensor system to determine coordinate locations.

Test 6: Wooded Area—Accuracy from Geophysical Data Analysis for Surface Points

- The 46 points from Test 5 were traversed dynamically by the integrated system and were picked from the instrument peaks shown in the data set and reported. These were directly compared to the ground truth for position accuracy and to the locations from Test 5.

Test 7: Wooded Area—Area Mapping

- The approximately 1-acre area was mapped with the data analysis using the GFE G-858 sensor (with magnetometer base station), integrated with the navigation equipment at approximately 1 m spacing in an approximately E-W direction. The

steel pins were removed from the 40 points described in Test 5 so as not to affect the subsurface anomaly results.

- The selection threshold for anomaly selection for the wooded area was based on the instrument reading for all items larger than the 57mm M86, as shown by the Calibration Lanes area mapping from Test 1.

Test 8: Wooded Area—Dynamic Anomaly Interrogations

- Ten well-defined anomalies were selected from the Test 7 results for interrogation. The 10 anomalies then had a dynamic 3-D data set acquired as in Test 4 by walking an approximately 2 m square area with the sensor head at multiple heights or by swinging and lifting the handheld sensor over the anomaly area, as required by the individual systems. Based on the 3-D data captured, a revised dig list location was selected.

Test 9: Wooded Area—Dynamic Anomaly Positioning

- An anomaly array board 1.2 m square was utilized for Test 9. It had an irregular array of nails inserted (point into the ground) for point source anomalies. This board was randomly placed in an area clear of subsurface anomalies adjacent to each of the six rebar points and mapped in a similar manner to Test 8. The individual nail location positions were selected as a dig list from the instrument peaks.

Test 10: Mogul Area—Accuracy with Positioning System for Surface Points

- The mogul area has 20 unknown points established in a varied array traversing a portion of the large and medium moguls with widely varying slope and elevation. The points are PVC pipe with removable steel pins (to trigger the magnetometer when required). Each was occupied by the integrated navigation and geophysical sensor system to determine coordinate locations.

Test 11: Mogul Area—Accuracy from Geophysical Data Analysis for Surface Points

- The 20 points from Test 10 were traversed dynamically by the integrated system. These points were picked from the instrument peaks shown in the data set and reported. These were directly compared to the ground truth for position accuracy and to the locations from Test 10.

3.7 Selection of Analytical and Testing Methods

This section is not applicable.

3.8 Selection of Analytical and Testing Laboratory (may not be applicable to UXO)

This section is not applicable.

3.9 Management and Staffing

This section is not applicable.

3.10 Demonstration Schedule

Demonstration testing was performed December 1 through 5, 2003.

4. Performance Assessment

4.1 Performance Criteria

Performance objectives were defined above in Table 3-1.

4.2 Performance Confirmation Methods

Some tests conducted during Phase III included two methods of collecting positional data. The first method (Test 5) included statically locating the RTS prism as accurately as possible over the survey location and collecting a point. The second method (Test 6) included collecting a profile over a series of locations, then processing the data, picking the anomaly peak, and recording the position of that peak. As these methods included both statically and dynamically collected positions, we were able to compare those points collected methodically and those collected quickly similar to an efficient real-time survey.

Table 4-1 is a listing of data collected in the wooded area over known, upright, PVC pipes with bolts inserted into them to create a geophysical anomaly. This is an example of the high accuracy of the RTS/geophysical sensor combination. All positions were collected with the entire geophysical/RTS sensor setup. The static tests displayed in columns 2 and 3 were collected only with the RTS collecting data, not utilizing the geophysical sensor for aid in location. The RTS prism was located as accurately as possible over the top of the PVC pipe, extending up from the ground and collected as a single point at a time. The dynamic locations (columns 5 and 6) were collected in profile by walking over all PVC locations with a steel bolt placed in each PVC location. A geophysical data collection rate of 10 Hz was utilized. The dynamic locations were processed and picked from the geophysical sensor data anomalies, and the offset was subsequently calculated (columns 7 and 8). Figure 4-1 exhibits a profile of the geophysical data with corresponding data location in map view. These were utilized for picking anomaly peaks and associating them to data locations.

As evident in the X and Y offset columns, the dynamic data provided a very accurate assessment of the anomaly location. It should also be noted that much of the wooded survey area was covered by 6 to 18 in of water and ice, which made walking a profile directly over all survey

points challenging in itself. Even with these obstacles, the average overall offset was only 0.13 m. Table 4-1 is a sample of the data collected during the demonstration. Further raw and processed data is available in the Appendix D compact disc.

Table 4-1. Comparison of Static and Dynamic Locations of Known Points in Wooded Area

Point_Id	Static_X	Static_Y	Elevation	Dynamic_X	Dyanmic_Y	X_offset	Y_offset
65	402676	4369531	10.775				
69	402650.5	4369539	10.76	402650.58	4369538.51	-0.119	0.077
70	402643.6	4369541	10.719	402643.49	4369541	0.143	-0.126
71	402641.6	4369510	10.688	402641.55	4369510.59	0.001	-0.103
72	402631.7	4369522	10.738	402631.48	4369522.04	0.207	-0.224
73	402629.6	4369498	10.659	402629.21	4369498.26	0.372	-0.145
102	402672.8	4369532	10.702	402672.64	4369531.62	0.181	0.044
103	402671.9	4369518	10.673	402671.82	4369518.38	0.041	0.072
104	402671	4369505	10.684	402670.75	4369505.35	0.25	0.027
105	402670	4369492	10.688	402669.85	4369492.05	0.18	-0.002
106	402669.2	4369479	10.691	402668.68	4369478.86	0.487	0.127
107	402668.3	4369466	10.668	402667.99	4369465.83	0.274	-0.032
108	402667.3	4369453	10.687	402667.11	4369452.9	0.169	-0.134
109	402653.9	4369459	10.665	402654	4369459.04	-0.113	-0.012
110	402655.6	4369470	10.687	402655.62	4369470.54	-0.02	-0.276
112	402659.6	4369496	10.683	402659.74	4369496.32	-0.122	-0.175
113	402660.6	4369508	10.665	402660.66	4369508.07	-0.05	-0.056
114	402662.2	4369520	10.684	402662.22	4369520.33	0.006	0.001
115	402665	4369533	10.687	402665.01	4369532.89	-0.055	-0.099
116	402665.3	4369544	10.746	402665.09	4369544.59	0.168	-0.212
118	402655	4369534	10.7	402654.9	4369534.21	0.083	0.092
119	402652.9	4369524	10.677	402652.82	4369523.98	0.077	0.108
120	402649.4	4369511	10.66	402649.26	4369510.67	0.156	0.044
121	402624.2	4369516	10.806	402624.32	4369515.92	-0.086	0.115
122	402623.9	4369508	10.692	402623.49	4369507.77	0.362	-0.173
123	402643.5	4369476	10.66	402643.41	4369475.87	0.101	0.07
124	402641.8	4369464	10.661	402641.59	4369463.88	0.188	0.148
125	402628.7	4369469	10.709	402628.69	4369469.11	0.038	-0.132
126	402630.2	4369479	10.649	402630.35	4369479.42	-0.17	-0.056
127	402634	4369492	10.63	402634.03	4369492.52	-0.032	-0.269
129	402639.9	4369513	10.69	402639.9	4369513.3	-0.012	-0.25
130	402643	4369524	10.704	402643.09	4369524.43	-0.137	-0.204
131	402646.2	4369536	10.702	402646.33	4369535.63	-0.126	0.011
132	402649.4	4369547	10.732	402649.66	4369546.54	-0.258	0.399
133	402641.3	4369548	10.674	402641.14	4369547.65	0.155	-0.051
134	402637.5	4369537	10.779	402637.51	4369536.81	0.022	0.133
135	402634.3	4369527	10.73	402634.43	4369527.1	-0.173	-0.104
138	402624.9	4369495	10.656	402625.04	4369494.72	-0.122	-0.068
139	402620.3	4369484	10.685	402619.92	4369484.28	0.38	0.11

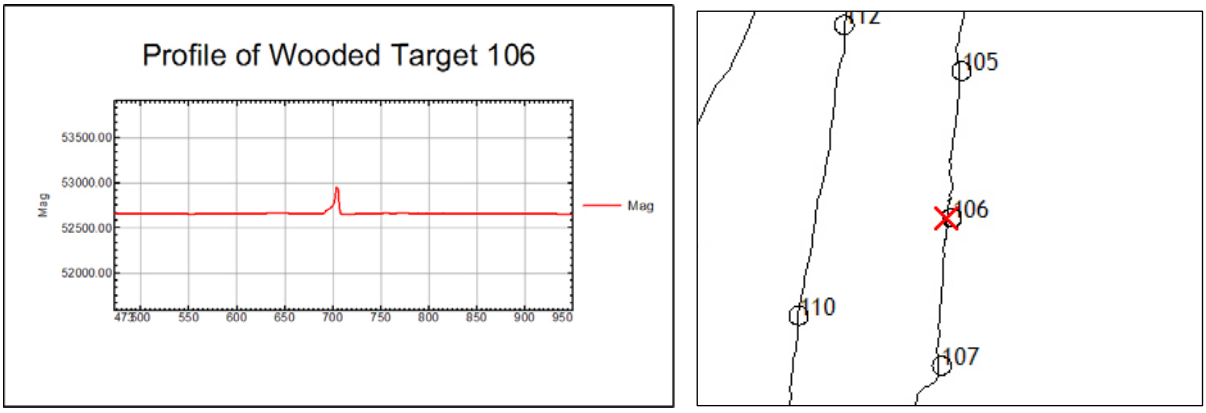

Figure 4-1. Geophysical Data Profile and Location of Anomaly Peak (plotted [red 'X'] on map with data track [black line] and static points [black circles])

4.3 Data Analysis, Interpretation, and Evaluation

The following includes descriptions of test results. For further information regarding testing methods, refer to Section 3.6.

Tests 1 and 7 represent the calibration lane and wooded area mapping, respectively. Both tests worked efficiently, and data appeared very clean with well formed dipoles. Figure 4-2 displays a color contour map of the wooded area. The RTS worked very well in the woods with only minor data gaps that were filled in by moving the position of the gun. With minimal movement of the gun, the entire area was easily surveyed.

Test 2 consisted of reacquisition of 19 items in the calibration area. The original intent of this test was to pick the anomaly locations from the calibration area processed and reacquire these coordinates. Incorrect northing and easting coordinates were provided the first day, and extra equipment for staff configuration that was to be shipped to the site was lost by the shipping company, so the calibration area mapping was performed on the second day. There was not enough time to process the data and pick anomaly positions before locating these points in the calibration grid. Therefore, it was determined that we could locate the anomalies dynamically in real-time with the magnetometer and provide an RTS point for the peak of that anomaly.

Tests 3 and 4 represent static and dynamic anomaly interrogations of individual targets in the calibration grid at sensor heights of 6, 12, and 18 in. Data overall appeared to be of good

quality, although there were large targets that exhibited a signal much larger than the 1 m area surveyed as well as some anomalies that were too deep to exhibit a signal that was distinguishable from the nearby shallower targets. And some static cell data paths did not line up well with the assigned survey points. Figure 4-3 demonstrates static calibration cells 8C and 8A, respectively. Cell 8C appears to have the data point locations in a fairly evenly spaced orientation while cell 8A does not appear to have followed an evenly spaced grid. It is believed that this positional error is as high as approximately 0.2 m due to the speed in which the survey was being conducted in order to finish within time restraints (because of loss of time on the first day) as well as the extremely gusty winds and cold temperatures that were present the first two to three days of fieldwork. It is not believed that this positional error is due to geophysical or positional sensor error.

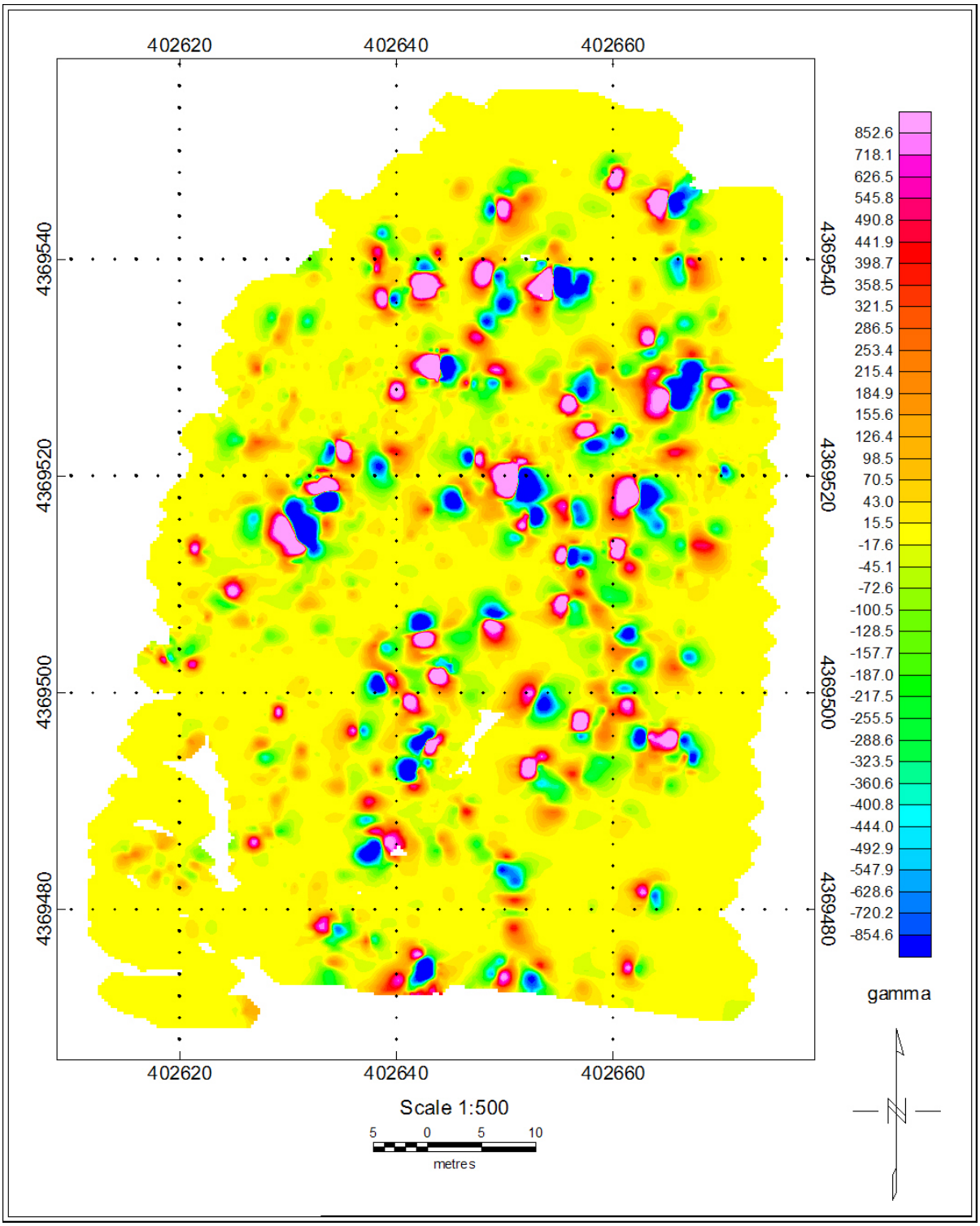

Figure 4-2. Map of Wooded Data Collected with RTS/Geophysical Data Sensor Setup

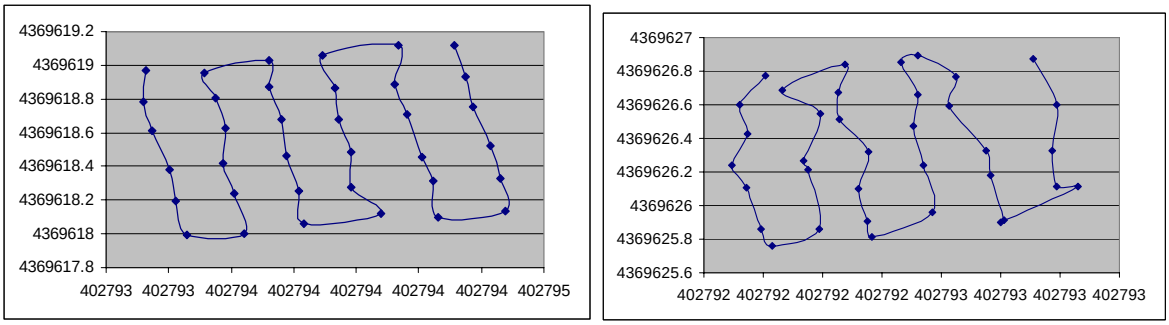

Figure 4-3. Locational Data Track of Calibration Cells 8C (left) and 8A (right)

Test 5 and 6 represent the static and dynamic location tests, respectively, collected in the wooded area. Test 5 consisted of RTS positions of 40 PVC and six rebar location measurements while Test 6 was a dynamic profile across all 46 points with the geophysical sensor and RTS utilized together. Bolts were placed into the vertical PVC pipes that extended slightly above the ground surface. Overlaying the ground path of the dynamic profile over the static points collected (as evident in Figure 4-1) confirmed the accuracy of the dynamic location when combined with magnetic signal across those points. An example of these tests is exhibited in Table 4-1 and Figure 4-1.

Test 8 included 10 anomaly interrogations picked from targets in the wooded area. Twenty targets were picked due to the possibility that some of these picks may lie in the large areas of water pooled across the site. Overall data quality is high, but the accelerations caused by the back and forth movement of the staff coupled with the high accuracy and data collection rate while trying to perform a survey such as this create more very small positional errors than when traversing a straight, constant velocity path. This phenomenon is likely exacerbated by the rapid data collection rate of the RTS system and the distance from the RTS prism to geophysical sensor on the staff. Errors typically appear to be on the order of approximately 0.2 m and could likely be minimized by placing the RTS prism as close to the geophysical sensor as possible.

Test 9 included a 1.2 m square board with concentric semicircles of increasing size with four nails in each circle. It appears the same small positional errors were also present in this survey as in Test 8 due to quickly changing accelerations. Also, the corner of the 1.2 m board included a small hole that was placed over each of the six pieces of rebar in the wooded area. These

pieces of rebar exhibited a much stronger signal than the nails in the board and masked most of the nail signal.

Tests 10 and 11 represented the static and dynamic location surveys for the mogul area similar to Tests 5 and 6. Results were also very similar to those of Tests 5 and 6.

5. Cost Assessment

5.1 Cost Reporting

When compared against GPS technologies, cost saving with the RTS is significant in almost all aspects of UXO geophysical surveying, stakeout, feature identification, and target relocation activities. Table 5-1 provides a listing of the cost savings potential of the RTS approach.

Table 5-1. Cost Assessment

Cost Saving Issue	Notes
Capital Equipment	Approximately 50% of the cost of RTK GPS
Survey Efficiency	Reduced set-up times, data download times, and the absence of required navigation post-processing reduces unit survey cost by approximately 15%.
Survey Capability – Intermittent wooded areas	Ability of RTS to survey in areas adjacent to trees and in intermittent tree-covered areas allows for complete coverage in many areas where GPS is only a partial solution. Depending on site conditions, this could save up to 50% of survey costs.
Survey Capability – Full wooded areas	Ability of RTS to survey in wooded areas offers substantial savings. Cost comparisons against GPS are not relevant. Cost savings versus ultrasonic system should be approximately 50%.
Feature Collection and Way-pointing	Savings for these activities will be commensurate with above.
Target Detection	Relative to GPS, the RTS has navigational accuracy capabilities that will improve geophysical data quality in many different survey conditions. The added quality of the data will lead to greater target detection rates of UXO, which will provide significant savings to the Department of Defense (DoD).
Target Discrimination	The RTS has navigational accuracy capabilities that will improve geophysical signature fidelity significantly compared to GPS in many different survey conditions. This will allow application of target discrimination techniques, which will provide significant savings to DoD.

6. Implementation Issues

6.1 Environmental Checklist

There are no permits or regulations that impact this technology.

6.2 Other Regulatory Issues

No known regulatory issues.

6.3 End-User Issues

No known end-user issues.

7. References

No references

8. Points of Contact

Point of Contact	Address	Phone/Fax/Email	Role in Project
Martin Miele	1326 North Market Boulevard Sacramento, CA 95834	Ph: 916-565-4165 Fax: 916-565-4356 Martin.miele@shawgrp.com	Project Manager

APPENDIX A - Compact Disc of Raw and Processed Data

Appendix H:

GIS
Phase III Report

GeoVizor

Innovative Navigation Systems to Support Digital Geophysical Mapping
Phase III
Aberdeen Proving Ground (APG) Demonstrations

Completed for The
U.S. Army Corps of Engineers
Huntsville Center

By
Gifford Integrated Sciences

Acronyms

APG	Aberdeen Proving Ground
DGM	digital geophysical mapping
EM	electromagnetic
ESTCP	Environmental Security Technology Certification Program
GFE	government-furnished equipment
GIS	geographic information system
GPS	global positioning system
RTK	real-time kinematic
UTM	Universal Transverse Mercator
UXO	unexploded ordnance
VR	virtual reality

INTRODUCTION

This report describes the test performed at Aberdeen Test Center January 12 through 22, 2004. The purpose of the test was to validate the performance of the positioning subroutines of the GeoVizor system. GeoVizor is a real-time geophysical data acquisition, visualization, and analysis system. It was designed and built by Gifford Integrated Sciences under a cooperative agreement with the U.S. Army Corps of Engineers, Huntsville Center.

The GeoVizor positioning system is a hybrid system that uses one subsystem (primary) to maintain the location of the operator in a global coordinate system and another system (secondary) to maintain the position of the instrument head relative to the operator.

The primary positioning system currently has two methods for maintaining operator location during a survey. The first method is a real-time kinematic (RTK) global positioning system (GPS) system (NovAtel) with 2 cm accuracy. The second method can act as a backup to the GPS system when satellite lock is lost or as a stand-alone system when GPS use is not applicable. The second primary method uses an electronic compass, a laser range finder, and an ultrasonic pedometer. The operator shoots a line before walking it with the laser range finder and compass. The data is then allocated along the preset line using the ultrasonic pedometer. Any method that establishes the position of the operator in a global coordinate system and provides immediate position information at the operator location can be substituted for the primary positioning system.

The secondary positioning system is an ultrasonic system that tracks the instrument head relative to the primary system origin. The head information is correlated real time with the primary system information to show the location of the operator on the grid and to correctly georeference the geophysical data. This system is relatively inexpensive, costing less than $1,500.

The Aberdeen test was only partly successful. We experienced numerous equipment problems and lapses in survey control. While many of these problems can be traced to the extremely cold weather during the test (subzero with wind chill), this does not excuse the design failures that allowed the weather to impact the equipment and the survey method. However, since the test, we have taken the lessons to heart and designed and built a new survey platform that we feel addresses all the issues brought to light by the test. This new survey platform will be covered in detail in the last section.

Because of the problems we had with the weather and equipment, the entire test as represented was completed January 21-22, 2004. Due to this time constraint, not all the test tasks were completed nor were we able to demonstrate the manual mode of the primary positioning system. Using the new survey platform, we would welcome the opportunity to rectify these deficiencies.

The organization of this report follows the test outline as provided by the Corps of Engineers.

Test 1: Calibration Lane—Area Mapping

- Area map the 29 m by 37 m site (0.25 acre) using the government-furnished equipment (GFE) G-858 sensor (with magnetometer base station) integrated with the navigation equipment at 1 m spacing in an approximately E-W direction.
- Post process the data set (prior to the wooded area mapping) to create a dig list for the anomalies that are above a threshold established by the typical 57 mm M86 items in the Calibration Lanes. The dig list selected based on this threshold will be compared to the ground truth in Appendix G for position accuracy. This threshold value will also be used for anomaly selection for the wooded area mapping dig list.

This survey was completed on January 22 from 2:54 to 3:28 p.m. The survey was conducted in backpack mode with the primary positioning system set as the NovAtel GPS and the secondary system the ultrasonic system. Because of a set-up error, the base station diurnal is not available for removal. However, because GeoVizor is a real-time system, we don't typically use a diurnal correction. It is sitting over on the base station while we are visualizing and analyzing the data in the field.

The data files are in the Test_1 directory.

Directory Contents:

alldata.datV2 – UHUNTER Grid of raw data
alldata.log - UHUNTER log of raw data
AllData.xls – Excel spreadsheet of raw data (East North Value)
AllData.xyz – ASCII file of raw data (East North Value)
Alldata_headingremoved.datV2 - UHUNTER Grid of data with heading error removed
Alldata_headingremoved.log - UHUNTER log of data with heading error removed
Alldata_headingremoved.xls - Excel spreadsheet of data with heading error removed
Alldata_headingremoved.xyz - – ASCII file of data with heading error removed
AllData_picks.xls – Excel spreadsheet of picked anomalies in calibration grid
Dat_1_1_l*.txt – raw serial instrument inputs for each line of data
KP.kbdat – UHUNTER KB file for known locations of targets
Line_*_ Data.xyz – post-processed line data created when operator signals he is at the end of a line. (East North Value)
Picker.art - UHUNTER art file of picks
Picker.datV2 - UHUNTER grid – mode adjusted

Figure 1 shows a scatter plot in Easting Northing of the entire post-processed data set. Figure 2 shows data for line 27. The blue line is the straight up GPS positioning along the line. The magenta line is the GPS plus ultrasonic position resulting in the head position. Figure 3 shows the U-HUNTER representation of the grid (Picker.datV2) using AllData_headingremoved.xyz as the input file.

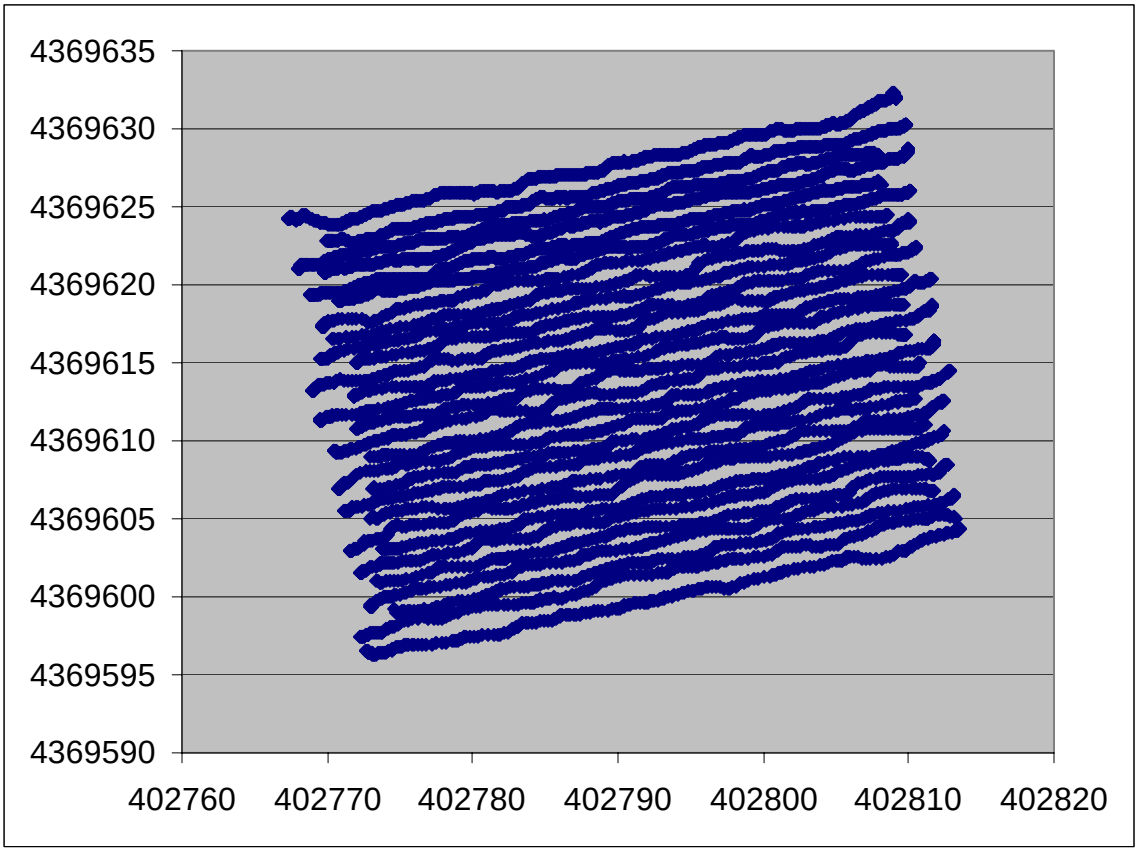

Figure 1. Post-processed survey data

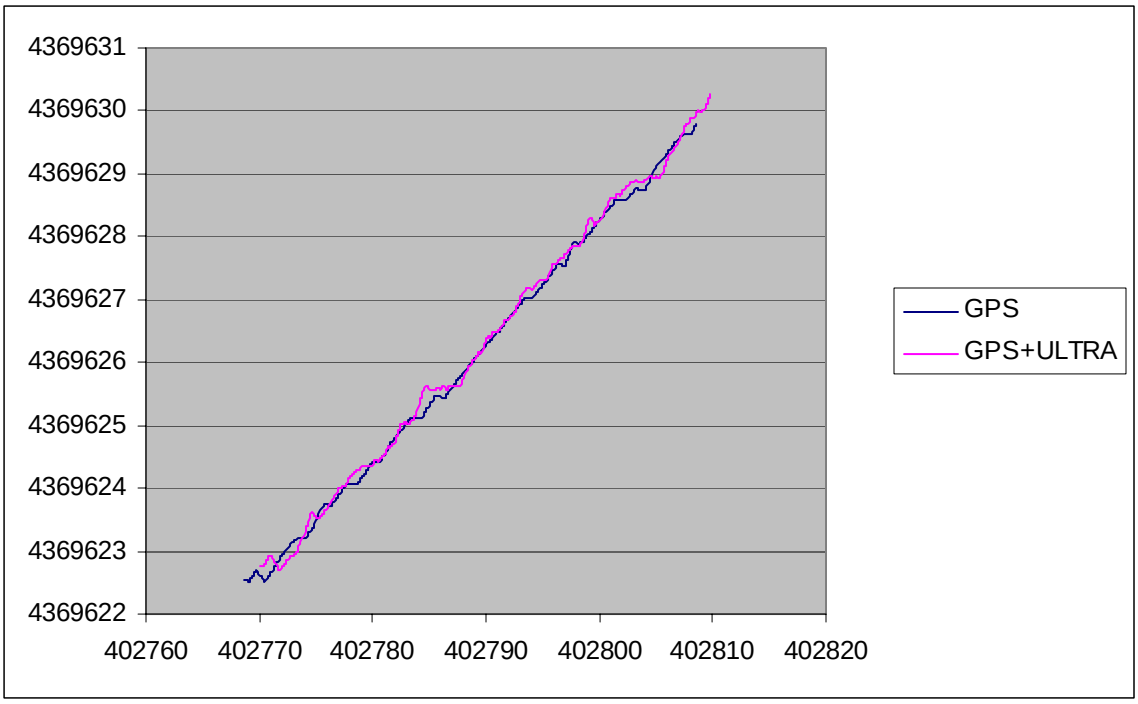

Figure 2. Line 27, GPS versus head position

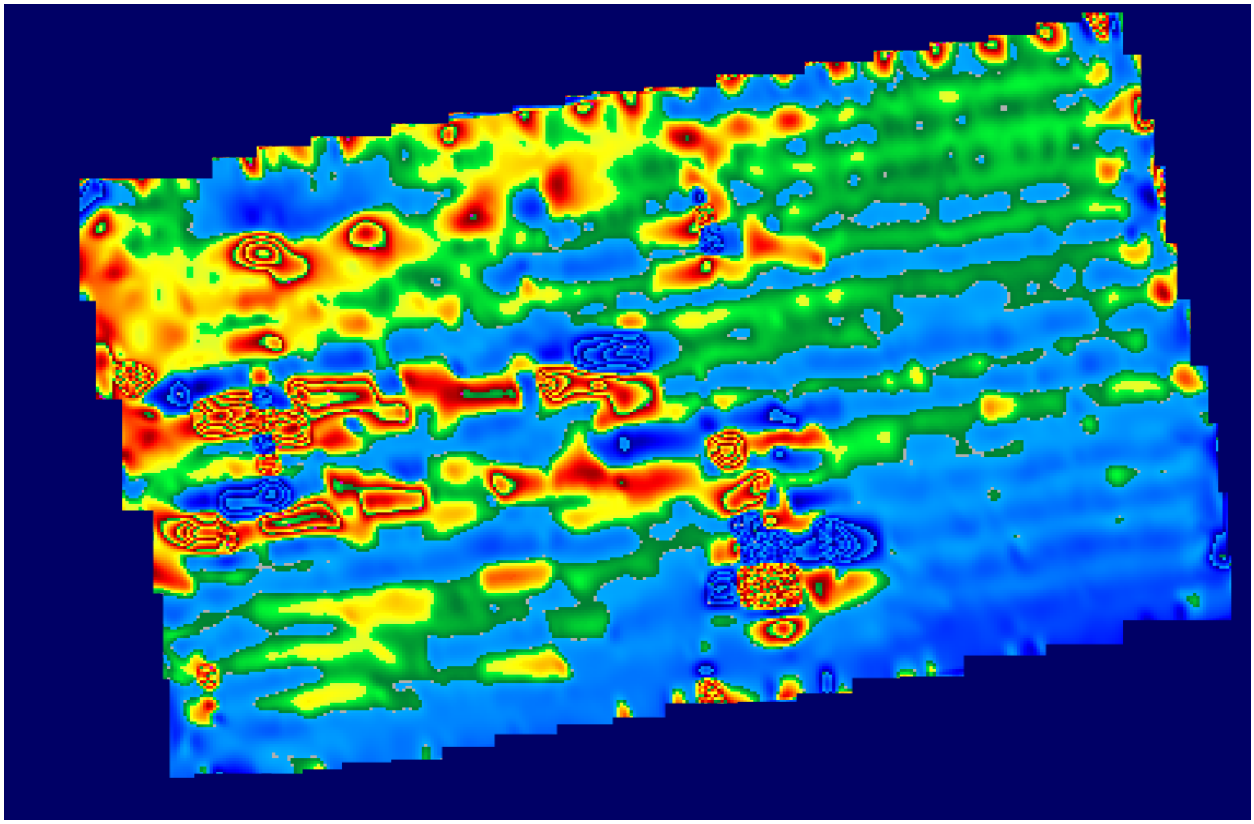

Figure 3. U-HUNTER Grid

Test 2: Calibration Lane—Reacquisition

- The contractor shall reacquire the coordinates of 19 items. They include three each of 57 mm, 60 mm, 81 mm, 2.75 in, 105 mm, and 155 mm seeded items at different orientations/depths as well as one 8# shotput. The items are lane 6 A, C, & D; 7 A, C, E, H, J, & L; 8 A, C, &E, 13 B, F, & J; 14 B, F, & J; and Shotput lane 10 G. They are shown in Appendix G as highlighted in yellow. Use the integrated system to reacquire and flag the position real time. The reacquired coordinate will be compared to the seeded location coordinates.

Figure 4 is the real-time reacquisition/interrogation view from GeoVizor. The 3-D response of an individual anomaly (#2, C6 57 mm at 0.4 m depth, 90° dip) is on the left side of the screen. The crosshair shows the current location of the instrument head in the volume above the target. The previously completed digital geophysical mapping (DGM) survey and the anomalies picked for investigation are on the right hand side of the screen. The dragger crosshair shows the current location of the instrument head in Universal Transverse Mercator (UTM) and the direction it is pointing relative to the GPS antenna.

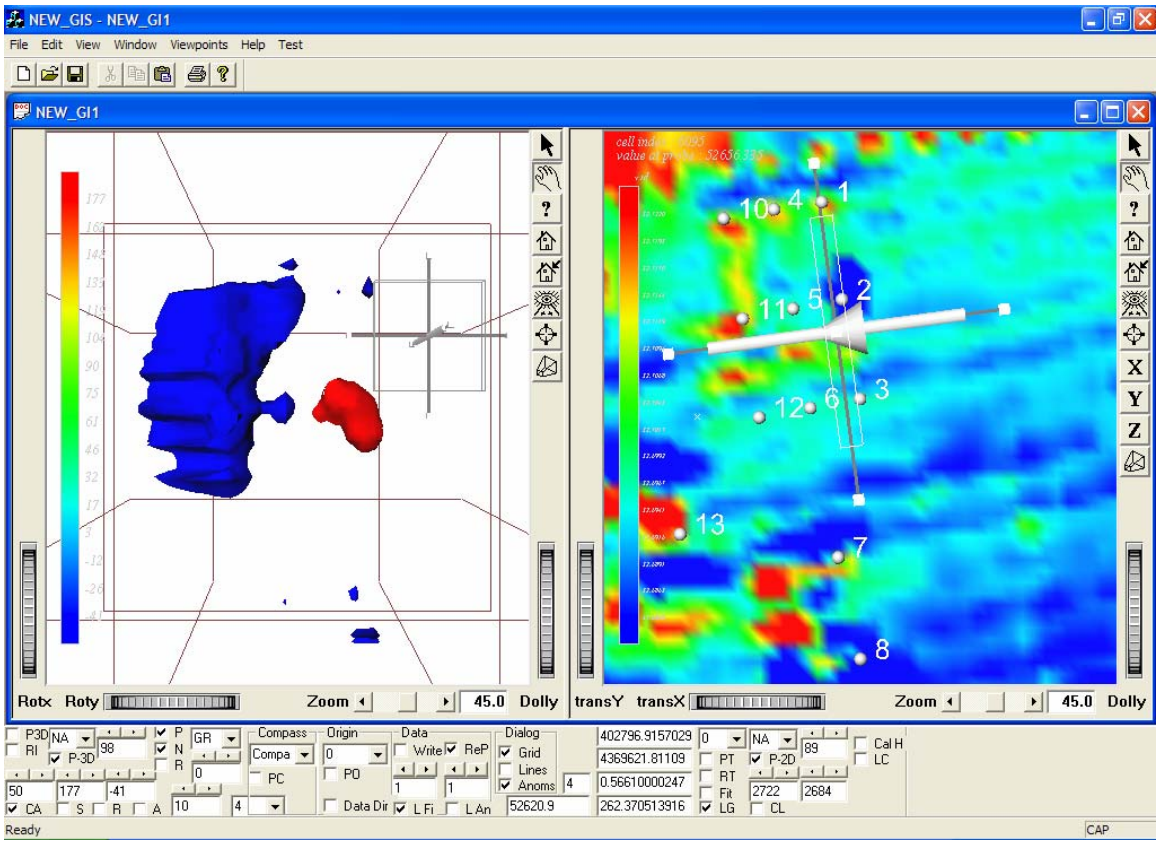

Figure 4. Real-time Reacquisition/Interrogation View from GeoVizor

The picked points we used in the test were the true coordinates of the objects, as we had not done the pick prior to the reacquisition test. This was because of time constraints. We demonstrated the ability to reacquire these points during the survey; however we did not save specific coordinates, as they would be the same as the picked points (white spheres,

right side). When migrating to a point, we know what direction we are headed because the arrow on the crosshair is pointing in that direction. We simply move until our crosshair is over the point.

Test 3: Calibration Lane Area—Fixed Grid Anomaly Interrogations Evaluations

- These 19 locations will be interrogated in both a fixed grid and dynamic mode. The fixed grid data set will be gathered based on a fixed grid mesh or marked carpet centered on the reacquired location for a 1.2 m square area at .2 m intervals with a sensor height at .15, .30, and .45 m heights (147 points). Standoff will be established by plastic head spacers or movement of the head position up a position pole. The individual point data captured will be compared from relative positioning among the points captured to the fixed grid. Based on the 3-D data captured, a revised dig list location will be selected. The refined dig list coordinates will be compared to the seeded location coordinates from Appendix G, area mapping dig list coordinates from Test 1, and the flagged coordinates from Test 2.

Table 1 contains the anomaly identifications used by GIS.

Anomaly #	ATC ID	Target ID	Depth (m)	Azimuth	Dip
1	A6	57mm M86	0.4	0 az	45
2	C6	57mm M86	0.4	0 az	90
3	E6	57mm M86	0.91	0 az	0
4	A7	60mm M49A3	0.5	0 az	45
5	C7	60mm M49A3	0.5	0 az	90
6	E7	60mm M49A3	1	0 az	0
7	H7	81mm M374	0.5	0 az	45
8	J7	81mm M374	0.5	0 az	90
9	L7	81mm M374	1.5	0 az	0
10	A8	2.75" M230	0.5	0 az	45
11	C8	2.75" M230	0.5	0 az	90
12	E8	2.75" M230	1.2	0 az	0
13	G10	8# SHOT	0.2		
14	B13	105mm M60	0.9	0 az	45
15	F13	105mm M60	0.9	0 az	90

Table 1. Anomaly Identification used by GIS.

The data files for this test are contained in the directory Test_3.

Directory Contents:

calibration_fixed_grids_final.xls – test results in Corps supplied format
CP_*_1_*.txt. – Data points as saved in field
CP_*_1_*.txt.final – data points with compass correction applied

This test demonstrates a procedure problem on our part. In order to determine the bearing of the ultrasonic array, we use an electronic compass which is susceptible to perturbations in the magnetic filed caused by large electromagnetic (EM) sources. On the Aberdeen site, we calibrated the compass approximately 100 ft from the trailer. We assumed that this calibration would be valid over in the calibration grid several hundred yards away and for the woods grid also. This was not the case. A large EM source affects the site, growing stronger from West to East. In the field we saw the compass error, but our procedures were not robust enough to deduce that it was not a constant offset (like a declination error). Therefore we applied a constant correction. As it turns out, the error was variable with the maximum error when pointing North and South and the minimum error (essentially zero) when pointing East and West. The maximum error in the calibration grid was 4°. The maximum error in the woods was 12°. We believe the source may be the large power lines at the edge of the woods.

After we discovered this calibration error, we reprocessed the data with the variable function. This reprocessed data is in files labeled **CP_*_1_*.txt.final**.

On the new platform, we have added the ability to conduct comprehensive compass checks and calibrations in a minimum amount of time and with relative ease. Where a single-point compass calibration is not sufficient, such as for a variable source, we have added the ability to map the variation in the grid and apply a variable correction real-time. The correction we made on the data for this test is more of a Band-Aid and does not represent the quality we can expect in the future. Nevertheless, this error only affects the global positioning of the head. What is really important for analysis of the 3-D volume is the coherency of the secondary positioning system, in other words, how accurate the incremental positioning of the head reports in the local volume.

Due to time constraints we were able only to complete 15 of the 19 targets. We actually did the test twice, but the first time we were having problems with our GPS software, causing the primary position to be way off. We got this problem corrected, but by this time, we were having problems with the ultrasonic units. Our power supply was acting flaky because of the cold. This caused a voltage fluxuation, which meant that the positioning would wander. The error was not too bad, but we know the system works better than this. In the new platform we have put in new much larger power supplies in a protected container that can be heated if necessary. Additionally, by this time our composite ultrasonic array had cracked due to the cold. This caused a warping in it, which accounts for some of the warping in the array images. We made the receiver array on the new platform with aluminum tubing.

Figure 6 shows a scatter plot of the array at the 15 cm level. Loss of continuity is evident, especially along the edges of the array. Figure 7 shows the scatter plot of the 30 cm level, and Figure 8 shows the scatter plot of the 45 cm level. In spite of the voltage problems with ultrasonic units and the array frame cracking, the internal coherency is still fairly good.

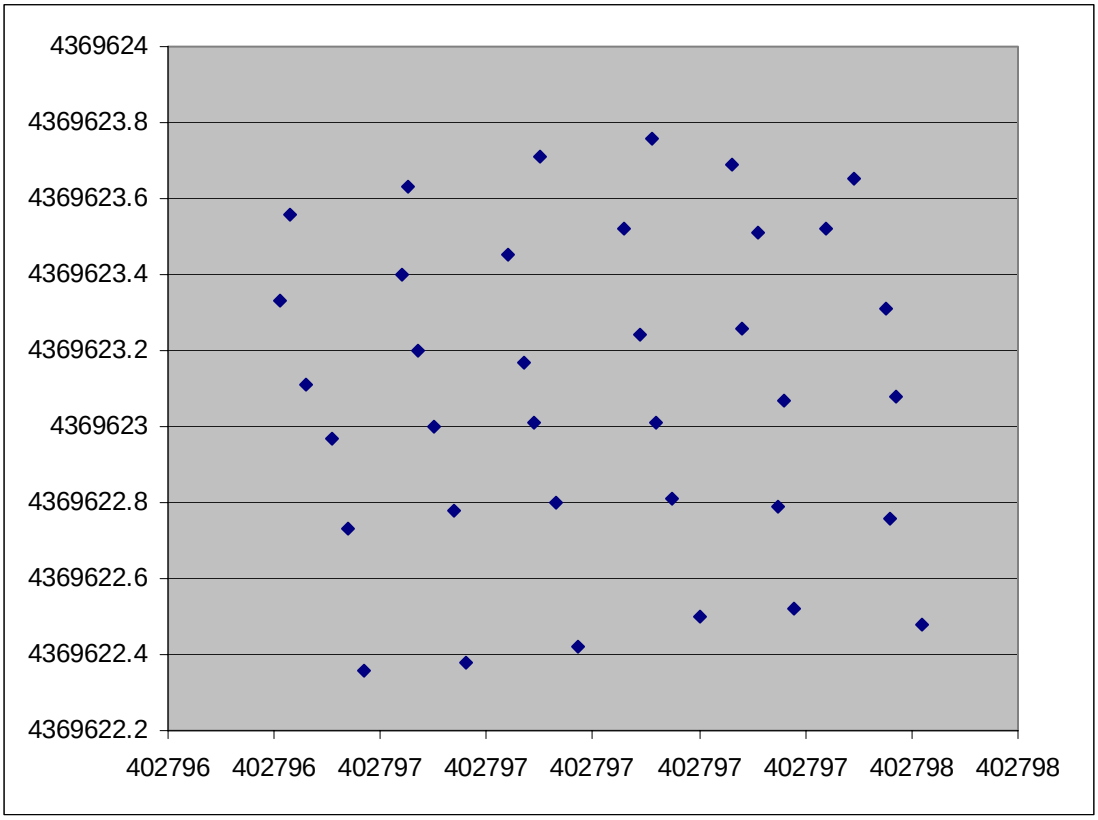

Figure 5. Target 6C, 15 cm Level

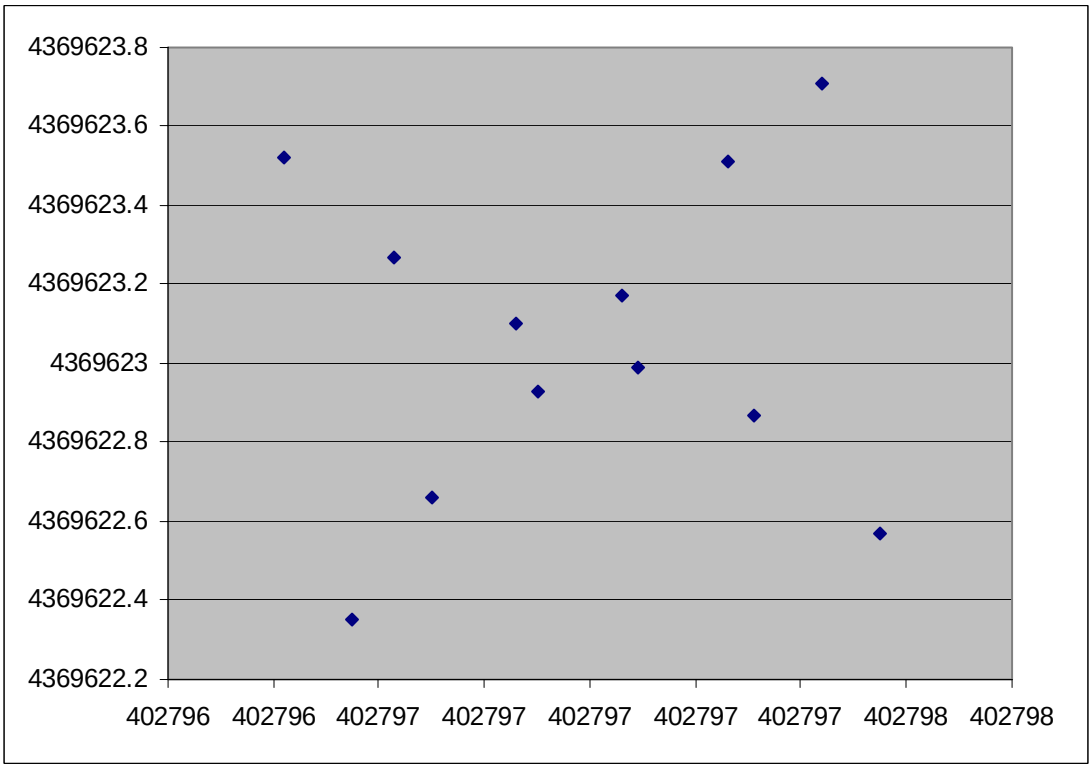

Figure 6. Target 6C, 30 cm Level

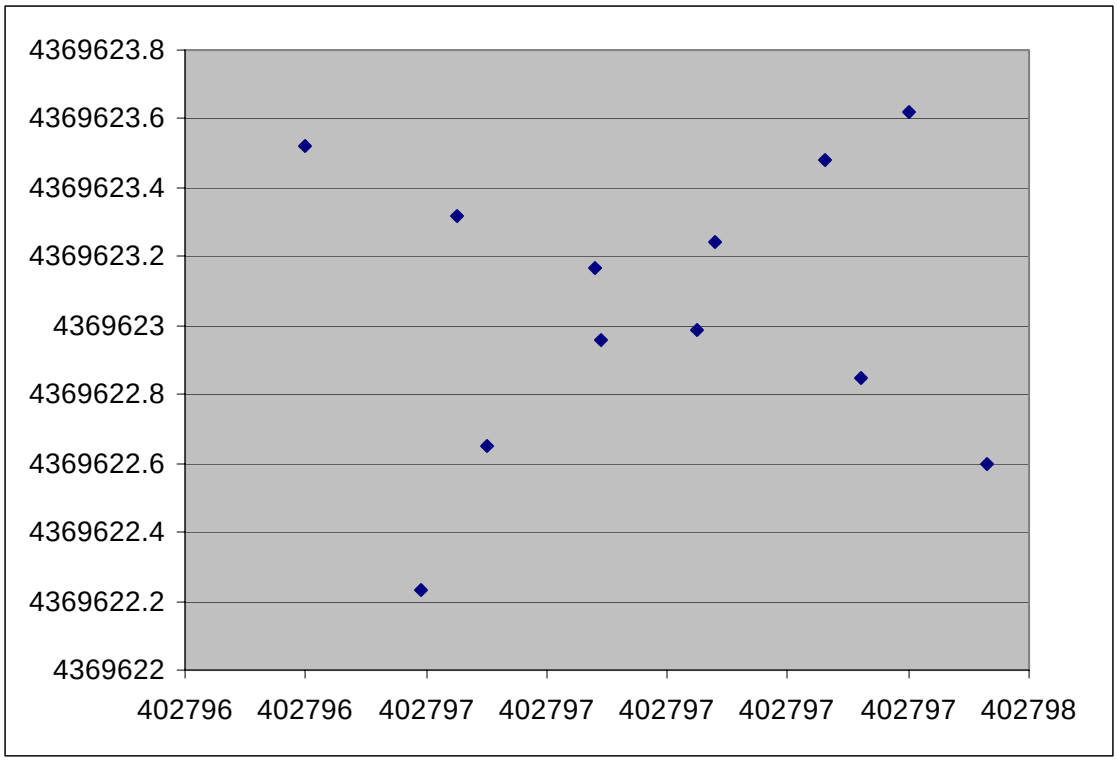

Figure 7. Target 6C, 45 cm Level

Test 4: Calibration Lane Area—Dynamic Anomaly Interrogations Evaluations

- The 19 anomalies will then have a dynamic 3-D data set acquired by walking an approximately 2 m square area with the sensor head at multiple heights or by swinging and lifting the handheld sensor over the anomaly area as required by the individual systems. The objective will be to capture a similar data set as in Test 3 but in a rapid more random unguided field methodology that will rely upon the navigation system's dynamic position accuracy with a continuous sensor and navigation data stream. Based on the 3-D data captured, a revised dig list location will be selected. The refined dig list coordinates will be compared to the seeded location coordinates from Appendix G, area mapping dig list coordinates from Test 1, the flagged coordinates from Test 2, and fixed grid location from Test 3.

This data is in the directory Test_4

Directory Contents:

Dat_*_*_A*.txt - Raw serial output from all the system devices.
XYZDat_*_*_A*.xyz. – Contains the ASCII post-processed data in the form below. The file is created when the operator tells the system he is finished with the current anomaly.
AllDynamicAnomalies.xls – Excel spreadsheet containing all the data from the anomalies in the form below:

Data Form:

Head East,
Head North,
Head Elevation off the Ground,
Instrument Reading,
Hour,
Min,
Sec,
Blank,
Total Head Elevation

A*_AnalysisGrid3D_*.txt. – Sparse matrix. The file is written with the following code. Each pixel in the matrix represents 40 mm.

```
for (lev=0; lev<m_gridLevels; lev++)
{
        for (i=0; i<m_gridRows; i++)
        {
                for (j=0; j<m_gridColumns; j++)
                {
                        fprintf(OUTANOM2,"%lf\n",m_gridDouble[i][j][lev]);
                }
        }
}
```

The 3-D dynamic volumes are visualized real-time in GeoVizor. Figure 8 shows three representations of the volumes of a 60 mm buried at .5 m with a 90° dip (C7). The upper left image shows a dipole view of the raw geophysical signature. This image is made by defining the skins to represent a value of 99% of the positive pole (Red) and 99% of the negative pole (Blue). The upper right image is made by defining the skins to represent a value of 95% of the positive pole (Red) and 95% of the negative pole (Blue). The lower left image shows the result of “Frag Zone” algorithm, which will be described later for Test 9.

Figure 8 also demonstrates that attempting to use a 2-D slice survey (single height DGM) will not capture the maximums of both poles, thus making accurate inversion modeling difficult.

As with the previous test, this test was done twice, the GPS did not work in the first series, and the ultrasonics were flaky in the second. Because we are being judged by the total positioning accuracy, we are submitting the second series for analysis. The first series is available for review in the subdirectory labeled FirstSeries.

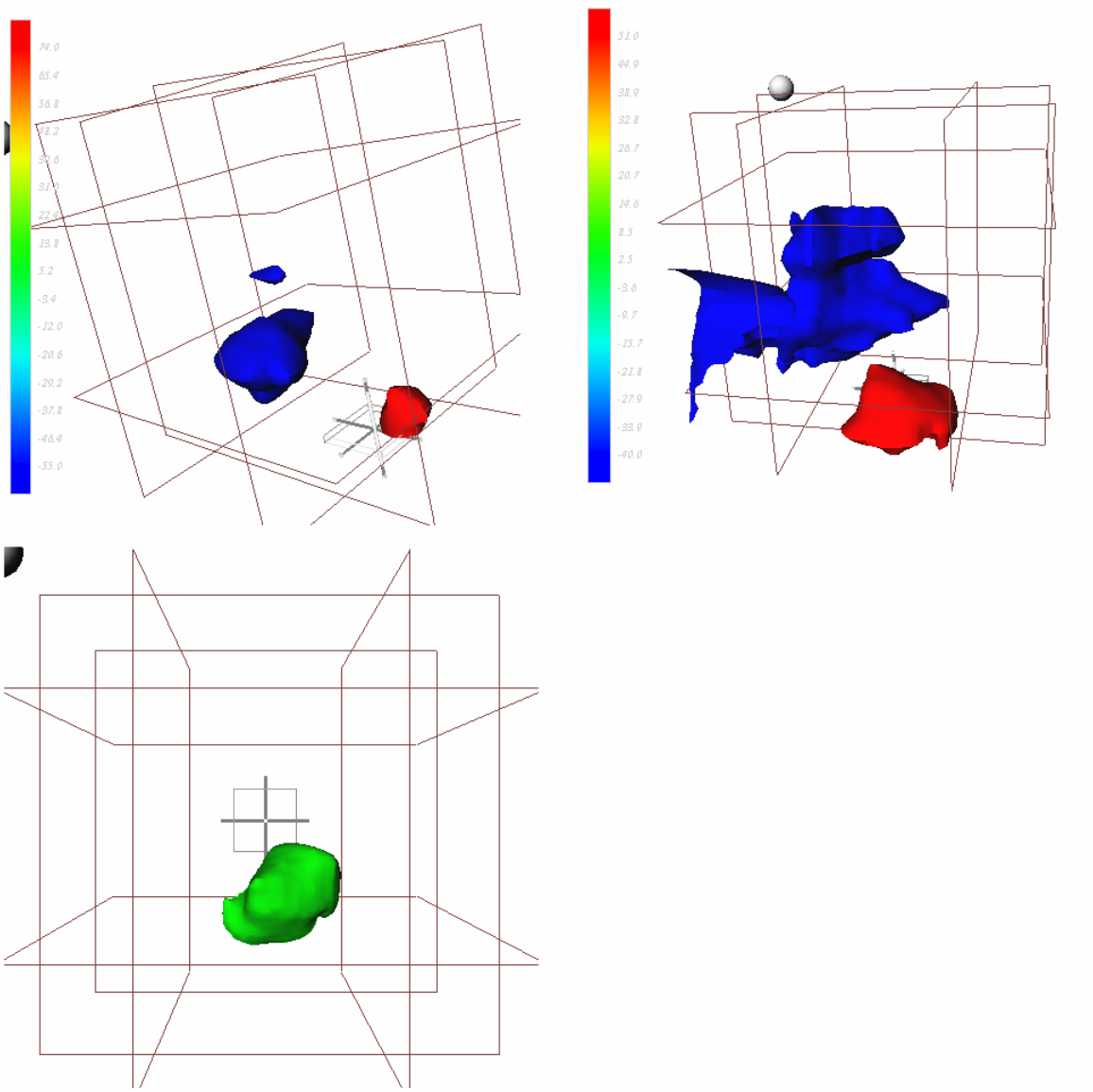

Figure 8. Volume Representation (C7) 60 mm, 0.5 m depth, 90° dip (Second Series). Top views are oblique from top. Bottom is looking down on volume.

Figures 9 and 10 represent, respectively, the scatter plot of the East North positioning for the above object, first series (Bad GPS, Good ultrasonic) and the scatter plot of the East North positioning for the above object second series (Good GPS, Bad ultrasonic). It is clear how tight and consistent the ultrasonic reporting is in the first series. We can expect this quality from the new platform (Good GPS, Good ultrasonic). The magenta dots are the true target location and the board corners.

Figure 11 shows the same representation for the Figure 8 target but using the first series as the input. In spite of the ultrasonic problems in the second series, the volume images from Figure 8 and Figure 11 are fairly close in location, structure, and value because the GeoVizor system has such dense sampling that the positioning errors in the second series

are pretty much “averaged out.” Nevertheless, we are not satisfied with the “averaged out” solution so we fixed the problem in the new platform. Appendix A contains the 3-D volume images for all 15 targets we imaged (Second Series).

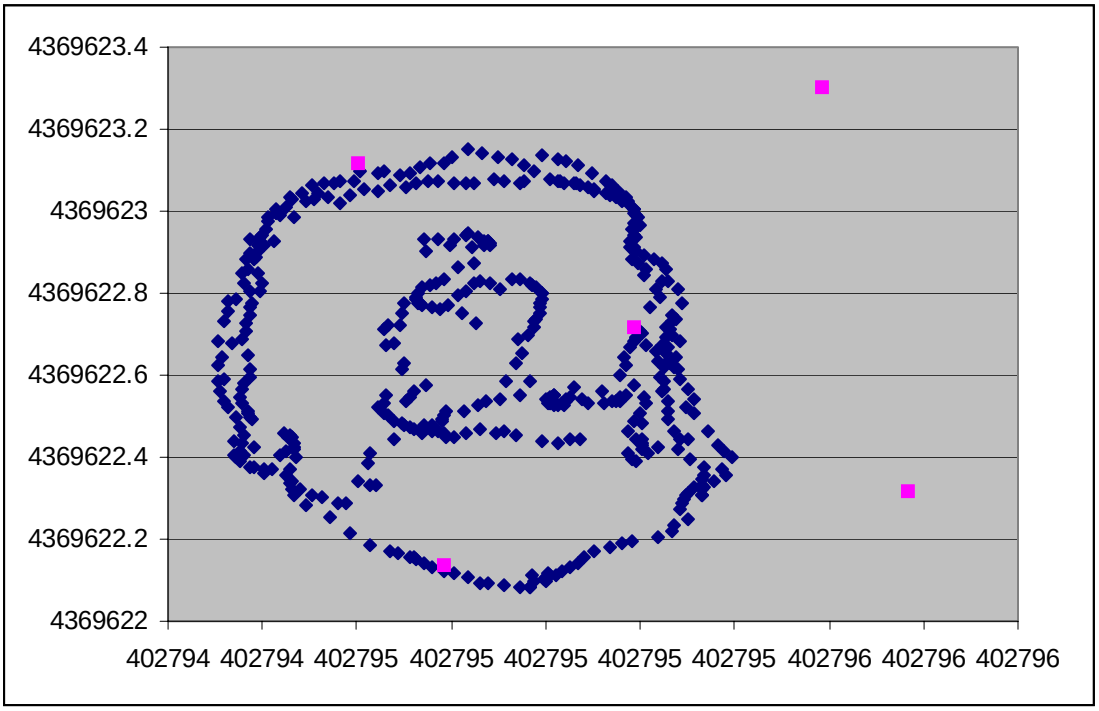

Figure 9. (C7) First Set (Bad GPS, Good Ultrasonic)

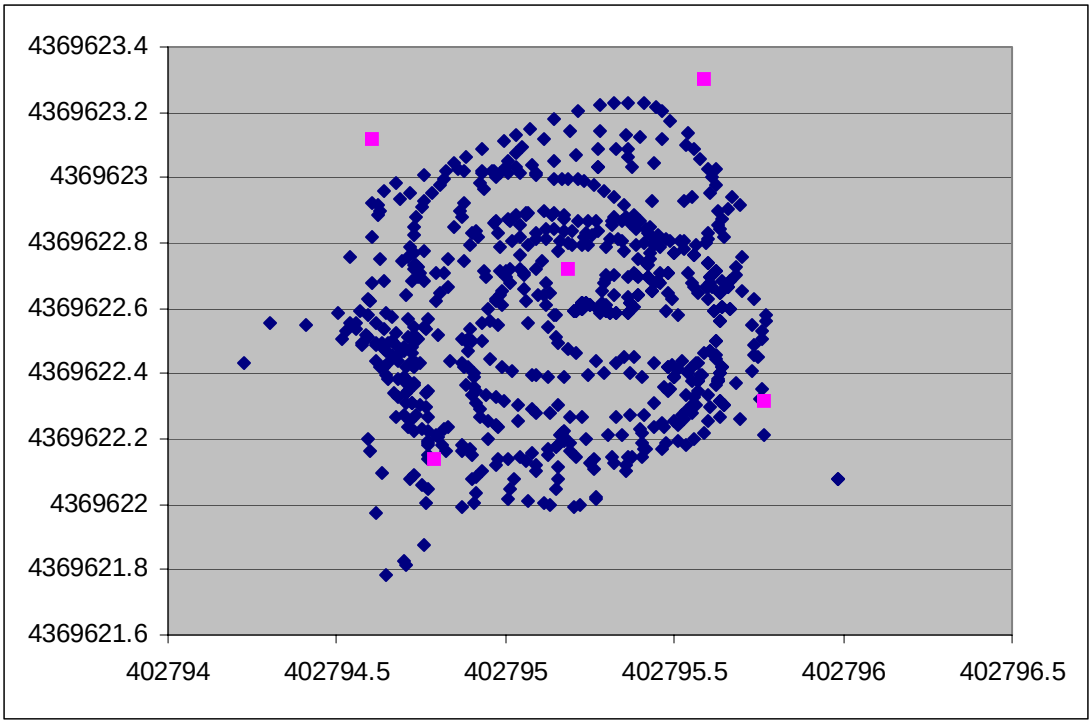

Figure 10. (C7) Second Set (Good GPS, Bad Ultrasonic)

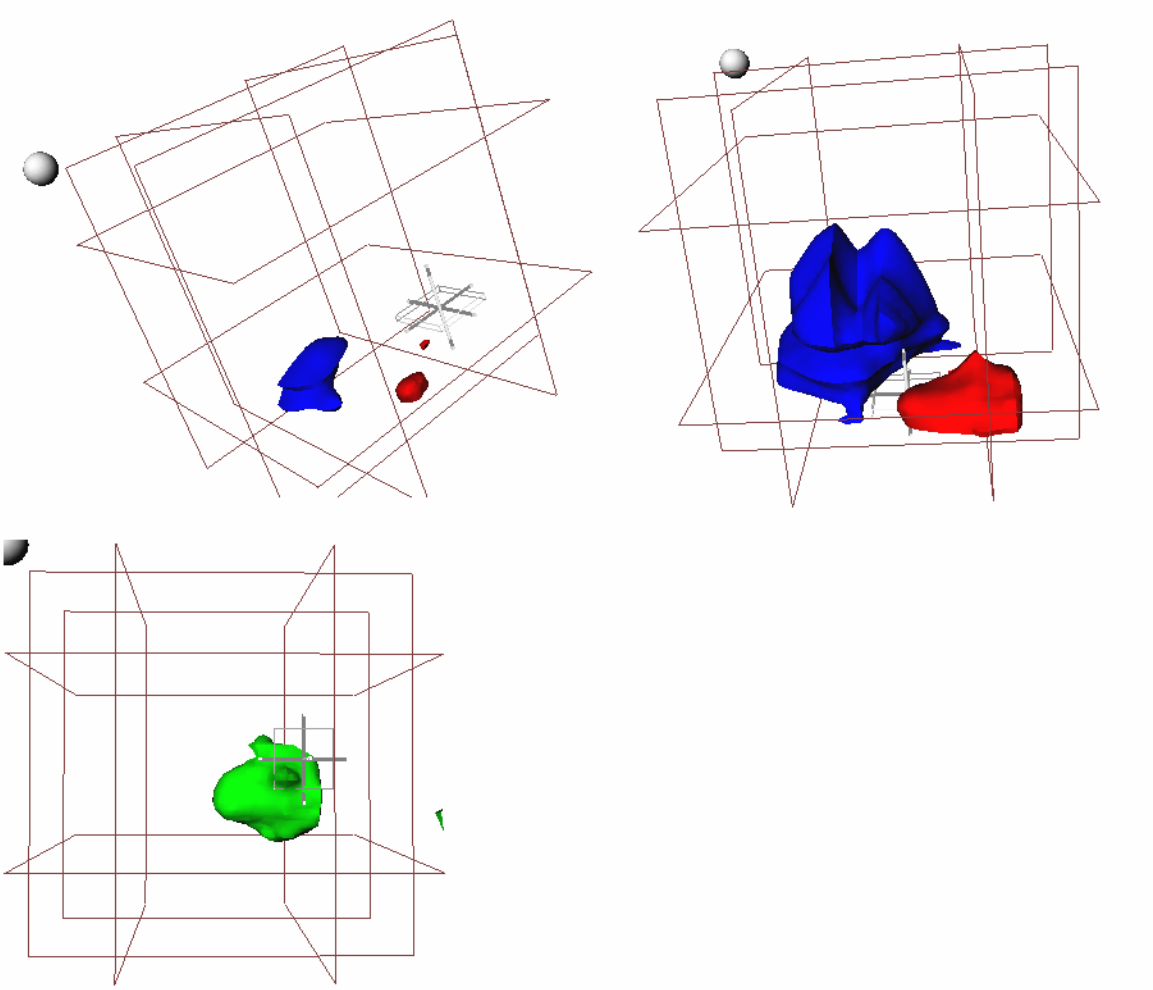

Figure 11. Volume representation (C7) 60 mm, 0.5 m depth, 90° dip (First Series). Top views are oblique from top. Bottom is looking down on volume.

Test 5: Wooded Area—Accuracy with positioning system for surface points

- The wooded area has six unknown permanent rebar points within the interior. These positions are placed in areas without nearby adjacent geophysical anomalies. Forty additional, widely scattered points are established by PVC pipe with removable steel pins (when required to trigger the magnetometer). Each shall be occupied by the integrated navigation/geophysical sensor system to determine coordinate locations. These will be directly compared to the ground truth for position accuracy.

Test results are in the directory Test_5

WoodsStaticPoints.xls – Excel spreadsheet with data in the form:

East North Elevation Instrument_Reading Hour Min Sec.

Figure 12 shows the static test points in the woods. Our conclusion from the comparison of the static and dynamic tests is that the GPS did not work very well in the woods except for the outermost targets.

We did not have time to demonstrate our alternative laser/compass primary positioning system for this test.

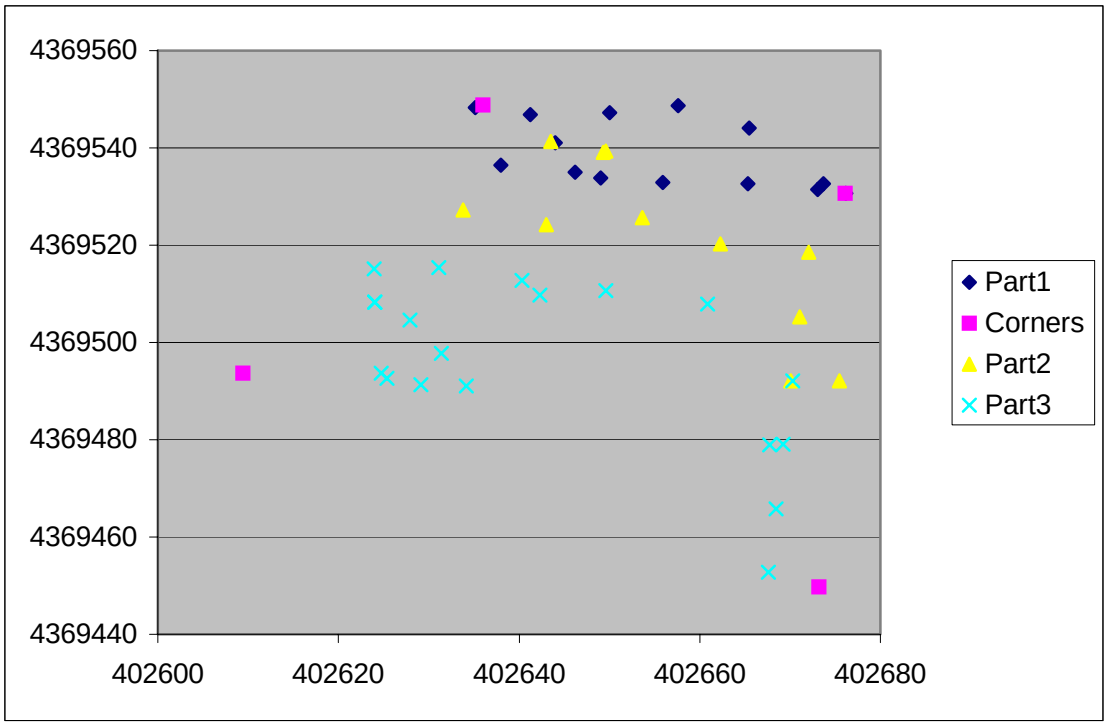

Figure 12. Woods Static Points

Test 6: Wooded Area—Accuracy from Geophysical Data Analysis for surface points

- The 46 points from Test 5 will be traversed dynamically by the integrated system. These points shall be picked from the instrument peaks shown in the data set and reported. These will be directly compared to the ground truth for position accuracy and to the locations from Test 5.

The data from this test is found in directory Test_6

Directory Contents:

Dat_*_*_A*.txt - Raw serial output from all the system devices.
Line_*_Data.xyz. - Contains the ASCII post-processed data. The file is created when the operator tells the system he is finished with the current line.
WoodsdynamicPoints.xls – Excel spreadsheet containing all the data from the lines including the comparison with the static points.

The points that were traversed were walked using 21 line segments.

Our conclusion from the comparison of the static and dynamic tests is that the GPS did not work very well in the woods except for the outermost targets. Even in the outermost points, our compass problems described earlier compromised the test. Figure 13 shows the tracks for the woods dynamic survey. As each segment was walked as a straight line, you can see the wander of the GPS in the trees.

We did not have time to demonstrate our alternative laser/compass primary positioning system for this test.

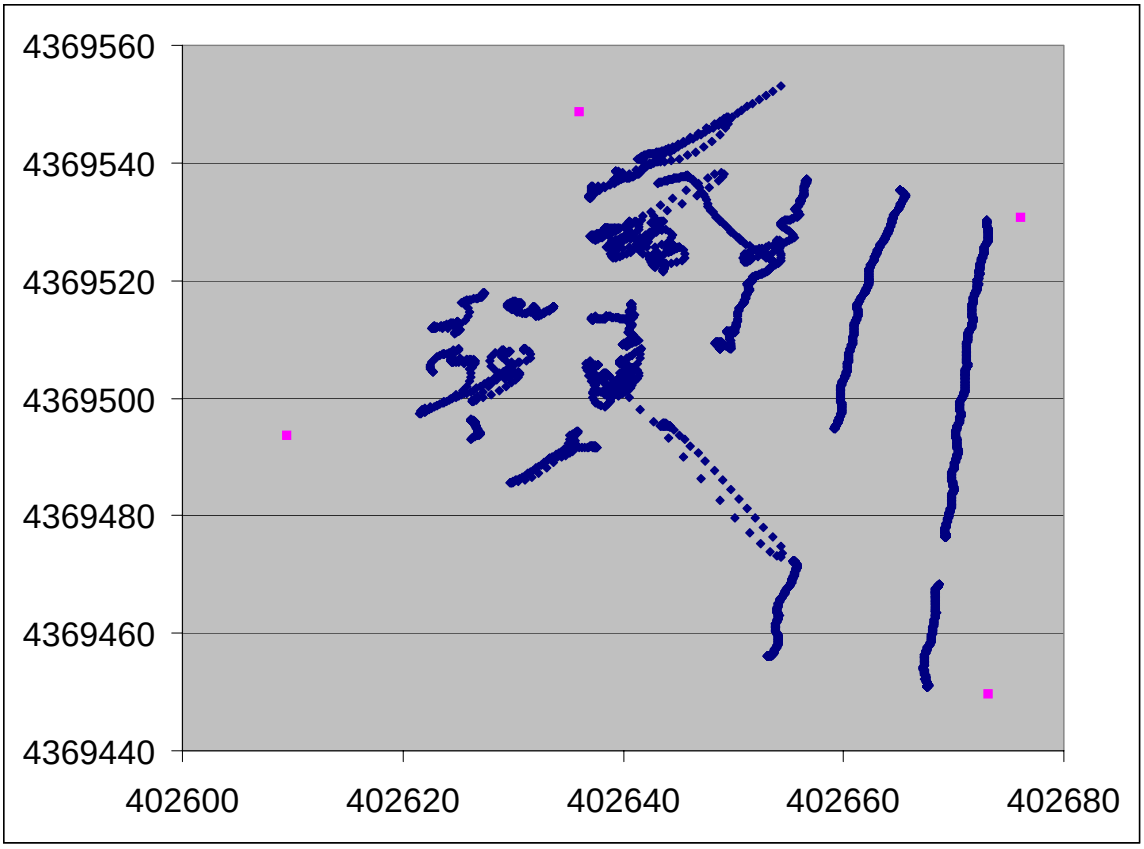

Figure 13. Woods Dynamic Lines

Test 7: Wooded Area—Area Mapping

- The approximately 1 acre area will be mapped with the data analysis using the GFE G-858 sensor (with magnetometer base station) integrated with the navigation equipment at approximately 1 m spacing in an approximately E-W direction. The steel pins will be removed from the 40 points described in Test 5 so as not to affect the subsurface anomaly results.
- The selection threshold for anomaly selection for the wooded area will be based upon the instrument reading for all items larger than the 57 mm M86, as shown by the Calibration Lanes area mapping from Test 1. The dig list selected will be evaluated by Aberdeen Proving Ground (APG) with emphasis based upon position accuracy. Ground truth locations will be available for more in-depth evaluations in August 2004.

This test was not completed.

Test 8: Wooded Area—Dynamic Anomaly Interrogations

- Ten well-defined anomalies will be selected from the Test 7 results for interrogation. The 10 anomalies will then have a dynamic 3-D data set acquired as in Test 4 by walking an approximately 2 m square area with the sensor head at multiple heights or by swinging and lifting the handheld sensor over the anomaly area as required by the individual systems. Based on the 3-D data captured, a revised dig list location will be selected. The data will be used by others to help evaluate and develop geophysical modeling and discrimination algorithms when the ground truth locations are available in August 2004.

This test was not completed.

Test 9: Wooded Area—Dynamic Anomaly Positioning

- An anomaly array board 1.2 m square will be created. It will have an irregular array of nails inserted (point into the ground) for point source anomalies. This board will be randomly placed in an area clear of subsurface anomalies adjacent to each of the six rebar points. This shall be mapped in a similar manner to Test 8. The individual nail location positions shall be selected as a dig list from the instrument peaks. The government will compare the relative position of the dig list points to the array positions and report the deviation from the location.

This test was completed for five rebar points. The data for this test is found in the directory Test_9.

Directory Contents:

Dat_*_*_A*.txt - Raw serial output from all of the system devices.
XYZDat_*_*_A*.xyz. - Contains the ASCII post-processed data in the below form. The file is created when the operator tells the system he is finished with the current anomaly.
AllNailBoards.xls – Excel spreadsheet containing all of the data from the anomalies in the below form:

Data Form:

Head East,
Head North,
Head Elevation off the Ground,
Instrument Reading,
Hour,
Min,
Sec,
Blank,
Total Head Elevation

A*_AnalysisGrid3D_*.txt. – Sparse matrix. The file is written with the following code. Each pixel in the matrix represents 40 mm.

```
for (lev=0; lev<m_gridLevels; lev++)
{
        for (i=0; i<m_gridRows; i++)
        {
                for (j=0; j<m_gridColumns; j++)
                {
                        fprintf(OUTANOM2,"%lf\n",m_gridDouble[i][j][lev]);
                }
        }
}
```

Appendix B contains the images from the five nail boards that were imaged.

The 3-D dynamic volumes are visualized real-time in GeoVizor. Figure 14 shows three representations of the volume over the nail board. This was anomaly 5 in the directory. The upper left image shows a dipole view of the raw geophysical signature. This image is made by defining the skins to represent a value of 99% of the positive pole (Red) and 99% of the negative pole (Blue). The upper right image is made by defining the skins to represent a value of 95% of the positive pole (Red) and 95% of the negative pole (Blue). The lower left image shows the result of Frag Zone algorithm. The Frag Zone algorithm isolates small dipoles and monopoles that are typically overwritten by a larger nearby emitter. The green is the positive pole of the rebar. The red and blue are the small poles created by the nails in the board.

Note that every target in the Calibration grid (Appendix A) was imaged using the same Frag Zone algorithm with the same input parameters, and none of them indicate the presence of small emitters, indicating that the small poles are not artifacts of the algorithm.

Note that the nail dipoles do not correspond directly with the locations of the nails on the board. This is not a positioning error of the system. The G-858 magnetometer cannot see directly underneath it. There is a dead zone extending in a cone from the center of the head downward with a cone slope of about 20°. Therefore, the dipoles are amalgamations of the emitter responses surrounding the head at any given moment.

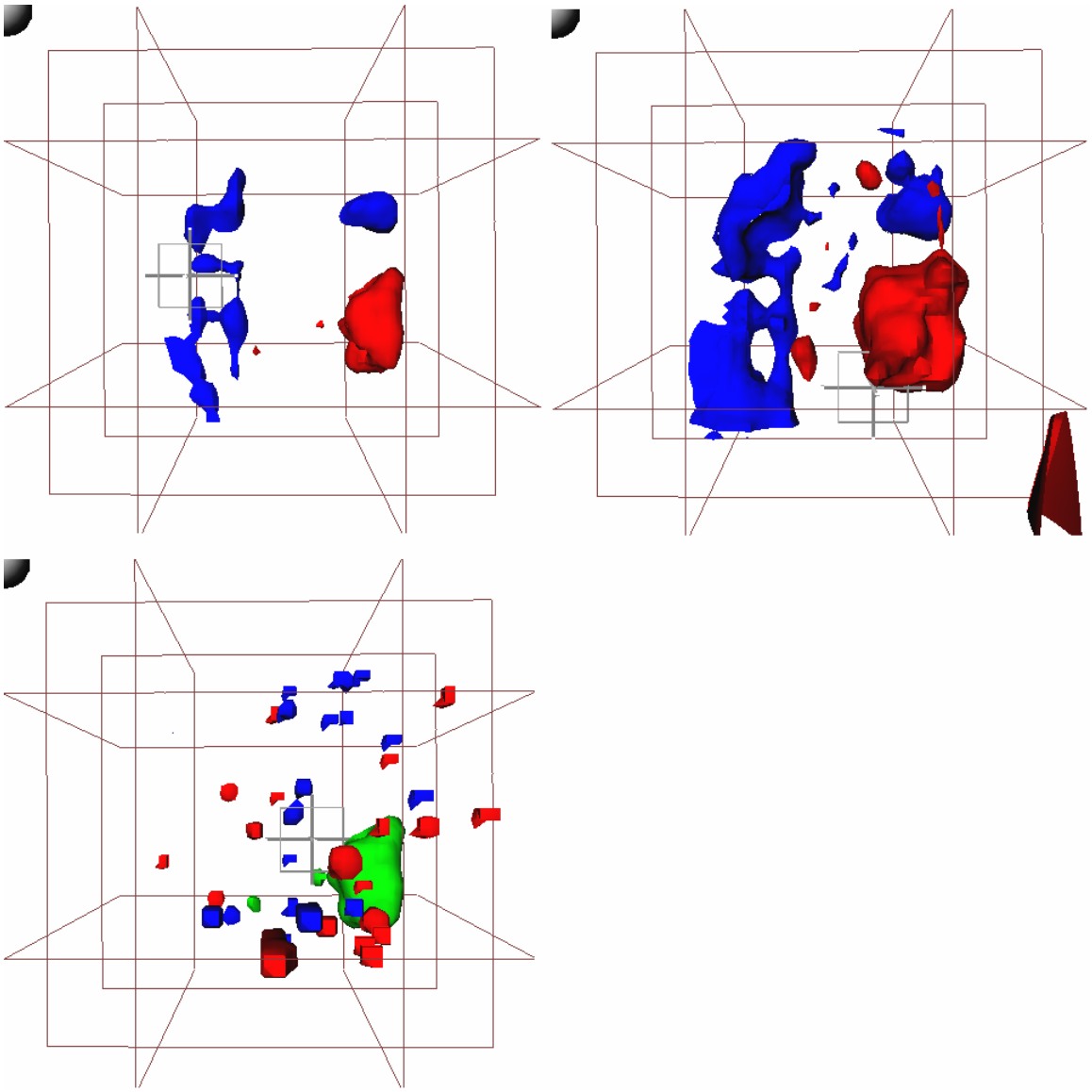

Figure 14. Nail Board—Top View

Figure 15 shows an example where the nail board was randomly laid over a piece of UXO in the woods grid. Note that two primary emitters are isolated in this case.

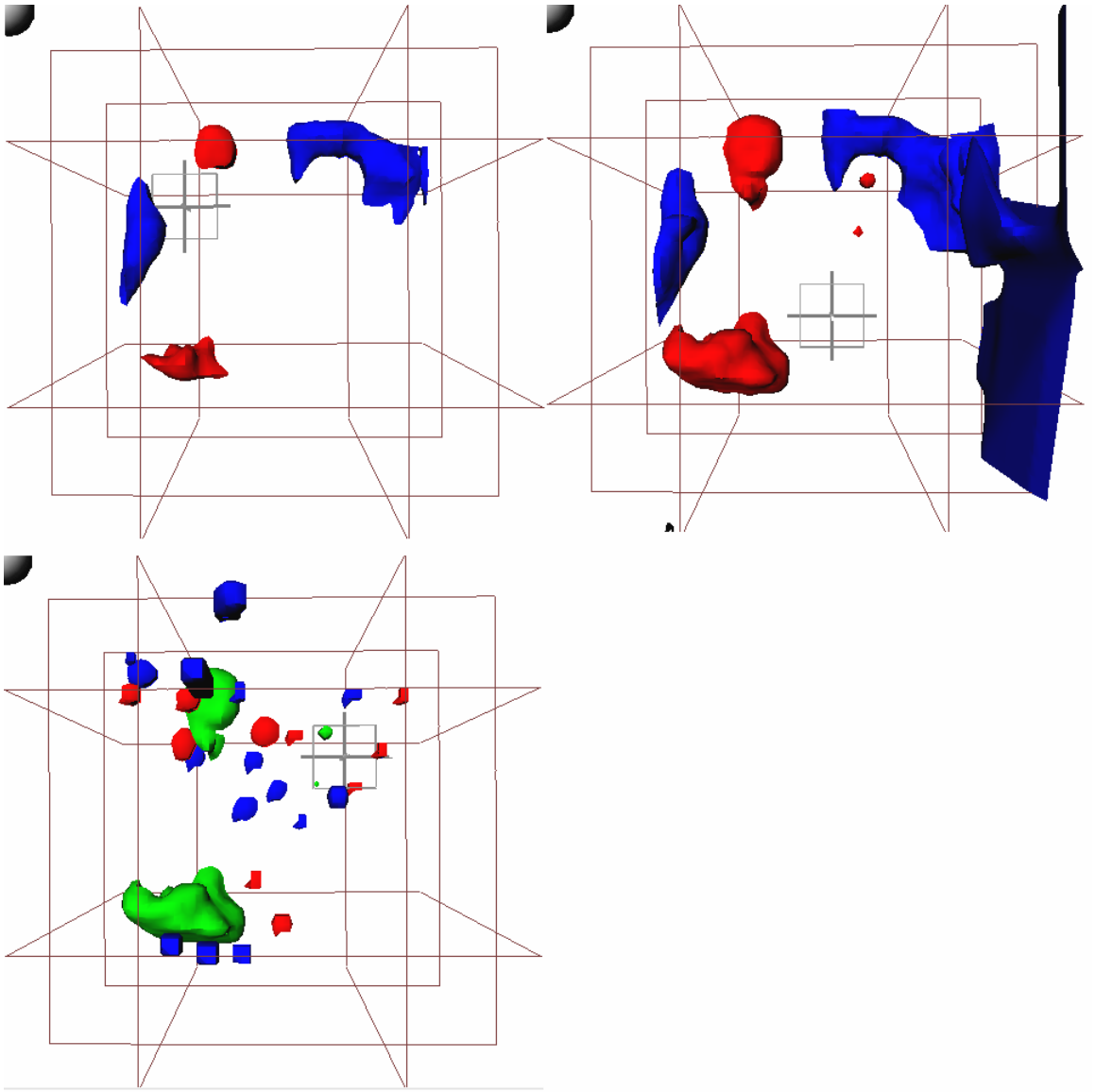

Figure 15. Nail Board over UXO—Top View

The Frag Zone algorithm also vividly demonstrates why 2-D digital geophysical mapping has failed to produce data that can consistently be used for analysis, such as inversion modeling. Figure 16 shows two views of the nail board volume from Figure 14 and two views of the nail board volume from Figure 15.These images are made real-time just by spinning the volume. All images are taken from the side of the volumes so that the ground is at the bottom of the image, as opposed to Figures 14 and 15, which are looking down at the board from the top of the volume. This image demonstrates that attempting to use a 2-D slice survey (single-level DGM) will often not capture the maximums of both poles and will result in losing most of the nail (frag) dipoles.

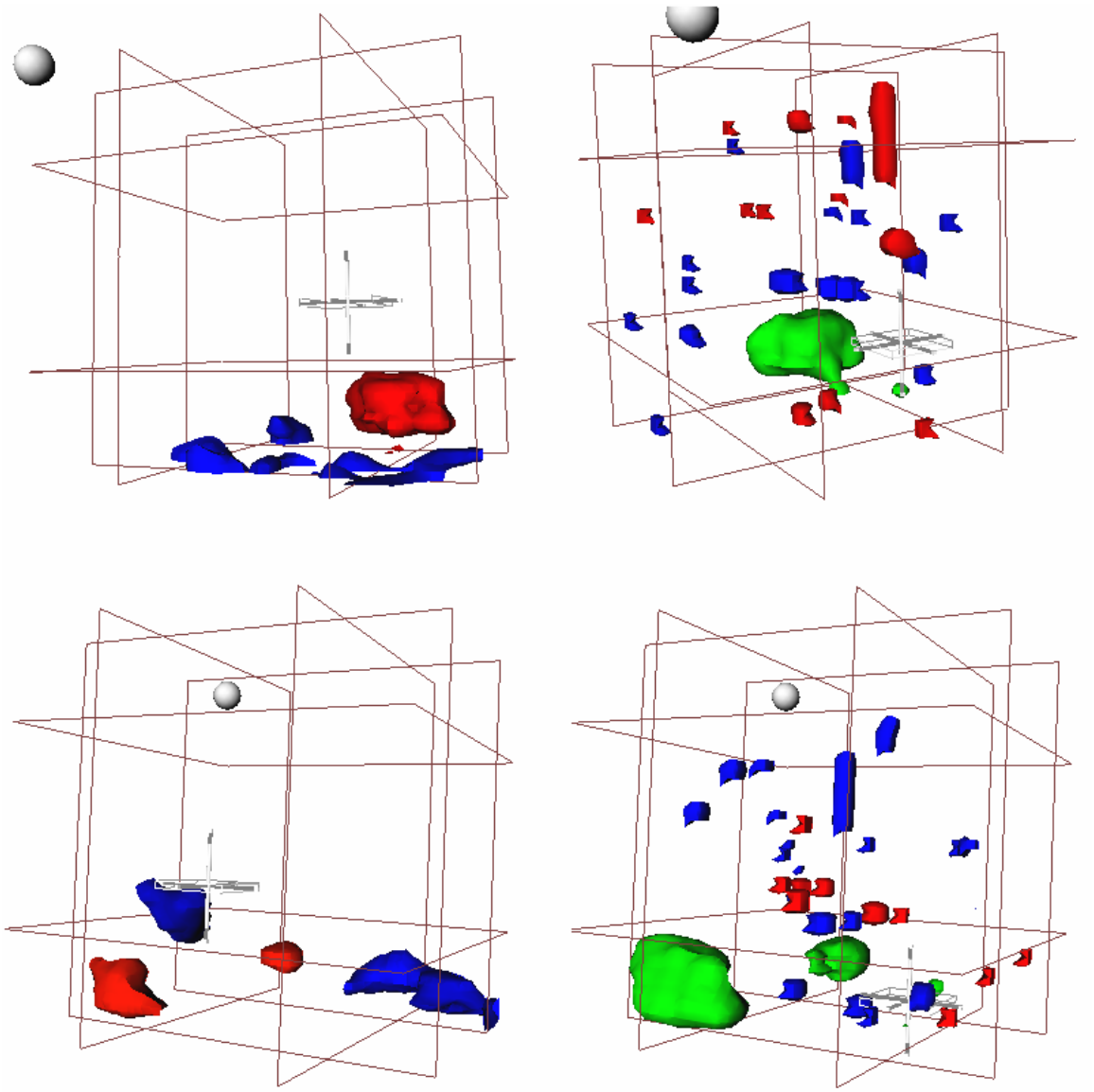

Figure 16. Side Views of Data Volumes

Test 10: Mogul Area—Accuracy with positioning system for surface points

- The mogul area has 20 unknown points established in a varied array traversing a portion of the large and medium moguls with widely varying slope and elevation. The points are PVC pipe with removable steel pins (to trigger the magnetometer when required). Each will be occupied by the integrated navigation/geophysical sensor system to determine coordinate locations. These will be directly compared to the ground truth for position accuracy.

The data from this test is found in the Test_10 directory.

Directory contents:

CP_*_*_*.txt – original point locations
Moguls.final.xls – Excel spreadsheet with compass adjusted positions

East
North
Elevation
Instrument Value
Hour
Min
Sec

Figure 17 shows the scatter plot for the static positions.

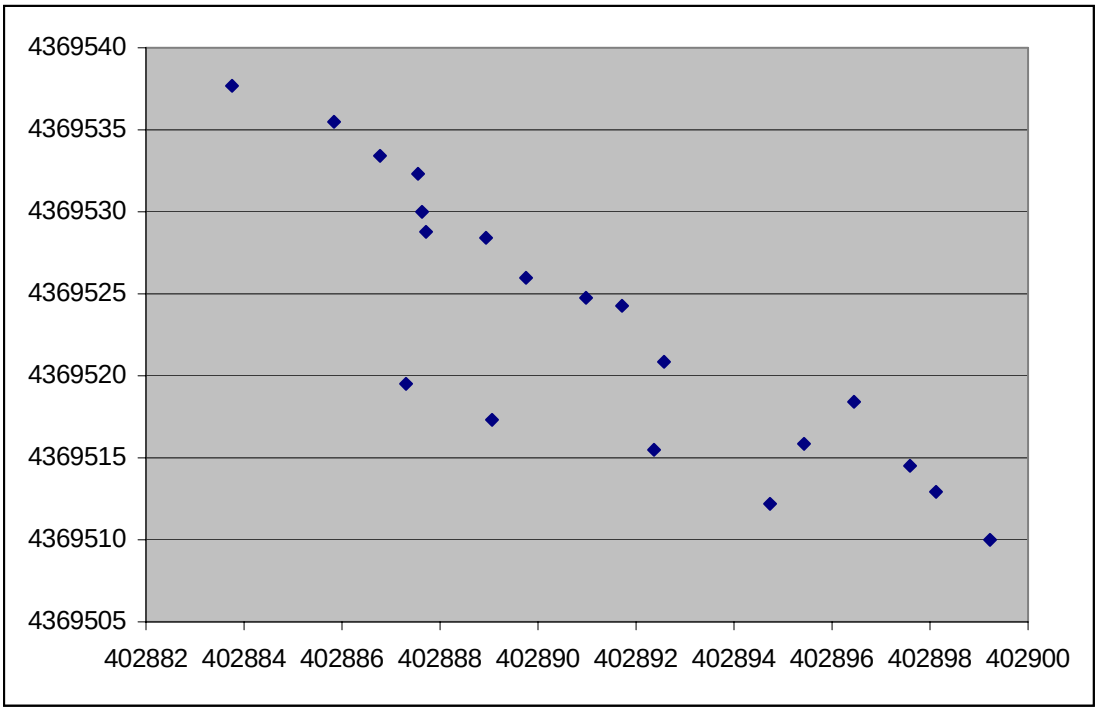

Figure 17. East-North Scatter Plot of Static Positions—Moguls

Test 11: Mogul Area—Accuracy from Geophysical Data Analysis for surface points

- The 20 points from Test 10 will be traversed dynamically by the integrated system. These points will be picked from the instrument peaks shown in the data set and reported. These will be directly compared to the ground truth for position accuracy and to the locations from Test 10.

Directory Test_11 contains the data from this test.

Directory Contents:

Dat_1_1_L*.txt. - Raw serial output from all of the system devices.
Line_*_Data.xyz. - The post-processed files that are dropped when you tell the computer you are at the end of a line.
Line_*_Data.xls. - The post-processed files in Excel spreadsheet form that are dropped when you tell the computer you are at the end of a line.
LinePicks.xls - Excel spreadsheet contains the comparison between the static and dynamic tests.

Figure 18 contains the locations of the static acquisitions and the picks made by us. The average error of these picks from the static positions is .33 m. Where multiple targets were found along a line (buried unexploded ordnance [UXO]), all were picked and the closest one to the static point was selected. Figure 19 contains the closest actual positions to the static points along each line. The average error of these points is .15 m.

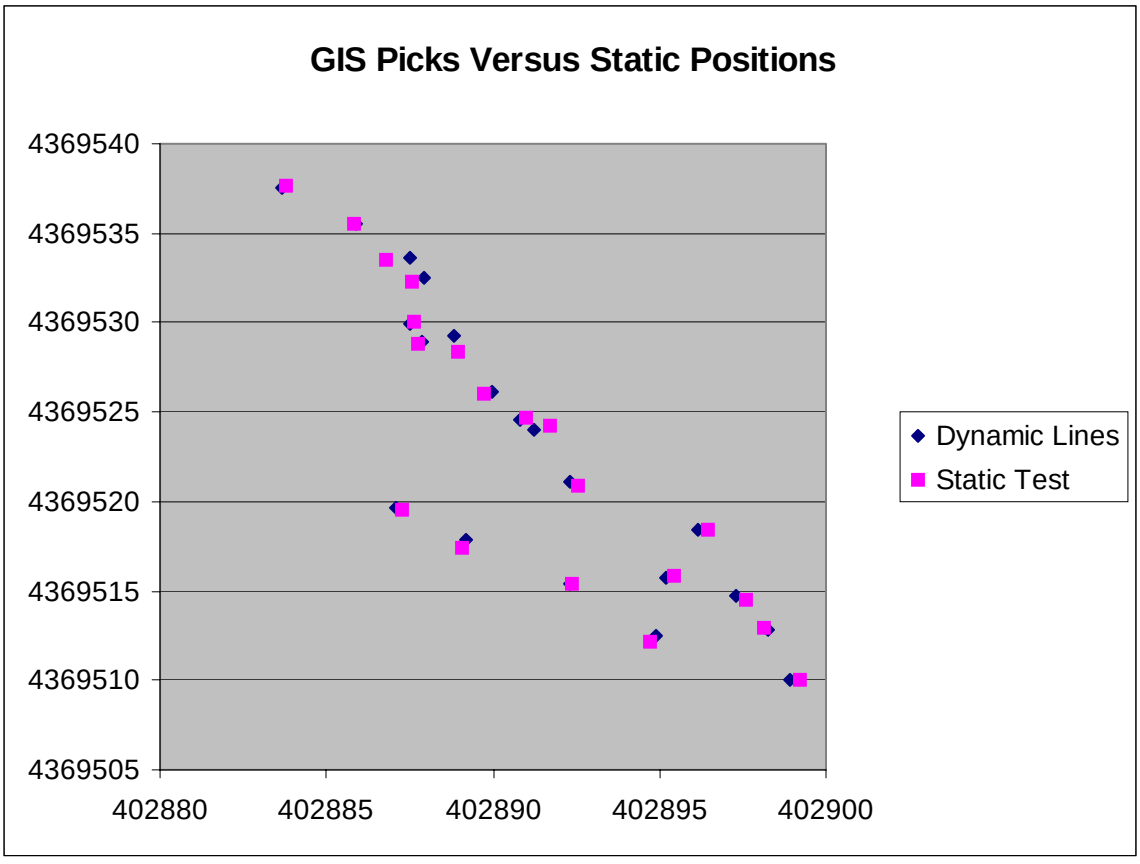

Figure 18. Locations of Static Acquisitions and Picks Made.

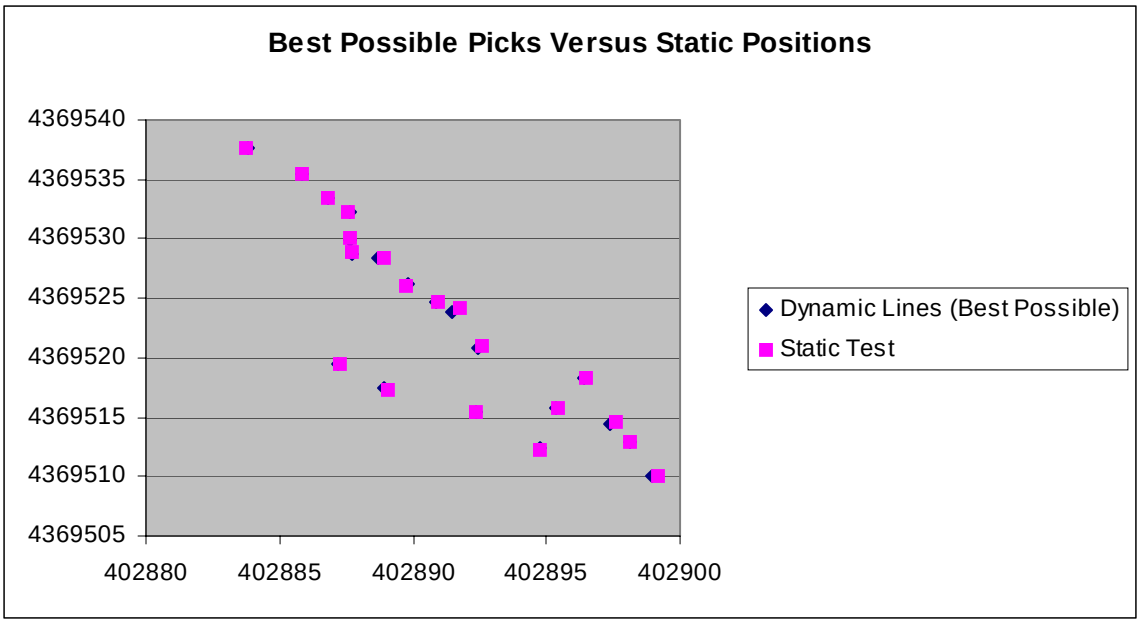

Figure 19. Closest Actual Static Positions to Static Points

New Survey Platform

The Aberdeen test demonstrated several weaknesses in the hardware configuration of the GeoVizor system. The first is that, in spite of the changes made since the McKinley test, the backpack configuration was not working for the Reacquisition/Interrogation mode. Because of the image stability requirements of the Corps of Engineers, the ultrasonic array needed to be independent of the operator, actually sitting on the ground. This requirement removes most of the advantages of the integrated backpack and adds new complexities in mandating a long cable tether going from the frame to the backpack. When all the equipment was added, the backpack became much too complex with wires and very overweight (approximately 50 lb).

Another issue was the difficulty in setting up and balancing the ultrasonic array on a tripod for every image. This could take up to five minutes, depending on the complexity of the terrain, which is much longer than the time required to image the anomaly (approximately 1 minute).

When we returned to Colorado, we initiated the construction of a new survey platform for the Reacquisition/Interrogation mode (see Figure 20). It is an all-aluminum cart that has the array ultrasonic attached to it in manner that takes only a few moments to balance it. The cart has no axle, so it can go practically anywhere with a 24-in clearance. The cart has a compartment to carry all the system electronics and a large battery compartment so the system can be run all day without changing the battery. The compartments are completely waterproof and can be heated if necessary. The system can be pulled and operated by one person with little or no fatigue over the day. The entire cart can be broken down to fit into a shipping container for airline transport.

Figure 20. New Survey Platform

Current Mode of Operation

The operator wears the virtual reality (VR) glasses and the computer mouse and pulls the cart to each anomaly using the interactive positioning system (Figure 4). When he is over the anomaly, stops the cart, balances the array, and images it. He makes a dig decision, saves the data, and moves on.

System cost:

Ultrasonic units - $1,500
Cart - $1,000
Laptop computer - $1,500
VR glasses - $1,200
Software - $4,500

GPS – $29,000
Laser range finder- $3,000
Compass -$1,500

Total system cost is approximately $41,000.

Alternate System

An alternate mode of operation is to have a reacquisition team flag the anomalies. The operator then pulls the cart to the flag and tells the computer he is at X flag. He can see the DGM survey and flag position in his glasses (Figure 4). He images the anomaly and saves the data referenced to the flag position. This mode is much less expensive and

provides the same quality of 3-D image and decision tools as the GPS-enabled system. The only difference is that you would only know the true position of the anomaly within a meter for data archiving.

System costs:

Ultrasonic units - $1,500
Cart - $1,000
Laptop computer - $1,500
VR glasses - $1,200
Software - $4,500

The total cost for this high quality, 3-D imaging system would be less than $10,000.

Conclusion

The GeoVizor system provides an important new capability to the ordnance and explosives community. The ability to collect, visualize and analyze volumetric geophysical data in the field will make a large difference in being able to eliminate non-OE from excavation (Frag Zone algorithm, Test 9) and ensuring the OE is not left in field simply because it is too deep and had a marginal response in the original DGM survey.

We are anxious to take GeoVizor to the next level by completing the analysis subsystem and testing and validating the new survey platform with a full Environmental Security Technology Certification Program (ESTCP) test project.

Appendix I:

ArcSecond
Phase III Report

US Army Corps of Engineers
Engineering and Support Center,
Huntsville

Environmental Security Technology Certification Program

Innovative Navigation Systems to Support Digital Geophysical Mapping Phase III

APG Demonstrations

ArcSecond

Report

17 February 2005

ARMY Environmental Quality Technology Program

EQT

Acronyms

APG	Aberdeen Proving Ground
EDM	electronic distance measurement
GFE	government-furnished equipment

1.0 Experimental Design

Testing will be performed to validate performance. All surface points for navigation performance evaluations were previously surveyed in traditional civil surveying techniques by Aberdeen Proving Ground (APG) using a Total Station electronic distance measurement (EDM). This is planned for one-week field campaigns at APG. Testing order may be adjusted to facilitate production. Each area will have four known surface control points established along the perimeter of the area for establishing the local coordinates reference grid.

Test 1: Calibration Lane—Area Mapping

- Area map the 29 m by 37 m site (0.25 acre) using the government-furnished equipment (GFE) G-858 sensor (with magnetometer base station) integrated with the navigation equipment at 1 m spacing in an approximately E-W direction.
- Post process the data set (prior to the wooded area mapping) to create a dig list for the anomalies that are above a threshold established by the typical 57 mm M86 items in the Calibration Lanes. The dig list selected based on this threshold will be compared to the ground truth in Appendix G for position accuracy. This threshold value will also be used for anomaly selection for the wooded area mapping dig list.

Test 1: ArcSecond Results

Figures 1-1 through 1-4 show the results from the ArcSecond Test 1. The average error for the survey equaled 0.181 m, and the standard deviation equaled 0.146 m, as shown in Figure 1-1.

19 Anomalies	**Tolerances**		
	Easting	Northing	Radial
Average Error	-0.0284	0.0928	0.1812
Standard Deviation	0.1531	0.1500	0.1456

Figure 1-1. Summary ArcSecond Results from Test 1

Figure 1-2. Integrated ArcSecond/G858 Instrument

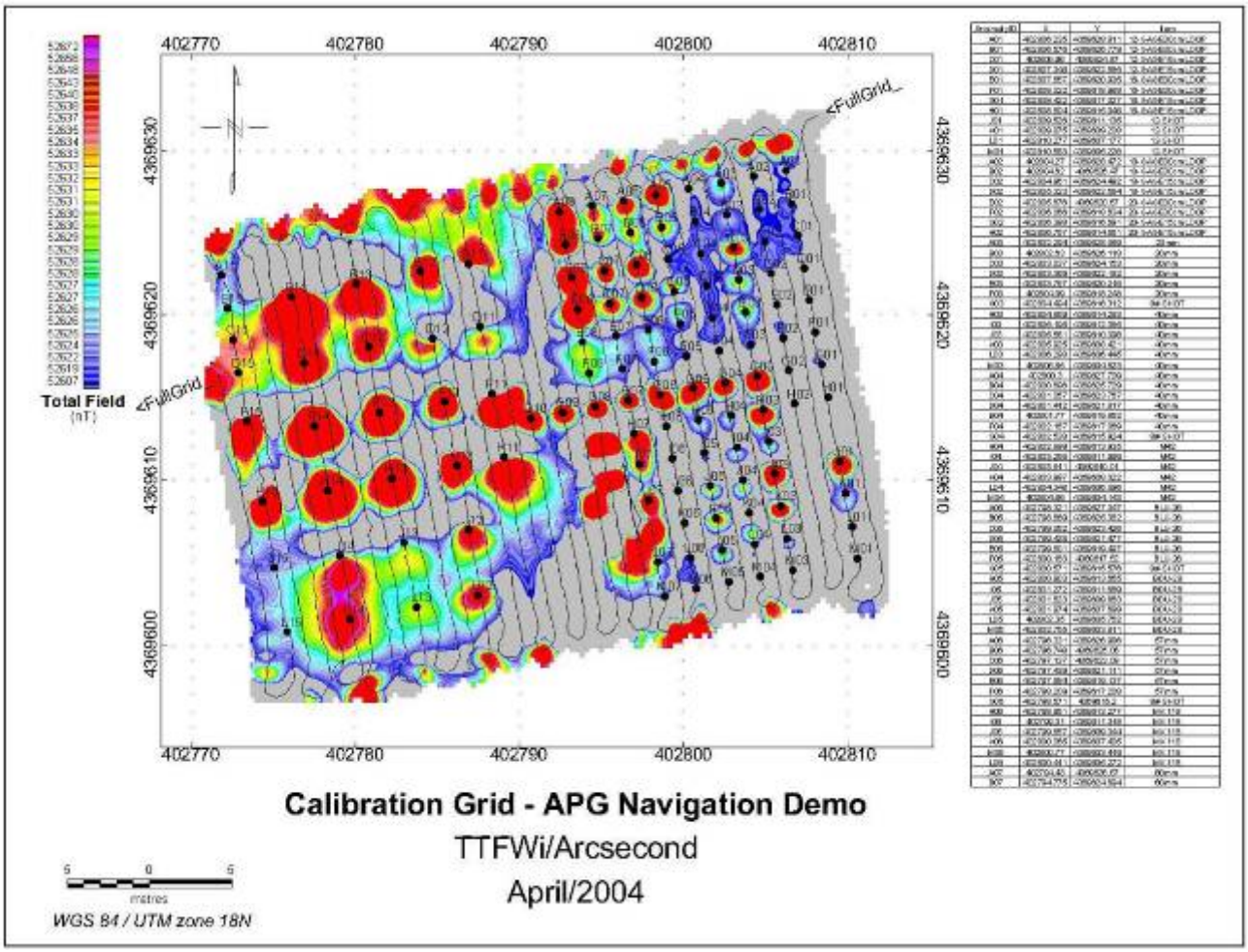

Figure 1-3. Calibration Grid—ArcSecond Results in Map Form

ArcSecond - Test 1								
UTM coordinates								
ID	**Grid Location**	**Easting (Control)**	**Northing (Control)**	**East (Measured)**	**North (Measured)**	**Easting (Tolerance)**	**Northing (Tolerance)**	**Radial Error**
155mm M483A1	B14	402776.104	4369621.141	402776.167	4369621.025	-0.063	0.116	0.132
155mm M483A1	F14	402777.510	4369613.288	402777.517	4369613.297	-0.007	-0.009	0.011
155mm M483A1	J14	402779.063	4369605.419	402779.123	4369605.139	-0.060	0.280	0.286
105mm M60	B13	402780.068	4369621.924	402780.054	4369621.913	0.014	0.011	0.018
105mm M60	F13	402781.483	4369614.115	402781.503	4369614.086	-0.020	0.029	0.035
105mm M60	J13	402782.970	4369606.210	402782.971	4369605.992	-0.001	0.218	0.218
8# SHOT	G10	402790.697	4369613.755	402790.756	4369613.709	-0.059	0.046	0.075
2.75" M230	A08	402792.426	4369626.304	402792.628	4369626.485	-0.202	-0.181	0.271
2.75" M230	C08	402793.186	4369622.320	402793.265	4369622.240	-0.079	0.080	0.113
2.75" M230	E08	402793.836	4369618.401	402793.856	4369618.175	-0.020	0.226	0.227
60mm M49A3	A07	402794.430	4369626.670	402794.403	4369626.533	0.027	0.137	0.140
60mm M49A3	C07	402795.185	4369622.719	402795.261	4369622.728	-0.076	-0.009	0.076
60mm M49A3	E07	402795.871	4369618.778	402795.896	4369618.308	-0.025	0.470	0.471
57mm M86	A06	402796.331	4369626.986	402796.378	4369627.059	-0.046	-0.073	0.087
81mm M374	H07	402796.984	4369612.829	402797.258	4369612.941	-0.274	-0.112	0.296
57mm M86	C06	402797.137	4369623.090	402797.145	4369623.014	-0.008	0.076	0.076
57mm M86	E06	402797.854	4369619.137	402797.937	4369618.945	-0.083	0.192	0.209
81mm M374	J07	402797.874	4369608.786	402797.958	4369608.654	-0.084	0.132	0.157
81mm M374	L07	402798.446	4369605.029	402797.917	4369604.895	0.529	0.134	0.546
							Average Error	0.181
							Standard Deviation	0.146

Figure 1-4. Calibration Grid—All ArcSecond Results

Test 2: Calibration Lane—Reacquisition

- The contractor shall reacquire the coordinates of 19 items. They include three each of 57 mm, 60 mm, 81 mm, 2.75 in, 105 mm, and 155 mm seeded items at different orientations/depths as well as one 8# shotput. The items are lane 6 A, C, and D; 7 A, C, E, H, J, and L; 8 A, C, and E; 13 B, F, and J; 14 B, F, and J; and Shotput lane 10 G. They are highlighted in yellow in Appendix G. Use the integrated system to reacquire and flag the position real time. The reacquired coordinate will be compared to the seeded location coordinates.

Test 2: ArcSecond Results

ArcSecond performed the "reacquire" test using the navigation screen on its PDA software application. The PDA and interface screen are shown in the following figures. The anomaly points were flagged using standard survey flags.

Figure 1-5. Rugged Pocket PC PDA

The navigation screen allows the user to navigate back to the target point (reacquire point) based on the user's acceptable tolerance. For Test 2, ArcSecond used 5 mm (0.5 cm) as the acceptable tolerance. Once within this tolerance zone, the reacquisition point was flagged (see navigation steps in Figure 1-6).

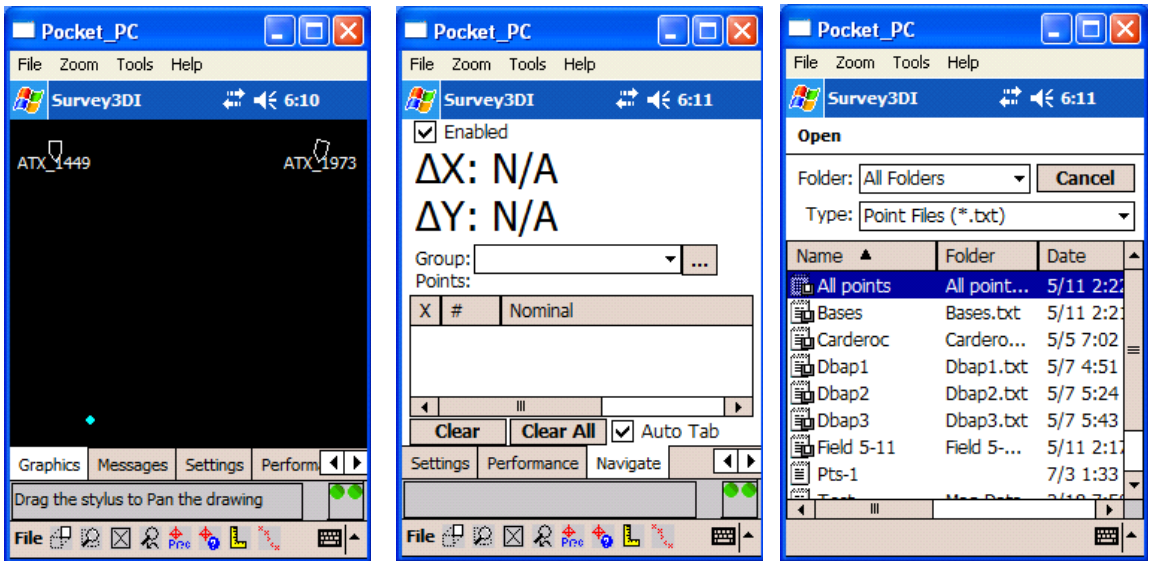

Step 1: Set-Up System **Step 2: Go to Navigate Screen** **Step 3: Select Point File**

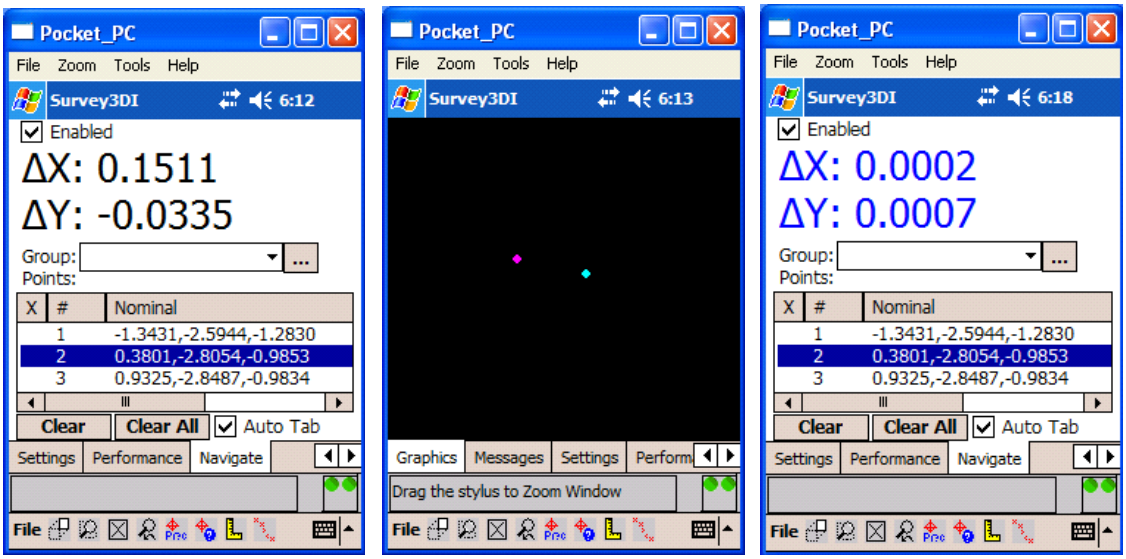

Step 4: Select Reacquire Point **Step 5: Navigate to Point** **Step 6: Final navigation Tolerance**

Navigation Process Summary: Perform a system setup, select the Navigation tab, and then load the "Reacquire Point" file. Then select the target point from within the list—the interface will show the delta difference between the target point and the current location. The user may then use the map screen and text screen to navigate to within the desired tolerance of the target point.

Figure 1-6. Navigation screens

The following chart shows navigation results from the calibration grid. For the purposes of this test, we set the tolerance for the navigation to 5 mm. The following tables show (a) the navigation tolerance compared to the "ArcSecond mapped" reacquisition point and (b) the tolerance of the reacquire point to the "known" Army control point.

ID	Grid Location	East (Measured)	North (Measured)	Easting (Navigation)	Northing (Navigation)	Easting (Tolerance)	Northing (Tolerance)	Radial Error
155mm M483A1	B14	402776.167	4369621.025	402776.170	4369621.022	-0.003	0.003	0.005
155mm M483A1	F14	402777.517	4369613.297	402777.519	4369613.296	-0.002	0.001	0.002
155mm M483A1	J14	402779.123	4369605.139	402779.124	4369605.138	-0.001	0.001	0.002
105mm M60	B13	402780.054	4369621.913	402780.053	4369621.913	0.001	0.000	0.001
105mm M60	F13	402781.503	4369614.086	402781.504	4369614.086	-0.001	0.000	0.001
105mm M60	J13	402782.971	4369605.992	402782.969	4369605.991	0.003	0.001	0.003
8# SHOT	G10	402790.756	4369613.709	402790.755	4369613.709	0.001	0.000	0.001
2.75" M230	A08	402792.628	4369626.485	402792.628	4369626.487	0.000	-0.002	0.002
2.75" M230	C08	402793.265	4369622.240	402793.265	4369622.238	0.001	0.002	0.002
2.75" M230	E08	402793.856	4369618.175	402793.855	4369618.176	0.001	-0.001	0.002
60mm M49A3	A07	402794.403	4369626.533	402794.403	4369626.532	0.000	0.001	0.001
60mm M49A3	C07	402795.261	4369622.728	402795.260	4369622.730	0.001	-0.002	0.002
60mm M49A3	E07	402795.896	4369618.308	402795.894	4369618.311	0.002	-0.003	0.004
57mm M86	A06	402796.378	4369627.059	402796.376	4369627.061	0.002	-0.002	0.003
81mm M374	H07	402797.258	4369612.941	402797.258	4369612.943	0.000	-0.002	0.002
57mm M86	C06	402797.145	4369623.014	402797.149	4369623.017	-0.003	-0.003	0.004
57mm M86	E06	402797.937	4369618.945	402797.938	4369618.948	-0.001	-0.003	0.003
81mm M374	J07	402797.958	4369608.654	402797.958	4369608.655	0.000	-0.001	0.001
81mm M374	L07	402797.917	4369604.895	402797.916	4369604.895	0.001	0.000	0.001
							Average Error	0.002
							Standard Deviation	0.001

Figure 1-7. Calibration Grid—Tolerance of ArcSecond Reacquisition Point to Target Reacquisition Point (Mapped by ArcSecond)

ArcSecond - Test 2								
UTM coordinates								
ID	**Grid Location**	**Easting (Control)**	**Northing (Control)**	**Easting (Navigation)**	**Northing (Navigation)**	**Easting (Tolerance)**	**Northing (Tolerance)**	**Radial Error**
155mm M483A1	B14	402776.104	4369621.141	402776.170	4369621.022	-0.066	0.119	0.136
155mm M483A1	F14	402777.510	4369613.288	402777.519	4369613.296	-0.009	-0.008	0.012
155mm M483A1	J14	402779.063	4369605.419	402779.124	4369605.138	-0.061	0.281	0.288
105mm M60	B13	402780.068	4369621.924	402780.053	4369621.913	0.015	0.011	0.018
105mm M60	F13	402781.483	4369614.115	402781.504	4369614.086	-0.021	0.029	0.035
105mm M60	J13	402782.970	4369606.210	402782.969	4369605.991	0.001	0.219	0.219
8# SHOT	G10	402790.697	4369613.755	402790.755	4369613.709	-0.058	0.046	0.074
2.75" M230	A08	402792.426	4369626.304	402792.628	4369626.487	-0.202	-0.183	0.273
2.75" M230	C08	402793.186	4369622.320	402793.265	4369622.238	-0.079	0.082	0.113
2.75" M230	E08	402793.836	4369618.401	402793.855	4369618.176	-0.019	0.225	0.226
60mm M49A3	A07	402794.430	4369626.670	402794.403	4369626.532	0.027	0.138	0.141
60mm M49A3	C07	402795.185	4369622.719	402795.260	4369622.730	-0.075	-0.011	0.076
60mm M49A3	E07	402795.871	4369618.778	402795.894	4369618.311	-0.023	0.467	0.467
57mm M86	A06	402796.331	4369626.986	402796.376	4369627.061	-0.045	-0.075	0.087
81mm M374	H07	402796.984	4369612.829	402797.258	4369612.943	-0.274	-0.114	0.297
57mm M86	C06	402797.137	4369623.090	402797.149	4369623.017	-0.012	0.073	0.074
57mm M86	E06	402797.854	4369619.137	402797.938	4369618.948	-0.084	0.189	0.207
81mm M374	J07	402797.874	4369608.786	402797.958	4369608.655	-0.084	0.131	0.155
81mm M374	L07	402798.446	4369605.029	402797.916	4369604.895	0.530	0.134	0.546
							Average Error	0.181
							Standard Deviation	0.145

Figure 1-8. Calibration Grid—Tolerance of ArcSecond Reacquire Point to Known Anomaly Location

Test 3: Calibration Lane Area—Fixed Grid Anomaly Interrogations Evaluations

- These 19 locations will be interrogated in both a fixed grid and dynamic mode. The fixed grid data set will be gathered based on a fixed grid mesh or marked carpet centered on the reacquired location for a 1.2 m square area at .2 m intervals with a sensor height at .15, .30 and .45 m heights (147 points). Standoff will be established by plastic head spacers or movement of the head position up a position pole. The individual point data captured will be compared from relative positioning among the points captured to the fixed grid. Based on the 3-D data captured, a revised dig list location will be selected. The refined dig list coordinates will be compared to the seeded location coordinates from Appendix G, area mapping dig list coordinates from Test 1, and the flagged coordinates from Test 2.

Test 3: ArcSecond Results

ArcSecond performed the required interrogations on 10 of the 19 anomalies. Initially, this subset was chosen due to time constraints – and pending weather. However, the decision was made (mutually) that the 10 samples were enough to determine the system's overall performance. This decision was based on the quality of data from initial interrogations.

Figure 1-9 shows the plywood grid template used for all interrogations. The template was placed directly over the anomaly's seeded location, as marked by flags placed by the customer and the four corner pins. While care was taken to place the template accurately over each cell, the template did not perfectly match each cell. We estimated that the placement error could easily have been 1-2 cm in some cases with respect to the pins.

The PVC offsets are also shown in Figure 1-9. These offsets were attached directly to the G-858 sensor head, and the positioning system was aligned directly over the head. Figure 1-10 shows the mounting of the positioning sensor over the geophysical sensor (though the picture was from Test 4 – the Dynamic Interrogation).

Figure 1-9. Fixed Grid Template—with 6 in, 12 in, and 18 in PVC Offset Tubes

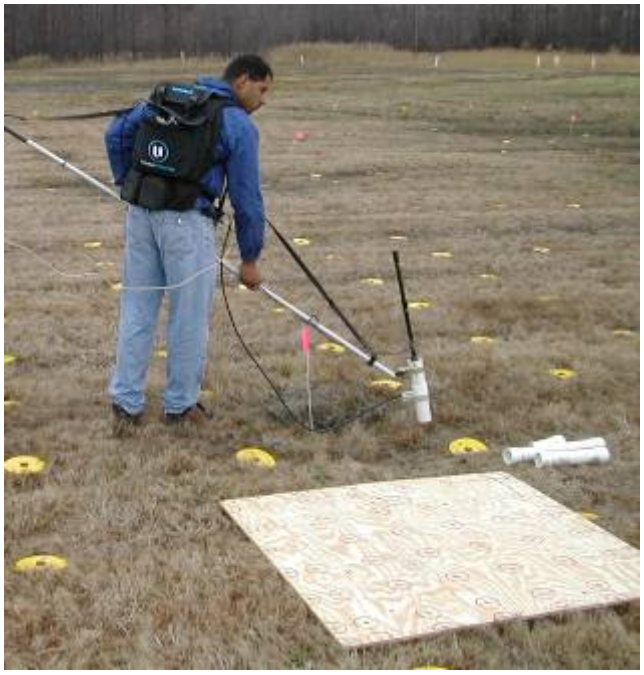

Figure 1-10. Fixed Grid Template—Positioning Sensor over G-858 Sensor (shown for Dynamic Testing – Test 4)

Figure 1-11 shows screen shots of the Fixed Grid interrogations. The screen shots show several individual anomaly cells. The green points show the 6 in offset interrogations, the yellow points show the 12 in offset interrogations, and the red points show the 18 in offset interrogations. The blue points represent the streaming data points from Test 4.

The 6 in offset points were collected in a 6 x 6 grid (36 points total) that covered the 1 m^2 square meter plywood template; the 12 in and 18 in offset points were collected in "cross pattern" that included 12 points total.

Figure 1-12 contains the accumulated results of Test 3. Specifically, it compares the Fixed Anomaly calculated positions to the Seeded positions.

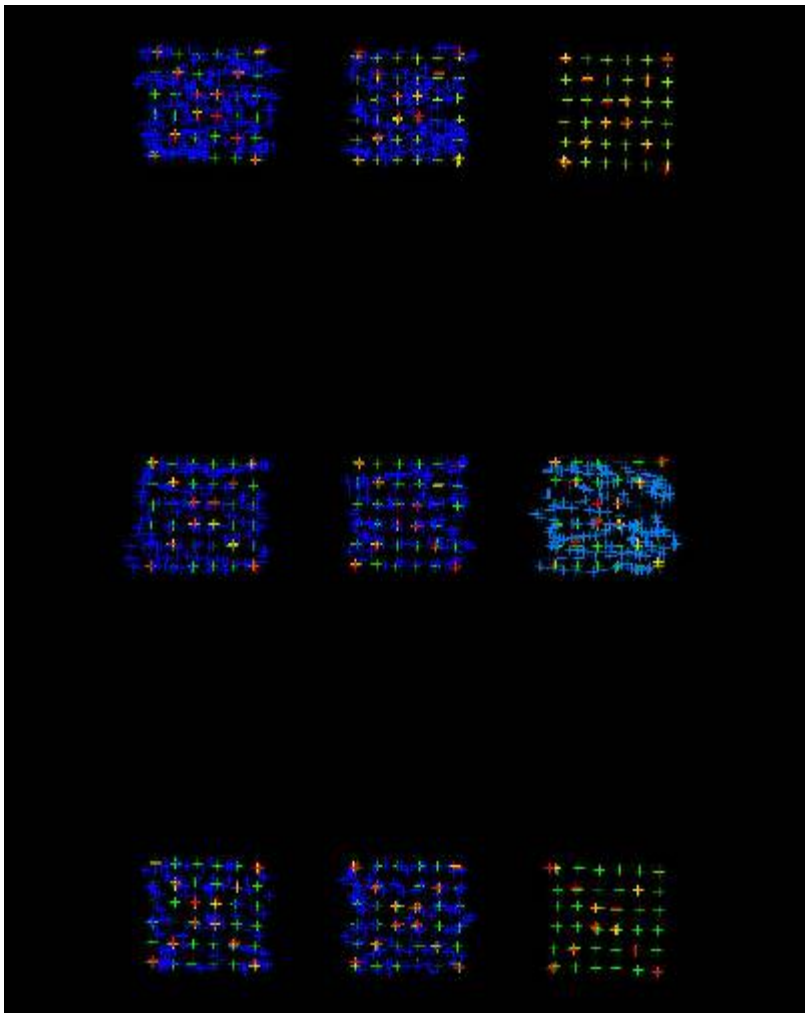

Plan View of Grid Interrogations

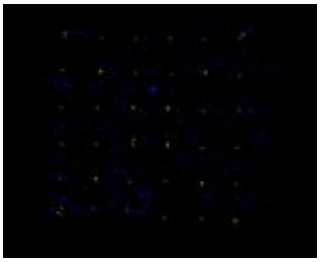

Plan View of A8 Fixed Grid Interrogation

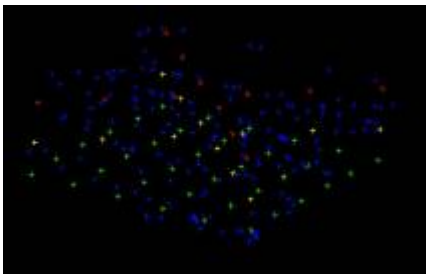

Perspective View of A8 Fixed Grid Interrogation

6 in offset = Green
12 in offset = Yellow
18 in offset = Red
Stream = Blue

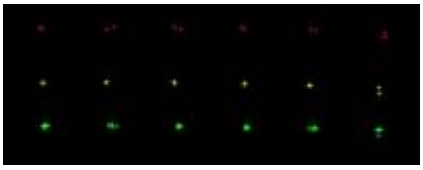

Side View of A8 Fixed Grid Interrogation

Figure 1-11. Fixed Grid Interrogations—Graphical Point Data

ArcSecond Entry- Test 3 (15 cm)

ID	grid location	East	North	East	North	Tolerance Easting	Tolerance Northing	Error	
155mm M483A1	B14	402776.104	4369621.141	NA	NA	NA	NA	NA	
155mm M483A1	F14	402777.510	4369613.288	NA	NA	NA	NA	NA	
155mm M483A1	J14	402779.063	4369605.419	NA	NA	NA	NA	NA	
105mm M60	B13	402780.068	4369621.924	NA	NA	NA	NA	NA	
105mm M60	F13	402781.483	4369614.115	NA	NA	NA	NA	NA	
105mm M60	J13	402782.970	4369606.210	NA	NA	NA	NA	NA	
8# SHOT	G10	402790.697	4369613.755	402790.7237	4369613.8027	-0.0267	-0.0477	0.054656294	
2.75" M230	A08	402792.426	4369626.304	402792.3273	4369626.3592	0.0987	-0.0552	0.113060895	
2.75" M230	C08	402793.186	4369622.320	402793.2035	4369622.3997	-0.0175	-0.0797	0.081632971	
2.75" M230	E08	402793.836	4369618.401	402793.7921	4369618.2987	0.0439	0.1023	0.111315581	
60mm M49A3	A07	402794.430	4369626.670	402794.4870	4369626.7119	-0.0570	-0.0419	0.070746531	
60mm M49A3	C07	402795.185	4369622.719	402795.1976	4369622.7729	-0.0126	-0.0539	0.055336609	
60mm M49A3	E07	402795.871	4369618.778	402795.9569	4369618.8667	-0.0859	-0.0887	0.123443636	
57mm M86	A06	402796.331	4369626.986	402796.3402	4369627.0554	-0.0092	-0.0694	0.069970418	
81mm M374	H07	402796.984	4369612.829	NA	NA	NA	NA	NA	
57mm M86	C06	402797.137	4369623.090	402797.2160	4369622.9515	-0.0790	0.1385	0.159434388	
57mm M86	E06	402797.854	4369619.137	402797.9032	4369619.2098	-0.0492	-0.0728	0.087878411	
81mm M374	J07	402797.874	4369608.786	NA	NA	NA	NA	NA	
81mm M374	L07	402798.446	4369605.029	NA	NA	NA	NA	NA	
						-0.0194	-0.0269	0.0927	**Average Error**
						0.0562	0.0794	0.0336	**Standard Deviation**

ArcSecond Entry- Test 3 (30 cm)

ID	grid location	East	North	East	North	Tolerance Easting	Tolerance Northing	Error	
155mm M483A1	B14	402776.104	4369621.141	NA	NA	NA	NA	NA	
155mm M483A1	F14	402777.510	4369613.288	NA	NA	NA	NA	NA	
155mm M483A1	J14	402779.063	4369605.419	NA	NA	NA	NA	NA	
105mm M60	B13	402780.068	4369621.924	NA	NA	NA	NA	NA	
105mm M60	F13	402781.483	4369614.115	NA	NA	NA	NA	NA	
105mm M60	J13	402782.970	4369606.210	NA	NA	NA	NA	NA	
8# SHOT	G10	402790.697	4369613.755	402790.7304	4369613.8170	-0.0334	-0.0620	0.070422723	
2.75" M230	A08	402792.426	4369626.304	402792.3291	4369626.3554	0.0969	-0.0514	0.109679774	
2.75" M230	C08	402793.186	4369622.320	402793.2170	4369622.4124	-0.0310	-0.0924	0.097483058	
2.75" M230	E08	402793.836	4369618.401	402793.7664	4369618.4804	0.0696	-0.0794	0.105561794	
60mm M49A3	A07	402794.430	4369626.670	402794.4781	4369626.7453	-0.0481	-0.0753	0.089302934	
60mm M49A3	C07	402795.185	4369622.719	402795.1963	4369622.7569	-0.0113	-0.0379	0.039518006	
60mm M49A3	E07	402795.871	4369618.778	402795.9106	4369618.8520	-0.0396	-0.0740	0.083908806	
57mm M86	A06	402796.331	4369626.986	402796.3299	4369627.0316	0.0011	-0.0456	0.045584383	
81mm M374	H07	402796.984	4369612.829	NA	NA	NA	NA	NA	
57mm M86	C06	402797.137	4369623.090	402797.1788	4369623.1554	-0.0418	-0.0654	0.07763896	
57mm M86	E06	402797.854	4369619.137	402797.8643	4369619.2097	-0.0103	-0.0727	0.073475787	
81mm M374	J07	402797.874	4369608.786	NA	NA	NA	NA	NA	
81mm M374	L07	402798.446	4369605.029	NA	NA	NA	NA	NA	
						-0.0048	-0.0656	0.0793	**Average Error**
						0.0494	0.0167	0.0233	**Standard Deviation**

ArcSecond Entry- Test 3 (45 cm)

ID	grid location	East	North	East	North	Tolerance Easting	Tolerance Northing	Error	
155mm M483A1	B14	402776.104	4369621.141	NA	NA	NA	NA	NA	
155mm M483A1	F14	402777.510	4369613.288	NA	NA	NA	NA	NA	
155mm M483A1	J14	402779.063	4369605.419	NA	NA	NA	NA	NA	
105mm M60	B13	402780.068	4369621.924	NA	NA	NA	NA	NA	
105mm M60	F13	402781.483	4369614.115	NA	NA	NA	NA	NA	
105mm M60	J13	402782.970	4369606.210	NA	NA	NA	NA	NA	
8# SHOT	G10	402790.697	4369613.755	402790.7103	4369613.8080	-0.0133	-0.0530	0.054667777	
2.75" M230	A08	402792.426	4369626.304	402792.3217	4369626.3513	0.1043	-0.0473	0.114484565	
2.75" M230	C08	402793.186	4369622.320	402793.2126	4369622.3958	-0.0266	-0.0758	0.080309089	
2.75" M230	E08	402793.836	4369618.401	402793.7931	4369618.3020	0.0429	0.0990	0.107907364	
60mm M49A3	A07	402794.430	4369626.670	402794.4801	4369626.7483	-0.0501	-0.0783	0.092938924	
60mm M49A3	C07	402795.185	4369622.719	402795.1963	4369622.7569	-0.0113	-0.0379	0.039518006	
60mm M49A3	E07	402795.871	4369618.778	402795.9209	4369618.8635	-0.0499	-0.0855	0.098986637	
57mm M86	A06	402796.331	4369626.986	402796.3245	4369627.0323	0.0065	-0.0463	0.046714359	
81mm M374	H07	402796.984	4369612.829	NA	NA	NA	NA	NA	
57mm M86	C06	402797.137	4369623.090	402797.1784	4369623.1453	-0.0414	-0.0553	0.069040621	
57mm M86	E06	402797.854	4369619.137	402797.8643	4369619.2097	-0.0103	-0.0727	0.073475787	
81mm M374	J07	402797.874	4369608.786	NA	NA	NA	NA	NA	
81mm M374	L07	402798.446	4369605.029	NA	NA	NA	NA	NA	
						-0.0049	-0.0453	0.0778	**Average Error**
						0.0475	0.0532	0.0258	**Standard Deviation**

Figure 1-12. Fixed Anomaly Interrogation Compared to Seeded Values

Test 4: Calibration Lane Area—Dynamic Anomaly Interrogations Evaluations

- The 19 anomalies will then have a dynamic 3-D data set acquired by walking an approximately 2 m square area with the sensor head at multiple heights or by swinging and lifting the handheld sensor over the anomaly area as required by the individual systems. The objective will be to capture a similar data set as in Test 3 but in a rapid, more random, unguided field methodology that will rely on the navigation system's dynamic position accuracy with a continuous sensor and navigation data stream. Based on the 3-D data captured, a revised dig list location will be selected. The refined dig list coordinates will be compared to the seeded location coordinates from Appendix G, area mapping dig list coordinates from Test 1, the flagged coordinates from Test 2, and fixed grid location from Test 3.

  Note that the sensor data sets from the Calibration Lanes with the true seeded location and orientations will be used by others to help evaluate and develop geophysical modeling and discrimination algorithms.

Test 4: ArcSecond Results

Figure 1-10 shows the user collecting data in the streaming mode for one of the anomalies in Test 4. Likewise, Figure 1-11 shows the dynamic data points (shown in blue). The results from Test 4 are shown in Figure 1-13.

Contractor Entry- Test 4 (Streaming at approximitely 30cm)

ID	grid location	East	North	East	North	Tolerance Easting	Tolerance Northing	Error	
155mm M483A1	B14	402776.104	4369621.141	NA	NA	NA	NA	NA	
155mm M483A1	F14	402777.510	4369613.288	NA	NA	NA	NA	NA	
155mm M483A1	J14	402779.063	4369605.419	NA	NA	NA	NA	NA	
105mm M60	B13	402780.068	4369621.924	NA	NA	NA	NA	NA	
105mm M60	F13	402781.483	4369614.115	NA	NA	NA	NA	NA	
105mm M60	J13	402782.970	4369606.210	NA	NA	NA	NA	NA	
8# SHOT	G10	402790.697	4369613.755	402790.7058	4369613.7924	-0.0088	-0.0374	0.038436925	
2.75" M230	A08	402792.426	4369626.304	402792.3943	4369626.3238	0.0317	-0.0198	0.03735614	
2.75" M230	C08	402793.186	4369622.320	402793.1714	4369622.3544	0.0146	-0.0344	0.037336822	
2.75" M230	E08	402793.836	4369618.401	402793.9157	4369618.3742	-0.0796	0.0268	0.084023205	
60mm M49A3	A07	402794.430	4369626.670	402794.4870	4369626.7119	-0.0570	-0.0419	0.070746531	
60mm M49A3	C07	402795.185	4369622.719	402795.1904	4369622.7486	-0.0054	-0.0296	0.0301271	
60mm M49A3	E07	402795.871	4369618.778	402795.8788	4369618.7346	-0.0078	0.0434	0.044113994	
57mm M86	A06	402796.331	4369626.986	NA	NA	NA	NA	NA	
81mm M374	H07	402796.984	4369612.829	NA	NA	NA	NA	NA	
57mm M86	C06	402797.137	4369623.090	402797.0949	4369623.0520	0.0421	0.0380	0.056734134	
57mm M86	E06	402797.854	4369619.137	NA	NA	NA	NA	NA	
81mm M374	J07	402797.874	4369608.786	NA	NA	NA	NA	NA	
81mm M374	L07	402798.446	4369605.029	NA	NA	NA	NA	NA	
						-0.0088	-0.0069	0.0499	**Average Error**
						0.041633595	0.03640369	0.018961211	**Standard Deviation**

Figure 1-13. Dynamic Anomaly Interrogation Compared to Seeded Values

Test 5: Wooded Area—Accuracy with Positioning System for Surface Points

- The wooded area has six unknown permanent rebar points within the interior. These positions are placed in areas without nearby adjacent geophysical anomalies. Forty additional widely scattered points are established by PVC pipe with removable steel pins (when required to trigger the magnetometer). Each will be occupied by the integrated navigation/geophysical sensor system to determine coordinate locations. These will be directly compared to the ground truth for position accuracy.

Test 5: ArcSecond Results

ArcSecond measured the six rebar and 40 PVC points using the standard ArcSecond Pole Receiver. The raw data and the summary results are shown in Figure 1-14. (Note: ArcSecond does not have the Army values for the rebar and PVC points, but the Army provided the summary comparison in Figure 1-14.)

Static_X	Static_Y
402609.422	4369493.623
402620.281	4369484.173
402623.812	4369507.429
402624.307	4369515.865
402625.036	4369494.559
402626.837	4369504.279
402628.727	4369468.778
402629.292	4369490.200
402629.539	4369497.923
402630.370	4369479.229
402631.463	4369516.264
402631.709	4369521.753
402633.975	4369492.150
402634.285	4369526.926
402635.939	4369548.822
402637.207	4369502.143
402637.598	4369536.752
402641.581	4369510.379
402641.748	4369463.808
402643.049	4369524.160
402643.665	4369540.854
402643.679	4369475.772
402646.247	4369535.461
402649.429	4369510.585
402649.432	4369546.786
402650.570	4369538.457
402653.013	4369524.046
402653.932	4369458.840
402655.112	4369534.165
402655.681	4369470.175
402657.869	4369547.785
402659.736	4369496.070
402660.659	4369507.786
402662.313	4369520.281
402665.105	4369532.610
402665.259	4369544.347
402667.399	4369452.554
402668.350	4369465.725
402669.177	4369478.919
402670.157	4369492.033
402671.056	4369505.187
402671.991	4369518.363
402672.889	4369531.482
402673.190	4369449.263
402676.081	4369530.669

Raw Data from Test 5

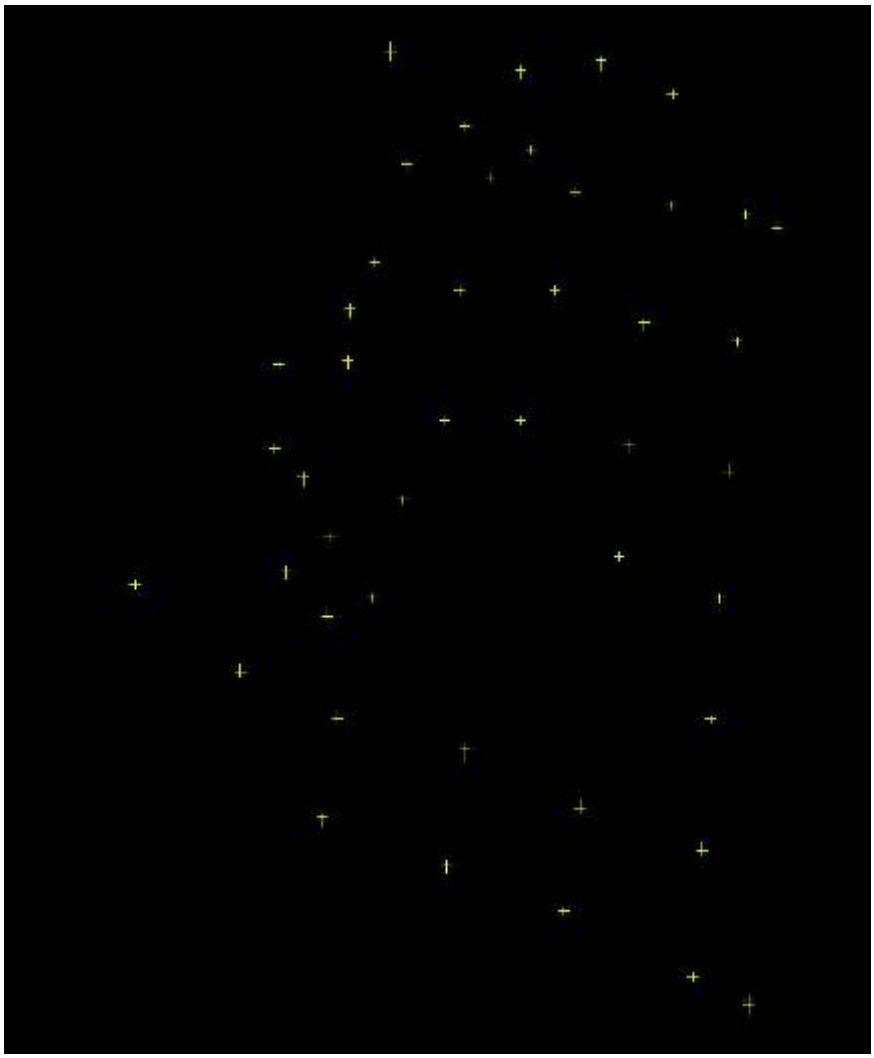

Plan View of Surveyed Points for Test 5

Test 5- Wooded Surface Points (Navigation)

	6-Rebars				40-PVC Points			
	Tolerance	Tolerance			Tolerance	Tolerance		
Contractor	Easting	Northing	Distance		Easting	Northing	Distance	
Shaw/IT	0.0727	-0.0689	0.1125		0.0809	-0.0811	0.1339	Average Error
	0.0460	0.0462	0.0403		0.0608	0.0645	0.0538	Standard Deviation
GIS	-0.3843	-0.0321	0.9254		-0.1241	0.0826	0.5310	Average Error
	0.9183	0.5268	0.6428		0.3514	0.6130	0.4788	Standard Deviation
ArcSecond	0.0332	0.0282	0.0503		0.0175	0.0500	0.0649	Average Error
	0.0225	0.0225	0.0196		0.0271	0.0404	0.0303	Standard Deviation
Ensco	-0.3022	0.0300	0.4044		0.1117	-0.0631	0.5659	Average Error
	0.4155	0.1300	0.1570		0.3707	0.5213	0.3068	Standard Deviation

Army Summary Results from Test 5

Figure 1-14. ArcSecond Results from Test 5

Test 6: Wooded Area—Accuracy from Geophysical Data Analysis for Surface Points

- The 46 points from Test 5 will be traversed dynamically by the integrated system. These points will be picked from the instrument peaks shown in the data set and reported. These will be directly compared to the ground truth for position accuracy and to the locations from Test 5.

Test 6: ArcSecond Results

ArcSecond dynamically measured the six rebar and 40 PVC points using the integrated positioning and geophysical system. The point coordinates were picked using instrument peaks. (Note: ArcSecond does not have the Army values for the rebar and PVC points, but the Army provided the summary comparison in Figure 1-15.)

Dynamic_X	Dyanmic_Y
402665.0885	4369532.506
402664.3028	4369526.192
402662.2574	4369520.342
402661.1693	4369511.208
402671.0098	4369505.256
402670.2113	4369491.96
402663.4936	4369482.133
402668.2945	4369465.643
402664.7712	4369458.7
402667.4665	4369452.525
402653.9184	4369458.809
402654.7224	4369465.726
402660.237	4369498.062
402660.3163	4369504.183
402653.0752	4369523.813

Raw Data from Test 6

Test 6- Wooded Points (Geophysics)

	6-Rebars			40-PVC Points				
	Tolerance	Tolerance		Tolerance	Tolerance			
Contractor	Easting	Northing	Distance	Easting	Northing	Distance		
Shaw/IT	0.1928	-0.1743	0.2651	0.1314	-0.1052	0.2493	Average Error	
	0.1302	0.0866	0.1473	0.1588	0.1371	0.0953	Standard Deviation	
GIS	0.8672	-0.5186	1.0105	-0.2748	0.0769	0.9007	Average Error	
				0.5865	0.9501	0.6753	Standard Deviation	
ArcSecond				-0.0112	0.1137	0.1397	Average Error	
				0.0569	0.0922	0.0660	Standard Deviation	
Ensco	0.2968	-0.3200	0.4369	0.1991	-0.2591	0.4666	Average Error	
	0.1360	0.1801	0.2154	0.2947	0.3841	0.3429	Standard Deviation	
Gtek (RTS)	0.0046	0.0283	0.1543	0.0410	-0.1158	0.2598	Average Error	
	0.1744	0.0493	0.0994	0.0626	0.3124	0.1898	Standard Deviation	
Gtek (String)	-0.0066	0.3300	0.3308	Average Error				
	0.0196	0.1766	0.1764	Standard Deviation				

Army Summary Results from Test 6

Figure 1-15. ArcSecond Results from Test 6

Test 7: Wooded Area—Area Mapping

- The approximately 1 acre area will be mapped with the data analysis using the GFE G-858 sensor (with magnetometer base station) integrated with the navigation equipment at approximately 1 m spacing in an approximately E-W direction. The steel pins will be removed from the 40 points described in Test 5 so as not to affect the subsurface anomaly results.
- The selection threshold for anomaly selection for the wooded area will be based on the instrument reading for all items larger than the 57 mm M86, as shown by the Calibration Lanes area mapping from Test 1. The dig list selected will be evaluated by APG with emphasis on position accuracy. Ground truth locations will be available for more in-depth evaluations in August 2004.

Test 7: ArcSecond Results

ArcSecond mapped the wooded area, as shown in Figure 1-16. The "pick points" are identified in Figure 1-17, and the geophysical map that resulted is shown in Figure 1-18. (Note: ArcSecond is awaiting final results from Army on wooded area test.)

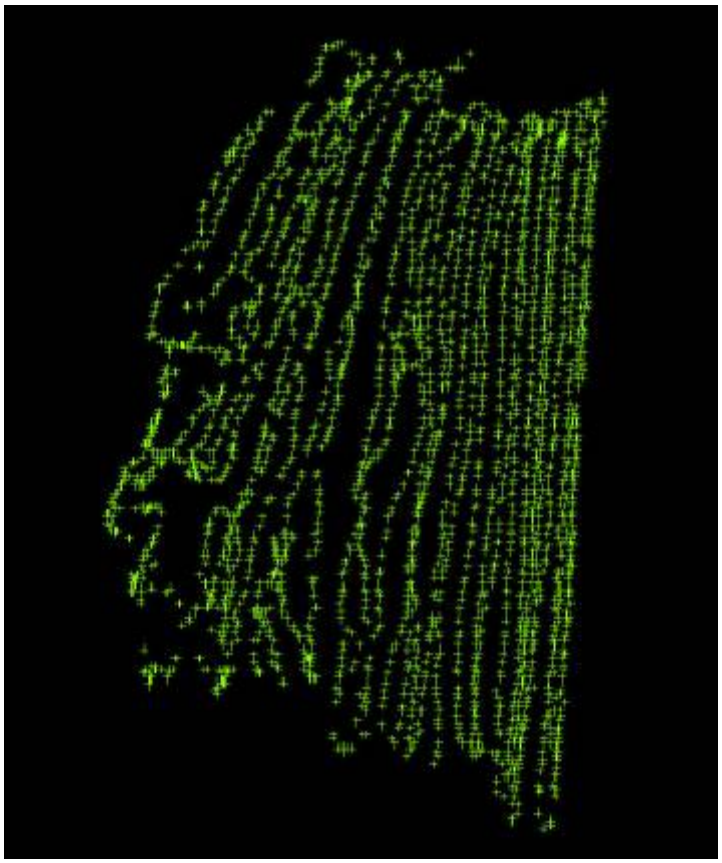

Figure 1-16. Area Mapping Samples in Wooded Area

Contractors picks

Point_Id	X	Y
1	402664.04	4369458.62
2	402655.94	4369465.20
3	402662.63	4369470.24
4	402657.23	4369472.47
5	402653.95	4369475.29
6	402651.13	4369470.36
7	402650.43	369477.52
8	402643.27	4369473.18
9	402639.28	4369472.01
10	402633.05	4369478.58
11	402618.03	4369482.57
12	402625.89	4369484.92
13	402628.83	369487.26
14	402629.06	4369491.25
15	402639.98	4369487.50
16	402620.96	4369503.23
17	402629.42	4369498.06
18	402636.22	4369496.54
19	402651.48	4369492.55
20	402656.88	4369493.02
21	402656.41	4369487.03
22	402663.81	4369494.31
23	402666.98	369492.66
24	402665.45	4369497.83
25	402665.68	4369502.64
26	402659.93	4369497.36
27	402652.19	4369499.94
28	402649.60	4369505.11
29	402655.00	4369506.98
30	402659.70	4369506.16
31	402668.38	4369512.73
32	402662.28	4369510.15
33	402655.12	369512.03
34	402660.40	4369513.79
35	402660.05	4369518.02
36	402665.22	4369522.36
37	402669.68	4369528.70
38	402663.69	4369527.41
39	402663.92	4369533.39
40	402670.15	4369535.15
41	402658.41	4369537.74
42	402655.47	4369539.61
43	402656.06	4369524.47
44	402651.01	4369529.28
45	402648.20	4369532.22
46	402652.89	4369536.91
47	402647.84	4369538.44
48	402651.13	4369544.07
49	402643.97	4369541.26
50	402638.69	4369541.14
51	402628.95	4369533.63
52	402633.17	4369537.03
53	402642.44	4369536.56
54	402641.74	4369530.81
55	402627.89	69521.07
56	402629.06	4369513.09
57	402630.94	4369503.23
58	402639.16	369501.70
59	402642.44	4369503.93
60	402646.44	4369512.50
61	402640.92	4369510.27
62	402636.11	4369509.21
63	402632.00	4369521.19
64	402635.28	4369523.18
65	402638.92	4369525.18
66	402640.45	4369521.30
67	402648.90	4369518.72
68	402658.41	4369530.22
69	402616.50	4369492.31
70	402668.38	4369537.74
71	402660.64	4369486.56
72	402639.16	369534.57

Figure 1-17. Contractor Picks for Wooded Area

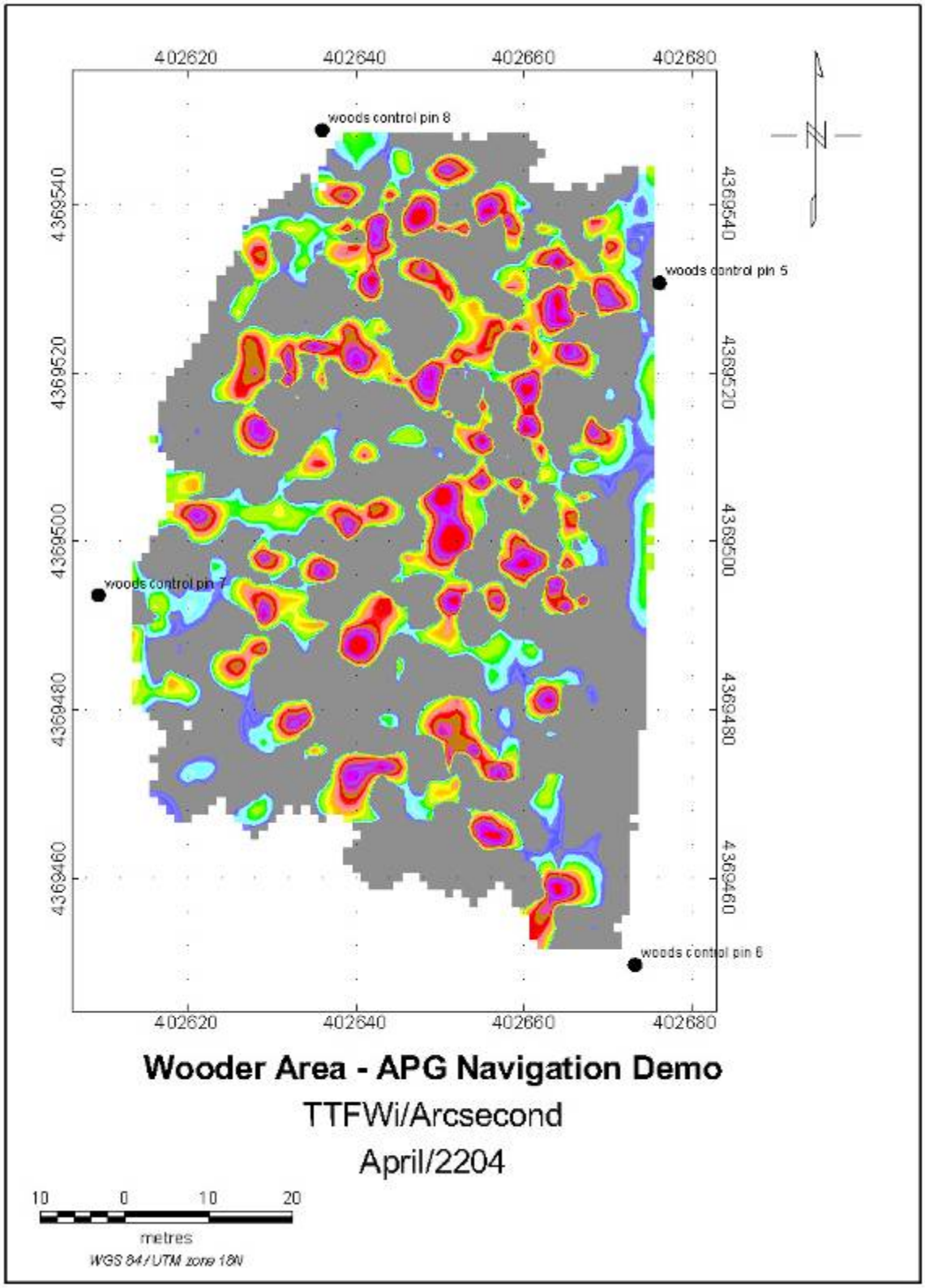

Figure 1-18. ArcSecond Geophysical Map from Test 7

Test 8: Wooded Area—Dynamic Anomaly Interrogations

- Ten well-defined anomalies will be selected from the Test 7 results for interrogation. The 10 anomalies will then have a dynamic 3-D data set acquired as in Test 4 by walking an approximately 2 m square area with the sensor head at multiple heights or by swinging and lifting the handheld sensor over the anomaly area, as required by the individual systems. Based on the 3-D data captured, a revised dig list location will be selected. The data will be used by others to help evaluate and develop geophysical modeling and discrimination algorithms once the ground truth locations are available in August 2004.

Test 8: ArcSecond Results

This test was not performed. The test will be conducted by the Army in coming months.

Test 9: Wooded Area—Dynamic Anomaly Positioning

- An anomaly array board 1.2 m square will be created. It will have an irregular array of nails inserted (point into the ground) for point source anomalies. This board will be randomly placed in an area clear of subsurface anomalies adjacent to each of the six rebar points. This will be mapped in a similar manner to Test 8. The individual nail positions will be selected as a dig list from the instrument peaks. The government will compare the relative position of the dig list points to the array positions and report the deviation from the location.

Test 9: ArcSecond Results

This test was not performed. The test will be conducted by the Army in coming months.

Test 10: Mogul Area—Accuracy with Positioning System for Surface Points

- The mogul area has 20 unknown points established in a varied array traversing a portion of the large and medium moguls with widely varying slope and elevation. The points are PVC pipe with removable steel pins (to trigger the magnetometer when required). Each will be occupied by the integrated navigation/geophysical sensor system to determine coordinate locations. These will be directly compared to the ground truth for position accuracy.

Test 10: ArcSecond Results

ArcSecond used its standard two-detector pole receiver to measure the mogul surface points. The benefit of this approach is twofold: (1) the pole does not need to be held level, and (2) the height of the pole may be adjusted in order to see over obstacles. The survey results are presented in figure 1-19. (Note: ArcSecond does not have the Army values for the mogul points, but the Army provided the summary comparison also shown in Figure 1-19.)

Test 10 Fixed Position

Point_Id	Easting	Northing	Elevation
141	402883.906	4369537.544	12.400
142	402885.677	4369535.437	13.605
143	402886.707	4369533.208	12.722
144	402887.440	4369532.197	12.164
145	402887.929	4369530.101	11.788
146	402888.045	4369528.918	12.032
147	402888.709	4369528.135	12.466
148	402889.950	4369526.057	12.696
149	402890.691	4369524.975	12.660
150	402891.443	4369523.688	12.216
151	402892.468	4369520.630	11.957
152	402887.167	4369519.395	12.267
153	402888.992	4369517.196	11.952
154	402892.553	4369515.439	12.163
155	402896.300	4369518.355	12.077
156	402895.217	4369515.786	12.394
157	402897.412	4369514.705	12.282
158	402898.306	4369512.738	12.107
159	402894.597	4369512.115	12.178
160	402899.108	4369510.001	12.730

ArcSecond Measured Data

20-PVC Points

	Tolerance	Tolerance					
Contractor	Easting	Northing	Distance		Elevation		
Shaw/IT	-0.0562	-0.0392	0.0900		-0.1486	Average Error	
	0.0449	0.0551	0.0383		0.0261	Standard Deviation	
GIS	-0.0538	-0.0782	0.2545		1.0938	Average Error	
	0.1914	0.1883	0.1157		0.0896	Standard Deviation	
ArcSecond	-0.0001	0.0115	0.0150		0.0100	Average Error	
	0.0065	0.0097	0.0061		0.0105	Standard Deviation	
Ensco	0.0900	-0.0098	0.2111		N/A		
	0.1400	0.1691	0.0991				

ArcSecond Measured Data compared to Army Known Values

Figure 1-19. Survey Results for Mogul Surface Points

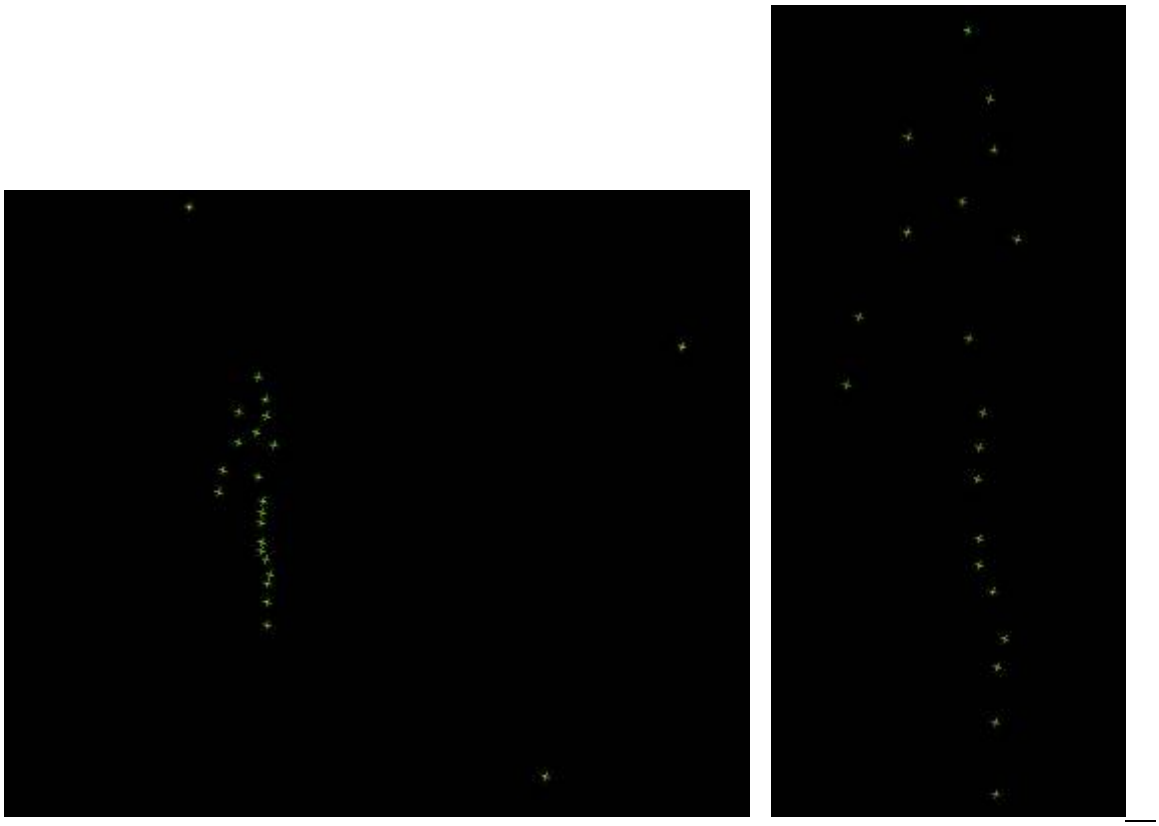

Plan View with Control Points Shown **Plan View of Surface Points Only**

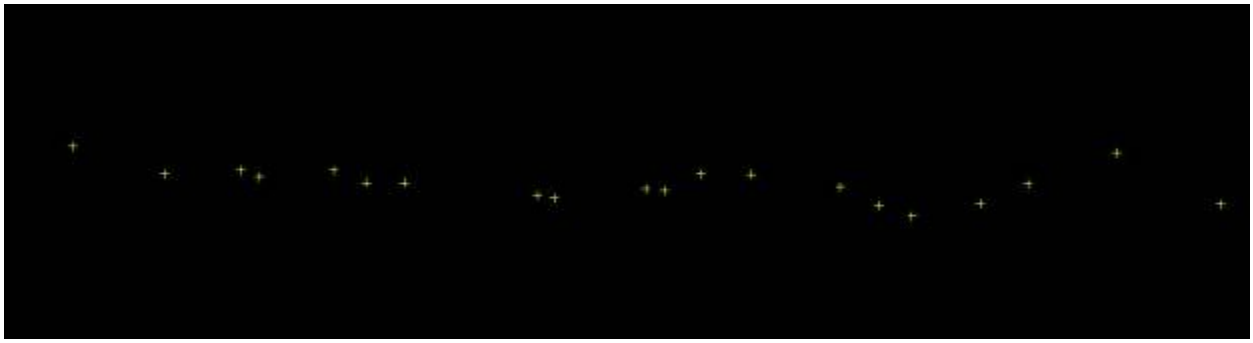

Side View of Surface Points Only

Figure 1-20. Survey of Mogul Surface Points

Test 11: Mogul Area—Accuracy from Geophysical Data Analysis for Surface Points

- The 20 points from Test 10 will be traversed dynamically by the integrated system. These points will be picked from the instrument peaks shown in the data set and reported. These will be directly compared to the ground truth for position accuracy and to the locations from Test 10.

Test 11: ArcSecond Results

ArcSecond used a two-detector pole mounted directly over the G-858 sensor head (shown in Figure 1-2). This allowed the operator to collect data without being concerned about orienting the sensor precisely vertical to the surface. To collect the data, the operator walked a path around the moguls, continuously collecting data, stopping to get more data (fine interrogation) at the flag locations. The survey results – and path – can be seen in Figure 1-21. (Note: ArcSecond does not have the Army values for the mogul points, but the Army provided summary comparison in the second table in Figure 1-21.)

Point_Id	Dynamic_X	Dyanmic_Y
141.000	402883.714	4369537.282
142.000	402885.703	4369535.347
143.000	402886.707	4369533.097
144.000	402887.352	4369532.162
145.000	402887.946	4369530.064
146.000	402888.049	4369528.953
147.000	402888.705	4369528.156
148.000	402889.891	4369526.112
149.000	402890.689	4369524.964
150.000	402891.467	4369523.701
151.000	402892.421	4369520.629
152.000	402887.197	4369519.351
153.000	402889.015	4369517.162
154.000	402892.652	4369515.379
155.000	402896.301	4369518.344
156.000	402895.376	4369515.830
157.000	402897.326	4369514.704
158.000	402898.292	4369512.702
159.000	402894.619	4369512.094
160.000	402899.057	4369510.046

ArcSecond Measured Data

Test 11- Mogul Points (Geophysics)

20-PVC Points

	Tolerance	Tolerance			
Contractor	Easting	Northing	Distance		
Shaw/IT	0.0010	0.0455	0.1786	Average Error	
	0.1464	0.1475	0.1041	Standard Deviation	
GIS	0.0062	-0.0536	0.2318	Average Error	
	0.1591	0.1919	0.0931	Standard Deviation	
ArcSecond	-0.0023	0.0263	0.0649	Average Error	
	0.0583	0.0441	0.0405	Standard Deviation	
Ensco	-0.1195	0.0562	0.3354	Average Error	
	0.2558	0.2178	0.1089	Standard Deviation	

ArcSecond Measured Data compared to Army Known Values

Figure 1-21. Survey Results for Mogul Surface Points Using Geophysical Data

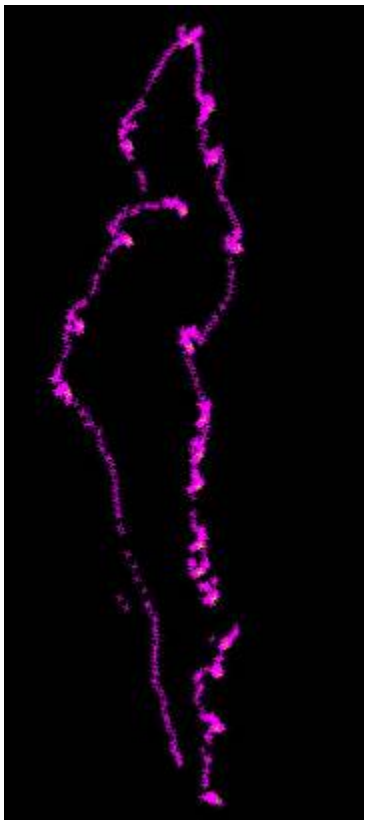

Plan View of Dynamic Survey

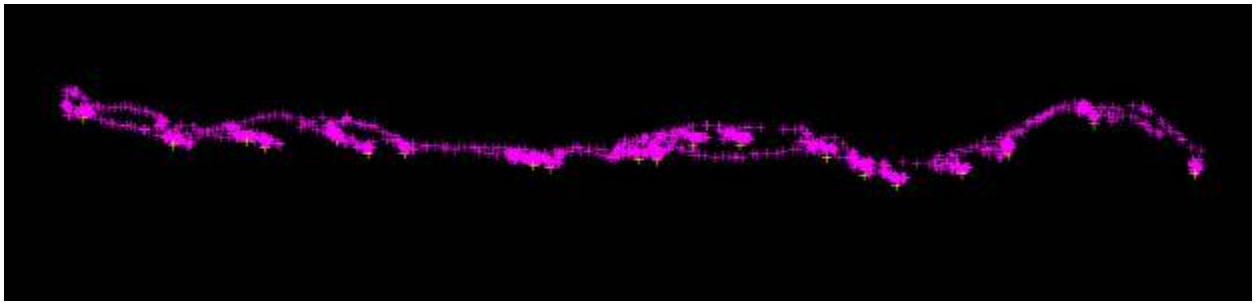

Side View of Dynamic Survey

Figure 1-22. Dynamic Survey Results for Mogul Surface Points

Appendix J:

Gtek
Application of Robotic Total Station Navigation to Sub-Audio Magnetic Surveys

REPORT

BETTER BY DEFINITION

Application of Robotic Total Station Navigation to Sub-Audio Magnetics Surveys

Aberdeen Proving Ground, Aberdeen MA

POST-ACTIVITY REPORT

G-tek Australia Pty Limited
[ABN 47 099 519 034]

Brisbane
3/10 Hudson Road
Albion Qld 4010
Ph 07 3862 2588
Fax 07 3862 3418

Sydney
Suite 1A, 802 Pacific Highway
Gordon NSW 2072
Ph 02 9844 5413
Fax 02 9844 5445

Armidale
Earth Sciences Building, UNE
Geology North Road
Armidale NSW 2351
Ph 02 6773 3927
Fax 02 6773 3307

Sunshine Coast
PO Box 2002
Buddina Qld 4575
Ph 07 5493 8577
Fax 07 5493 7405

Project Reference:	USAC02095
Prepared For:	United States Army Corps of Engineers
Authorisation No:	DACA87-03-H-00021
Issuing Office:	Brisbane Office
Date of Issue:	July 2004

DISCLAIMER AND COPYRIGHT NOTICE
G-TEK AUSTRALIA PTY LIMITED
DISCLAIMER

Please Read This Disclaimer
This Disclaimer is an important legal document. The use of this report is governed by and subject to this Disclaimer.

G-tek's Client
The entity who commissioned this report, and who is G-tek's client is the United States Army Corps of Engineers ("the Client").

Purpose Of This Report

This report describes 3 days of SAM data collection at the Aberdeen Proving Ground, Aberdeen, Maryland from 28th May -1st June 2004. ("the Purpose")

Disclaimer

G-tek accepts no responsibility or liability for any use of this report or any reliance upon this report by any person, other than the use of the whole of this report by the Client consistent with the Purpose.

G-tek accepts no responsibility or liability to any person who relies upon a part of this report. This report must at all times be considered in its entirety.

COPYRIGHT

Copyright
G-tek is the owner of the copyright subsisting in this report.

License
G-tek grants to the Client a non-exclusive license for the full term of copyright throughout the world to use and reproduce this Report for any reason consistent with the Purpose.

Infringement
The reproduction of any part of this report by any person other than the Client, or for any reason not consistent with the Purpose is an infringement of copyright, and will be prosecuted by G-tek.

Prepared by:  Malcolm K. Cattach

Reviewed by:  John M. Stanley

DOCUMENTATION CONTROL	
Copy Number	Issued To
1	USACE - Huntsville
2	USACE - Huntsville
3	G-tek Australia Pty Limited
4	G-tek Australia Pty Limited

Copy of 4

Table of Contents

APPLICATION OF ROBOTIC TOTAL STATION NAVIGATION TO SUB-AUDIO MAGNETICS SURVEYS

Aberdeen Proving Ground, Aberdeen MA

POST-OPERATIONS REPORT

EXECUTIVE SUMMARY

In recent years, a new technology known as the Robotic Total Station (RTS) has gained wide acceptance in the cadastral surveying community. The RTS employs laser sight and servo motor technology to track a moving target with great precision. It has been suggested that the RTS has potential as a positioning system for the acquisition of geophysical data for UXO detection. Several researchers have successfully integrated RTS into their survey platforms.

Sub-Audio Magnetics (SAM) is a high resolution geophysical survey technique which enables the simultaneous acquisition of Total Magnetic Intensity (TMI) and Total Field Electromagnetic Induction (TFEMI) data. During 2003, Geophysical Technology Limited (G-tek) designed and constructed a very fast sampling total field magnetometer, codenamed the "TM-6 ," in collaboration with the USACE and sponsored by ERDC. This newly developed system is currently undergoing Certification trials for the detection of UXO in a program funded by ESTCP and administered by the United States Army Corps of Engineers (USACE). The technique generally uses survey quality DGPS to position data when working in open areas where line-of-sight to satellites is available. In areas of thicker vegetation where tree canopy can block access to satellites, a Cotton Thread Odometer (CTO) system is employed, usually with very acceptable results.

In February 2004, G-tek was asked to integrate RTS technology with the TM-6 in order to evaluate its application to the conduct of SAM surveys. In particular, the performance of RTS was to be compared with the performance of CTO systems in wooded areas and with DGPS in open areas. G-tek conducted field trials of the RTS during SAM Certification trials at Aberdeen Proving Ground (APG), Aberdeen, Maryland. Testing was undertaken over 3 days of SAM data collection from 28th May to 1st June 2004 in the "Wooded " area of the UXO Test Site. The RTS evaluation was funded by the Department of the Army Research Development and Testing (RDT&E) Program and administered by the Corps of Engineers Engineering Research and Development Center (ERDC), Vicksburg MS and the Army Environmental Center.

Detail in this report is given to preparation of the system, acquisition and processing of data and final results of the data collected. Conclusions and recommendations are made from this testing as to the effectiveness of such a system for future surveys. It was determined that the Leica TPS1100 is suitable for integration with the TM-6 data recorder and the SAM survey method. However, it was concluded that RTS should only be used as a method of last resort in wooded conditions due to time consuming logistical difficulties.

The trials demonstrated that:

- The use of RTS in Wooded situations will significantly increase the cost of the survey compared with using CTO systems due to greatly increased setup costs and slow production rates.
- RTS is a very precise positioning system when line-of-sight is available between the RTS unit and the mobile reflector. However, if used as the sole positioning method, RTS will most likely result in less accurate positioning of targets than using CTO as a result of inadequate positional coverage due to obstructions.
- If used in collaboration with a CTO, the target positional accuracy may exceed that possible with CTO only systems. However, RTS is still very slow to use and it must be assessed as to whether the extra cost is justified by a small improvement in accuracy and any consequent savings which may be achieved by slightly reduced relocation costs.
- When used in open areas, the performance of RTS was considered similar to that achievable with DGPS although setup time may be slightly greater for RTS than DGPS.
- The probability of detection of potential UXO was not affected by the choice of the positioning systems trialled.

SCOPE AND OBJECTIVES OF THE SURVEY

Positioning using DGPS is inherently limited in heavily wooded areas due to the tree canopy blocking access to the satellite constellation. Other options for data positioning are Cotton Thread Odometer (CTO) or Robotic Total Station (RTS). RTS has not been widely used for positioning of geophysical survey platforms. However, field experiments previously performed at APG have demonstrated that the Leica RTS system could be used with some success in the more heavily wooded areas.

The three main objectives of the APG demonstration were:

1. To evaluate RTS navigation with the TM-6 in the Wooded Area of the UXO test site where its performance could be compared with a selection of sensor technologies that have been previously investigated by the United States Army Corps of Engineers (USACE).

2. To compare the performance of the RTS implementation with the performance of a standard CTO system in Wooded Areas.

3. To compare RTS with DGPS in open areas.

PROJECT PERSONNEL

The data acquisition team consisted of Dr John Stanley, Dr Malcolm Cattach, Mr Stephen Griffin and Mr Jared Townsend from G-tek's Research & Development Division. Data was processed by Mr Jared Townsend and Mr Stephen Griffin. All team members contributed to the report.

The crew were supervised on-site by Mr Rick Fling who also provided the photographs shown in this report. Local Maryland Leica Agent, Mr Bill Murphy assisted with the RTS system on site for the first day of acquisition.

SURVEY AREA

The density of vegetation in the Wooded Area of the APG UXO test site increased from East to West, as shown in Figure 1. In order to implement the SAM survey methodology, the area was divided into 6 adjacent 30m x 30m grids for the trial. The nomenclature used for the survey grids is shown in Figure 2 and is consistent with the nomenclature used for the SAM certification trials being conducted at APG.

On the open edge of the Wooded area, the corners of each block were accurately located using DGPS and pegged with plastic flags. Deeper under the tree canopy where DGPS was not available, RTS was used to accurately locate the corner points.

Figure 1: Photograph (looking West) of APG Wooded area. Note felled tree (extending across Grid B-07).

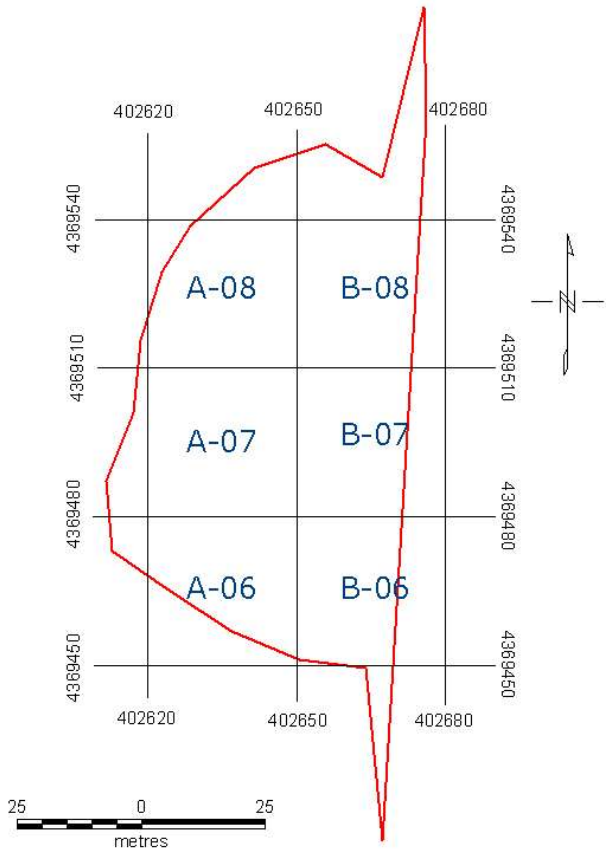

Figure 2: Map showing APG UXO Wooded Area, separated into 30m blocks for the SAM EMI survey.

SURVEY INSTRUMENTATION

The Leica TPS 1100 Robotic Total Station System

The following RTS hardware was used for the survey:

i. TPS 1100 Theodolite
ii. RCS 1100 Remote Controller
iii. 360° Prism (mounted on sensor frame)
iv. Mini Prism and Bipod (used for backsight)
v. GDF121 Tribrach and GST120 Tripod

The TPS1100 theodolite, shown in Figure 3, transmits a laser beam towards the reflector which is illuminated so that the reflection of the laser beam is able to be easily detected by a CCD element in the theodolite. The reflectors are engineered so they have a characteristic signature that is easily recognised by the CCD element, so it is very easy to distinguish this reflection from any others that may have also been illuminated by the laser beam.

As the reflector moves across the ground, the theodolite is controlled by servo motors to track the motion by continuously adjusting the horizontal and vertical alignment of the sight, so that the optimal reflection is maintained. The basic data that are being continuously recorded are the constantly changing horizontal and vertical angles between the theodolite and reflector, and the straight line distance. The computer in the theodolite converts these data into eastings and northings.

A radio modem is used to link the theodolite with the remote controller, which is an exact duplicate of the control panel mounted on the theodolite itself. The eastings and northings are calculated in the theodolite, then transmitted to the remote controller in real time, where they are output through an RS232 port.

A laser beam will spread out with distance, which means the system operates best when the reflector is located well away from the theodolite (hundreds of metres). As the reflector moves across the ground, the angular velocity that the theodolite has to maintain in order to keep tracking the reflector will be much less with a greater separation distance. Furthermore, because the beam has spread out more with distance, it is easier for the optical sight to maintain lock on the reflector since the spot reflection is located in a larger field of view of the CCD.

For this trial the RTS system was used in its rapid tracking mode which has an accuracy of 10 mm ± 2 ppm, and a measurement time of approximately 0.15 –0.3 seconds.

Figure 3 The Leica TPS1100 Robotic Total Station (RTS).

Note: The latest model TPS 1200 was trialled prior to this survey and found to be more difficult to interface with the TM-6. The output baud rate from the remote controller was too high for the TM-6 to maintain, along with all of its other tasks. This baud rate could not be set to a lower figure in the current version of the system. The TPS1100 system configured with certain application programs essentially duplicated the performance of the newer model.

The TM-6 Magnetometer

Detailed descriptions of the SAM technique and the TM-6 magnetometer have been previously provided and are beyond the scope of this report.

Data were acquired using a quad-magnetic sensor array, held at a nominal elevation of 0.4m above the ground. The four Cs-vapour sensors were equally separated by 40cm and supported on a non-metallic frame, as shown on the right side of the photograph in Figure 3 below. The RTS reflector was mounted behind the operator, directly below the GPS antenna. The forward offset between the sensors and the reflector was measured at 1.0m.

In practice, SAM surveys require a two-man survey crew. One operator carries the frame and is responsible for maintaining consistent sensor height and line direction. The second operator controls the TM-6's operation and recording functions and monitors data input and quality. The two operators maintain a distance of several metres from each other in order to ensure that there is no electromagnetic interference from the control and data logging electronics (see Figure 5).

Figure 4 Photograph of the SAM acquisition system showing the four Cs vapour magnetometer sensors at the front of the array (right of photo) and the reflective prism (red cube) mounted directly below the GPS antenna at the rear of the frame (top left of photo).

Figure 5 SAM surveys require a two-man acquisition crew. A distance of several metres is maintained between the operators to ensure that there is no electromagnetic interference from the control and data logging electronics.

Technical Summary of the Survey Equipment

The technical specifications of the SAM RTS survey system is summarised below in Table 1.

Table 1 Acquisition Instrumentation specifications used for the survey.

Roving Magnetometer Acquisition System	
Magnetometer	Geophysical Technology proprietary TM-6 Magnetometer Controller
Sensor	Scintrex CS-2 Cs Vapour
Number of Sensors	4 at sensor separation of 400mm
Array Setup	cm from centre of frame: -60, -20, 20, 60
Sensor Elevation	0.4m
Sample Rate	1200 samples per second
Sample Resolution	0.01nT
Data Positioning	
Robotic Total Station	Leica TPS1200
Datum	NAD83
Sample Rate	Non-constant - up to ~ 4Hz when lock is available
Nominal Survey Direction	000-180

The TM-6 Data Logging Process

When lock is achieved, the output data stream from the RTS remote controller is continuous at a non-constant time interval with a rate of approximately 0.3 Hz. If lock is lost then the RTS ceases to output data. The format of the data stream is a proprietary Leica format referred to as the GSI-16 Cartesian format. The data string includes an ID number, easting, northing, elevation and reflector height.

The TM-6 is designed to time stamp every input with an accurate time value that has better than 1 ppm accuracy, maintained by continuous reference to a GPS time strobe. As the RTS position string is input through an RS-232 serial input, the time stamp is embedded with the string which is then reformatted and recorded along with all other system inputs such as the sensor measurements.

In normal DGPS operations, the TM-6 continuously corrects the internal clock every second, based on the precise timing signal received from the satellites. During an RTS survey in an area where GPS reception is not possible due to obstructions from trees, the internal TM-6 clock will still maintain the required accuracy for at least half-an-hour, before it is necessary to re-establish a GPS lock to reset the internal clock with the satellite timing signal. Each SAM survey grid is approx. 30 m x 30 m, and takes approximately 20 minutes to complete. Therefore, the required timing precision can be easily maintained by simply moving the sensor frame to a location where it can see the satellites between each grid set up. Thus, if GPS lock is lost for any length of time, the TM-6 clock will be reset well within the required 30 minute interval that is necessary to ensure an accuracy of <10μs.

The TM-6 data logging software was modified specifically for this project to enable parameter settings that specify that the system is being used in RTS mode. That is, the software is configured to read in the Leica GSI-16 format rather than the usual NMEA GGA string that is input with DGPS operations. Once the RTS position data is incorporated into the data file, it is processed in much the same manner as if the positions were obtained from the NMEA GGA string. The only significant difference is the fact that the NMEA GGA string stores position in latitude and longitude which needs to be transformed into UTM eastings and northings, whereas the RTS position is already in the required UTM eastings and northings.

Leica 1100 RTS Setup Procedure

The procedure to set up the RTS is described as follows:

i. Set up the theodolite mounted on a tripod over a known point and level.
ii. Set up a reflector mounted on a bipod over a known point (see Figure 6).
iii. Configure the theodolite with the required settings.
iv. Type in known UTM coordinates of the theodolite position.
v. Type in known UTM coordinates of the reflector position.
vi. Measure with the theodolite, the distance between the theodolite and reflector and compare the measured value against the known value as an accuracy check.
vii. Move the reflector to another known point and measure the distance and coordinates then compare these measured coordinates with the known position to check the instrument is working to the required accuracy.
viii. Sight the theodolite towards the reflector mounted on the sensor frame.
ix. Use the remote control unit to initiate the continuous recording of position and commence surveying the grid.

Power Search

The TPS1100 system is able to provide a power search option through the implementation of an application program (specifically installed firmware). This refers to a search option that enables the instrument to find the prism at any location in a very short period of time, if it loses the signal through obstruction or loss of direct line of sight.

Associated with the power search option is the ability to define a 'working area' which restricts the horizontal and vertical angle the theodolite can move during the power search. In this way, the time to regain lock after it has been lost will be minimized. The search area is defined through manual programming of the allowable boundaries of the theodolite movement both horizontally and vertically.

Figure 6 Reflector mounted on bipod setup on a known point. This instrument is used to confirm the position where the theodolite is setup.

Auto Record Mode

An advanced application program was used to configure the instrument into the most appropriate mode for this type of survey. In this mode, the calculated position of the reflector is continuously output from the remote controller (and logged by the TM-6) at rates up to 0.3 Hz, depending on the quality of the lock being maintained during movement of the reflector across the ground.

The position is only output while direct line of sight between the theodolite and reflector is maintained. If this line of sight is interrupted (say by a tree) the data stream is stopped but the theodolite will continue to move based on it predicting the track of the reflector. In this way, as soon as the direct line of sight is re-established, the data stream output resumes. If the theodolite estimate of the reflector track is poor, the theodolite switches into the power search mode until the required level of signal is re-established. The operator has to be constantly aware of this situation so as to stop walking until the lock is re-established.

Scale Factor

GPS positioning and UTM coordinates have to take into account the fact that the earth's surface is curved. RTS surveying assumes it is working on a flat surface. If the distances involved become significant (hundreds of metres), there will be a discrepancy between UTM coordinates measured using a DGPS system, and coordinates determined from the RTS system. This discrepancy is easily dealt with through the use of a scale factor that adjusts the RTS measurements so they match the DGPS UTM data. The scale

factor is programmed into the TPS1100 during the initial set up so that all measured positions are automatically adjusted according to the scale factor, prior to output to the data logger.

The standard approach adopted by the TPS1100 is to specify the scale factor at the Central Meridian of the UTM Zone (in this case 0.9996) and then to specify the distance in metres between the Central Meridian and the survey location (in this case 97215 metres).

Survey Reference Information

The wooded area at the APG UXO test site was set up into 6 grids referred to as A-06, A-07, A-08, B-06, B-07 and B-08. It was not possible to use the same theodolite position for all 6 grids as no single location provided good line-of-sight for all grids. Four different theodolite positions were selected to provide optimal coverage for each grid as shown in Figure 7.

The main selection criteria in each case were that the reflector needed to have a direct line-of-sight to the theodolite at all start and end points of each survey line. All theodolite positions were in the open field, shooting into the wooded area, as shown in Figure 8. One of the major obstacles to the survey was maximizing line-of-sight in areas which contained the felled tree shown in Figure 1.

Table 2 summarises the positions of the various Theodolite Stations and describes which station was used for each grid surveyed.

Table 2 Reference Coordinates of Theodolite Stations

Survey Grid	Theodolite Station	Easting (mE)	Northing (mN)
A6	7F	402770.102	4369479.962
A7	10D	402710.018	4369569.940
A8	10D	402710.018	4369569.940
B6	Stn500	402684.529	4369503.032
B7	Stn15	402902.446	4369486.106
B8	Stn15	402902.446	4369486.106

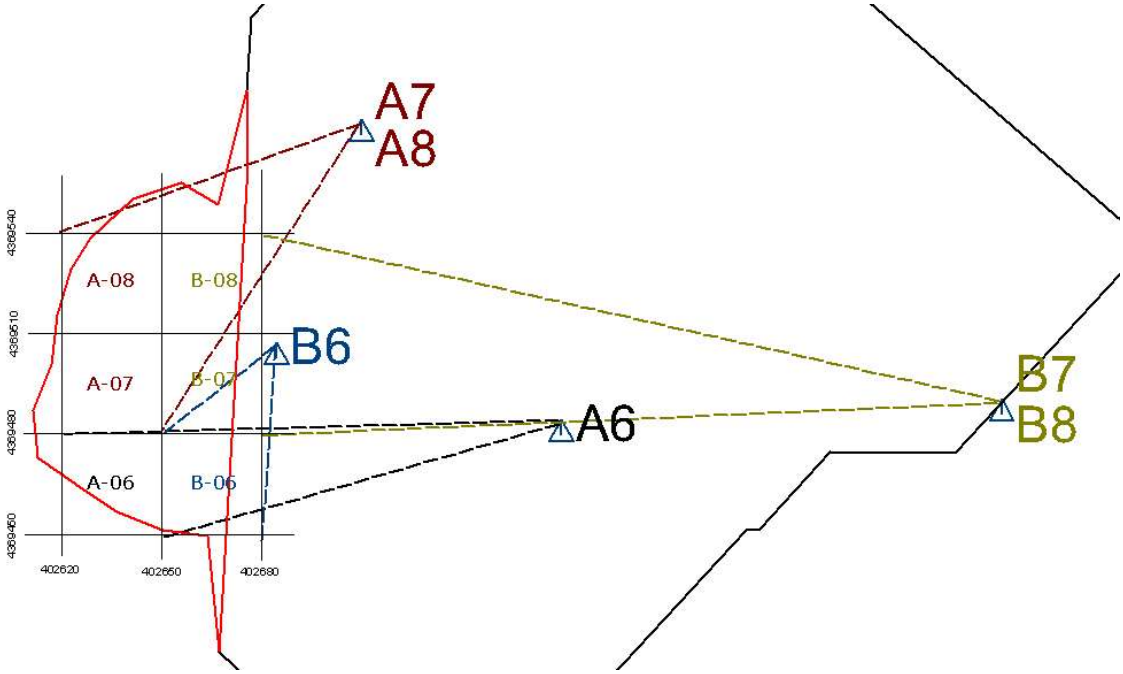

Figure 7 Location of RTS Theodolite Stations showing the location used for each grid.

Figure 8 RTS shooting into wooded area from Theodolite Station 10D. The butt of the felled tree can be seen just to the right of the theodolite.

All of the above theodolite positions except Stn15 were established by G-tek. Stn15 was a location surveyed in by Aberdeen Test Centre (ATC) Geodetic personnel, and was used as the main backsight check point for each of the theodolite station locations. The typical error in the backsight measurements was of the order of 0.01 –0.02 m. This figure was used to confirm the theodolite had been accurately set up over its known position. The listed coordinates are referred to in this report as the reference locations and are the actual numbers typed into the theodolite to establish the station location. A number of checks were conducted during the survey and are summarized in the following two tables:

Table 3 RTS Measured Coordinate Checks

ID	Easting 1 (mE)	Northing 1 (mN)	Easting 2 (mE)	Northing 2 (mN)	delta East (m)	delta North (m)	Difference (m)
15 (stn)	27 May RTSDEMO2.GSI		402902.446	4369486.106			
16	402947.650	4369538.298	402947.653	4369538.303	0.003	0.005	0.006
500	402684.535	4369503.034	402684.529	4369503.032	0.006	0.002	0.006
500 (stn)	29 May RTSDEMO4.GSI		402684.529	4369503.032			
M478	402785.683	4369305.448	402785.686	4369305.416	0.003	0.032	0.032
15	402902.428	4369486.111	402902.446	4369486.106	0.018	0.005	0.019
M478 (stn)	29 May RTSDEMO4.GSI		402785.686	4369305.416			
7F	402770.107	4369479.980	402770.102	4369479.962	0.005	0.018	0.019
15	402902.434	4369486.111	402902.446	4369486.106	0.012	0.005	0.013
500	402684.574	4369503.029	402684.529	4369503.032	0.045	0.003	0.045
10D	402710.006	4369569.943	402710.018	4369569.940	0.012	0.003	0.012
7F (stn)	1 Jun RTSDEMO5.GSI		402770.102	4369479.962			
10D	402710.018	4369569.943	402710.018	4369569.940	0.000	0.003	0.003
500	402684.524	4369503.048	402684.529	4369503.032	0.005	0.016	0.017
500	402684.534	4369503.046	402684.529	4369503.032	0.005	0.014	0.015
104	402671.000	4369505.293	402671.039	4369505.242	0.039	0.051	0.064
113	402660.628	4369507.888	402660.667	4369507.840	0.039	0.048	0.062
120	402649.422	4369510.677	402649.459	4369510.629	0.037	0.048	0.061
105	402670.092	4369492.162	402670.134	4369492.105	0.042	0.057	0.071
107	402668.266	4369465.860	402668.313	4369465.799	0.047	0.061	0.077

	Temporary Bench Mark established by G-tek
	RTS measured by G-tek
	Provided by Aberdeen Test Centre
	DGPS measured by G-tek

Table 4 DGPS Measured Coordinate Checks.

ID	Easting 1 (mE)	Northing 1 (mN)	Easting 2 (mE)	Northing 2 (mN)	delta East (m)	delta North (m)	Difference (m)
15	402902.420	4369486.130	402902.446	4369486.106	0.026	0.024	0.035
10D	402710.020	4369569.970	402710.018	4369569.940	0.002	0.030	0.030
7F	402770.110	4369479.980	402770.102	4369479.962	0.008	0.018	0.020
500	402684.530	4369503.090	402684.529	4369503.032	0.001	0.058	0.058
500	402684.530	4369503.090	402684.524	4369503.048	0.006	0.042	0.042
104	402671.010	4369505.330	402671.039	4369505.242	0.029	0.088	0.093
104	402671.010	4369505.330	402671.000	4369505.293	0.010	0.037	0.038
104	402671.000	4369505.320	402671.039	4369505.242	0.039	0.078	0.087
104	402671.000	4369505.320	402671.000	4369505.293	0.000	0.027	0.027
113	402660.660	4369507.900	402660.667	4369507.840	0.007	0.060	0.061
113	402660.660	4369507.900	402660.628	4369507.888	0.032	0.012	0.034
105	402670.100	4369492.190	402670.134	4369492.105	0.034	0.085	0.091
105	402670.100	4369492.190	402670.092	4369492.162	0.008	0.028	0.029
107	402668.280	4369465.890	402668.313	4369465.799	0.033	0.091	0.097
107	402668.280	4369465.890	402668.266	4369465.860	0.014	0.030	0.033
M478	402785.670	4369305.440	402785.686	4369305.416	0.016	0.024	0.029

Table 3 above provides RTS measured coordinates for a range of locations as indicated by the ID in the first column, with the theodolite station set up at four different locations, namely Stn 15, Stn 500, Monument 478 and Stn 7F. The RTS measured coordinates labelled as Easting 1 and Northing 1 (coloured green) are compared against the reference coordinates, labelled as Easting 2 and Northing 2, which were either RTS derived (coloured orange and listed in Table 1) or provided by Aberdeen Test Centre (coloured yellow). The columns labelled delta East, delta North and Difference indicate the comparison between the measured and reference coordinates. ID points 104, 113, 120, 105 and 107 refer to locations set up by ATC, listed as 'woods magpoints ,'and marked on the ground with PVC tube.

It is worth noting the average differences in the rightmost column, if they are considered as two groups. The average of the group of differences associated with the G-tek established station locations (light green) is 0.02 m. The average of the group of differences associated with the 'woods magpoints '(light blue) is 0.07 m. These figures at the very least indicate that the standard of the G-tek surveying was being conducted to

an acceptable level of precision. The slightly greater difference related to the 'woods magpoint' locations could be explained by the ATC positions being slightly incorrect.

In order to test the accuracy of the position data supplied by ATC, the G-tek DGPS was used to measure DGPS coordinates at all of the points in question. On the eastern edge of the wooded area, where vegetation was not dense, these points were open to be surveyed with the G-tek DGPS. The results of this survey are summarized in Table 4.

The data coloured blue represents the DGPS positions, the data coloured yellow represent the ATC data and the green represent measurements using the RTS system. Again comparing the average of the differences (rightmost column) in the two groups results in the ATC data having an average difference of 0.085 m and the RTS data having an average difference of 0.034 m.

In practice, all of this data would have to be considered well within acceptable limits.

Instrument Latency (Time Lag)

The sequence of events that provide a given position estimate are summarized as follows:

i. The laser beam illuminates the reflector
ii. The reflection from the reflector is detected by the CCD element in the theodolite
iii. The horizontal and vertical angle of the theodolite is adjusted by servo motors so the reflected position is centred on the field of view
iv. The horizontal and vertical angles and the distance are measured and converted to position coordinates by the theodolite computer
v. The data is transmitted to the remote controller via the radio modem
vi. The data is transferred to the TM-6 via a serial port RS-232 link
vii. The position string is time stamped by the TM-6 so that position can then be related to other time stamped data such as the sensor output.

This sequence of events from the moment the reflector is initially illuminated until the time the data is time stamped takes a finite amount of time to occur. However, it is generally constant for each measurement. Therefore, even though the data may be output at a rate of the order of 0.3 Hz, each of these measurements will be recorded by the TM-6 a short time after the sequence begins. This delay is known as the instrument latency.

A simple field procedure was followed to estimate this latency by surveying a profile across a target from two directions 180° apart, and adjusting the timing of the position data until the two peaks coincide. For this trial, the time lag was estimated to be 0.3 seconds, which was found to be in agreement with other people using the same instrument, but with different recording hardware.

Figure 9 presents the line profiles recorded over four targets which were used to measure the latency. These included the rebar points #11, #13 and #14 in the woods. The lag correction in the processing software was adjusted until all peak anomalies matched.

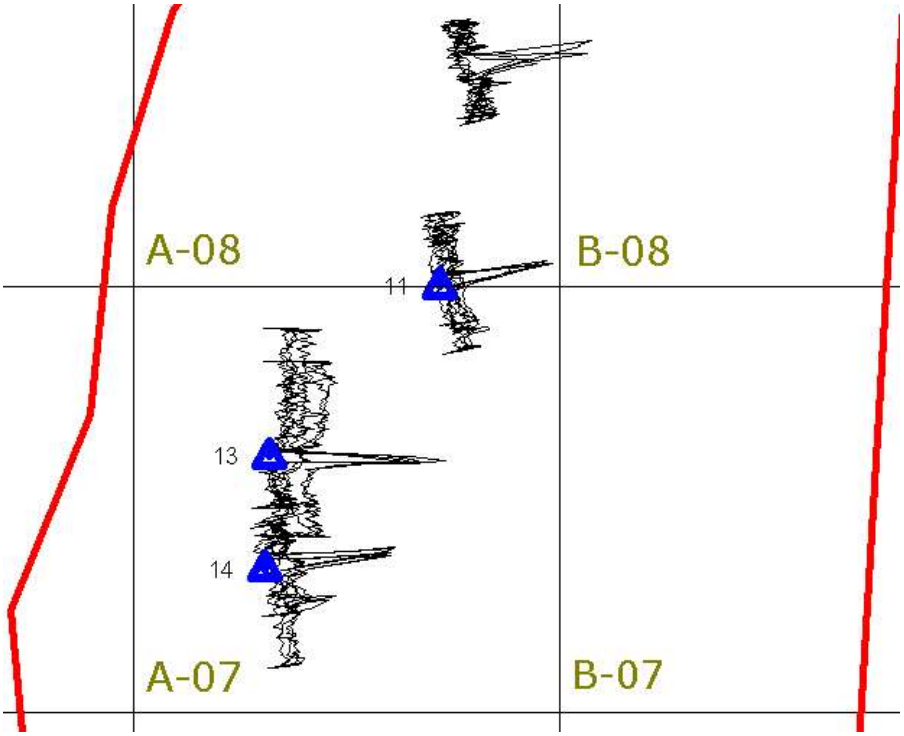

Figure 9 Line profiles of EM response over rebar used for RTS lag corrections

SURVEY METHODOLOGY

SAM Survey Field Procedures

Transmitter loops of side length approximately 38m x 38m were laid out around each survey block at a distance of about 5m from the edge of the survey area. The loop wire was made up of 4 conductors, doubled over to effectively make an 8 turn loop.

A Zonge GGT-10 geophysical transmitter, controlled by a Geophysical Technology Limited (GTL) SAM signal controller was used to transmit a square waveform into the loops at a frequency of 15Hz (50% duty cycle). The controller was synchronized to GPS timing strobes. These same timing strobes were also utilized by the TM-6 magnetometer thereby providing precise synchronization between the transmitter and the TM-6 receiver.

An objective of the trials was to make a direct comparison between RTS positioning in the Wooded area and that which could be achieved with the use of a CTO. The most effective means by which that comparison could be facilitated was to operate both positioning systems concurrently. Consequently, a

CTO was also used for all six RTS navigated grids. A GTL proprietary odometer was used for the surveys. This unit outputs an electronic strobe pulse which was logged by the TM-6 at intervals of 5cm.

In order to enable a survey time comparison between using the CTO and using RTS, two of the grids, A-08 and B-06 were surveyed twice –once with RTS and once with the CTO only.

The grids were surveyed using the RTS in a similar manner to the DGPS positioning system.

The following procedure was followed:

- Polychains were laid out along the northern and southern boundaries of the survey area.
- Sighters were positioned at the ends of each of the survey lines to provide visual guides as the grids were surveyed. The survey lines were spaced 1.5 metres apart, and oriented north-south.
- The actual start and end points used for each line were determined by the need to have a clear line-of-sight between the reflector on the sensor frame and the theodolite. In most cases, the lines started a short distance away from the first polychain and finished a short distance past the other polychain. This was to ensure that positional data were being recorded at the moment the lines started and ended.
- At the start of each line, the cotton thread was attached to a fixed object and once RTS data were being received by the TM-6, the survey was commenced.
- During the traverse, the operator monitored the position data on the remote controller and if RTS lock was lost due to an obstruction of the line-of-sight between the reflector and the theodolite, the survey continued past the obstruction to allow the RTS to reacquire. If reacquisition did not occur very quickly, the traverse was halted while the RTS completed its power search and reacquired lock. The traverse was restarted as soon as the TM-6 again received the RTS output.
- If an obstacle was met while surveying the lines, GTL's convention is to shift the array to the left of and around the obstruction whilst maintaining the same array orientation. This convention was employed at Aberdeen. Normally, while using a CTO, these shifts are recorded in the data file as a note which is available to the interpreter. Notes were not recorded at Aberdeen as the RTS generally provided this information instead.

STATISTICAL COVERAGE ACHIEVED WITH RTS

One of the major issues with positioning systems in vegetated areas is the degree of coverage achieved, as too little coverage will result in poor positioning of the geophysical data. Typically, when using DGPS systems, a position is available at least once per second. At walking speed, this would translate to a position about every metre.

With the TM-6, after post-processing the raw magnetic data, the SAM parameters of TMI and TFEMI are generated at the rate of typically 15 measurements per second. This means that there are 15 samples recorded within and therefore constrained by a distance of approximately one metre of traverse. The speed of traverse is assumed to be constant within that one second period and the position of each data point is determined by linearly interpolating between the known positions. Any error due to slightly non-constant speed is therefore distributed between each data point within that second. Consequently, the accuracy of the positioning method, be it DGPS, RTS or CTO, will be largely dependent on the number of positional "fixes" along each line.

Some locations within a grid will have no positional data points due to trees obstructing line-of-sight between the RTS and the reflector, while others will have many data points if the survey is slowed by obstacles on the ground. Therefore, it is not possible to determine the statistical coverage achieved with RTS by simply determining the average number of positional data points per square area of survey.

In determining the statistical coverage achieved with the RTS, the following assumptions were made:

- Speed of traverse is constant within any one second period.
- A positional measurement every metre provides adequate positional control for UXO surveys.
- Positional measurements at intervals closer than one metre do not significantly improve positional control. For example, four identical positional measurements taken at one location while the sensor is stationary will not provide any improvement over one measurement at that location.

The statistical coverage was therefore determined as follows:

The RTS position data were re-fiducialed (interpolated to a new sample spacing) using a Geosoft utility, to a sample interval of one metre. However, if no positional data were available within a distance of greater than one metre a gap was left in the data. The number of new positions on each 30m line would therefore be 31 if the line had adequate positional information. Accordingly, in a 30m x 30m grid surveyed at 1.5 m line spacing, there would be 21 lines of 31 positional data points or 651 data points. By counting the number of re-fiducialed positions within each grid, it was possible to determine the % areal coverage achieved for each grid. These statistics are shown in Figure 10.

As can be seen from the figure, high coverage rates were achieved (>94%) in grids B-06, B-07 and B-08. This would be expected as there was little vegetation in these grids. However, it is also apparent that the percentage coverage dropped off quickly as the surveys extended into the Wooded areas on grids A-06, A-07 and A-08. It is difficult to determine what would be an acceptable coverage rate for these grids for UXO detection. However, it is clear that the RTS coverage of Grids A-06, A-07 and A-08 are less than adequate (less than 65% and as low as 37%).

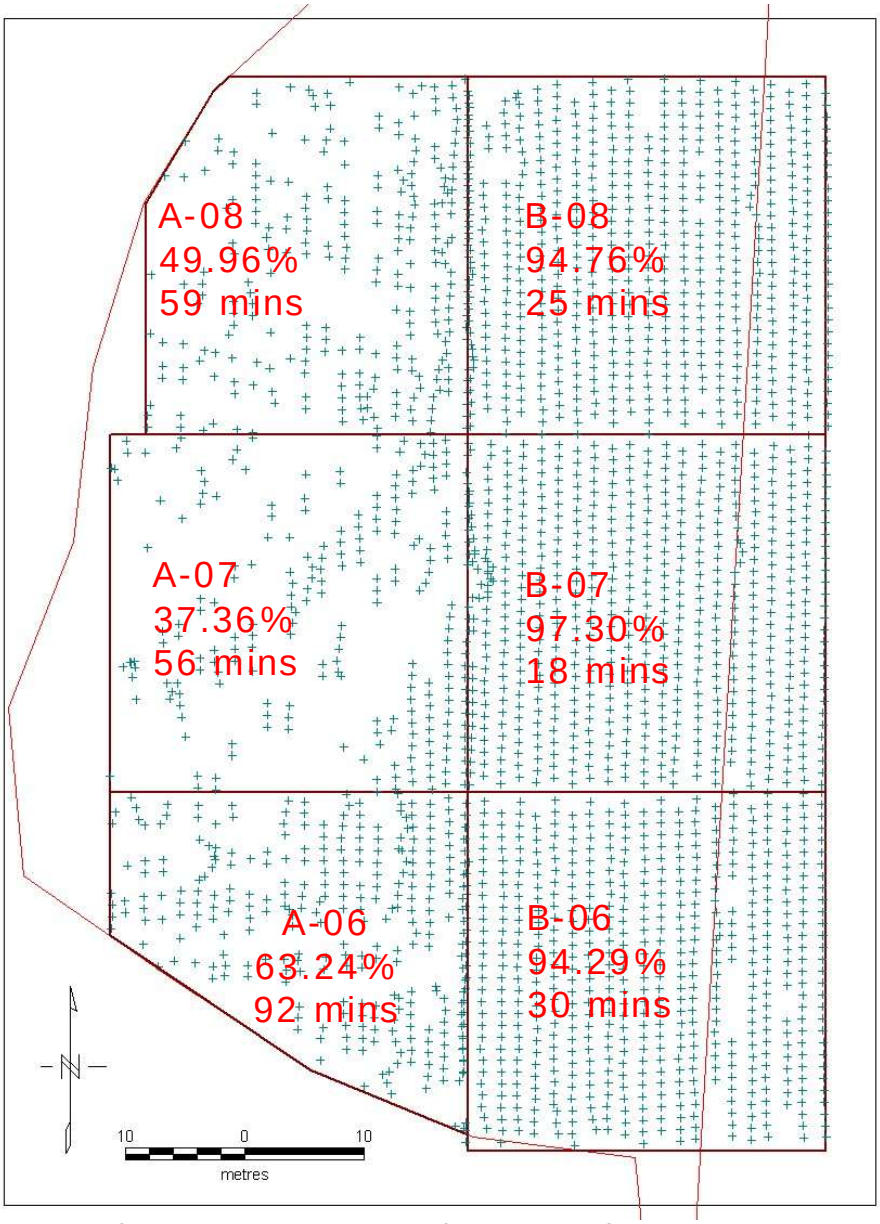

Figure 10 Map of survey area showing re-fiducialed RTS data points as crosses and estimated coverage achieved. The time taken to complete the grid using RTS is also shown (excluding repeats due to operator error).

Also shown on Figure 10 are the times taken to survey each of the grids. These times are determined directly from the data logs and exclude any time taken to repeat lines which were lost due to operator error. As would be expected, the times required to survey the grids in the wooded areas were greater due to the need to stop and wait for reacquisition once RTS lock was lost. It was estimated that reacquisition time took less than 30 sec about 70% of the time, 1 to 5 minutes about 20% of the time and greater than 5 minutes about 10% of the time.

DATA PROCESSING CONSIDERATIONS

MagPi - Sub-Audio Magnetics Processing Package

As part of the SAM Certification trials, a new software package name 'MagPi' has been written to process the Sub-Audio Magnetics data. Several modifications were required to the package to enable processing of the RTS data. These included:

- Ability to read the RTS data format.
- Modifications to the interpolation procedure for RTS positional information including smoothing (Renner Spline) of the line paths where coincident or near-coincident points occur.
- Ability to merge RTS and cotton thread odometer data.

Interpolation of positional data between RTS positions

As mentioned previously, the TM-6 used four sensors for the surveys. Consequently, the line paths for each of the four sensors were determined from the RTS positions by calculating forward and lateral offsets from the RTS reflector. Two major issues were encountered with interpolating positions based on the RTS data. These were due to the non-constant sample interval resulting from situations where:

1. RTS lock was lost due to trees etc obstructing line-of-sight between the RTS and the reflector, sometimes resulting in long gaps in the positional data (up to ten metres).
2. The survey speed slowed considerably while negotiating difficult terrain or trees (sometimes reversing). At these times, RTS data were recorded at very close spatial intervals and were sometimes coincident.

The result of these situations was that the distance interval between RTS data points varied widely along the profiles. This provided quite a challenge to the interpolation software which had difficulty coping as demonstrated in Figure 11. In order to improve the interpolation process, Renner Spline smoothing was applied to the RTS track prior to calculating the sensor offsets. The much improved result of this process is shown in Figure 12.

The smoothing process overcomes the effect of sharp angles in the traverse due to positional data points being too close together. However, it cannot compensate for loss of RTS positions over a significant distance. Where this occurs, there is no option but to linearly interpolate positions for each geophysical data point with the assumption that the sensor is moving at constant speed –which it isn't. An example of where this has been applied to TMI data is shown in the leftmost image of Figure 13.

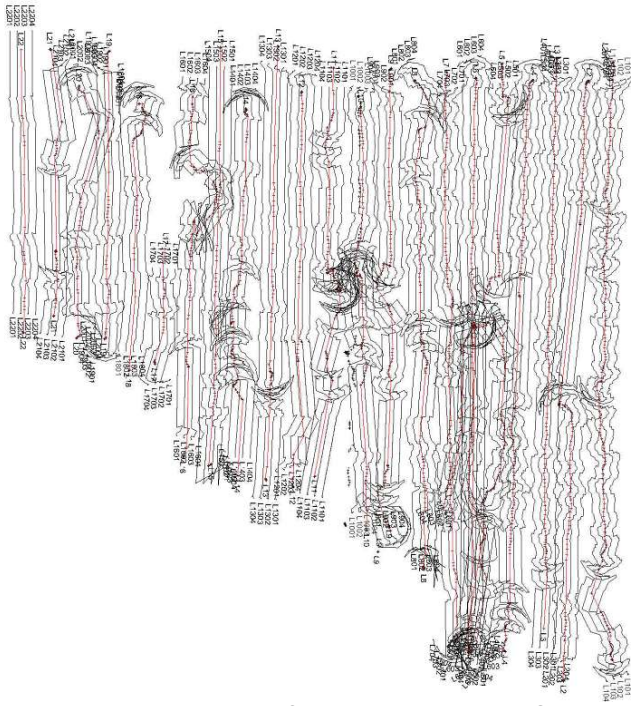

Figure 11 Grid A-06 - Poor interpolation of variably spaced RTS data points. RTS tracks are shown in red, calculated tracks for each of the four sensors are shown in black.

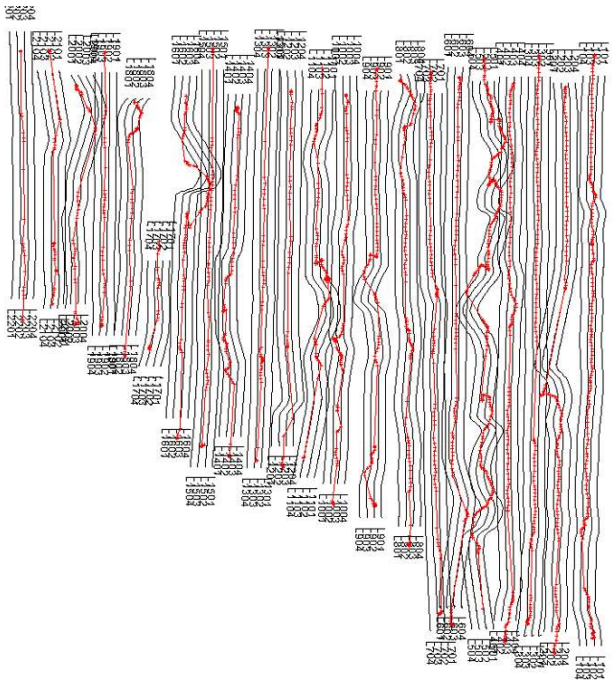

Figure 12 Grid A-06 - Improved interpolation after using Renner spline smoothing of RTS tracks and then applying sensor offsets. RTS tracks are shown in red, calculated tracks for each of the four sensors are shown in black.

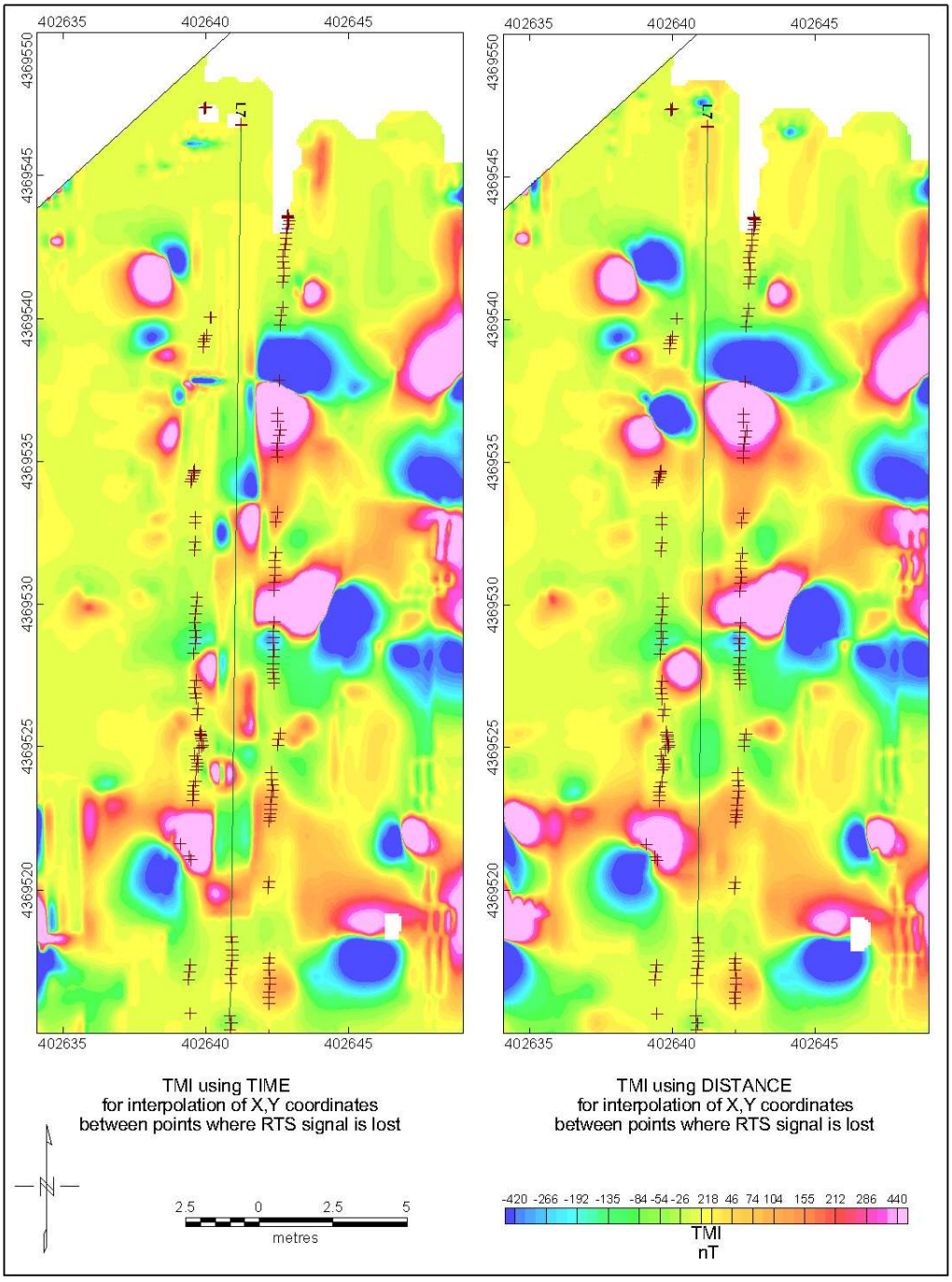

Figure 13 Section extracted from Grid A-08. Left - An example of time-based interpolation over a period where RTS has been lost for a significant time. Right – The same dataset where distance-based interpolation has been applied based on strobe inputs from the cotton thread odometer.

As can be seen from the image, the anomalies in the centre of the image have been distorted due to the fact that inadequate positional control was available in the data. The ripple visible on the right of the image was due to overlapping lines. As the CTO was also used for the survey, it was possible to integrate the two datasets by using the RTS positions as control points where they were available and using the strobe inputs from the cotton thread odometer to constrain data to 5cm increments of distance between the RTS points. This strategy was implemented in the data processing and the results shown in the rightmost image of Figure 13.

As can be seen from that image, the anomalies have been significantly improved by this means. The example shown is rather extreme as there was a large gap in the data where there were no RTS positions. Normally, if RTS was being relied on solely, this line would have needed resurveying. Nevertheless, the example demonstrates the effect that would occur over smaller gaps in the RTS data as well.

By running the RTS and cotton thread odometer concurrently, it was possible to process data using three different positioning strategies:

1. Use RTS positions only.
2. Use CTO positioning only.
3. Use a combination of RTS positions and CTO infill.

As the major objective of this project was to compare positioning techniques, a great advantage of running both the RTS and cotton thread odometer concurrently was that the only variable in the comparison was the positioning technique. That is, if the RTS and CTO surveys had been run independently, it would have been impossible to walk exactly the same path and the data acquired would have been slightly different.

The three positioning techniques mentioned above were tested at known locations within the grid. Figure 14 shows images of TMI data recorded at 'Woods Rebar 12 'using the three positioning systems. The RTS was found to be more accurate than the CTO only positioning technique. The RTS/CTO combination technique was also demonstrated to be very accurate in locating the anomaly.

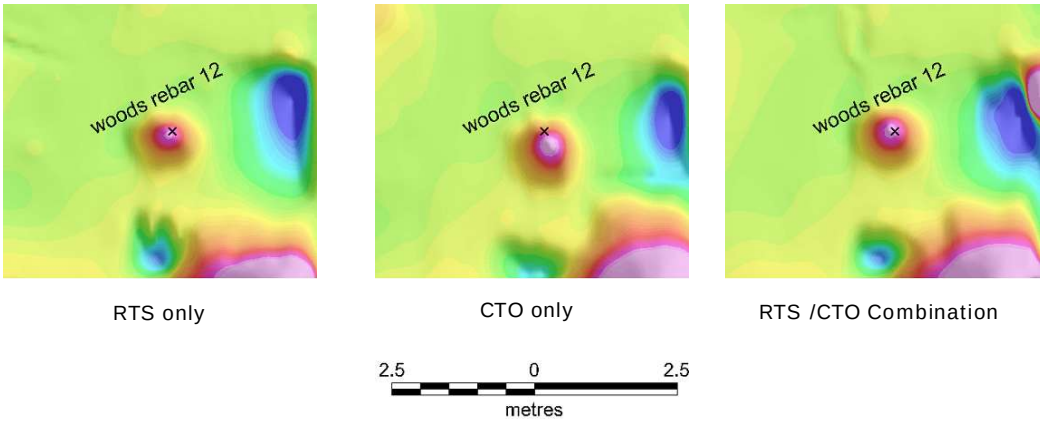

Figure 14 TMI anomalies, located using the three different methods

SURVEY RESULTS

Two of the grids, A-08 and B-06, were surveyed with CTO only as well as with the RTS / CTO combination. The purpose of this was to fulfil two objectives:

1. To compare survey times when using either RTS or CTO.
2. To compare the effectiveness of using polychains to mark the start and end of lines compared to the more accurate RTS positioning.
3. To compare the repeatability of data quality using either technique.

A-08 was fairly representative of the Wooded Area while B-06 was more representative of open country. The times taken to survey each grid are shown in Table 5. In the open area of Grid B-06, the survey times are very similar as RTS lock wasn t'lost very often. However, in the more heavily treed area, Grid A-08, the time required to conduct the survey was doubled due to the significant amount of time spent waiting to reacquire RTS lock. Interestingly, there was little difference in the time required to survey the two grids by the CTO only method.

Table 5 Comparison of Survey times for cotton thread odometer positioning and RTS positioning.

Grid ID	Survey Time - Cotton	Survey Time - RTS
A-08	29 min	59 min
B-06	28 min	30 min

Figure 15 shows images of the TMI data recorded from Grid A-08, surveyed with CTO only (Top Image) and with CTO using the endpoints only from the RTS survey (Bottom Image). That is, they were surveyed at different times. In both images, the data processing assumed straight lines from the start to the end points. In reality, the sensor array was manoeuvred around trees and the result of this is the presence of some linear processing artefacts in both images. The two images appear to be essentially the same although the start of a small anomaly is visible at the south-western corner on the Bottom Image which is not visible on the Top Image. This is probably due to having a slightly different endpoint in the RTS positioned data. The CTO only survey must have stopped just short of the anomaly. From the point-of-view of interpretation, the two surveys appear to be essentially the same.

Figure 16 shows images of the TMI data also recorded from Grid A-08, but surveyed with RTS only (Top Image) and with the RTS/CTO combination (Bottom Image). The Top Image shows severe tears in the data resulting from inadequate positional control as described previously. In comparison, the Bottom Image is of quite good quality. The ripples present on the eastern edge of the grids are due to the effect of gridding overlapping lines which result from traverses skirting around trees.

The RTS / CTO combination appears to correlate very well with both images from Figure 15.

Similarly, Figure 17 shows images of the TMI data recorded from Grid B-06, surveyed with CTO only (Top Image) and with CTO using the endpoints only from the RTS survey (Bottom Image). Grid B-06 was relatively open with very few trees as indicated by the very high quality images. The two images appear are remarkably similar, thus attesting to the repeatability of the CTO positioning.

Figure 18 shows images of the TMI data also recorded from Grid A-08, but surveyed with RTS only (Top Image) and with the RTS/CTO combination (Bottom Image). Because there were few trees in this grid, the RTS coverage was very high as discussed earlier (94%). Consequently, the data has been well positioned and the image is of high quality. As would be anticipated, the Bottom Image shows little improvement compared to the Top Image.

Both the RTS and RTS/CTO combination images appear to correlate very well with both images from Figure 17.

All grids were processed with the RTS positioning option and appended to produce the image shown in Figure 19. All grids were also processed with the RTS/CTO combination processing option to produce the image shown in Figure 20. The RTS/CTO image is clearly superior to the RTS only image, particularly in the western grids where RTS coverage was inadequate.

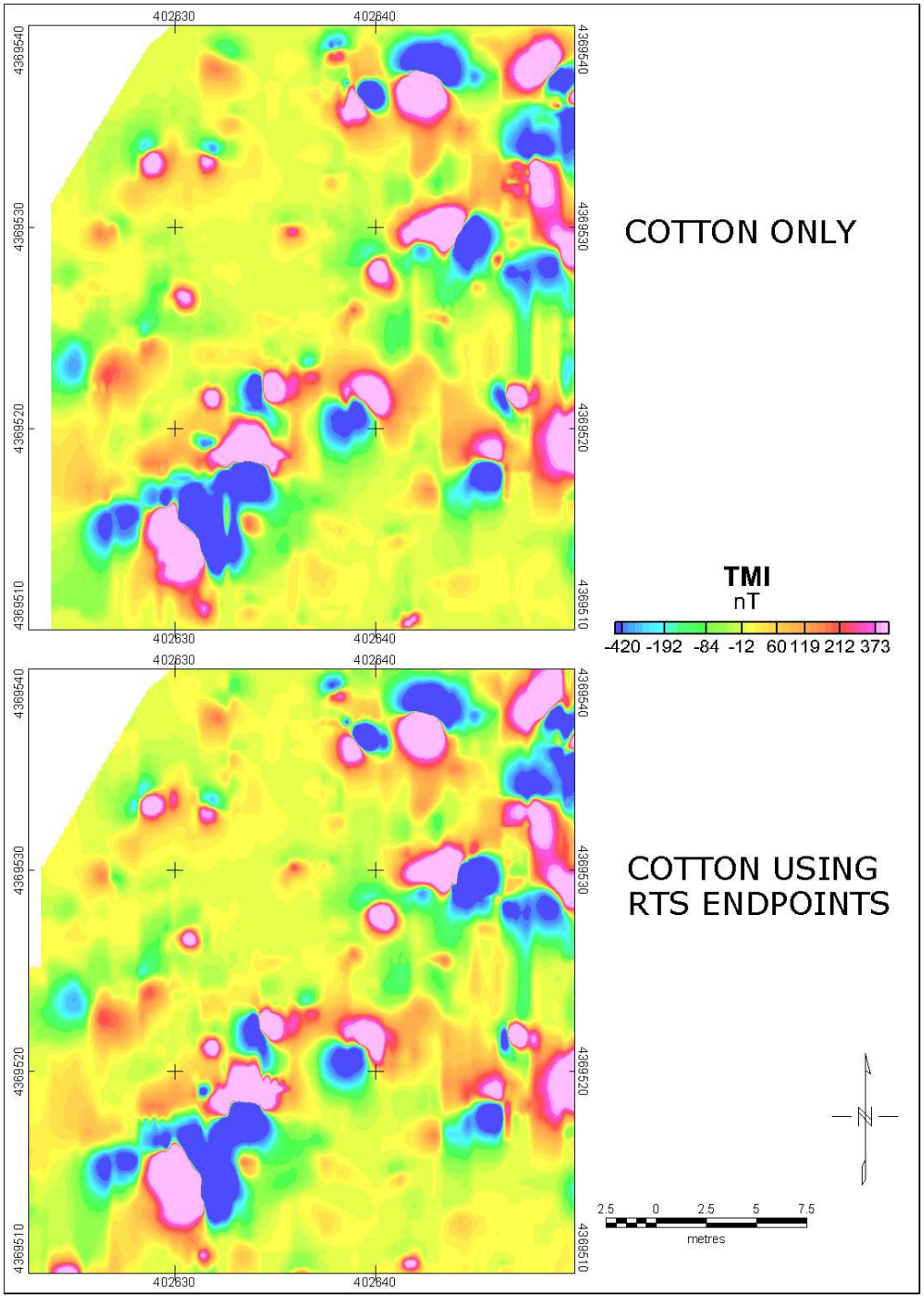

Figure 15 Grid A-08 TMI images. Top – CTO positioning only using polychains as end points. Bottom - CTO positioning only using RTS positions as end points.

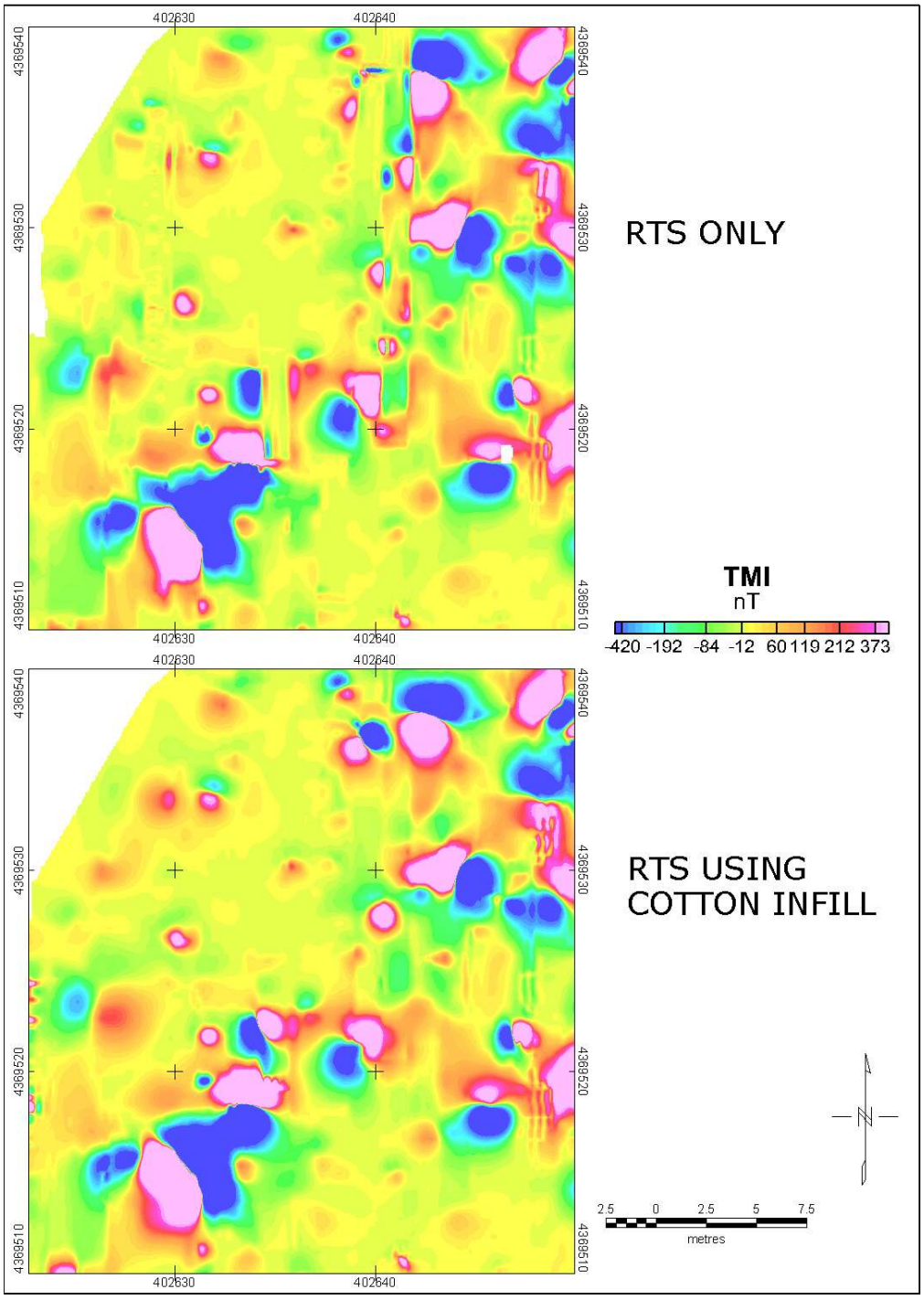

Figure 16 Grid A-08 TMI images. Top – RTS positioning only. Bottom – RTS using cotton thread odometer infill.

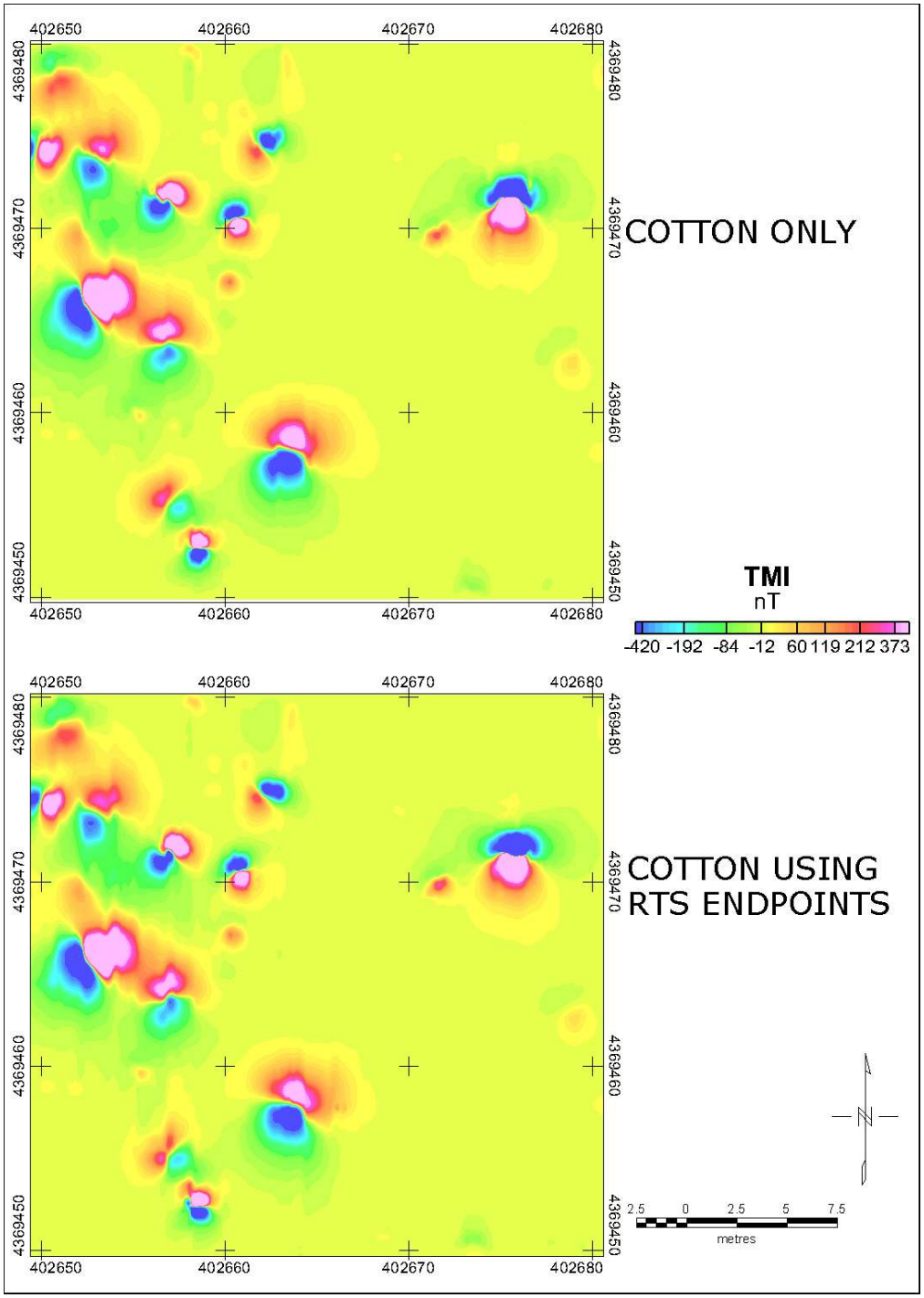

Figure 17 Grid B-06 TMI images. Top – CTO positioning only using polychains as end points. Bottom - CTO positioning only using RTS positions as end points.

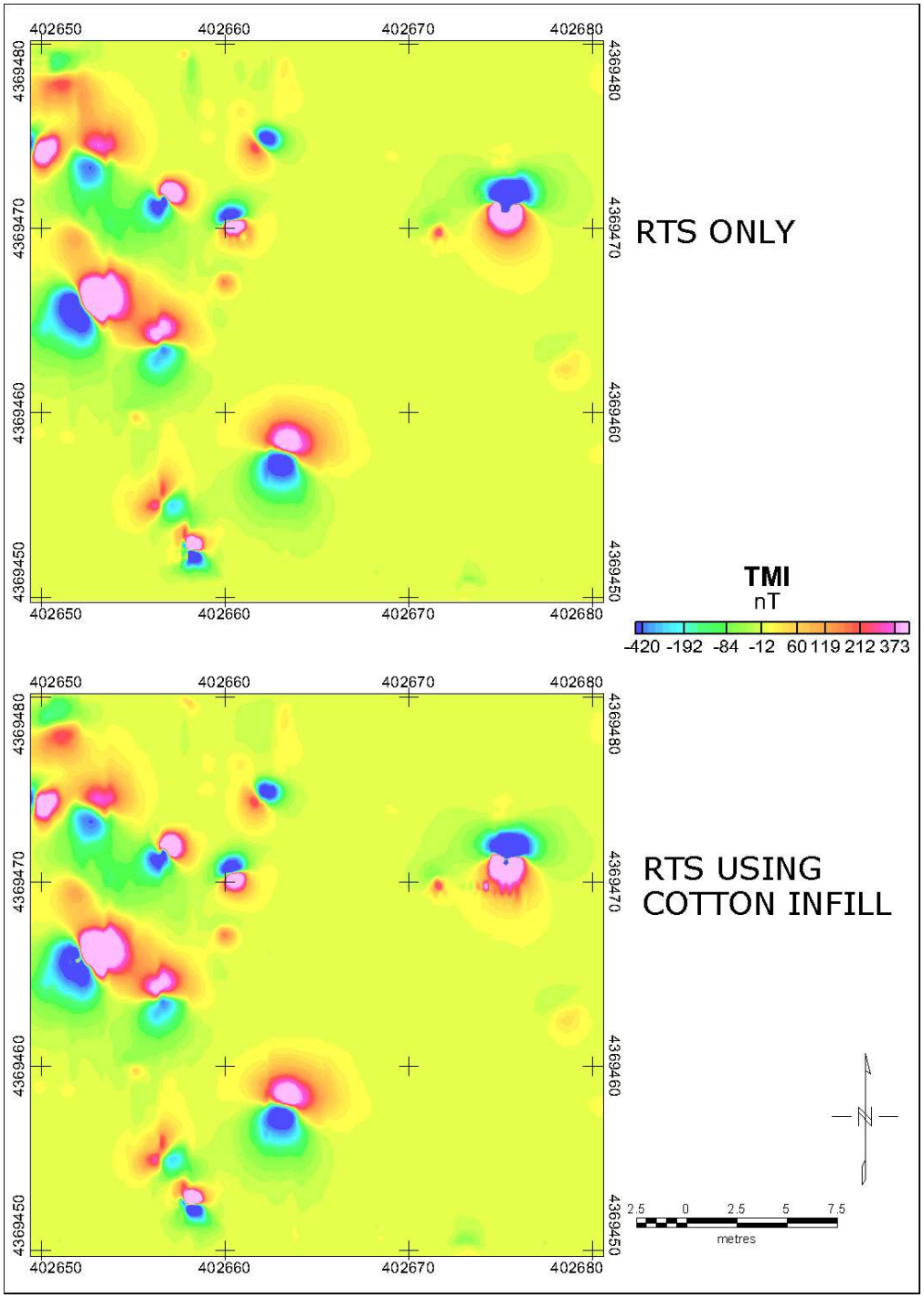

Figure 18 Grid B-06 TMI images. Top – RTS positioning only. Bottom – RTS using CTO infill.

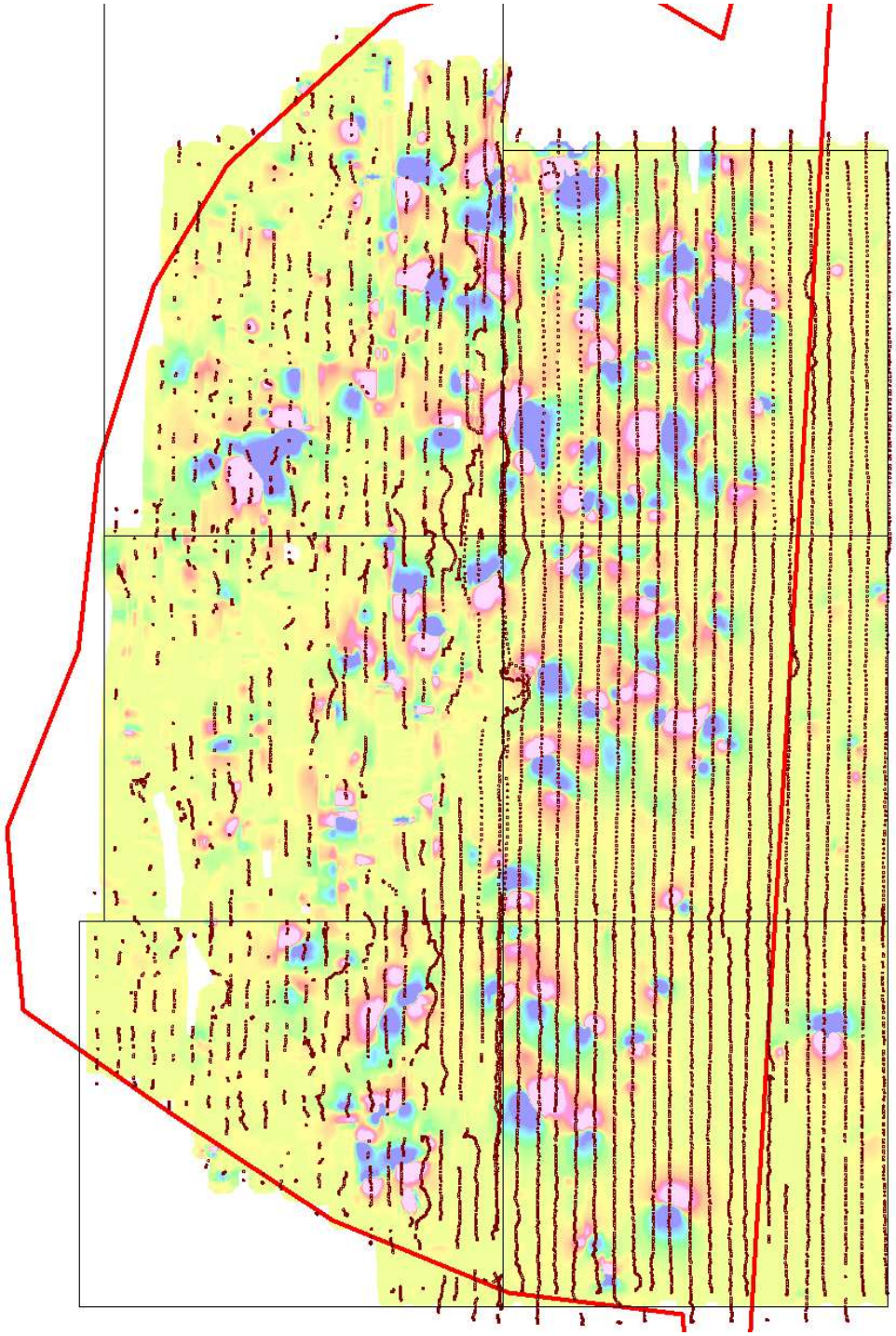

Figure 19 Combined TMI data for all Grids – Positioning using RTS Only. Actual RTS positions are also shown.

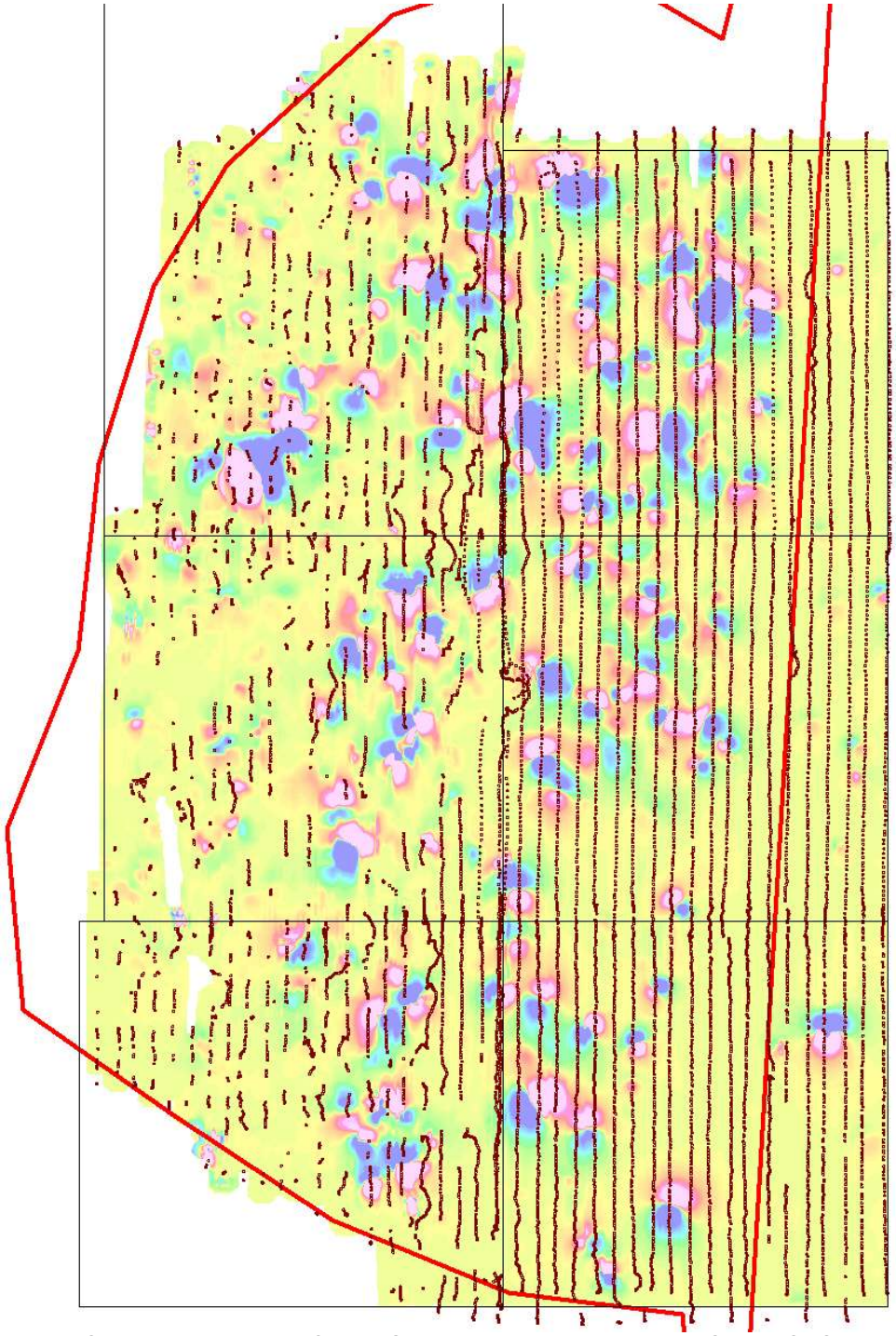

Figure 20 Combined TMI data for all Grids – Positioning using RTS and CTO combined. Actual RTS positions are also shown.

DISCUSSION

The TM-6 is a newly developed instrument which has been specifically designed as a geophysical data logger. In designing the TM-6, particular emphasis was placed on accurately time stamping all input data streams. For this reason, integration of the RTS positioning system with the TM-6 was technically quite straightforward requiring only minor hardware and software modifications. More effort was spent on the data processing software than anticipated, largely due to the relatively poor RTS coverage in the Wooded areas.

The results of the project were quite informative and enabled an excellent assessment of the benefits and limitations of both RTS and CTO positioning systems. Both RTS and CTO systems as well as the combination RTS/CTO positioning system were assessed on the basis of key performance criteria as described below:

Setup / Evacuation Time

RTS and CTO surveys in wooded areas both require control points to be established prior to surveying. Survey chains and sighters are also required for navigation purposes. Consequently, the costs involved in establishing these controls are common to both surveys. However, RTS requires the additional establishment of accurate theodolite stations where the RTS is situated for the duration of the survey. These stations need to be selected for optimal coverage of the survey area and indeed one or more new stations may be required for each survey area.

The time taken to establish a new theodolite station will depend on the level of expertise of the operator. The process requires selecting the location, installing and levelling the RTS, back sighting to at least two known benchmarks to ensure accuracy and setting up survey settings. Because of the amount of walking involved, this process took us at least an hour but it would be anticipated that an experienced operator would reduce the time required (most likely about 30 mins).

Use of CTO requires some cleanup at the end of the survey. Generally, it would take only a few minutes to remove the expended cotton.

Speed of Acquisition

The speed of survey using CTO will depend solely on the rate at which the ground can be traversed ie restricted by terrain, vegetation and ground surface conditions. RTS will also be dependent on these conditions but the greatest impediment to speed for the RTS system was the time taken to reacquire lock after passing behind obstacles such as trees. From our experience at Aberdeen, it could be safely assumed that use of RTS in wooded areas would at least double the survey time compared to using CTO only.

Logistics

Apart from the requirement to establish the RTS stations, the main logistical difference between RTS and CTO navigated surveys was the constant requirement to maintain line-of-sight between the RTS and the

reflector. Apart from trees, operators had to be aware of their position relative to the survey platform at all times as it was possible for the second operator to inadvertently obstruct line-of-sight.

Achievable Coverage Rate in Wooded Areas

Based on our experience, we would recommend that there should be a positional control point within every metre of traverse. RTS coverage in the survey areas diminished quite rapidly as the survey progressed further into the trees and by this definition, grids A-06, A-07 and A-08 all suffered from inadequate positional control in the RTS only surveys. The integration of CTO information with the RTS positions resulted in the best positional control of the three systems tested.

Absolute Positional Accuracy

One of the greatest advantages of RTS compared to CTO was the precision of location possible (~10mm) when lock was achieved. CTO is capable of quite good along-line accuracy (typically within 0.3% of the distance between control lines). However, CTO cross-line positioning (in the direction perpendicular to the line direction) is generally much less accurate as it is very dependent on how straight the line is. If it is necessary to deviate around trees etc, RTS can accurately track the deviation as long as lock is not lost. When using CTO, it is general practice to note that a deviation has occurred in the data file. That information is then carried through the processing stream and is available to the interpreter.

The most important requirement for any navigation system used for UXO surveying is that it must provide "adequate" positional control. The definition of "adequate positional control" is a little subjective. While target positional accuracy of better than 30cm might be nice where it can be achieved in open areas, extending this error to 1.0m in wooded areas may be acceptable if the survey cost saving is great. In this case, the requirement is clearly met most efficiently with a CTO. When using RTS, the resulting accuracy will depend on the ability of the operators to walk at constant speed during the period when lock is not available. During such periods, RTS accuracy may not be significantly better than 1.0m anyway (walking at constant speed in a wooded environment is virtually impossible because of the various obstacles which need to be negotiated. This is even more of an issue for RTS surveys where regular loss of lock between the RTS and the reflector means that the survey needs to regularly cease while lock is reacquired).

The cost equation will be different in different situations but the terms to be balanced are the additional cost to achieve improvement in positional accuracy versus the additional cost in relocating targets which may be less accurately positioned. An important constant in this equation is the probability of detection. This demonstration has indicated that the detection performance is not enhanced using one or the other positioning device.

Ability to Work in Extensive Wooded Areas

The Wooded area at the APG UXO test site is quite narrow and is situated adjacent to open grassland. This enabled the establishment of RTS stations in open country and at distances from the survey areas where the field of view could be optimised and the "fan of obstruction" from individual trees could be minimised. Even so, the coverage rate achieved by the RTS did not provide adequate positional control as the effective penetration of the laser through the trees into the woods dropped off rapidly with distance.

Accordingly, the RTS would not operate well in more extensive wooded areas where greater penetration of the laser would be required.

As long as positional control is available for the corners of grids, CTO navigation can be used in extensive wooded areas.

Equipment Cost

RTS is marginally cheaper than a DGPS system at about US$30000 and as such would be a major component cost of any geophysical survey. A CTO would cost of the order of $1000. Consumable costs for CTO are of the order of $10 per Ha. Depreciation or hire costs of the RTS would be much higher.

Total Survey Cost

The total survey costs for RTS and CTO largely reflect the setup/evacuation times and the speed of acquisition. We estimate that CTO surveys would achieve 3-4 times the production rate of RTS positioned surveys. Consequently, the cost of conducting an RTS positioned survey is estimated to be 3-4 times that of a CTO positioned survey.

Ease of Use

G-tek has used other RTS systems prior to the Aberdeen trails. Our experience has been that these instruments require a considerable amount of training in order to operate them effectively. Inappropriate operation can result in significant errors in the surveys. In contrast, the CTO systems can be learnt in a very short time.

Summary of Comparisons

In order to summarise a comparison of the three positioning systems, each system was rated subjectively according to the above performance criteria by assigning a number from 1 to 10 where 1 corresponds to very poor performance and 10 corresponds to very good performance. The results were summed and are listed in Table 6.

As can be seen from the Totals, we rate the RTS quite poorly compared to the CTO system for this application, largely due to the poor coverage rate and slow production rate. By combining the RTS and CTO data, the quality of positioning exceeded that of either RTS or CTO only. However, the combined system still suffered from low production rates and consequent high cost due to the RTS.

Table 6 Summary of Comparisons of the three positioning systems.

Positioning Technique	RTS	CTO	RTS/CTO
Setup / Evacuation Time	2	9	2
Speed of Acquisition	2	9	2
Logistics	3	9	2
Absolute Positional Accuracy	10	8	10
Achievable Coverage Rate in Wooded Areas	4	8	9
Overall Positional Quality in Wooded Areas	2	8	9
Ability to Work in Extensive Wooded Areas	1	10	4
Equipment Cost	2	9	1
Total Survey Cost	2	10	1
Ease of Use	3	9	2
Total out of 100	31	89	42

CONCLUSIONS

The integration of RTS positioning with the TM-6 magnetometer was technically successful. When used in open areas, the system as demonstrated at APG worked as efficiently and accurately as DGPS positioning. However, when used in Wooded areas, the coverage achievable with the RTS system was demonstrated as being inadequate for the provision of complete positional accuracy.

By combining RTS with CTO, the positional accuracy exceeded that possible with CTO only. However, it was felt that the degree of improvement achieved with the combined system did not justify the significant extra cost of conducting the survey compared with using CTO only. Importantly, regardless of the positioning system used in the demonstration, the probability of detection did not appear to be affected.

Working in wooded environments will always require some compromises in positional data quality. This is due to obstacles which must be physically negotiated, resulting in deviation of the sensors around obstacles and the consequent variation in pitch and yaw of the survey platform. Regardless of what positioning technique is used, some error in positioning is unavoidable. Consideration must be given to this when interpreting data recorded in such environments. When working in these environments, relocation and interpretation needs to take into account the lesser degree of positional accuracy.

Appendix K:

ARM Group Inc.
Commercial Test of Ranger Positioning System

ARM Group Inc.

Geophysics Division

ARM Group Inc. working with RRR Inc. evaluated the Ranger system in field production mode at Ft. Devens, Massachusetts. The site was forested which would not allow for the use of GPS for position data for the ongoing DGM investigation at the site.

Productivity/Costs

Data was collected at the site using three different position techniques/systems; Ensco Ranger, Lieca 1200 Robotic Total Station (RTS), and Fiducial Surveying. Table 1 presents a comparison of productivity and data collection cost for the three methods. The DGM was conducted on uneven/steep heavily wooded terrain. For costing purposes, the Ranger rental was estimated at $3000 per month.

TABLE 1

Productivity and Costs

Position Method	Productivity (Acres/Day)	Cost (Dollars/Day)	Cost Per Acre (Dollars per Acre)
Ranger	1.25	$1,981	$1,585
RTS	1	$2,471	$2,471
Fiducials	1.5	$1,793	$1,195

Project Comments

The Ensco Ranger system is a radio navigation system with a lot of potential. The Ranger System is currently in the infancy stages of demonstrating the systems' capabilities in a production-oriented field geophysics environment and in that realm it is currently unproven. In its current form, it has some drawbacks as the system is not as stable as desired. We have outlined some positives and negatives of the system in bullet form below:

Positives

- The system when operating correctly should not require line of sight as it is radio wave based.
- The system when operating correctly should provide sub-meter accuracy within a wooded environment.
- The system is relatively easy to setup and operate

- The system when operating correctly should complete adequate positional sampling and comparable positional accuracy to other non-line-of-sight based position systems.
- Only one data logger is required.

Negatives

- Operational range appeared to be less then 200 feet. At no time was the ability of the system demonstrated to work consistently when areas greater than 200' x 200' were attempted in wooded or un-wooded areas of the project site.
- Poor radio antenna connectors
- Possibility of mobile radio losing memory
- Insufficient feedback on PDA of poor position data.
- No nulling ability on the Logger S/W
- Equipment is not ruggedized for varying field conditions (need longer cables with tighter connectors, PDA requires shell)
- Equipment requires occasional programming which requires extensive training or a lot of basic knowledge.
- Lack of definite, established and documented field procedures to conduct surveys in production environment.
- No way to integrate with other Geophysical surveying instruments.
- Only one EM-61 can be run with Ranger at this time.

The performance of the ranger system over a three week period at Devens varied. On the first 2-3 days of surveying, the system appeared function as needed. Later evaluation of the data indicated the position data was not usable. Toward the end of the first week, the system started to malfunction. Mobile radio 2 lost its internal memory because a battery was left on the radio overnight and hence discharged. This caused the radio to report ranges of 1400-1700 even when less than 10 meters away from the fixed radios. The loss of internal memory also changed two other settings (skips and fixed antenna mode) which caused the system to partially function and significant production time was lost to troubleshoot the system.

The self location functionality of the fixed radios needs to be made more reliable. The bias loops were conducted in accordance with prior training but after feedback from ENSCO, a new method of conducting the bias loop was put forward. With improved results from the bias loop, positioning accuracy should increase. Examples were seen where anomalies were positioned up to 20ft from their actual location. The most error was seen in survey areas with changing elevation. Because of the unreliable position data, RRR Inc had to go back and recollect data from almost three weeks of work with the Ranger utilizing the RTS and fiducial methods.

In summary, we have not seen the reliability that is desired but when the system has been working, the results have been good for the environment in which they are collected except in areas of varying elevation. The upside is extraordinary for positioning within

moderate to dense woods and the most common glitches appear to be related to the mobile radios, self location protocols, and durability.

Needed

The following are items that should be addressed before taking Ranger back into a field production environment:

1. The self location functionality of the fixed radios needs to be made more reliable.
2. Improve radio antenna connectors
3. Provide better feedback of poor data position on PDA.
4. Need nulling ability.
5. There needs to be more testing, trials, and work done between ENSCO and a partner-company entity that has expertise in production geophysics.
6. The system needs to be able to be unpacked, setup, and used ruggedly on a daily basis with only minor hiccups.
7. The radio power should be boosted so that the system can be used over areas larger than 200'x200' and in non-line of sight conditions.
8. A set of Standard Operating Procedures (SOPs) must be developed and documented.

Appendix L:

SKY Research Inc.
3-D Geophysical Data Analysis

Draft Report

3-D Geophysical Data Analysis

Cooperative Research and Development Agreement

DACA87-05-H-0005

Sky Research, Inc.

December 2005

Overview

Investigations were undertaken to determine if collecting magnetic data at multiple heights improves the ability to recover dipole moments and what the impacts of noise and positioning errors are on the recovered dipole parameters. Data supplied from Phase III Aberdeen Proving Ground (APG) demonstrations were inverted and the relevant dipole parameters compared. Because coverage was not ideal for many of the targets, these results were not completely conclusive and therefore Monte Carlo simulations were performed to further examine potential benefits from incorporating measurements from multiple elevations. In this paper, the analytical results are discussed, and field measurements to confirm the findings are suggested.

Inverting Phase III APG Data

The main goals of the work reported here were to:

(1) evaluate the positional accuracy required to obtain an accurate dipole model;

(2) determine whether data collected at multiple elevations provides any additional information.

For this investigation, six different datasets from measurements taken with one magnetometer and three different positioning systems (Millhouse, 2003) were evaluated. Efforts were made to survey in a consistent manner in order to minimize the effects of using different operators with different positioning systems. The consistent and repeatable geophysical sensor performance allows for data quality comparisons between the different positioning systems.

Evaluation of the datasets showed that data quality was an issue and, in some cases, precluded the ability to fit dipoles and obtain inversion results. A good rule of thumb is that the area surveyed should consist of a square centered on the object of interest with a minimum length of 4 to 5 times the sensor to target separation. However, in the datasets considered in this investigation, inadequate coverage of the magnetic anomaly was found to be an issue. For example, in Figure 1 we show data collected on a test stand over an 81 mm mortar at 65 cm from the sensor. In order to cover the area spanned by the anomaly, we require coverage of most of the 3 m by 3 m shown; however, only a 1 m square grid was covered during the data collection.

Now, consider the gridded images of the data collected in this study. In Figure 2, the results shown are for the magnetic response for a 60 mm mortar buried at 0.5 m depth with the sensor at the lowest height (0.15 m). Test 3 indicates measurements made when the sensor was stationary over the target, and Test 4 indicates measurements made using a mobile platform. Although these data were taken at the lowest sensor height and were of the highest quality data, in most cases the extent of dipole response could not be adequately contained in the 1 m square area. This contributes to difficulties in fitting a dipole. Therefore, a larger grid size should be considered for future measurements. Figure 2 also illustrates additional problems with the Test 3 and Test 4 datasets. The Test 3 ENSCO dataset shows both anomalous positions and amplitudes; all cells in that

particular dataset had similar problems so they were excluded from the current analysis. The Test 4 ENSCO dataset only contained measurements at two elevations. In addition, the ArcSecond datasets were incomplete (Test 3 contained measurements over only eight targets, and the Test 4 dataset was not of sufficient quality to perform inversions).

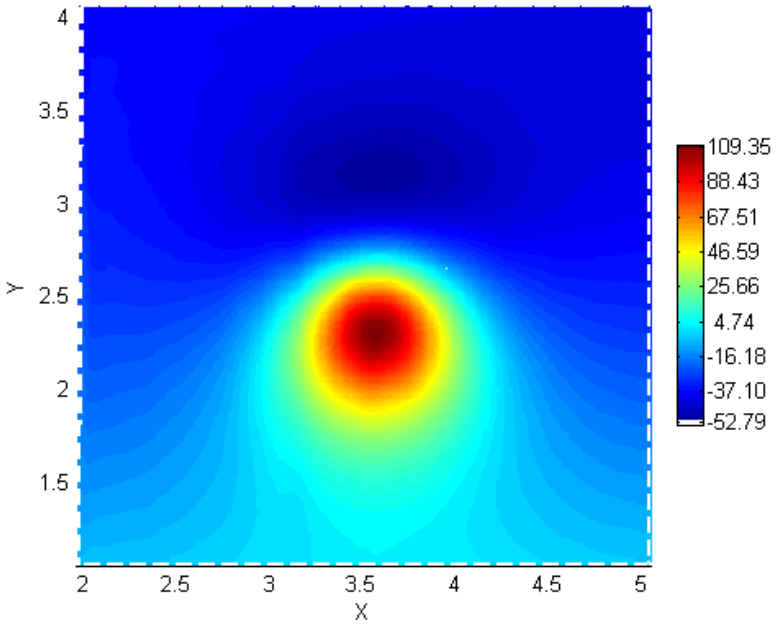

Figure 1: Dipole response from an 81mm mortar target at a depth of 65cm collected under ideal conditions on a test stand. Note that the entire dipole response cannot be contained within a 1m square grid.

Discussion of Inversion Results

The dipole parameters obtained through inversions of the supplied data are summarized in Tables 1-4. Results are provided for inverting with a single elevation only, two elevations, and three elevations (where available). The depths reported for the different objects can be used to examine benefits of the additional information. Because actual depths were also provided, comparisons can be made between depths inferred from inversions of single and multiple elevation data. In general, the single elevation data tends to overestimate the depth to the target with slight improvements as additional elevations are included in the data being inverted. There are also instances where the additional elevation information actually decreases the accuracy of the depth estimate.

Because there is a large range of possible moments for a given target which depend on both orientation (which is known) and remnant magnetism (which is not known), it is difficult to compare the moment measurements to a known value for each target as was possible with the recovered depths. The moments recovered from the inversion mostly fall within the expected range based on recovered models of similar items measured on a test stand. One exception is the 105 mm at location B14, which is consistently higher than the test stand measurements, possibly indicating significant remnant magnetism present in that particular target.

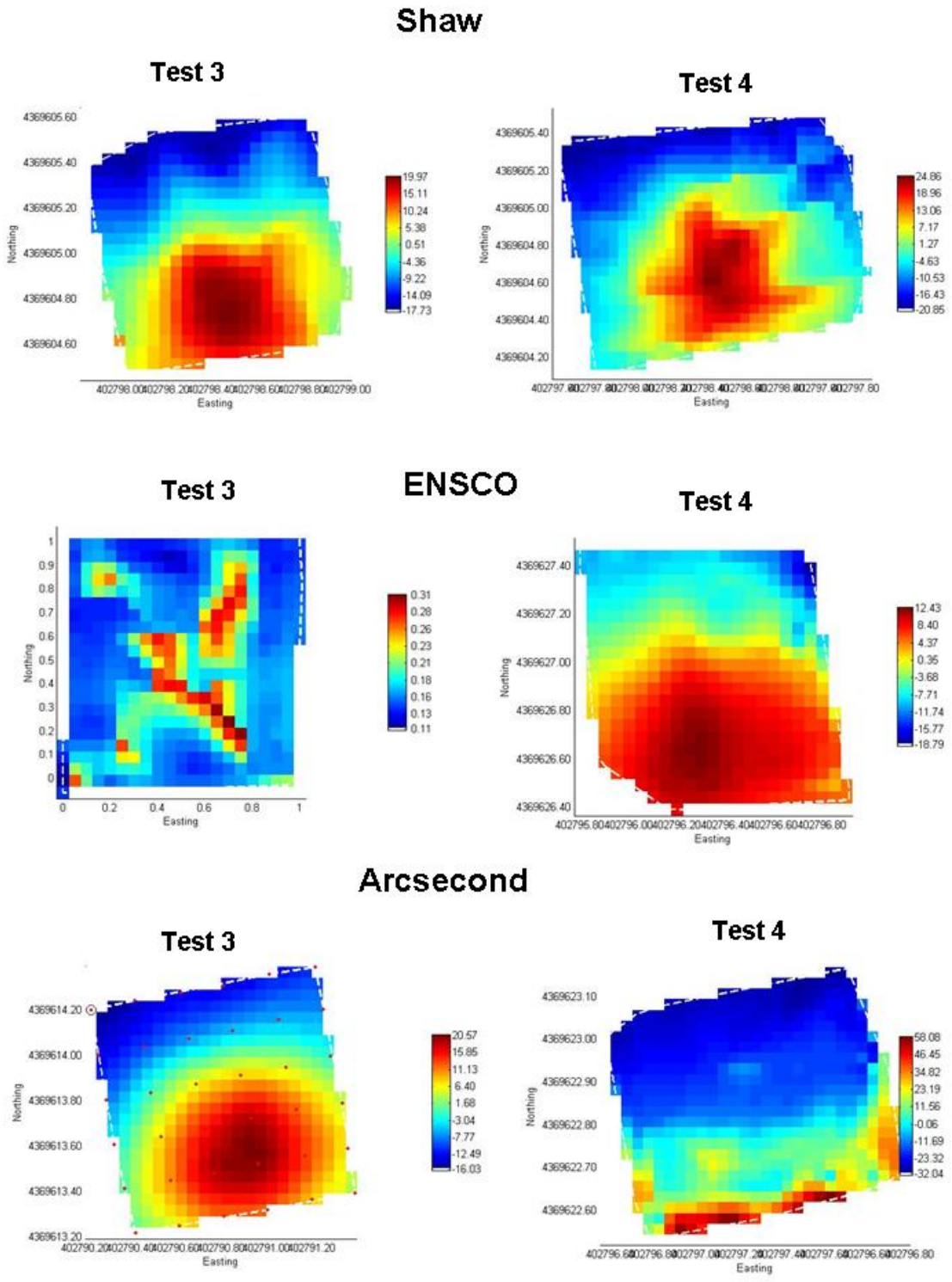

Figure 2: Gridded image of the data response for a 60 mm M49A3 target buried at a depth of 0.5 m with the sensor at a height of 0.15 m. Test 3 measurements were obtained by stopping at discrete points to collect data while Test 4 measurements were obtained on a mobile platform.

The angle relative to the Earth's field is also a difficult recovered parameter to compare with a known, absolute value. For the majority of targets, the additional elevations do not change the recovered values significantly. While the values are generally consistent for a given target at a given measurement setup, there are significant differences between the values of the recovered angle between different measurement methods (e.g., compare the results of the recovered angle relative to the Earth's field for Target A6 in Tables 1-4). The available data suggests that there are not sufficient improvements in the recovered inversion parameters to warrant the collection of multiple elevation data. It is also noted that the additional elevation data was not as densely sampled as the initial elevation and this may have contributed to the limited returns. Because the inversion results were not entirely conclusive, efforts were made via Monte Carlo simulations to obtain analytic results to further investigate whether collecting data at multiple elevations improves the ability to recover a dipole moment.

Monte Carlo Simulations

The first objective of these simulations was to determine if collecting data at multiple heights improved the ability to recover a dipole moment. A secondary goal was an investigation of the impact that noise and positioning errors have on the accuracy of the recovered dipole parameters.

In the results presented here, the following steps were repeated multiple times to arrive at a suite of results shown in Figures 5 to 8. First, a dipole was generated with random orientation and a moment of 0.05 Am^2 (typical for a 76 mm projectile at unfavorable orientation). The total magnetic field was then calculated both for a one-layer model where all the measurements were made at a single elevation and a two-layer model, in which measurements were made at two different elevations (see Figure 3). The systems were configured so that the same level of effort was required to cover a given area. Thus, one can view this as a test of the optimal way in which to deploy magnetometers. Next, noise was added to both the total magnetic field as well as the measured positions. A dipole model was then computed for both the one-layer and two-layer models. The entire process was repeated numerous times as the signal-to-noise ratio (SNR) and errors in position and depth to the target were varied.

The Monte Carlo findings are summarized in Figures 5 to 8 with each figure representing a different depth of the target. For each depth, plots are included for median deviations of each of the dipole model parameters (position, depth, moment, and angle relative to the Earth's field) versus standard deviation of the noise. Each plot contains results for both the one-layer and two-layer measurement scenarios. Note that the median deviation represents the magnitude of the error where 50% of the simulations had a smaller error and 50% had a larger error.

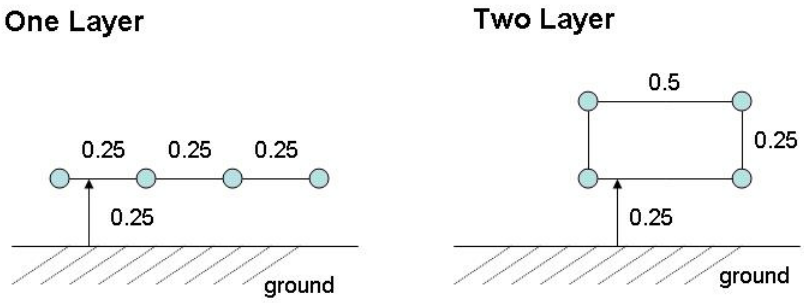

Figure 3: Scenarios for one- and two-layer measurements

Discussion of Monte Carlo Results

The plots of Figures 5 to 8 confirm some of the expected results. The parameters of the shallower targets are recovered with less error than the deeper targets. This is particularly true at low positional errors where the median deviations in the recovered parameters are small over the full range of noise values while for the deeper targets the deviations increase much more rapidly at higher noise values. This behavior is expected as a consequence of reduced SNR due to the weaker signals generated by the deeper targets. The second major observable result is that the one-layer measurement scenario (indicated by the dashed blue line in the plots) generally produces better results than the two-layer scenario (solid black line in plots). The reason for this is that the SNR is higher when the sensor is closer to the target. Deploying the sensors further from the target reduces the SNR but does not provide enough additional information to compensate for that reduction in SNR.

Other observations can be drawn from the Monte Carlo results. Errors in the recovered depths and positions are comparable to the positional errors of the observations, as shown in Figure 5 for a target at 0 meters in depth. Errors in the moment and angle also exhibit a strong correlation to the positional errors, as indicated in Figure 4. The positional errors are particularly dominant at the 0 meter depth case because the SNR is much higher than that for deeper targets.

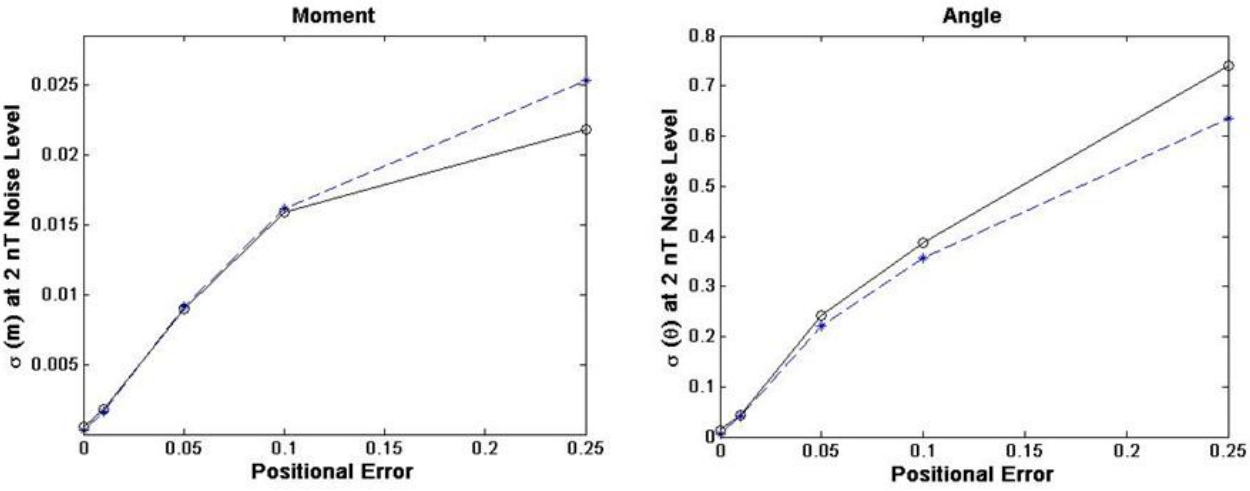

Figure 3: Correlation between the errors in the moment and the angle and the positional errors for a target at 0 meters depth. Results are plotted for a noise value of 2 nT.

For the target at a depth of 0.25 m (Figure 6) noise has a more significant impact on the recovery of the parameters of interest. This is evident in the linear increase in the median deviations that occurs with increasing noise. The positional errors are still the dominant contributors to the uncertainties in the recovered parameters. At a target depth of 0.5 m (Figure 7), the effects of noise are even more pronounced. With the noise at a 5 nT level, it is no longer possible to recover any of the parameters accurately, even with zero positional errors. Finally, at the target depth of 1.0 m (Figure 8) the effect of the noise is now much more important than the positional errors. Results for different positional errors are very similar. The effect of the noise on the recovered parameters is linear up to the 2 nT noise level, above which it becomes nonlinear. This represents the case where the noise is swamping the signal and there is very little structure in the measured data to constrain the inversion.

Conclusions

All of the results discussed here involve a single target in the field of view of the instrument. All indications are that the extra information from collecting data at multiple heights does not improve the ability to recover a dipole moment for a single target. In the future, simulations could be run that include multiple object scenarios. It is these situations that involve more than one target in the instrument's field of view where multiple elevation information may prove to be most useful. The Sky Research test plot in Ashland also provides an opportunity to acquire practical data using the one- and two-layer measurement scenarios discussed here (Figure 3) as it contains numerous multiple object areas with well-documented depths and orientations.

The maximum noise levels and positional error required to support advanced analysis depend on the size and shape of the small item of concern, as well as the expected depth distribution. For an object of the size of a 76 mm projectile, the Monte Carlo results indicate a minimum requirement of 10 cm positional error and 2 nT noise level (for less than 20% error in recovered parameters down to a depth of 1 m). If 0.75 m is an acceptable clearance depth, then a 5 cm positional error and 5 nT noise level would also suffice. There will always be a trade-off in the requirements for sensor noise and positional error. The more precise the positions, the more tolerant of sensor noise the recovered parameters will be (and vice versa).

References

Millhouse, D. S., 2003, *Innovative Navigation Systems to Support Digital Geophysical Mapping Phase III APG Demonstrations.* ESTCP Report.

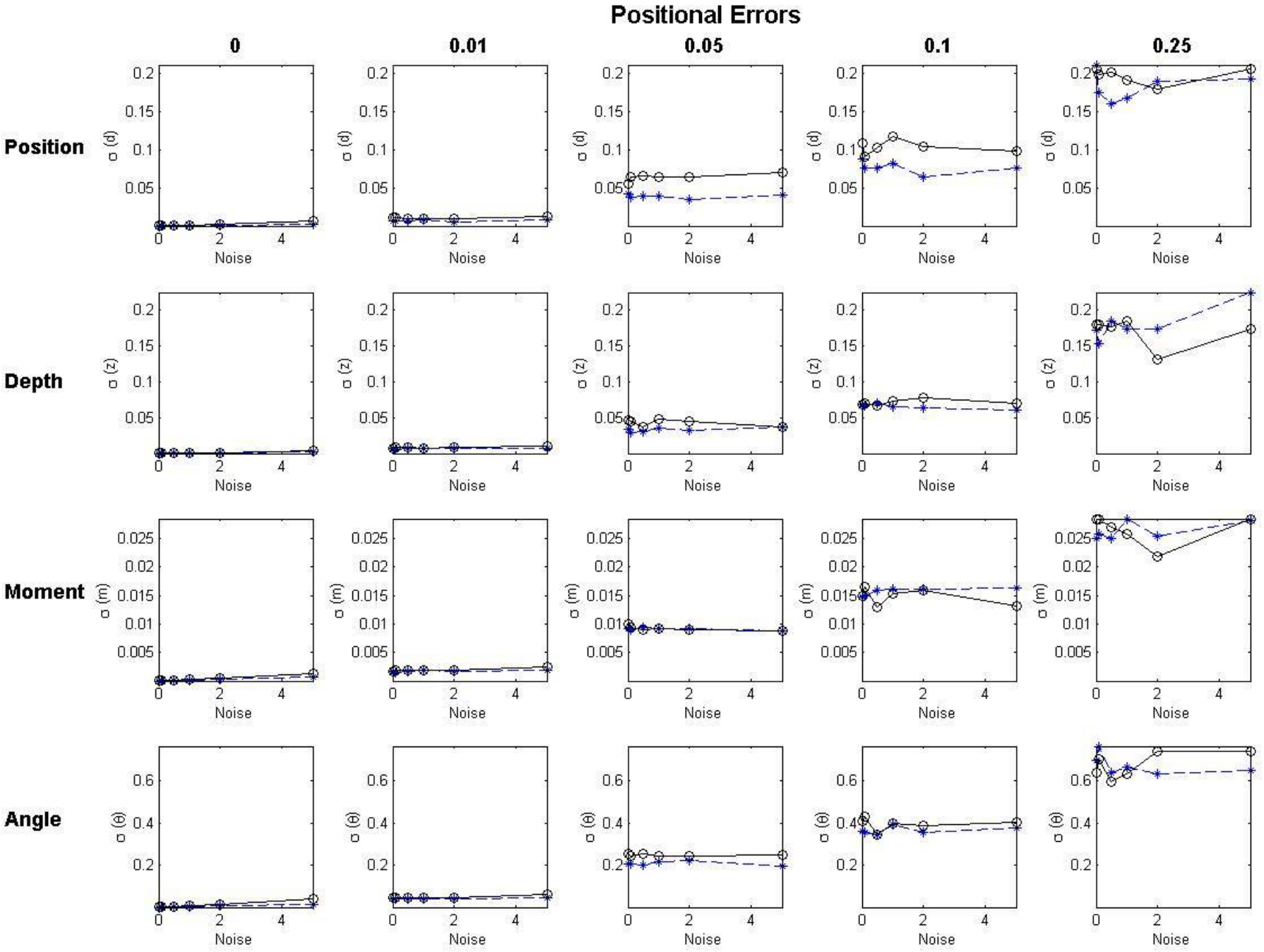

Figure 5: Monte Carlo results for a target depth of 0 m. Solid black line is two-layer measurement, and dashed blue line represents one-layer measurement.

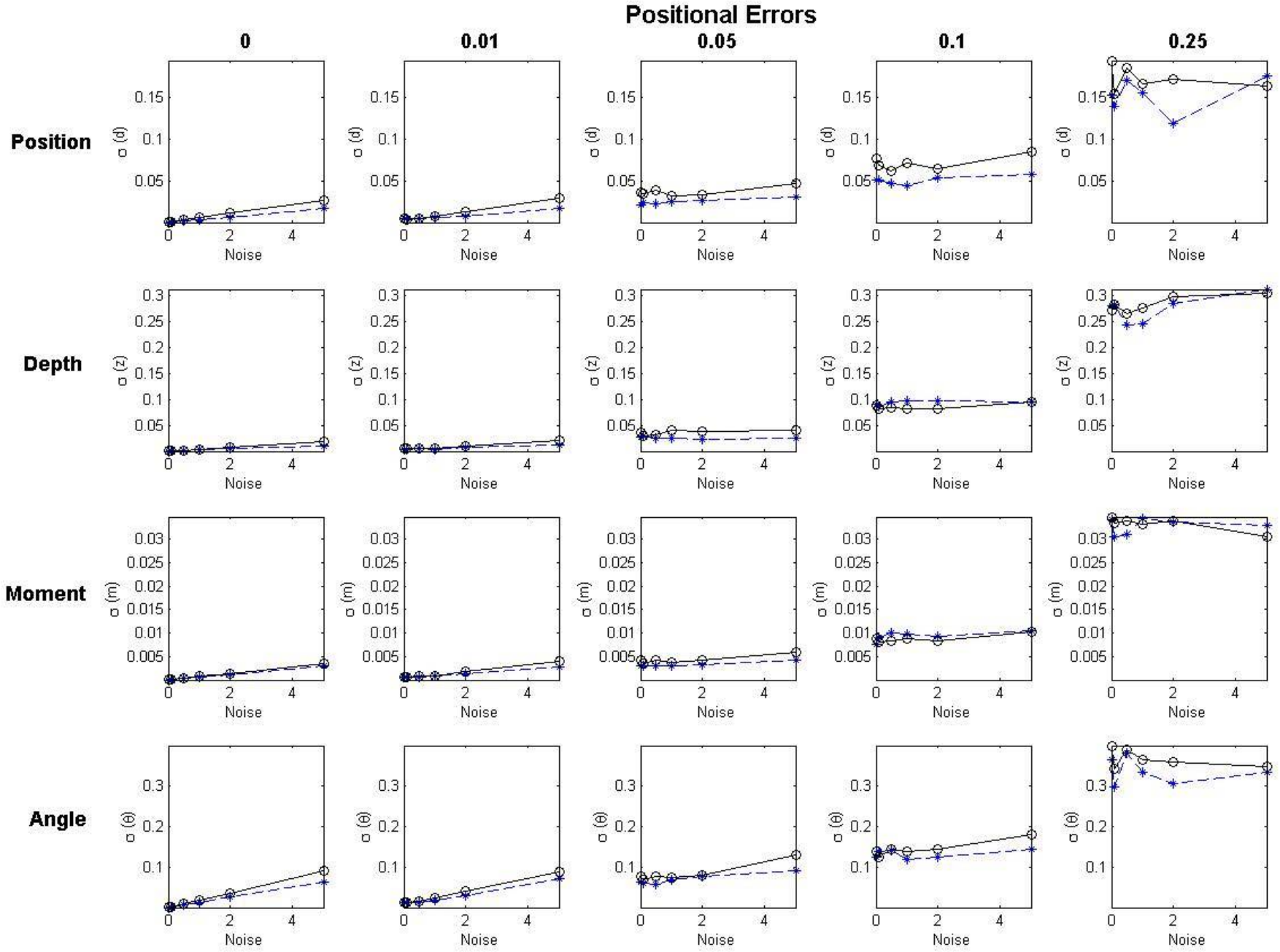

Figure 6: Monte Carlo results for a target depth of 0.25 m. Solid black line is two-layer measurement, and dashed blue line represents one-layer measurement.

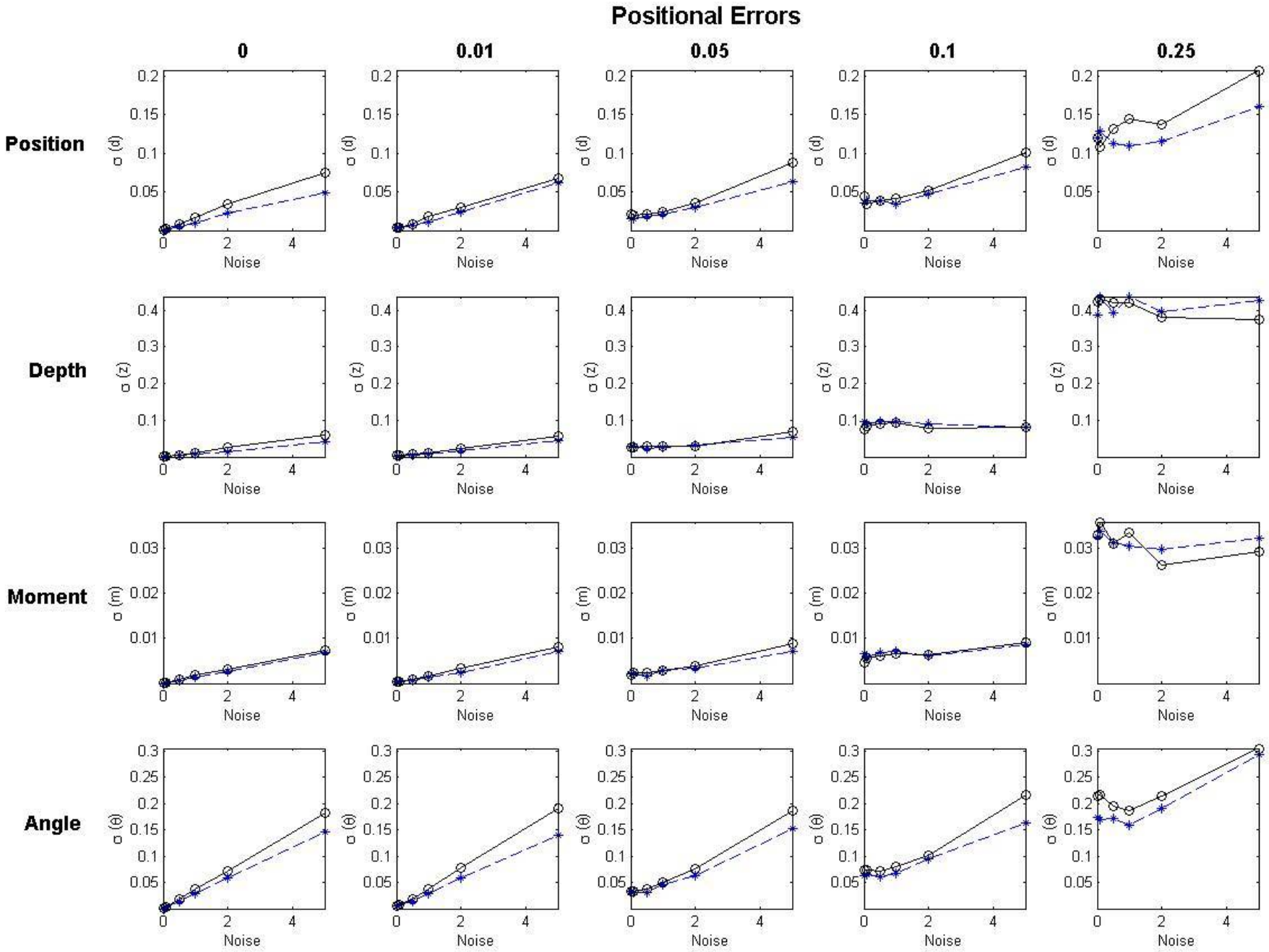

Figure 7: Monte Carlo results for a target depth of 0.5 m. Solid black line is two-layer measurement, and dashed blue line represents one-layer measurement.

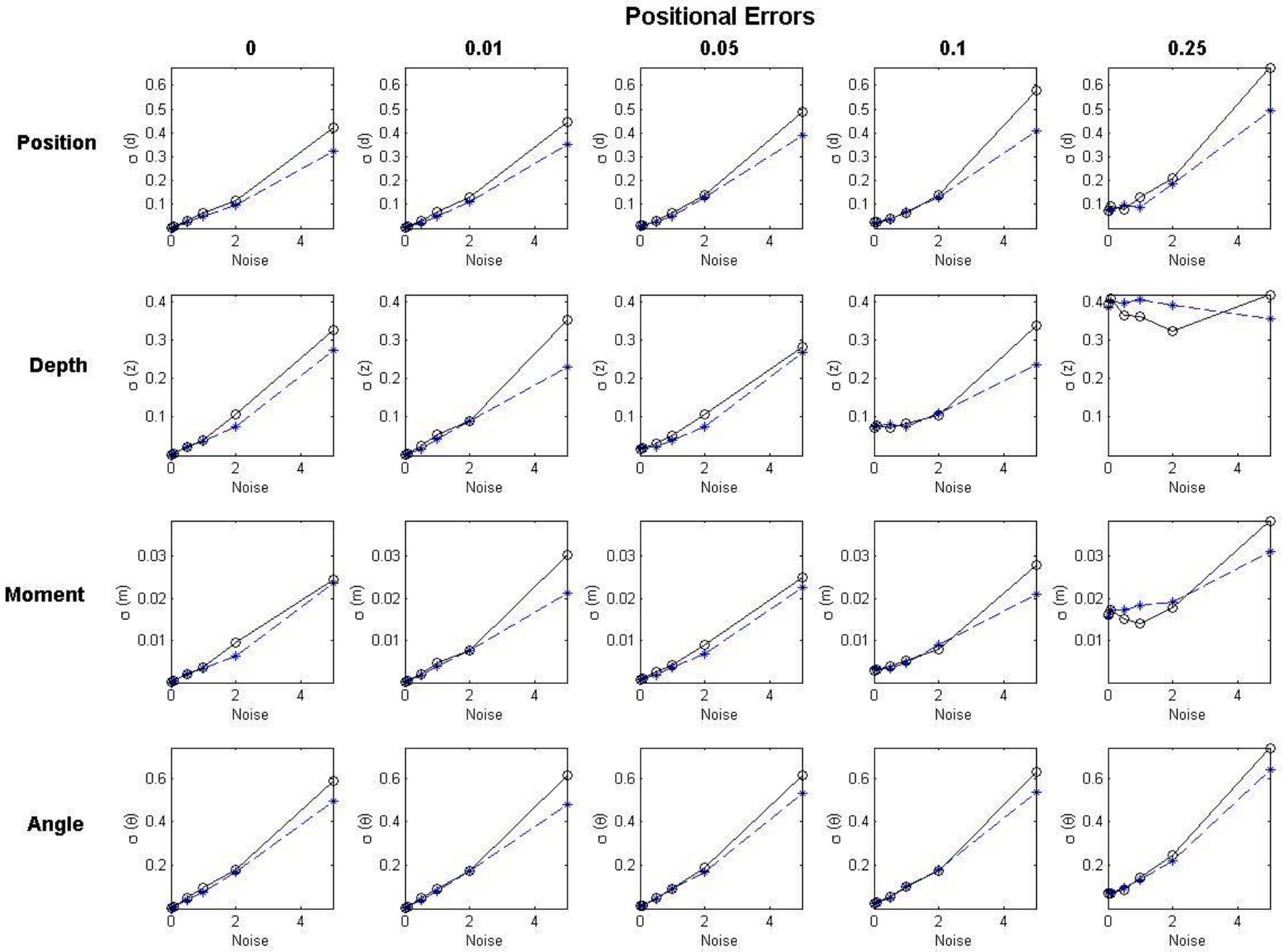

Figure 8: Monte Carlo results for a target depth of 1.0 m. Solid black line is two-layer measurement, and dashed blue line represents one-layer measurement.

Table 1: Test 3 ArcSecond

Target Information		Depth (m)			
Location	Description	Actual	1 Elevation	2 Elevations	3 Elevations
A6	57mm M86	0.4	0.501141	0.531046	0.553009
A7	60mm M49A3	0.5	0.697013	0.696483	0.678572
A8	2.75“ M230	0.5	0.733783	0.668256	0.631021
B13	105mm M60	0.9			
B14	105mm M60	0.9			
C6	57mm M86	0.4	0.612984	0.591747	0.610923
C7	60mm M49A3	0.5	0.71646	0.614059	0.572503
C8	2.75“ M230	0.5	0.732264	0.744905	0.735609
E6	57mm M86	0.91			
E7	60mm M49A3	1.0	NaN	NaN	NaN
E8	2.75“ M230	1.2	NaN	NaN	NaN
F13	105mm M60	0.9			
F14	155mm M483A1	0.9			
G10	8# shot	0.2	0.329084	0.331566	0.33349
H7	81mm M374	0.5			
J13	105mm M60	1.8			
J14	105mm M60	2.0			
J7	81mm M374	0.5			
L7	81mm M374	1.5			

Target Information		Moment (Am^2)		
Location	Description	1 Elevation	2 Elevations	3 Elevations
A6	57mm M86	0.099893	0.110218	0.119112
A7	60mm M49A3	0.121303	0.12263	0.11566
A8	2.75“ M230	0.293138	0.23735	0.209794
B13	105mm M60			
B14	105mm M60			
C6	57mm M86	0.125303	0.116659	0.126649
C7	60mm M49A3	0.187512	0.12254	0.099619
C8	2.75“ M230	0.493985	0.532577	0.515896
E6	57mm M86			
E7	60mm M49A3	NaN	NaN	NaN
E8	2.75“ M230	NaN	NaN	NaN
F13	105mm M60			
F14	155mm M483A1			
G10	8# shot	0.059722	0.062819	0.064095
H7	81mm M374			
J13	105mm M60			
J14	105mm M60			
J7	81mm M374			
L7	81mm M374			

Target Information		Angle Relative to Earth’s Magnetic Field		
Location	Description	1 Elevation	2 Elevations	3 Elevations
A6	57mm M86	34.72756	30.84426	27.32835
A7	60mm M49A3	24.1362	26.77767	29.73574
A8	2.75“ M230	21.21596	29.72546	36.30333
B13	105mm M60			
B14	105mm M60			
C6	57mm M86	33.51804	30.69088	32.87955
C7	60mm M49A3	58.62455	58.66335	57.09916
C8	2.75“ M230	10.84588	7.33035	5.497274
E6	57mm M86			
E7	60mm M49A3	NaN	NaN	NaN
E8	2.75“ M230	NaN	NaN	NaN
F13	105mm M60			
F14	155mm M483A1			
G10	8# shot	16.76506	21.06918	23.33947
H7	81mm M374			
J13	105mm M60			
J14	105mm M60			
J7	81mm M374			
L7	81mm M374			

Table 2: Test 4 ENSCO

Target Information		Depth (m)			
Location	Description	Actual	1 Elevation	2 Elevations	3 Elevations
A6	57mm M86	0.4	0.602027	0.595672	
A7	60mm M49A3	0.5	1.136562	0.809527	
A8	2.75“ M230	0.5	0.724782	0.699363	
B13	105mm M60	0.9	0.95221	0.945621	
B14	105mm M60	0.9	1.207533	1.216005	
C6	57mm M86	0.4	0.525167	0.521515	
C7	60mm M49A3	0.5	0.645577	0.481868	
C8	2.75“ M230	0.5	0.864965	0.898549	
E6	57mm M86	0.91	1.658995	1.976897	
E7	60mm M49A3	1.0	NaN	NaN	
E8	2.75“ M230	1.2	NaN	NaN	
F13	105mm M60	0.9	1.068963	1.301987	
F14	155mm M483A1	0.9	1.055534	1.101904	
G10	8# shot	0.2	0.436921	0.454946	
H7	81mm M374	0.5	0.763335	0.669142	
J13	105mm M60	1.8	NaN	NaN	
J14	105mm M60	2.0	1.153357	NaN	
J7	81mm M374	0.5	0.620028	0.767688	
L7	81mm M374	1.5	NaN	2.593372	

Target Information		Moment (Am^2)		
Location	Description	1 Elevation	2 Elevations	3 Elevations
A6	57mm M86	0.125884	0.128402	
A7	60mm M49A3	0.433178	0.130139	
A8	2.75“ M230	0.289789	0.259688	
B13	105mm M60	0.782346	0.765346	
B14	105mm M60	2.839428	2.906527	
C6	57mm M86	0.091397	0.089884	
C7	60mm M49A3	0.074406	0.032601	
C8	2.75“ M230	0.528804	0.631766	
E6	57mm M86	1.906609	6.784231	
E7	60mm M49A3	NaN	NaN	
E8	2.75“ M230	NaN	NaN	
F13	105mm M60	0.840099	1.954794	
F14	155mm M483A1	1.774079	2.167459	
G10	8# shot	0.060365	0.066409	
H7	81mm M374	0.316756	0.227355	
J13	105mm M60	NaN	NaN	
J14	105mm M60	0.216698	NaN	
J7	81mm M374	0.115847	0.253794	
L7	81mm M374	NaN	5.078272	

Target Information		Angle Relative to Earth’s Magnetic Field		
Location	Description	1 Elevation	2 Elevations	3 Elevations
A6	57mm M86	12.5995	19.9203	
A7	60mm M49A3	51.43141	49.51743	
A8	2.75“ M230	40.52778	37.62092	
B13	105mm M60	29.56425	29.47124	
B14	105mm M60	17.27914	15.26158	
C6	57mm M86	35.08199	30.87892	
C7	60mm M49A3	68.45837	66.25893	
C8	2.75“ M230	16.90034	42.25626	
E6	57mm M86	128.8811	167.8708	
E7	60mm M49A3	NaN	NaN	
E8	2.75“ M230	NaN	NaN	
F13	105mm M60	42.31408	63.67454	
F14	155mm M483A1	39.3261	45.11448	
G10	8# shot	38.74185	41.90012	
H7	81mm M374	31.76635	40.65393	
J13	105mm M60	NaN	NaN	
J14	105mm M60	32.37842	NaN	
J7	81mm M374	48.88637	69.26254	
L7	81mm M374	NaN	61.13174	

Table 3: Test 3 Shaw

Target Information		Depth (m)			
Location	Description	Actual	1 Elevation	2 Elevations	3 Elevations
A6	57mm M86	0.4	0.532569	0.514239	0.508437
A7	60mm M49A3	0.5	0.623634	0.568475	0.560188
A8	2.75“ M230	0.5	0.687836	0.700789	0.708918
B13	105mm M60	0.9	1.014997	0.992712	0.910642
B14	105mm M60	0.9	1.138566	1.160692	1.109983
C6	57mm M86	0.4	0.584425	0.548044	0.466515
C7	60mm M49A3	0.5	0.647594	0.577676	0.401636
C8	2.75“ M230	0.5	0.691489	0.68497	0.639493
E6	57mm M86	0.91	NaN	NaN	NaN
E7	60mm M49A3	1.0	NaN	NaN	NaN
E8	2.75“ M230	1.2	NaN	NaN	NaN
F13	105mm M60	0.9	NaN	NaN	1.036481
F14	155mm M483A1	0.9	1.064791	1.094057	1.087378
G10	8# shot	0.2	0.324049	0.311836	0.287347
H7	81mm M374	0.5	0.720181	0.713317	0.662743
J13	105mm M60	1.8	NaN	NaN	NaN
J14	105mm M60	2.0	1.459207	1.553314	2.484689
J7	81mm M374	0.5	NaN	NaN	NaN
L7	81mm M374	1.5	NaN	NaN	NaN

Target Information		Moment (Am^2)		
Location	Description	1 Elevation	2 Elevations	3 Elevations
A6	57mm M86	0.111478	0.104716	0.102811
A7	60mm M49A3	0.092841	0.076022	0.074263
A8	2.75“ M230	0.253545	0.264232	0.271121
B13	105mm M60	0.934652	0.857576	0.678831
B14	105mm M60	2.448752	2.561097	2.269357
C6	57mm M86	0.126767	0.108131	0.07312
C7	60mm M49A3	0.117363	0.088221	0.038227
C8	2.75“ M230	0.463742	0.45346	0.374884
E6	57mm M86	NaN	NaN	NaN
E7	60mm M49A3	NaN	NaN	NaN
E8	2.75“ M230	NaN	NaN	NaN
F13	105mm M60	NaN	NaN	1.522363
F14	155mm M483A1	2.215498	2.401487	2.348586
G10	8# shot	0.064114	0.06009	0.05221
H7	81mm M374	0.249114	0.245193	0.209028
J13	105mm M60	NaN	NaN	NaN
J14	105mm M60	0.615497	0.791767	4.697831
J7	81mm M374	NaN	NaN	NaN
L7	81mm M374	NaN	NaN	NaN

Target Information		Angle Relative to Earth’s Magnetic Field		
Location	Description	1 Elevation	2 Elevations	3 Elevations
A6	57mm M86	5.269197	10.88629	12.78771
A7	60mm M49A3	22.25141	28.1231	30.36111
A8	2.75“ M230	18.14987	18.44135	17.55439
B13	105mm M60	30.56331	25.36251	32.36401
B14	105mm M60	29.63468	24.28883	30.95027
C6	57mm M86	35.49107	33.14502	32.35058
C7	60mm M49A3	45.31232	44.93218	44.84467
C8	2.75“ M230	11.93422	11.1342	7.777159
E6	57mm M86	NaN	NaN	NaN
E7	60mm M49A3	NaN	NaN	NaN
E8	2.75“ M230	NaN	NaN	NaN
F13	105mm M60	NaN	NaN	90.6976
F14	155mm M483A1	11.98804	7.527781	7.215891
G10	8# shot	9.403697	8.080851	5.896939
H7	81mm M374	30.87343	33.45463	42.08515
J13	105mm M60	NaN	NaN	NaN
J14	105mm M60	34.53382	55.80856	84.46968
J7	81mm M374	NaN	NaN	NaN
L7	81mm M374	NaN	NaN	NaN

Table 4: Test 4 Shaw

Target Information		Depth (m)			
Location	Description	Actual	1 Elevation	2 Elevations	3 Elevations
A6	57mm M86	0.4	0.473267	0.411796	NaN
A7	60mm M49A3	0.5	0.762602	0.600987	0.580434
A8	2.75“ M230	0.5	0.654951	0.632909	0.620377
B13	105mm M60	0.9	0.997819	0.9463	0.925013
B14	105mm M60	0.9	1.089335	1.082356	1.037633
C6	57mm M86	0.4	0.524999	0.508413	0.448733
C7	60mm M49A3	0.5	0.559375	0.436608	0.436571
C8	2.75“ M230	0.5	0.644721	0.738701	0.579854
E6	57mm M86	0.91	NaN		NaN
E7	60mm M49A3	1.0	NaN	NaN	NaN
E8	2.75“ M230	1.2	NaN	NaN	NaN
F13	105mm M60	0.9	0.858157	0.861237	0.803303
F14	155mm M483A1	0.9			0.843728
G10	8# shot	0.2	0.225757	NaN	0.216065
H7	81mm M374	0.5	0.758335	0.715123	0.67981
J13	105mm M60	1.8			NaN
J14	105mm M60	2.0	NaN	1.80923	NaN
J7	81mm M374	0.5	NaN	0.78202	0.769265
L7	81mm M374	1.5	0.738679	NaN	NaN

Target Information		Angle Relative to Earth’s Magnetic Field		
Location	Description	1 Elevation	2 Elevations	3 Elevations
A6	57mm M86	34.45299	16.86428	NaN
A7	60mm M49A3	18.76019	28.61644	34.50131
A8	2.75“ M230	23.67622	26.04894	31.81796
B13	105mm M60	24.46164	29.15354	33.34383
B14	105mm M60	22.7136	21.5133	25.48991
C6	57mm M86	37.02038	40.82644	41.20343
C7	60mm M49A3	20.58963	28.27856	28.32122
C8	2.75“ M230	6.293871	44.2076	3.440319
E6	57mm M86	NaN		NaN
E7	60mm M49A3	NaN	NaN	NaN
E8	2.75“ M230	NaN	NaN	NaN
F13	105mm M60		45.95652	47.65167
F14	155mm M483A1	52.51058		5.386027
G10	8# shot	22.57867	NaN	32.53954
H7	81mm M374	30.84373	38.94739	44.3351
J13	105mm M60	NaN		NaN
J14	105mm M60	NaN	47.21118	NaN
J7	81mm M374	68.59161	83.44282	78.67748
L7	81mm M374	NaN	NaN	NaN

Appendix M:

AETC Inc.
Evaluations of Laser Based Positioning for Characterization of EMI Signals from UXO

EVALUATION OF LASER BASED POSITIONING FOR CHARACTERIZATION OF EMI SIGNALS FROM UXO

Bruce Barrow, AETC, Inc., Arlington, VA
Nagi Khadr, AETC, Inc., Arlington, VA
Thomas Bell, AETC, Inc., Arlington, VA

Abstract

A limiting factor in the inversion of electromagnetic induction (EMI) sensor data is the ability to accurately measure the position and orientation of the sensor coils. Without accurate 3-D positioning, the error in the inversion parameters that characterize unexploded ordnance (UXO) can be quite large. A variety of positioning systems (and combination of systems) are currently being used or considered: GPS, inertial navigation, radio frequency based, and laser based. We have combined a laser based system being developed by Arcsecond and ERDC with a Geonics EM61-HH and collected data under a controlled setting in order to evaluate its positioning accuracy and the effect of this accuracy on inverting EMI data. As a starting point, the combined instruments were constrained to move in a flat plane over test objects. The system was videoed as well to provide comparable ground truth. Next the instruments were rigged to be swept back and forth (in 3D) over test objects as if one were interrogating an anomaly in the field. Initial results indicate centimeter level accuracy with good EMI inversions, but there are indications that the error in position grows as the sensor moves faster than 0.5 to 1 meter per second.

Introduction

There are a number of issues currently being researched in the drive to use electromagnetic induction sensors to detect and identify buried unexploded ordnance. The main thrust is in fielding a practical instrument that can collect sufficiently high quality data to support an accurate model-based inversion. The model parameters can be used to determine if the object of interest is UXO. Error in the inverted parameters will reduce one's ability to differentiate between UXO and other metallic clutter. Typically, sensor noise is the limiting factor in the inversion of field data, but in the case of EMI sensors, accurate spatial positioning information has been found to be an even more important factor.

The authors have been researching the utility of combining an inertial motion sensor with a handheld EMI sensor to interrogate individual objects (Bell, 2004). The aim is to process both sensor data streams together to mutually constrain both the integration of the inertial motion sensor and the inversion the EMI data. As part of this effort, we needed highly accurate sensor positioning to ground truth our efforts. Initial experiments constrained the EMI sensor to motion on a flat platform. Video images of the motion were corrected for lens distortion and were found to provide 2D sensor trajectories accurate to a fraction of a centimeter.

In an effort to collect 3D positioned data from a swinging EMI sensor, we borrowed a positioning system being developed by Arcsecond, Inc (Millhouse, 2004). The system uses stationary rotating lasers to position roving light sensors with sub-centimeter accuracy. The system we used has four light sensors and measures both the 3D location and orientation of the EMI sensor.

We will present the results of inverting EMI data from a Geonics EM61-HH which is being swung over a 4 inch steel ball. Three sets of data are analyzed: 2D data positioned by videoing, 2D data

positioned by the Arcsecond and collected concurrently with the video positions, and lastly, 3D data positioned only by the Arcsecond system.

Arcsecond System

The company Arcsecond, Inc. makes and sells what they call “Indoor-GPS” positioning systems. Much of what they do is used for very precise measurements in manufacturing settings. Under several different UXO related research programs (Millhouse, 2004), an Arcsecond system that would be useful for UXO field surveys is being developed. The system is based on fixed rotating laser transmitters that they compare to GPS satellites. The transmitters have two rotating laser fans that are tilted relative to each other, plus a timing light strobe. By measuring the timing of the two laser fans relative to the timing strobe, one’s relative angular position from a transmitter can be measured. Given a set of two or more transmitters at known locations, all of these angular measurements can be used to calculate one’s position (Arcsecond, 2002). The “UXO” system makes use of four rigidly attached light sensors in a tetrahedral configuration to measure both the survey platform’s position and orientation. In post-processing software, the displacements from the Arcsecond sensors to the EMI sensor can be used to calculate the 3D position and orientation of the EMI coil. Limited by the laser rotation rate around 40Hz, the position of the platform is measured at a rate of 20 samples per second.

Experiments

These tests were done on a level wooden platform. Test objects could be placed roughly 30 centimeters below the platform. Photos of the test setups are shown in Figure 1. All of the data presented here is over a four inch diameter carbon steel sphere. The 2D video and 2D Arcsecond position data were collected simultaneously. The Geonics EM61-HH data was collected directly onto a laptop PC at a rate of 15 samples per second. The PC was also used to collect the Crossbow IMU data.

The 2D tests were done by attaching the equipment to a flat board and sliding the board along the platform surface. The EM61-HH coil head was detached from the usual pole and located at one end of the board. At the other end of the board, the Geonics electronics, the Crossbow IMU, and the Arcsecond sensors were attached (Figure 1a and 1b).

Three bright LED’s were placed on the coil to track its position and orientation in the video images. A video camera was located 2 meters over the platform, pointing down. A large, gridded board was imaged by the camera at the height of the LED’s. This gridded image was used to find a polynomial fit that would map camera pixel locations to a calibrated, rectangular X,Y coordinate system. The camera frame rate was 30 frames per second. The location of each LED was calculated from the centroid of its image over an eight pixel square. When the board was moved quickly (1 m/s), the image of each LED would noticeably smear out. As a sanity check, the separation of the two outer LED’s was measured at 25.4 cm and compared to the mapped images. The mean separation noted in the mapped images was 25.3 cm with a standard deviation of 0.2 cm as the board was swept about.

The Arcsecond system used for the 2D tests had a tetrahedral configuration of four sensors attached to the sensor board 75 cm back from the coil. The displacements from each Arcsecond sensor to the EM coil were measured for post-processing the EM coil’s position. When stationary, the RMS noise in the sensor positions is on the order of 0.2 millimeters and the calculated EM coil position noise is around 0.6 mm. For the 2D tests, only two laser transmitters were used.

For the 3D test, the EM61-HH coil was reattached to the standard Geonics rig. A flat board and a surveyor pole were attached to the rig to hold both the Crossbow IMU and the Arcsecond sensors. A shoulder strap held the rig over the experimenter’s shoulder, and the EM coil could be swept side-to-side

(a)

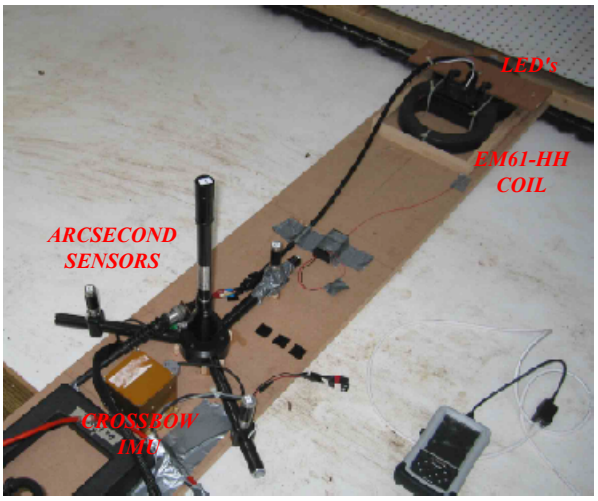

(b)

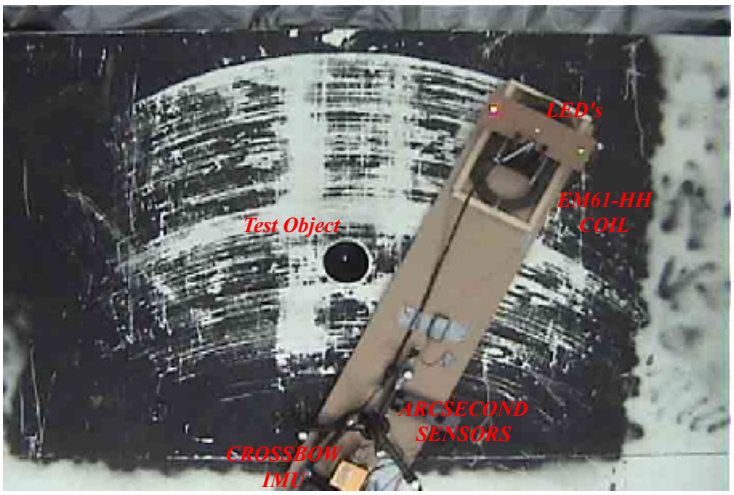

(c)

Figure 1. 2D and 3D EM61-HH sensor positioning experiments. In (a) sideview and (b) video camera view, the 2D sensor board is shown with EM61-HH coil, LED's, Arcsecond sensor, and Crossbow IMU. In (c), the 3D jig is shown with conventional EM61-HH pole, Arcsecond sensor, and IMU.

in a typical field survey interrogation of an object (see Figure 1c). For each data set, the coil would start flat and be lifted from the test platform. For half of the data collected, the coil would be placed flat on the platform surface at the end of each sweep (zero velocity updates for the IMU).

Results

Figure 2 plots sample trajectories of the EM coil from the three positioning data sets. An example of the concurrently collected video and Arcsecond positions are shown in 2a and 2c. The video data (red curve) was shifted in X, Y, and time to overlay with the Arcsecond positions. To compare the two sets, the video data was interpolated to the Arcsecond times. Across the central region of the video data, the standard deviations in the differences in X and Y were between 2 and 4 mm. The mean horizontal distance between the two position measurements was 3.5 mm with a standard deviation of 2.3 mm. Larger differences were noted around the edges of the video image. There is a distinct trend to differences at the edge and there maybe a residual error to the applied lens correction. The video data assumes a flat board, but the Arcsecond data in 2c shows almost 2 cm in variation. Along the Y direction, there is a distinct slope to the measured Z on the order of 1.0 cm over a distance of 100 cm. Over a narrow central region of the sweeps, the standard deviation in Z is 2.6 mm. Based on the reasonable agreement between these two systems; we conclude that their positioning is probably good to 5 mm or better. Figure 2b and 2d plot a sample 3D trajectory of the EM coil. The measured variation in Z as the coil is lifted and swept side-to-side over the platform is on the order of 10 cm.

The EMI data was fit with the standard induced magnetic dipole response model. The model parameters are object position (x, y, z), object orientation (θ, ϕ, ψ), and the object's magnetic polarization responses along its primary axes ($\beta_1, \beta_2, \beta_3$). Because the test object was a sphere, we simplified our fits with a single β value. Another important aspect of the inversion model was accounting for the temporal response of the EM61-HH. When sweeping the coil back and forth over a sphere, it was noted that the peak response was both delayed and distorted from the sphere's actual location. Using a simple wire coil with a gated on/off switch, the sensor's impulse response function was found (Bosnar, 2005). This response function was incorporated into the inversion model used here.

Results of fitting the measured data with the different positioning systems are shown in Figures 3 and 4. The black symbol/curves are the measured data and the green curve is the best model fit. In Figure 3, the data is plotted as a function of time. In Figure 4, it is plotted as a function of the X position. Note the displacements in X of the peak signals due to the sensor response; the actual sphere location is between the peaks.

For the 2D video/Arcsecond data, the measurements over the sphere were repeated and inverted seven times. For the 3D data, seventeen sets of measurements were made. Figure 5 presents the inversion results for all of this data (red X - video fit, green triangle – 2D Arcsecond, black diamond – 3D Arcsecond).

In Figure 5a, the fitted depths and response β's are plotted. These two fit parameters are highly correlated in the inversion model. Given measurements with both signal noise and positioning error, the inversion model tends to vary these two parameters the most in an attempt to get the best model fit to the data. For the three positioning sets, the mean sphere β's are: 6.70 – 2D Arcsecond, 6.88 – 2D video, and 6.94 – 3D Arcsecond. The standard deviations are: 0.18, 0.14, and 0.27, respectively. The sphere's depth was not noted accurately enough to check on the fitted depths. It was roughly 29 cm below the center of the EM coil when it was resting flat on the platform. For the three coordinate systems, $z = 0$ was only roughly matched to this coil height.

In Figure 5b, a measure of the fit quality is plotted versus the average swing speed of the EM61-HH coil. The peak speeds were on the order of 2 to 3 times greater. The fit quality parameter is the

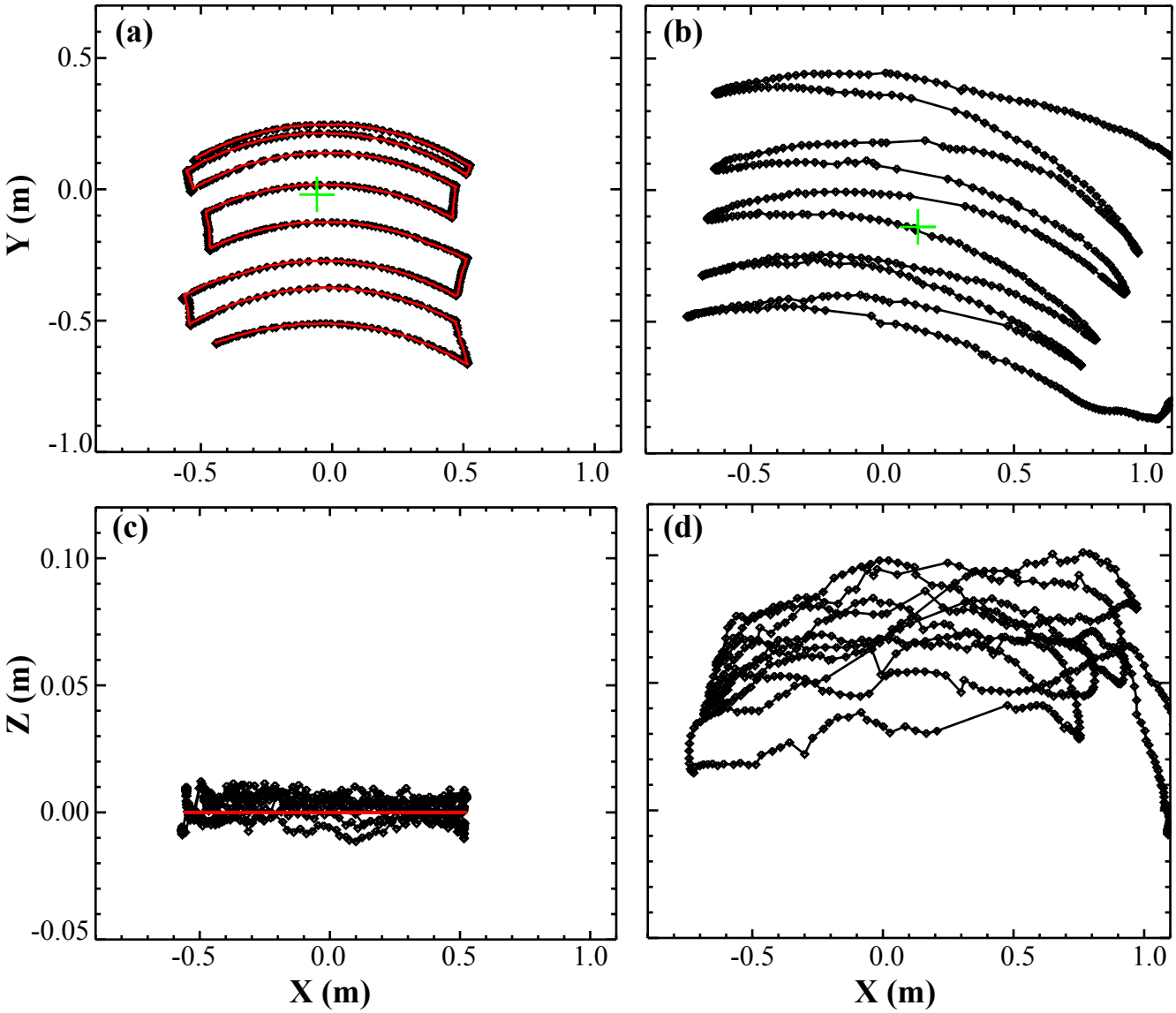

Figure 2. Sample X-Y and X-Z plots of the EM61-HH coil trajectories. In (a) and (c), the 2D coil motion on the sensor board as measured by the Arcsecond (black symbols) and the video (red curve). In (b) and (d), the 3D motion of the coil on the conventional EM61-HH pole. The green symbol is the object location.

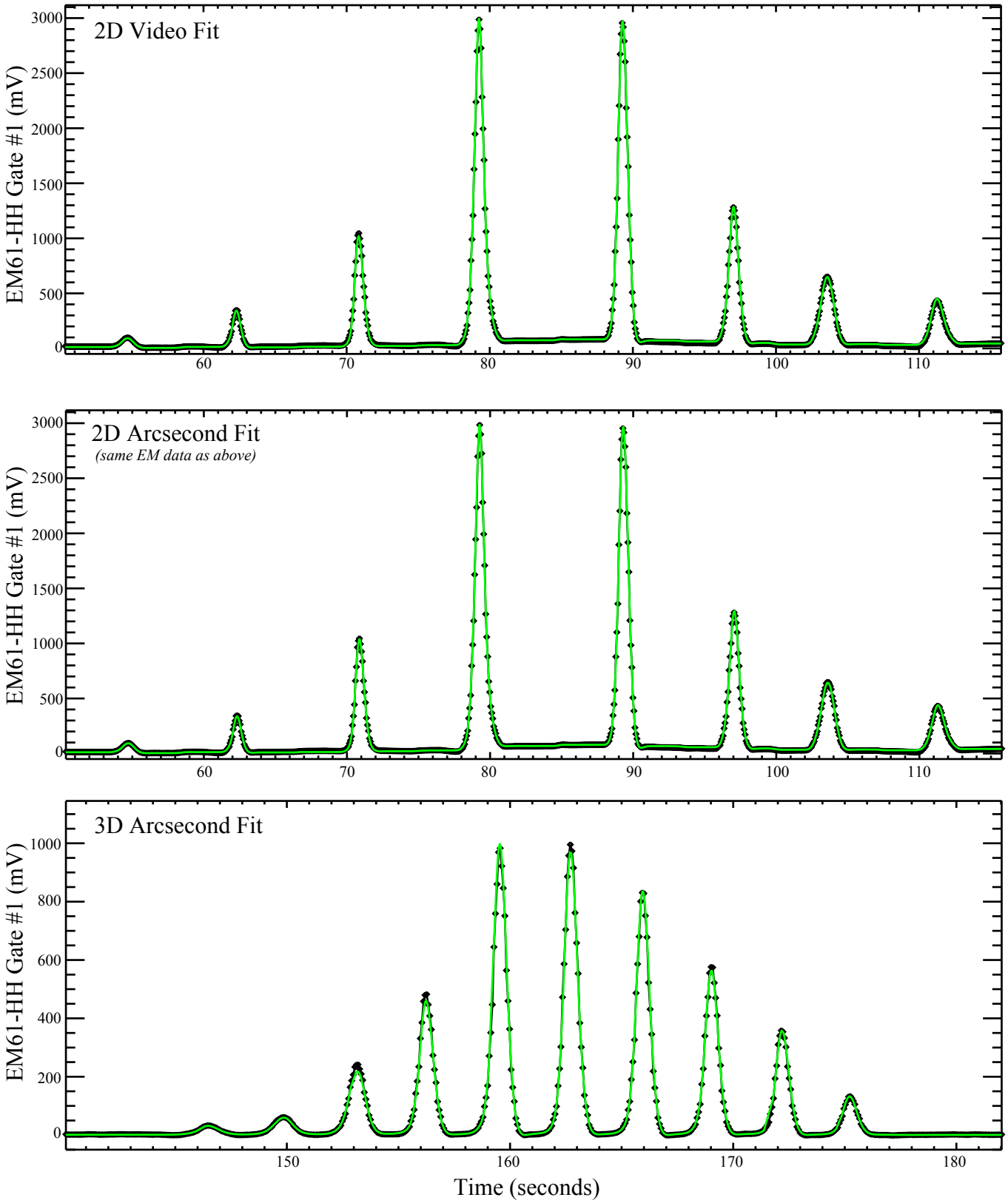

Figure 3. Time rasters of EM61-HH data (black curve and symbols) fitted to model (green curve).

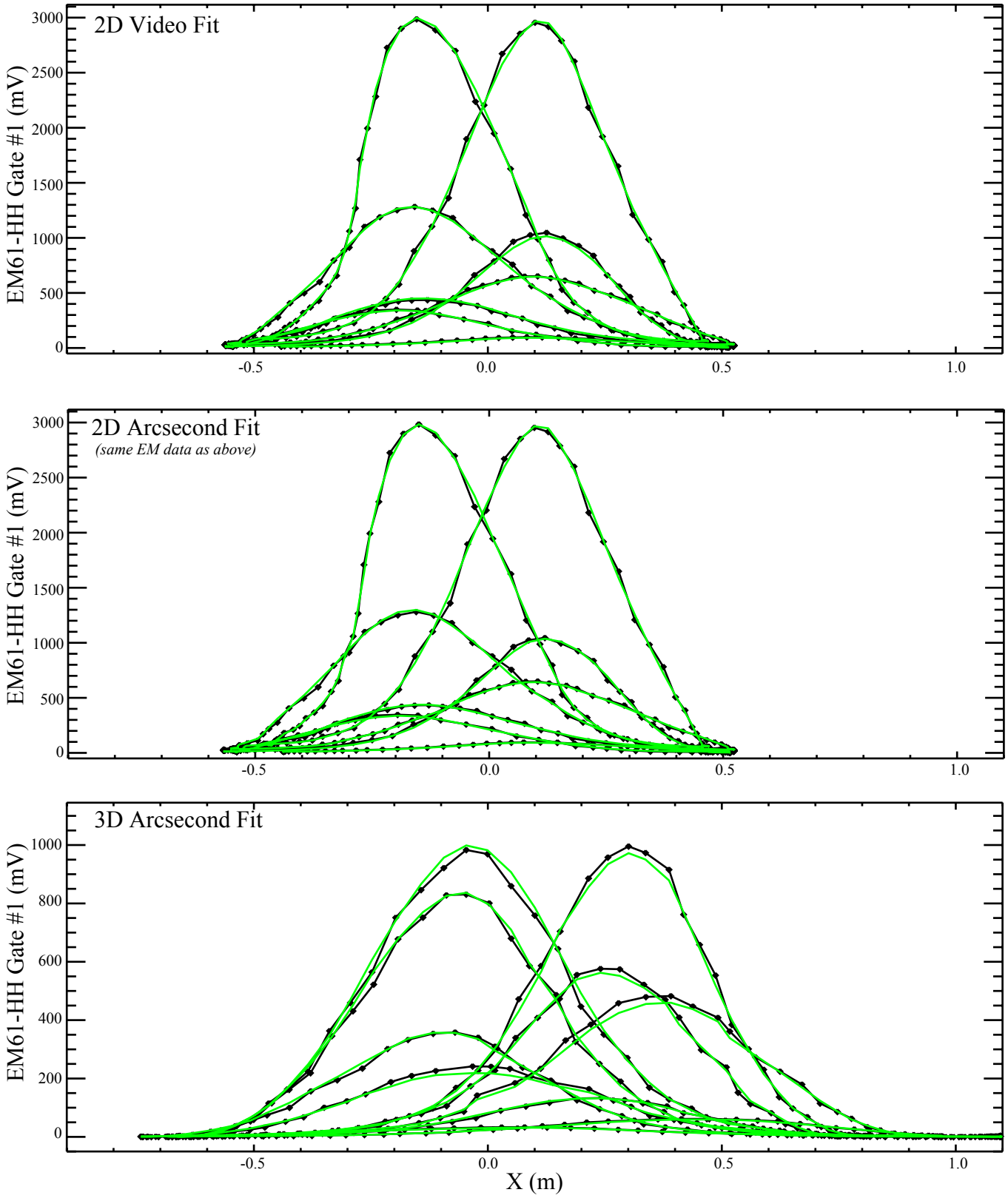

Figure 4. Plots along X of EM61-HH data (black curve and symbols) fitted to model (green curve).

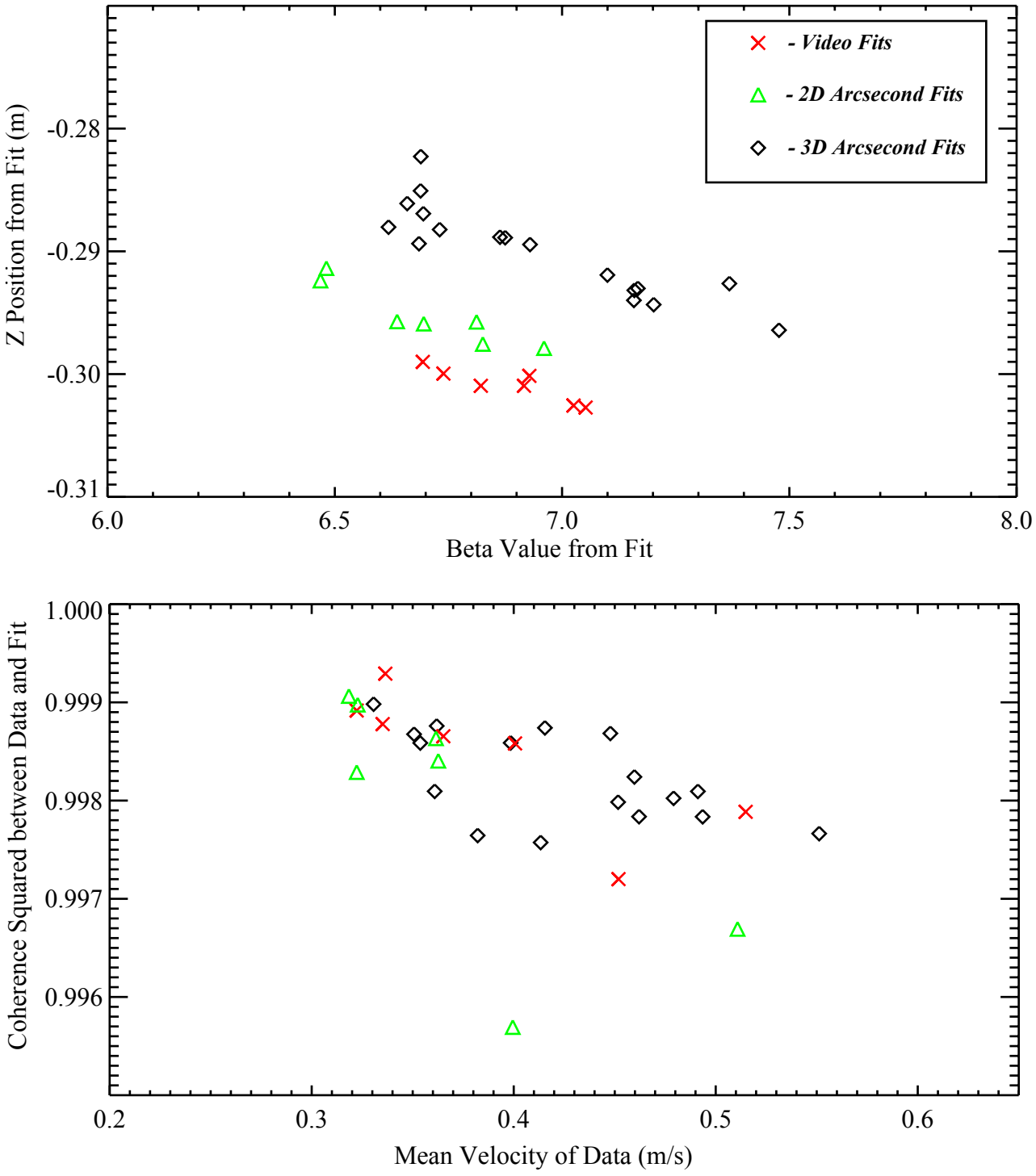

Figure 5. Results of fitting EM61-HH data with model using different positioning data.

square of the coherence between the best model fit and the data. There is a clear trend to poorer fits as the coil velocity increases. This is not surprising given the positioning system limitations of video frame rate (30 fps) and laser rotation rate (40Hz). At a speed of 1 m/s, the coil has moved 3.3 cm in a video frame and 2.5 cm during a single laser spin. Man portable survey systems move at comparable speeds and vehicle survey platforms exceed it.

In an effort to simulate the error in inverting the polarization responses as a function of positioning errors, a simple Monte Carlo simulation was run. Static measurements on a fixed grid with exact positioning were taken over a 40mm projectile. The data was inverted for the β responses. The same data was inverted repeatedly with increasing random errors added to the known grid positions. The results are shown in Figure 6. The variability in the fitted polarization responses and the coherence squared of the fit are plotted versus RMS position error in 5a and 5b respectively. At the level of 3 mm RMS position error, the average fit quality is about 0.998 and the spread in primary response is 15%. This is consistent with the Arcsecond 3D fits having an average fit quality of 0.9982 and a β spread of 13% (~0.9/6.94).

Conclusions

A laser based positioning system was used to position and invert EMI sensor data. In 2D tests, the positions mapped were found to match video mapped images at RMS position differences of 3-4 mm. Inverted 2D and 3D positioned data had high fit qualities of 0.9982. The fitted magnetic polarization responses had a narrow range of values (13%) over a set of seventeen 3D measurements of a steel sphere. However, the fit quality decreased at faster sensor motion rates, indicating larger positioning errors as speeds approach 1 m/s. Simulations of EMI data inversion with randomized position errors came up with similar fit qualities and response parameter errors at an RMS position error level of 3mm. All indications are that this laser based system is tracking the EMI sensor with sub-centimeter accuracy.

References

Bell, T.H., 2004, Strategic Environmental Research and Development Program web site, http://www.serdp.org/research/UX/UX-1381.pdf.

Millhouse, S.D., 2004, http://www.estcp.org/documents/techdocs/UX-0129.pdf, “ESTCP Cost and Performance Report (UX-0129) Innovative Navigation Systems to Support Digital Geophysical Mapping”.

Arcsecond, 2002, company web site, http://www.indoorgps.com/PDFs/wp_Error_Budget.pdf.

Bosnar, M, 2005, communications with Miro Bosnar at Geonics.

Acknowledgements

This work was supported by the Strategic Environmental Research and Development Program (SERDP) as Project UX-1381. The development of a UXO survey positioning system based on the Arcsecond equipment is managed by Scott Millhouse and funded by Environmental Security Technology Certification Program (ESTCP) as Project 200129. Additional funding comes from the Army Environmental Quality Technology Program (EQT) and the U.S. Army Corps of Engineers, Huntsville Engineering and Support Center (CEHNC). The authors would also like to thank Edmund Pendleton, Jay Bennett, and Scott Millhouse in providing and assisting with the Arcsecond equipment.

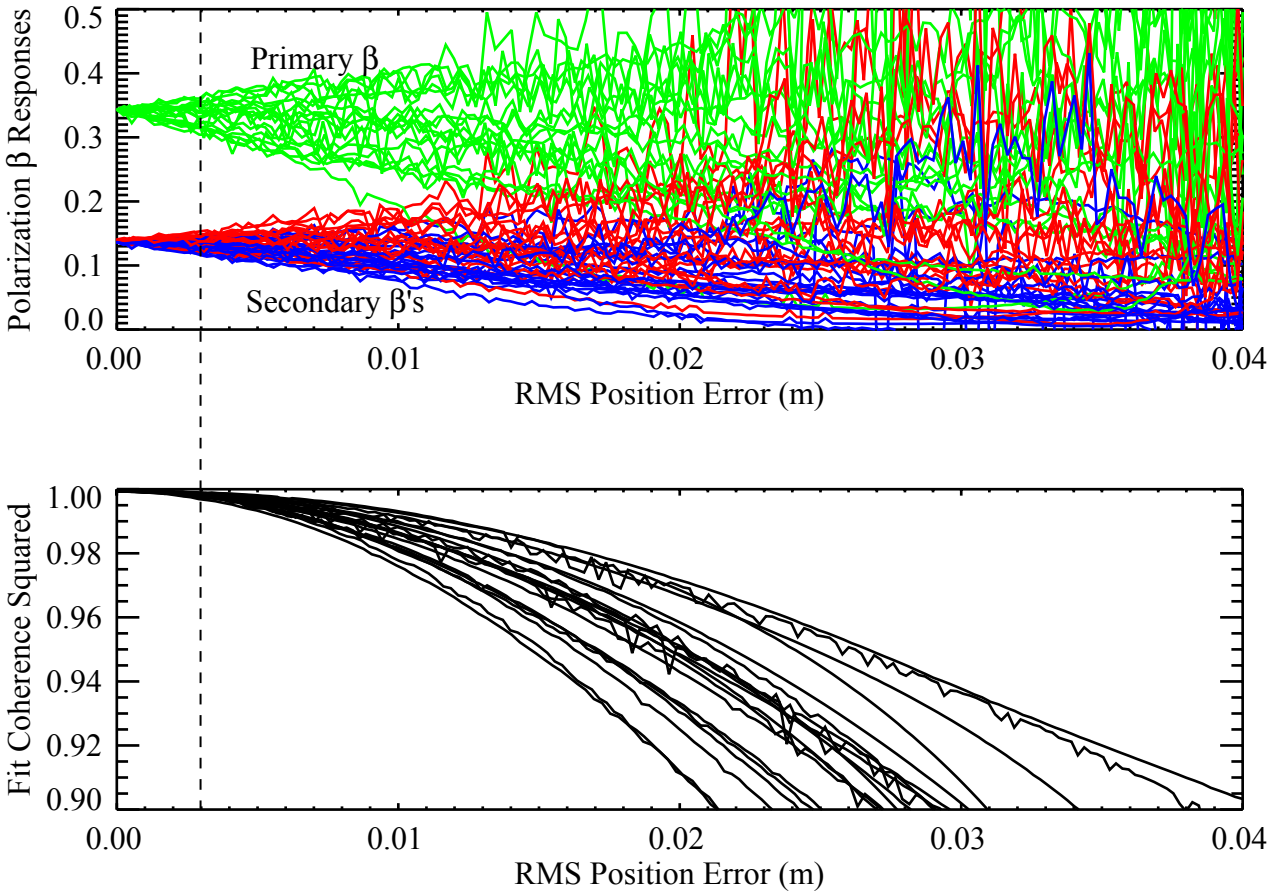

Figure 6. Monte Carlo simulation of inverting 40mm Projectile data with randomly generated position errors. Dashed line at RMS position error of 3 mm with an average fit coherence of 0.998 and a primary β spread of 15% (0.05/0.34).

Appendix N:

ENSCO Inc, Inertial Navigation System Improvements for Target Characterization using Small Area Inertial Navigation Tracking (SAINT)– Initial Study

Inertial Navigation System Improvements for Target Characterization using Small Area Inertial Navigation Tracking (SAINT) - Initial Study

February 13, 2006

ENSCO, Inc.
5400 Port Royal Road
Springfield, VA 22151

Introduction

Unexploded ordnance (UXO) poses a threat to human life and the environment. Millions of UXO are located in the United States on active test and training ranges and formerly used defense sites (FUDS). In addition to the millions of UXO, there are many times more cultural and debris anomalies. Digital geophysical mapping (DGM) is used to map the areas and to locate, identify and select the items for sampling and removal. Target characterization is one of the most important objectives of DGM. If we can accurately characterize and identify a buried target (as UXO, frag, fence post, etc.), then remediation resources can be focused on the truly hazardous targets, and nonhazardous targets can be left in place. The potential financial benefit of accurate characterization is tremendous. Prior studies have shown that detailed modeling and simulation of geophysical sensor data may provide the means to characterize targets, but such analysis will be ineffective without high-precision position data integrated with high-quality geophysical sensors.

Operationally, DGM is first conducted in a wide area search to locate targets with sub-meter accuracy. These targets are then relocated and marked (possibly flagged) for characterization. There is a need for a positioning system that can effectively be used to interrogate these targets over a small (~2 m x 2 m) area using standard geophysical sensors coupled with very precise 3-dimensional position data. ENSCO's approach to meet this positioning need initially consisted of using a tactical-grade inertial measurement unit (Honeywell's HG1700) coupled with a Geometrics G-858 total field cesium vapor magnetometer, innovative analytical techniques, and custom navigation software to successfully demonstrate a brass-board prototype system (capable of attaining an average radial error of 2.9 cm in the horizontal plane and an error of 1.9 cm in the vertical axis) for the EQT/ESTCP demonstration at Aberdeen Proving Ground (APG) UXO site during the week of July 12, 2004. SAINT, which stands for Small Area Inertial Navigation Tracking, was the name given to our system.

The objective of this effort was to use the experience that U.S. Army Engineering Support Center, Huntsville (USAESCH) and ENSCO have gained from the successful Environmental Quality Technology (EQT)/Environmental Security Technology Certification Program (ESTCP) demonstration as well as ENSCO's inertial navigation expertise based on other unrelated program areas to refine the usability of our Small Area Inertial Navigation Tracking (SAINT) technology for small area, high-resolution geophysical surveying. An initial demonstrable hardware system and related software was developed for this initial study effort funded by USAESCH.

Technology

Technology Description

Hardware

The primary sensor is the inertial measurement unit (IMU), which provides velocity and rotational information. The SAINT concept was originally demonstrated using a

Honeywell HG-1700 tactical grade IMU. During this project, the system was redesigned to accommodate a much smaller Honeywell HG-1930 IMU, as shown in Figure 1.

Figure 1. Honeywell HG-1930 Tactical Grade IMU

Just prior to final testing, the particular HG-1930 IMU unit we were using (an engineering unit of this soon-to-be commercially available device) failed internally. In order not to delay the evaluation further, we redesigned the sensor package to accommodate a larger HG-1700 IMU. The HG-1700 and HG-1930 are designed to have similar operating characteristics and are pin-compatible. The performance we describe below was achieved with the HG-1700; we expect the primary difference of using the HG-1930 (as we had planned) would have been a smaller and lighter device.

The prototype testing at APG indicated that it would be desirable for the SAINT to include its own source of heading information. The current design includes a Leica digital magnetic compass (DMC) to provide heading information. The DMC, however, is possibly affected by the magnetic anomalies created by the UXO being interrogated. These local magnetic effects are removed in software to provide a true magnetic north heading, as demonstrated during testing at ENSCO.

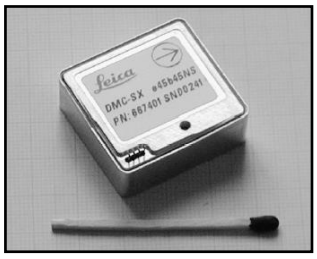

Figure 2. Leica Digital Magnetic Compass Sensor

The information from the navigation sensors and from the magnetic sensor are combined and stored on compact flash (CF) magnetic storage cards. This function is handled by a single-board computer. This computer operates positioning sensors, stores information,

and audibly guides the operator in the field. Figure 3 shows the computer board before installation in the SAINT enclosure.

Figure 3. Rabbit Single Board Computer

The SAINT components were integrated into a nonmetallic enclosure located at the opposite end of the survey staff from the magnetic sensor. Figure 4 shows the interior of this portion of the assembly along with the interface panel.

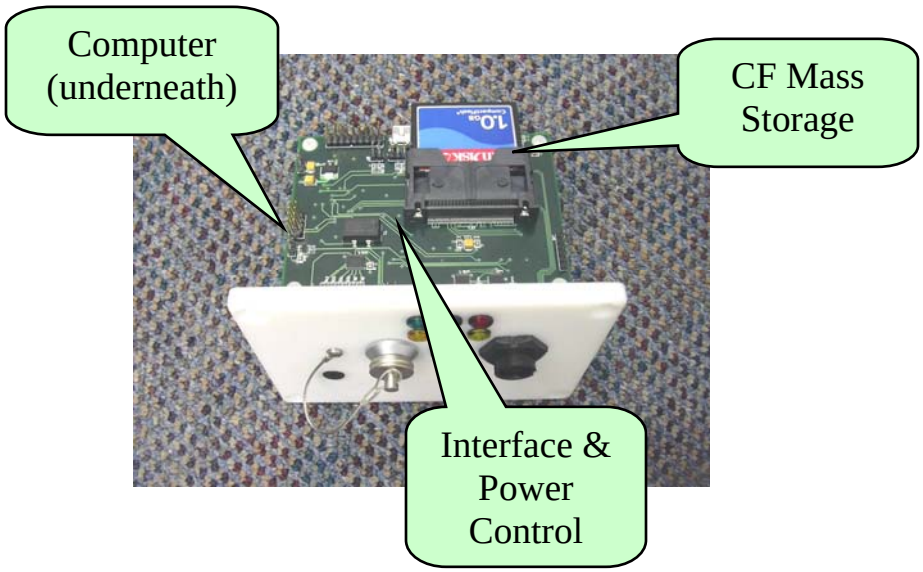

Figure 4. SAINT Interface Panel and Computer

The IMU, DMC, and other components are located below the computer board, as shown in Figure 5.

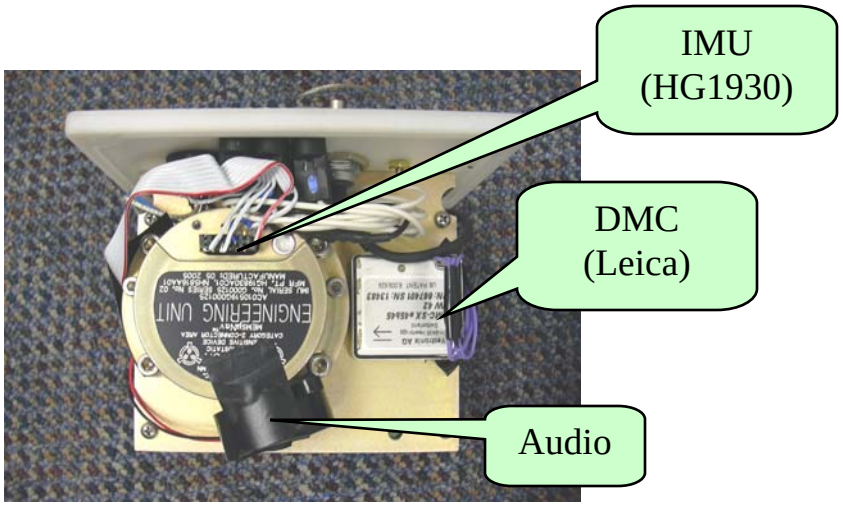

Figure 5. SAINT Components

The fully assembled SAINT system can easily be handled by one person. A belt pack contains batteries powering the unit. Figure 6 shows the complete SAINT system.

Figure 6. SAINT Shown with Geometrics G-858 Magnetometer

Software

All IMUs suffer from measurement errors that are integrated into the position, velocity, and attitude states and cause these states to drift, accumulating significant errors over short periods when unaided. By modeling the "position drift" as a function of time, we were able to determine the maximum duration of operation for the "free navigation" portion of the HG-1700 IMU collection to be approximately 30 seconds (to meet the demonstration's positional accuracy requirements).

The navigation software, developed under an unrelated program, consists of navigation equations, a 15-state Kalman filter and a Kalman smoother. Before and after the 30 seconds of collecting data over a target with the IMU, the IMU is placed stationary at its starting position. This allows the use of a position aid and a "zero velocity update" every time the IMU is stationary, which helps constrain the drift errors in the IMU. In post-processing, these errors are further reduced through the use of a Kalman smoother, which uses all the collected data to produce an optimal estimation of position and attitude over time.

Concept of Operations

The SAINT system is intended to help characterize targets found during UXO remediation activities. We assume that target locations have been previously marked with pin flags or by other means; the objective of data collection with the SAINT system is to acquire detailed sensor data for interrogation of the target location, combined with accurate position and orientation data for the sensor.

A single operator is necessary to collect data using the SAINT system. The system is battery-powered and requires no external power. Once powered on, the IMU begins data acquisition; raw data is stored on a built-in compact flash card until the system is powered down.

The operator sets the entire device on the ground for approximately 30 seconds. Then, the operator picks up the device, moves the sensor over the target in whatever pattern the operator desires, then returns the device back to the starting position. By limiting the time of free motion to 30 seconds or less, we are able to compute positions with standard deviations in radial position error of less than 1 cm. When the time of free motion exceeds 30 seconds, position errors increase exponentially with increasing time due to integrated measurement errors in the IMU. Greater data density can be achieved, however, by collecting multiple times over the same target.

Data processing is automated. The output data are oriented relative to the position of the original pin flag, with the orientation of the data determined by magnetic North.

Technology Enhancements

The primary tasks accomplished during this initial study effort were:

- Improvements to the mechanical integration of the inertial sensor and data acquisition electronics with the Geometrics G-858 magnetometer for robust, reliable, easy use. Also, operator ergonomics (grip switch, aural interface, etc.) have been implemented and the hardware has been developed to allow more tightly controlled foolproof operation.
- Improvements to the firmware and software, in the data logger and in post-processing analysis, to improve ease of use as well as to reduce the possibility of field data loss. This includes audible information to the user indicating timing for individual collections (*i.e.*, when to pick up the unit, when to set it back down), visual indications that the unit has successfully completed its position update phase and is ready for continued operation, and a simple USB field data download to the post-processing computer with data loss protection. Time alignment of position data with G-858 magnetic sensor data is performed internally; the magnetic data is being collected and stored by the SAINT data logger.
- Integration of a DMC to automate bearing information and development of methods to automatically integrate compass bearing with inertial computation, allowing for compass deviations due to presence of buried ferrous objects.
- Conducting a technology demonstration to interested parties.
- Interfacing with an EM-61-HH sensor in place of the G-858.

Calibration and Error Evaluation

Calibration

A calibration method is employed to determine the position offset between the SAINT cluster (contains IMU and compass) and the geophysical sensor prior to the first data acquisition with a given SAINT system. This calibration step is a one-time event per SAINT system, assuming sensors have not been moved, and consists of holding the center of sensitivity at a constant point while moving the SAINT cluster through a series of arcs. An algorithm was implemented to statistically estimate the position offset between the SAINT cluster and the geophysical sensor.

Error Validation Methodology

Position errors were validated by replacing the geophysical sensor with a pen (a Sharpie marker), rigidly attached to the SAINT sensor connection in place of the sensor, and using this pen to draw various random paths on a large (1.5 m x 1.5 m) sheet of paper placed on a horizontal surface, as seen in Figure 7. The SAINT cluster records its position and orientation, which is transferred (via a vector offset) to the position of the pen tip. The drawn path was digitally photographed, imported to our software, scaled (based on scale factors drawn on the paper), and then rotated and translated in a least-

squares routine to be plotted in conjunction with the pen path estimated by the IMU. The expected error in the ground truth path was limited by the resolution of the scanner and is expected to be no more than than 0.017 cm (based on 150 DPI) in the horizontal plane. The primary parameters for determining the navigation accuracy were the two-dimensional radial error (defined as the perpendicular distance from the IMU estimated path to the drawn path) and the z-axis position error in the IMU estimated path to the drawn path.

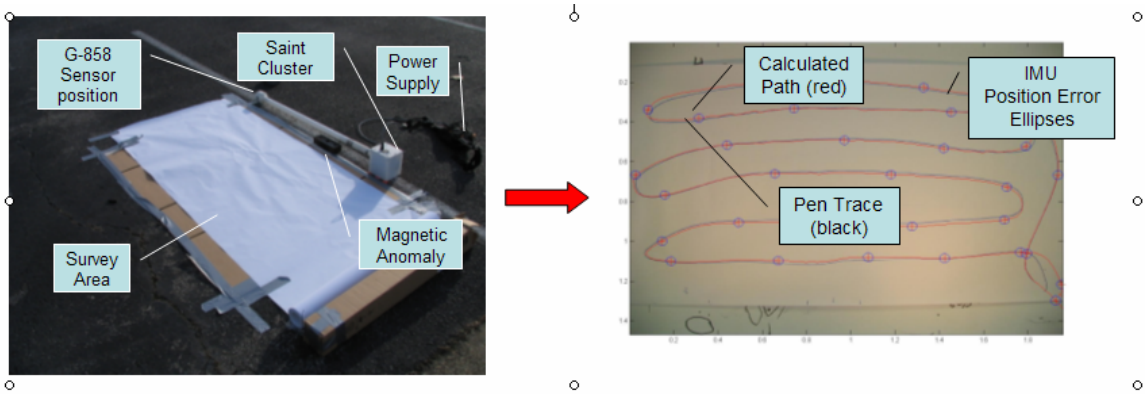

Figure 7: SAINT Position Error Validation Setup and Resulting Plot.

Performance

The performance of the SAINT system has steadily improved as the system development has continued. The initial prototype was tested at the APG UXO demonstration site. ENSCO demonstrated position accuracies ranging from 2.9 to 4.5 cm radial error (defined as the square root of the sum of the squares of the horizontal position errors) as achieved at the APG UXO demonstration site during the week of July 12, 2004, as shown in Table 1. For that demonstration, 19 locations were interrogated in a fixed grid. The fixed grid data set was gathered based upon a fixed grid boards centered on the reacquired location for a 1.0 m square area at .2 m intervals (36 points). For a sensor height of 15 cm, coordinates for all 36 points were acquired and for sensor heights of 30 and 45 cm; coordinates were acquired on the 12 points that form the diagonals of the grid. (The three sensor height standoffs were established by plastic head spacers attached to the grid board.) The results were very close to desired accuracy in both horizontal and vertical directions. A substantial amount of the estimated error was due to test conditions (e.g., warp of the reference wooden grid board) and not the data.

Using the improved SAINT system and the error validation methodology described above, position errors were computed at discrete intervals that were approximately 1 second apart. Discrete intervals are marked by center of error ellipsoids in right plot of Figure 7). Error statistics, shown in Table 1, indicate a marked improvement in the accuracy of the system. Although a portion of the reduced errors can be attributed to the improved calibration method described above, a significant portion of the errors at APG were due to test conditions, as stated above.

	APG Demo	Current effort
Average Radial Error (cm)	2.9 - 4.5	1.0
Minimum Radial Error (cm)	0.6	0.2
Maximum Radial Error (cm)	7.0	2.1

Table 1. Comparison of Position Errors Using Current SAINT System to the Prototype System Demonstrated at APG

Technology Transition

The purpose of this initial study phase was to refine the usability of our SAINT technology, first proven in the EQT/ESTCP demonstration in prototype form in 2004, for small area, high-resolution geophysical surveying. Improvements were made in the packaging, operational use, and accuracy of the SAINT system.

The objective for the next phase, to be sponsored by the U.S. Army Corps of Engineers (USACE) and ESTCP, is to provide a robust, fieldable system, able to provide very precise small-area position information through a common interface, usable with an EM-61 HH sensor.